

**PEPTÍDEOS BIOINSPIRADOS: ESTUDO DA INTERAÇÃO E O
MECANISMO DE AÇÃO SOBRE LEVEDURAS PATOGÊNICAS**

DOUGLAS RIBEIRO LUCAS

**UNIVERSIDADE ESTADUAL DO NORTE FLUMINENSE DARCY
RIBEIRO - UENF
CAMPOS DOS GOYTACAZES - RJ
FEVEREIRO/2025**

**PEPTÍDEOS BIOINSPIRADOS: ESTUDO DA INTERAÇÃO E O
MECANISMO DE AÇÃO SOBRE LEVEDURAS PATOGÊNICAS**

DOUGLAS RIBEIRO LUCAS

Tese apresentada ao Centro de Biociências e Biotecnologia, da Universidade Estadual do Norte Fluminense Darcy Ribeiro, como parte das exigências para obtenção do título de Doutor em Biociências e Biotecnologia.

Orientador: Prof. André de Oliveira Carvalho

Este trabalho foi desenvolvido no Laboratório de Fisiologia e Bioquímica de Microrganismos – LFBM no Centro de Biociências e Biotecnologia – CBB.

**CAMPOS DOS GOYTACAZES - RJ
2025**

FICHA CATALOGRÁFICA

UENF - Bibliotecas

Elaborada com os dados fornecidos pelo autor.

L933

Lucas, Douglas Ribeiro.

PEPTÍDEOS BIOINSPIRADOS : ESTUDO DA INTERAÇÃO E O MECANISMO DE AÇÃO SOBRE LEVEDURAS PATOGÊNICAS. / Douglas Ribeiro Lucas. - Campos dos Goytacazes, RJ, 2025.

178 f. : il.

Inclui bibliografia.

Tese (Doutorado em Biociências e Biotecnologia) - Universidade Estadual do Norte Fluminense Darcy Ribeiro, Centro de Biociências e Biotecnologia, 2025.

Orientador: André de Oliveira Carvalho.

1. transportador de poliaminas. 2. autofagia. 3. hiperpolarização mitocondrial. 4. morte celular. 5. ROS. I. Universidade Estadual do Norte Fluminense Darcy Ribeiro. II. Título.


CDD - 570

PEPTÍDEOS BIOINSPIRADOS: ESTUDO DA INTERAÇÃO E O MECANISMO DE
AÇÃO SOBRE LEVEDURAS PATOGÊNICAS


DOUGLAS RIBEIRO LUCAS

Tese apresentada ao Centro de Biociências e Biotecnologia, da Universidade Estadual do Norte Fluminense Darcy Ribeiro, como parte das exigências para obtenção do título de Doutor em Biociências e Biotecnologia.


APROVADO EM: 27/02/2025

Documento assinado digitalmente
 **ADRIANA FERREIRA UCHOA**
Data: 09/03/2025 17:13:48-0300
Verifique em <https://validar.iti.gov.br>


Prof. Adriana Ferreira Uchôa (Doutora em Biociências e Biotecnologia) -UFRN

Documento assinado digitalmente
 **LUIS GUILHERME MANSOR BASSO**
Data: 10/03/2025 11:59:38-0300
Verifique em <https://validar.iti.gov.br>

Prof. Luis Guilherme Mansor Basso (Doutor em Física) - UENF

Documento assinado digitalmente
 **SERGIO HENRIQUE SEABRA**
Data: 10/03/2025 10:59:33-0300
Verifique em <https://validar.iti.gov.br>

Prof. Sérgio Henrique Seabra (Doutor Ciências Biológicas (Biofísica)) – UFRJ

Documento assinado digitalmente
 **ANDRÉ DE OLIVEIRA CARVALHO**
Data: 08/03/2025 12:32:12-0300
Verifique em <https://validar.iti.gov.br>

Prof. André de Oliveira Carvalho (Doutor em Biociências e Biotecnologia) - UENF
(orientador)

DEDICO...

Ao meu pai Gilmar, minha mãe Maria Aparecida e meu irmão Gustavo Henrique
e meu sobrinho Lucas por todo apoio sempre.

2. AGRADECIMENTOS

A Deus, em primeiro lugar, por me conceder força para seguir em frente, mesmo nos momentos mais desafiadores, e por proteger meus caminhos ao longo dos mais de 80.000 km percorridos durante o Doutorado

Ao meu orientador, Prof. André de Oliveira Carvalho, pela orientação dedicada, pelos ensinamentos valiosos, pelo incentivo constante e pela amizade, além do apoio incansável em cada dúvida ao longo dessa jornada.

Aos membros da banca, minha sincera gratidão por aceitarem contribuir com sua experiência e conhecimento em minha defesa

Ao Prof. Sérgio Henrique Seabra e ao seu grupo pela colaboração com ensaio de toxicidade.

A todos os professores e funcionários do PGBB pelo apoio e pelos ensinamentos ao longo desta jornada, com um agradecimento especial à Dra. Anna Okorokova, ao Dr. Gabriel Bonan Taveira, ao Dr. Antônio Cogo e ao Dr. Luis Bastos, com quem tive maior proximidade

A todos amigos do grupo “CARVALHO ET AL” e “VAL-ANDRÉ”, pelas dicas, amizade e brincadeiras.

A todos os técnicos do LFBM pela manutenção e cuidado com o laboratório.

A meus amigos/irmãos da graduação para a vida Dr. Filipe Zaniratti e Leismarque Jr. e meu amigo irmão de infância Valber Augusto por toda ajuda, força e incentivo, ao longo de todos os anos.

A toda minha família pela força, incentivo e por acreditar em mim, em principal minha namorada Selmara Marcelino pela paciência, sempre me incentivando a dar o meu melhor.

À UENF e ao Programa de Pós-Graduação em Biociências e Biotecnologia, pela infraestrutura, pelo suporte, pela concessão da bolsa e pela oportunidade de realizar este curso.

Ao CNPq, à Capes e à Faperj, pelo apoio financeiro essencial para a concretização deste trabalho.

A todos que, de alguma forma, contribuíram para minha formação acadêmica e para a realização desta pesquisa, minha sincera gratidão

“Uma vida dedicada à ciência é uma vida bem vivida”.

Louis Pasteur

3. RESUMO

As doenças fúngicas e a resistência aos agentes antifúngicos estão crescendo globalmente, destacando a necessidade de novos tratamentos eficazes. Os peptídeos bioinspirados RR, D-RR e WR demonstraram potente atividade antifúngica contra *Candida tropicalis* e *Candida albicans*. Investigamos os modos de ação desses peptídeos, abordando aspectos como internalização celular, danos induzidos e vias de morte celular. RR e D-RR são internalizados em *C. tropicalis* em 1,2 e 1 minuto, respectivamente, enquanto WR é rapidamente internalizado em *C. albicans* em apenas 20 segundos, principalmente por transportadores de poliaminas. Inibidores de transporte (CCCP, NaN₃) e temperaturas baixas (4 °C) prejudicaram a internalização, protegendo os fungos da morte induzida pelos peptídeos. A espermina, um antioxidante, reduziu os níveis de espécies reativas de oxigênio (ROS), conferindo proteção aos fungos e atenuando os danos induzidos pelos peptídeos. Os peptídeos causaram intensos danos celulares, incluindo encolhimento celular devido ao efluxo de K⁺, hiperpolarização mitocondrial, acidificação do meio, permeabilização de membranas e degradação citoplasmática. Observamos alterações vacuolares, dano à parede celular e formação de poros. WR induziu especificamente *blebs* em *C. albicans*. Sob condições hipo-osmóticas, a morte celular foi acelerada. Estruturas similares à autofagia foram identificadas, sugerindo a ativação de processos de degradação celular. Além disso, a ligação dos peptídeos ao núcleo celular foi observada, indicando um possível alvo citoplasmático relevante para a ação antifúngica. Apesar do aumento de ROS, os antioxidantes demonstraram papel essencial na proteção celular, destacando sua relevância na modulação da toxicidade dos peptídeos. Os peptídeos não apresentaram toxicidade detectável em células LLC-MK2, reforçando seu potencial como candidatos promissores para o desenvolvimento de novos antifúngicos eficazes e seguros.

Palavras-chave: transportador de poliaminas; autofagia; hiperpolarização mitocondrial; ROS; morte celular.

4. ABSTRACT

Fungal diseases and resistance to antifungal agents are escalating globally, emphasizing the need for new effective treatments. The bioinspired peptides RR, D-RR, and WR demonstrated potent antifungal activity against *Candida tropicalis* and *Candida albicans*. We investigated the mechanisms of action of these peptides, focusing on cellular internalization, induced damage, and cell death pathways. RR and D-RR were internalized in *C. tropicalis* within 1.2 and 1 minute, respectively, while WR was rapidly internalized in *C. albicans* in just 20 seconds, primarily via polyamine transporters. Transport inhibitors (CCCP, NaN₃) and low temperatures (4 °C) impaired internalization, protecting fungi from peptide-induced death. Spermine, an antioxidant, reduced reactive oxygen species (ROS) levels, providing fungal protection and mitigating peptide-induced damage. The peptides caused extensive cellular damage, including cell shrinkage due to K⁺ efflux, mitochondrial hyperpolarization, medium acidification, membrane permeabilization, and cytoplasmic degradation. Vacuolar alterations, cell wall damage, and pore formation were observed. WR specifically induced blebs in *C. albicans*. Under hypoosmotic conditions, cell death was accelerated. Autophagic-like structures were identified, suggesting activation of cellular degradation processes. Furthermore, peptide binding to the cell nucleus was observed, indicating a possible cytoplasmic target relevant to their antifungal action. Despite increased ROS levels, antioxidants played an essential role in cellular protection, highlighting their importance in modulating peptide toxicity. The peptides exhibited no detectable toxicity toward LLC-MK2 cells, reinforcing their potential as promising candidates for the development of effective and safe new antifungal agents.

Keywords: polyamine transporter; autophagy; mitochondrial hyperpolarization; ROS; cell death.

5. SUMÁRIO

2. AGRADECIMENTOS	iv
3. RESUMO	vi
4. ABSTRACT	vii
5. SUMÁRIO	viii
1. INTRODUÇÃO GERAL	2
1.1 <i>O Cenário Atual das Infecções Fúngicas e Resistência Antifúngica</i>	2
1.2 <i>Peptídeos Antimicrobianos e Bioinspirados como Estratégia Terapêutica Inovadora</i>	4
1.3 <i>A Defensina Vu-Def1 como Modelo para o Design de Peptídeos</i> 6	
1.3 <i>Relevância do Estudo para Candida spp. como Alvo Terapêutico</i>	15
1.4 <i>Modo de Ação de Peptídeos Antifúngicos</i>	15
2. REFERÊNCIAS	18
3- OBJETIVOS	25
3.1 <i>Objetivo Geral</i>	25
3.2 <i>Objetivos Específicos</i>	25
4. CHAPTER 1: MANUSCRIPT PUBLISHED	27
4.1 <i>Grafical abstract (Resumo gráfico)</i>	29
4.2 <i>Figura Suplementar</i>	54
5. CHAPTER 2: MANUSCRIPT SUBMITTED	61
5.1 <i>Grafical abstract (Resumo gráfico)</i>	63
5.2 <i>Figura Suplementar</i>	110
6. CHAPTER 3: MANUSCRIPT SUBMITTED	118
6.1 <i>Grafical abstract (Resumo gráfico)</i>	120
6.2 <i>Figura Suplementar</i>	152
7. CONCLUSÕES	169

1 – INTRODUÇÃO GERAL

1. INTRODUÇÃO GERAL

1.1 O Cenário Atual das Infecções Fúngicas e Resistência Antifúngica

Os fungos representam uma ameaça crescente e séria para a saúde humana, causando milhões de infecções e mortes a nível mundial anualmente (Stewart & Paterson, 2021, Denning, 2024, Thambugala et al., 2024). Dados recentes apontam para cerca de 6,5 milhões de casos anualmente, resultando em 3,8 milhões de mortes, das quais 2,5 milhões são diretamente causadas por infecções fúngicas (GAFFI, 2022; Denning, 2024). No quadro 1 estão alguns destaques sobre o impacto dos fungos na saúde humana.

Quadro 1. Destaques do impacto de doenças fúngicas em humanos.			
Infecção Fúngica	Casos Anuais	Mortes Anuais	Taxa de Mortalidade
Aspergilose invasiva	2,1 milhões	1,79 milhões	85,20%
Aspergilose pulmonar crônica	1,8 milhões	340.000	18,50%
Candidemia e candidíase invasiva	1,5 milhões	954.000	63,60%
Pneumonia por Pneumocystis	505.000	214.000	42,40%
Meningite criptocócica	194.000	147.000	75,80%
Outras infecções fúngicas graves	300.000	161.000	53,70%
Asma fúngica	11,5 milhões	46.000	-

Fonte: Denning, 2024

A incidência de micoses invasivas tem apresentado um aumento preocupante, impulsionado por diversos fatores inter-relacionados. Evidências apontam para a influência do aquecimento global nesse processo, uma vez que o aumento da temperatura ambiental favorece a adaptação de fungos a condições térmicas mais próximas à temperatura corporal dos mamíferos, tornando-os mais suscetíveis a infecções (Crecy et al., 2009; Casadevall et al., 2021).

Um exemplo emblemático desse fenômeno é a emergência de *Candida auris*, uma levedura que, adaptada a temperaturas mais elevadas, tem causado infecções em humanos (Casadevall et al., 2021). Além disso, o aquecimento global promove alterações na distribuição geográfica de patógenos fúngicos, expandindo seu alcance e potencial de infecção (Nnadi & Carter, 2021).

Paralelamente, a crescente população de indivíduos imunocomprometidos, incluindo idosos, portadores de vírus da imunodeficiência humana (HIV, do inglês *human immunodeficiency virus*), pacientes oncológicos, transplantados e pessoas com infecções virais graves, contribui para o aumento da suscetibilidade às infecções fúngicas (Fisher et al., 2022).

Esse cenário foi amplificado pela pandemia de COVID-19, que evidenciou a gravidade das coinfeções fúngicas, como aspergilose, mucormicose e candidemia, as quais agravaram o quadro clínico dos pacientes e elevaram as taxas de mortalidade (Lockhart et al., 2023; Denning, 2024).

Conforme discutido previamente sobre o aumento das doenças fúngicas. Outro fator que chama a atenção é o aumento da resistência fúngica, o que torna o tratamento dessas infecções ainda mais desafiador (Fernández de Ullivarri et al., 2020, Fisher et al., 2022, Gow et al., 2022). Essa resistência pode ser intrínseca, caracterizada pela resistência natural de uma espécie fúngica a determinados antifúngicos. Um exemplo clássico é a resistência inerente de *Pichia kudriavzevii* (previamente identificada como *Candida krusei*) ao fluconazol, que ocorre devido a um polimorfismo de aminoácido em sua lanosterol desacetilase, impedindo a ligação do fluconazol à enzima e a inibição da síntese de ergosterol (Guinea et al., 2006, Lockhart et al., 2023).

Já a resistência adquirida surge quando uma espécie, inicialmente suscetível a um antifúngico, desenvolve mecanismos de resistência por meio de mutações ou alterações genéticas (Lockhart et al., 2023). Essa resistência pode ser adquirida *in vivo*, durante o tratamento, resultando em falhas terapêuticas, ou no ambiente, pela exposição prévia a fungicidas (Fisher et al., 2022). O desenvolvimento de resistência aos azólicos em *Aspergillus fumigatus*, associado ao uso disseminado de fungicidas azólicos na agricultura, ilustra a gravidade desta problemática (Strickland & Shi, 2021; Fisher et al., 2022; Gow et al., 2022).

Com essa realidade preocupante, torna-se urgente o desenvolvimento de novos antifúngicos eficazes para combater essas infecções fúngicas emergentes e reduzir a mortalidade associada, especialmente entre as populações mais vulneráveis (Figura 1) (Campoy & Adrio, 2017; Stewart e Paterson, 2021).

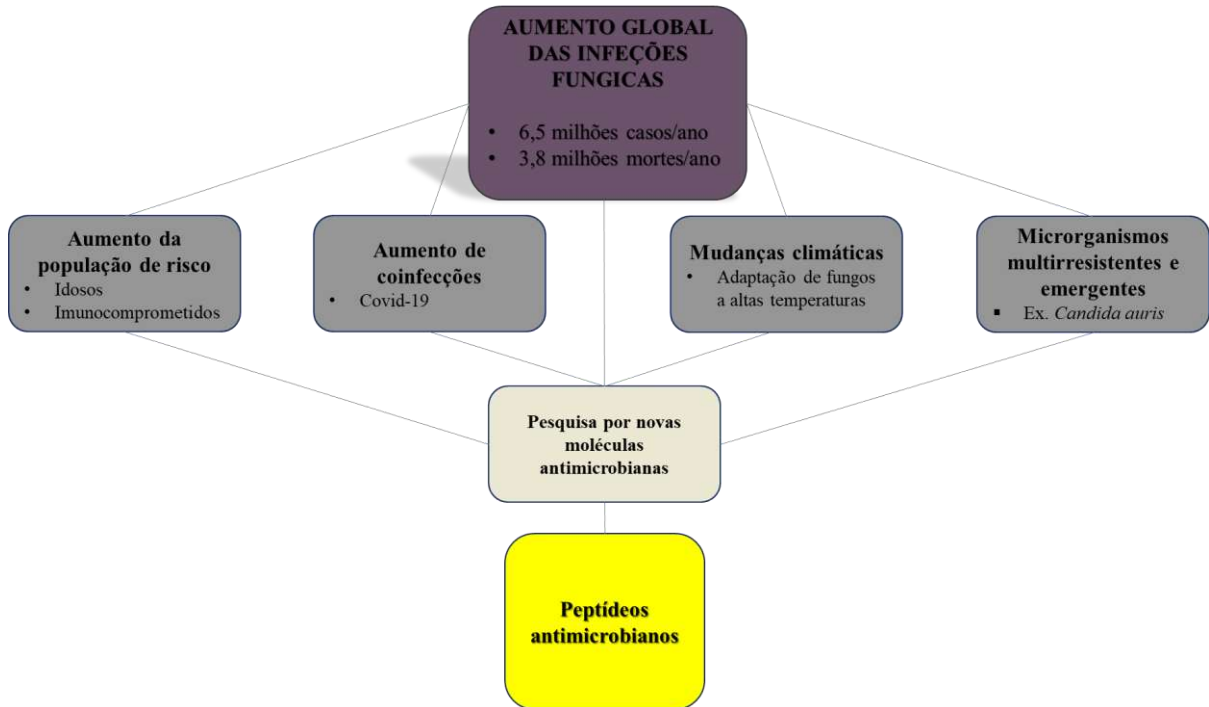


Figura 1: Fluxograma representando os fatores que contribuem para o aumento global das infecções fúngicas e a busca por novas moléculas antimicrobianas, com destaque para os peptídeos antimicrobianos.

1.2 Peptídeos Antimicrobianos e Bioinspirados como Estratégia Terapêutica Inovadora

Os peptídeos antimicrobianos (AMPs, do inglês *Antimicrobial Peptides*) são encontrados em uma ampla gama de organismos, de bactérias a humanos, e desempenham um papel crucial na imunidade inata contra invasões microbianas (Carvalho & Gomes 2009; Carvalho & Gomes, 2011; Fernández de Ullivarri et al., 2020; Răileanu et al., 2023). Os AMPs consistem em um pequeno número de aminoácidos, em geral são catiônicos, e a presença de aminoácidos, como argininas e lisinas, confere a eles uma carga positiva em pH fisiológico (Brunet et al., 2022).

A atividade dos AMPs abrange ações antibacterianas, antimicrobianas (fungos e parasitas), antivirais (incluindo HIV) e anticâncer, de acordo com o banco de dados ADP3

(Figura 2) (Huan et al., 2020).

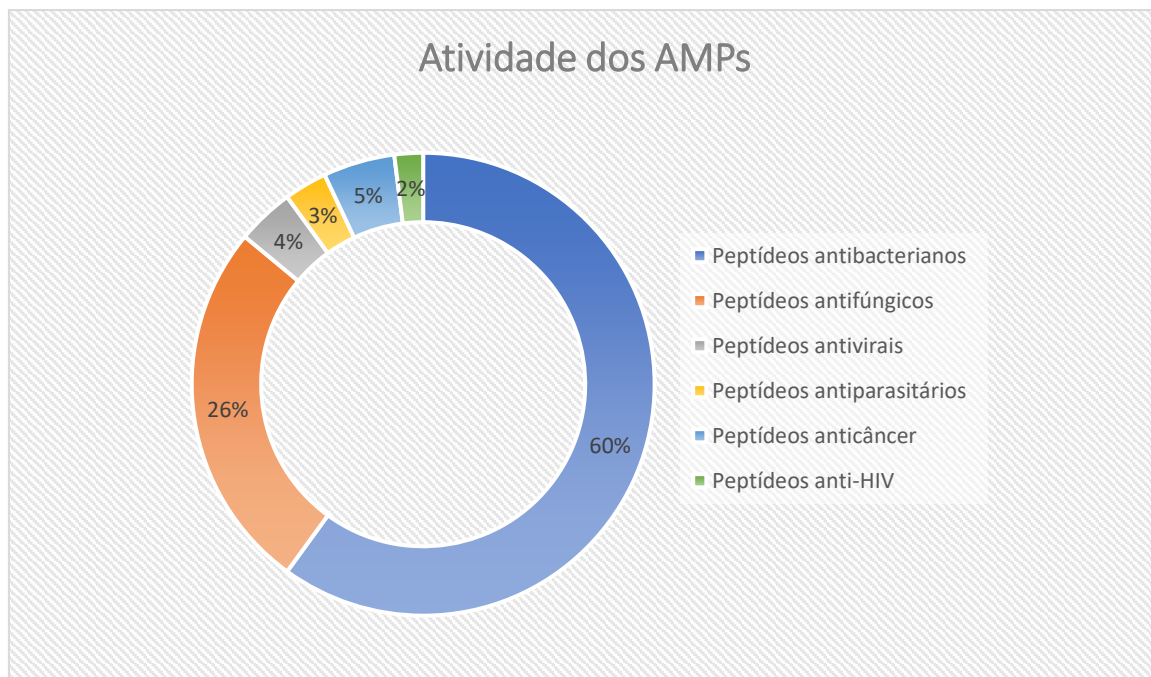


Figura 2. Estatísticas das principais atividades biológicas dos peptídeos antimicrobianos (adaptado de Huan et al., 2020)

Com base nas atividades e estruturas dos AMPs naturais, os peptídeos bioinspirados são moléculas sintetizadas de forma racional em laboratório, projetadas a partir de AMPs de ocorrência natural. Esses peptídeos apresentam uma ampla variedade de modificações estruturais, o que resulta em maior eficiência, segurança, especificidade e uma redução potencial da toxicidade para células não-alvo, quando comparados aos seus equivalentes naturais (Cary et al., 2000; Rajasekaran et al., 2012; Rajasekaran et al., 2018). O design de AMPs modificados com melhores propriedades terapêuticas, são relevantes para driblar os desafios clínicos enfrentados por esses peptídeos (Toledo et al., 2021).

Para aprimorar a estabilidade, prolongar a meia-vida, aumentar a atividade e melhorar a solubilidade e biodisponibilidade dos AMPs *in vivo*, modificações estruturais em AMPs nativos têm sido amplamente empregadas. Essas modificações podem incluir a adição, substituição ou exclusão de um ou mais resíduos de aminoácidos em sua sequência primária, permitindo a criação de variantes com propriedades otimizadas (Brogden & Brogden, 2011; Gentilucci et al., 2016).

O design de peptídeos segue estratégias que englobam cinco principais aspectos: o comprimento da cadeia, a estrutura secundária, a carga líquida, a anfifilicidade e a hidrofobicidade. Cada um desses elementos é cuidadosamente ajustado para maximizar a eficácia antimicrobiana, garantindo ao mesmo tempo a estabilidade estrutural dos peptídeos.

Além disso, a introdução de *D*-aminoácidos na sequência dos AMPs tem sido amplamente utilizada para melhorar a resistência contra proteases, prolongando sua estabilidade em ambientes biológicos complexos (Torres et al., 2019; Zhong et al., 2020; Huan et al., 2020).

Fatores adicionais, como o custo de produção, o pH ideal para a atividade antimicrobiana, a eficácia em condições ambientais adversas e a resposta imunológica do hospedeiro ao peptídeo, também devem ser considerados no processo de design. A otimização desses fatores é essencial para viabilizar o uso dos AMPs como terapias antimicrobianas eficazes e economicamente viáveis, especialmente em cenários clínicos desafiadores (Torres et al., 2019; Huan et al., 2020).

1.3 A Defensina Vu-Def1 como Modelo para o Design de Peptídeos

Nosso grupo tem se dedicado ao estudo de AMPs presentes nas sementes de *Vigna unguiculata* L. Walp. (feijão-de-corda). A partir desse material, foram isolados dois peptídeos ricos em cisteína: uma defensina e uma proteína transportadora de lipídeos (Figura 3), ambos com comprovada atividade biológica *in vitro* contra os fungos fitopatogênicos *Fusarium oxysporum* e *Fusarium solani*, além da levedura *Saccharomyces cerevisiae* (Carvalho et al., 2001).

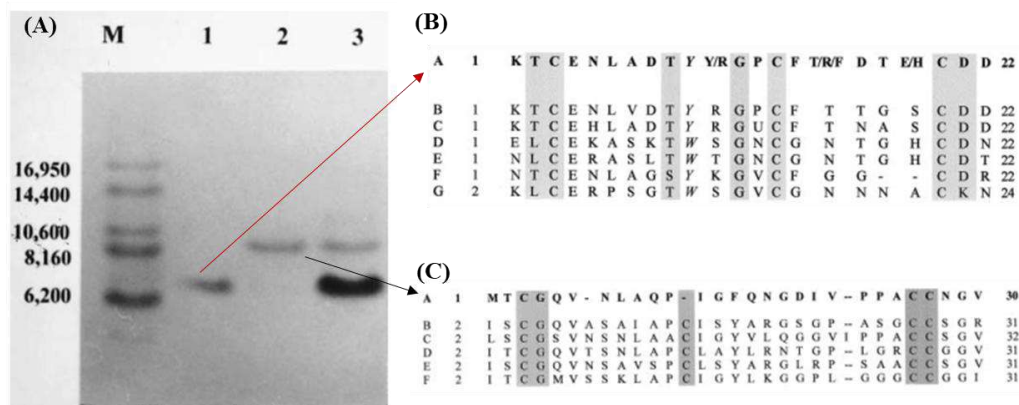


Figura 3. (A) Eletroforese em gel SDS-tricina de peptídeos purificados de sementes de caupi. 1, pico H1 da cromatografia líquida de alta eficiência (HPLC, do inglês *high performance liquid chromatography*); 2, pico H2 da cromatografia HPLC; 3, fração P3 do Sephadex G-50. Os números laterais na raia (M) referem-se a marcadores de massa molecular (Da). (B) Comparação das sequências de aminoácidos de defensinas deduzidas de cDNAs ou sequenciamento de proteínas. Resíduos de cisteína e glicina estão dentro de caixas. (C) Comparação das

seqüências de aminoácidos de proteínas transportadoras de lipídeos deduzidas de cDNAs ou sequenciamento de proteínas. Resíduos de cisteína e glicina estão dentro de caixas.

A defensina isolada foi clonada e a partir de seu cDNA obtido por RT-PCR no qual a seqüência completa do peptídeo foi obtida, recebendo a denominação Vu-Def1 (*Vigna unguiculata defensin one*) (Carvalho et al., 2006) (Figura 4).

```

AAGACGTGCGAGAACCTGGCGGATACATACAGGGGTCCGTGCTTCACCACTGGGAGC
K T C E N L A D T Y R G P C F T T G S

TGCGATGATCACTGCAAGAACAAAGAACACTTGCTGAGTGGCAGGTGCAGGGATGAT
C D D H C K N K E H L L S G R C R D D

GTCCGGTGTGGTGCACCAGAACTGTTAACTGGATTCTCTCCAAACCTAGACAAACG
V R C W C T R N C -

TGCATGCAGGGCATTTTATAAATAAAAACAACCATATATATATATACAATAAGCCTTCT

ACTGCATCTATATATCAACTTTGTACTGTACTATTACTTTTCGTGTCAGAACTATGTGTG

TAGTCTCTGTGACTCTGCATAACAGCAAGCTGAGTTATGCACTTATGAATATATAATC

AATAAAGTTCTTATGAATCAAAAAAAAAAAAAAAAAAAAAAAAAACCGGAATTCCGG

```

Figura 4. A seqüência nucleotídica do fragmento de 401 pb amplificado em RT-PCR usando iniciador desenhado a partir da defensina de sementes de *V. unguiculata* madura sem o peptídeo sinal, e clonado no pCR2.1-TOPO. A seqüência de aminoácidos deduzida de Vu-Def1 é mostrada abaixo da seqüência nucleotídica. O códon de parada é mostrado em negrito. A seqüência amino terminal usada para o desenho do iniciador é mostrada em cinza. (Adaptada de Carvalho et al., 2006, com modificações).

Dando continuidade às pesquisas, a Vu-Def1 foi expressa de forma recombinante e apresentou atividade antimicrobiana significativa contra promastigotas de *Leishmania amazonensis*, um patógeno humano de alta relevância médica (Souza et al., 2013) (Figura 5).

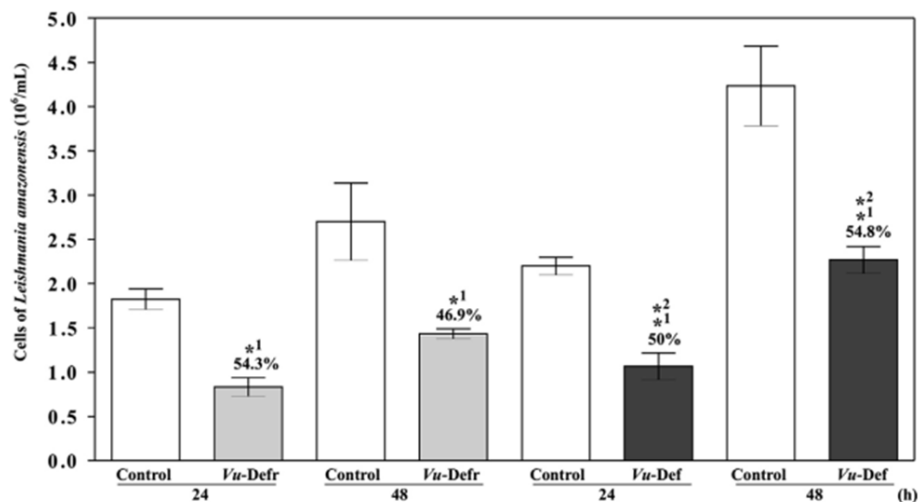


Figura 5. Ensaio de inibição do crescimento de *Leishmania amazonensis* na ausência (controle) e presença de 100 µg/mL de defensinas recombinante (*Vu-Defr*) e natural (*Vu-Def*). O crescimento foi observado após 24 e 48 h. (Adaptada de Souza et al., 2013, com modificações).

Dando continuidade aos estudos, foi projetado um peptídeo baseado na região de alça das fitas $\beta 2$ e $\beta 3$ da defensina *VuDef*₁, correspondente ao γ -core, uma região estrutural altamente conservada em AMPs e associada à sua atividade biológica (Figuras 6A). O γ -core é um elemento estrutural identificado por Yount & Yeaman (2004), que analisaram diversas classes de AMPs e descobriram um padrão comum em sua organização espacial. Eles demonstraram que essa região concentra a atividade biológica dos AMPs e a denominaram γ -core devido à similaridade estrutural com a letra grega " γ ". Para defensinas de plantas, o γ -core possui a fórmula NH₂-[X1-3]-[GXC]-[X3-9]-[C]-COOH, onde X representa qualquer aminoácido (Figuras 6C).

Com base nessas características, o peptídeo projetado contém 15 resíduos de aminoácidos, com a sequência L₃₂SGRARD₃₇D₃₈VRAWATR₄₆, e foi denominado A_{36,42,44} γ ₃₂₋₄₆*Vu-Def*. Nesse nome, A_{36,42,44} refere-se à substituição dos resíduos de cisteína por alanina, uma modificação feita para evitar a formação de pontes dissulfeto indesejadas e eliminar cisteínas livres. Já γ ₃₂₋₄₆ indica a posição correspondente do peptídeo na estrutura primária da *VuDef*₁. Para simplificar, o peptídeo foi abreviado como DD, devido aos dois resíduos adjacentes de ácido aspártico em sua sequência.

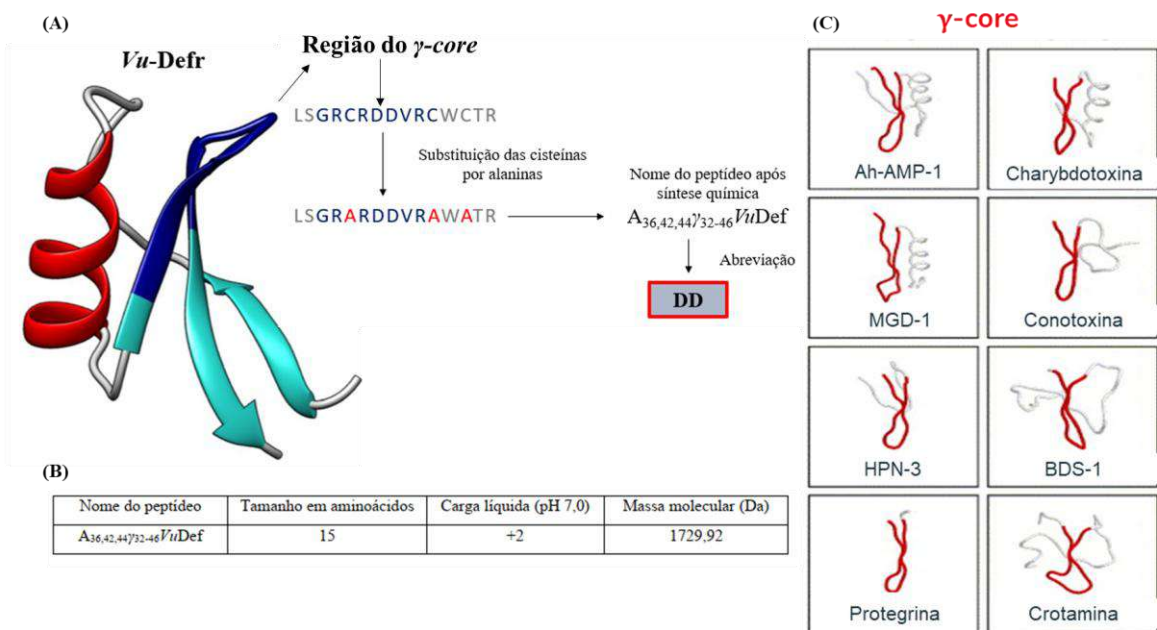


Figura 6. Representação esquemática da estrutura terciária de *Vu-Defr*. (A) Modelo estrutural de *VuDefr* de *Vigna unguiculata*. O cinza representa os elementos não estruturados, o vermelho representa a α -hélices o azul claro representa as folhas β e o azul escuro representa a região do γ -core e sua correspondente estrutura primária da qual

foi derivado do peptídeo $A_{36,42,44}\gamma_{32-46}$ VuDef (DD)(Adaptado de Souza et al., 2019). **(B)** Propriedades químicas do peptídeo sintético DD. **(C)** Representação estrutura terciária de diversos AMPs onde está destacado em vermelho o γ -core. Ah-AMP1 (defensina vegetal isolada de castanhas-da-índia); Charybdotoxina (toxina peptídica derivada do veneno de escorpião); MGD-1 (defensina isolada do mexilhão); Conotoxina (peptídeos neurotóxicos encontrados no veneno dos caramujos); HNP-3 (defensina isolada de neutrófilos humanos); BDS-1 (peptídeo isolado do veneno da anêmona marinha); Protegrina (peptídeo isolado de leucócitos suínos); Crotamina (peptídeo isolado do veneno de cascavel) (Adaptada Yount e Yeaman (2004), com modificações).

O peptídeo DD demonstrou manter sua atividade biológica contra a *L. amazonensis* e teve seu modo de ação parcialmente elucidado (Figura 7). Estudos revelaram que DD atua provocando perturbações na membrana do protozoário, induzindo a produção de espécies reativas de oxigênio (ROS, do inglês *reactive oxygen species*), promovendo a perda do potencial de membrana mitocondrial e desencadeando vias apoptóticas (Souza et al., 2019).

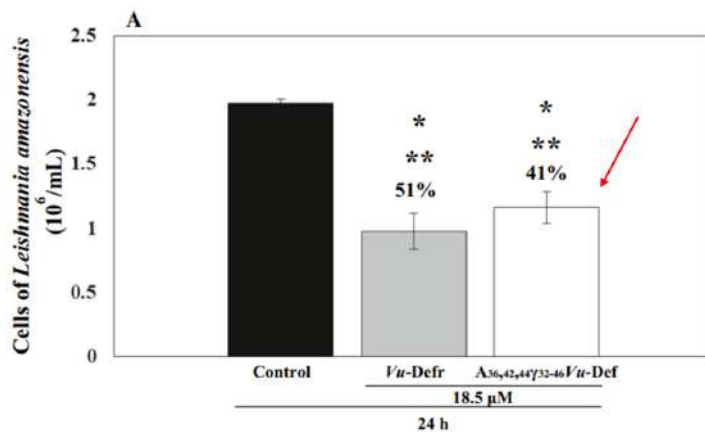


Figura 7. Ensaio de inibição do crescimento de *Leishmania amazonensis* na ausência (controle) e presença de 100 μ g/mL de defensas recombinante (Vu-Defr) e de $A_{36,42,44}\gamma_{32-46}$ Vu-Def (seta vermelha). A porcentagem de inibição do protozoário é mostrada acima das barras (Adaptado de Souza et al.,

2019).

A importância do γ -core se destaca não apenas pela sua função na atividade biológica dos AMPs, mas também por seu potencial no desenvolvimento de novas moléculas bioativas. A compreensão dessa região abre caminho para a criação de peptídeos antimicrobianos sintéticos, com aplicações terapêuticas voltadas ao combate de patógenos fúngicos e protozoários.

Com base nos resultados obtidos para o peptídeo DD em *L. amazonensis*, foi avaliada sua atividade inibitória contra cinco espécies de leveduras de interesse clínico, além da levedura modelo *S. cerevisiae*. No entanto, DD não demonstrou atividade inibitória significativa contra

essas leveduras (Figura 8) (Toledo et al., 2021).

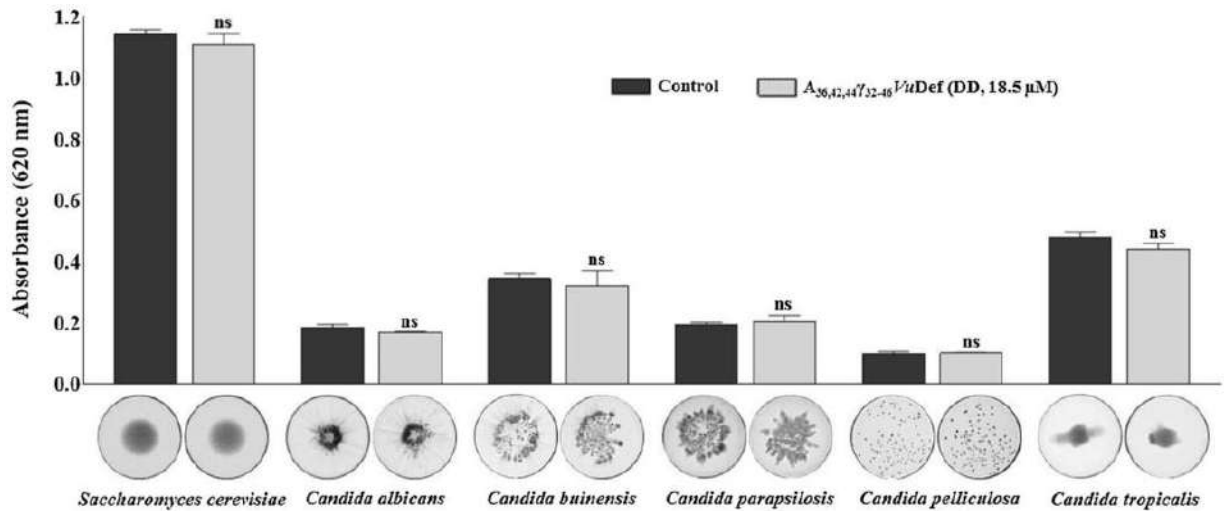


Figura 8: Crescimento das leveduras na ausência (controle) e na presença do peptídeo sintético DD na concentração de 18,5 μM por 24 h. As imagens dos fundos dos poços com o padrão de crescimento de cada espécie de levedura são mostradas abaixo das barras. A imagem é representativa de um ensaio em triplicata. ns = não significativo em relação ao controle (Adaptado de Toledo et al., 2021).

Esse resultado motivou esforços para aprimorar a atividade antifúngica de DD, especialmente contra leveduras, por meio do desenho de novos peptídeos. Para isso, foram realizadas alterações nos parâmetros bioquímicos do peptídeo, envolvendo substituições específicas de aminoácidos. O desenvolvimento desses novos peptídeos foi fundamentado em uma ampla pesquisa em bancos de dados, acompanhada de uma análise detalhada da literatura científica. Esse estudo compilou informações sobre a correlação entre as estruturas primárias de defensinas de plantas, suas atividades biológicas e parâmetros como carga elétrica e hidrofobicidade (Figura 9) (Toledo et al., 2021).

Defensina/nome do peptídeo	Estrutura Primária (Código de uma letra)						Carga Líquida (pH 7,0)	Hidrofobicidade (Kcal/mol)
	1	11	21	31	41	51		
VuDef ₁ A332-42-44Y32-44VuDef (DD)	---KTCENL-	ADTYRGGFCFT	TGSCDDHCKN	KEHLI-SGRC	R-----DDVA	-QWCTRNC	+2	+55,40
RS-AFF ₂	---QKLC-RF-	SGTWGGVCGN	NNACDM-CIR	LEK-ARHG	C-NVFF-AJ	C-CFFFC	+5,6	+34,78
	---QKLC-RF-	SGTWGGVCGN	NNACDM-CIR	LEK-ARHG	C-NVFF-AJ	C-CFFFC	+6,6	+35,74
	---QKLC-RF-	SGTWGGVCGN	NNACDM-CIR	LEK-ARHG	C-NVFF-AJ	C-CFFFC	+5,6	+36,64
	---QKLC-RF-	SGTWGGVCGN	NNACDM-CIR	LEK-ARHG	C-NYRFP-AJ	C-CFFFC	+6,6	+37,05
	---QKLC-RF-	SGTWGGVCGN	NNACDM-CIR	LEK-ARHG	C-NYVMP-AJ	C-CFFFC	+5,6	+35,82
	---QKLC-RF-	SGTWGGVCGN	NNACDM-CIR	LEK-ARHG	C-NYVFA-AJ	C-CFFFC	+5,6	+34,64
	---QKLC-RF-	SGTWGGVCGN	NNACDM-CIR	LEK-ARHG	C-NYVFP-R	C-CFFFC	+6,6	+36,09
	---QKLC-RF-	SGTWGGVCGN	NNACDM-CIR	LEK-ARHG	C-NYVFP-AJ	C-CFFFC	+4,6	+32,75
		M R	RG R	M	R R	W		R IR
	---QKLC-RF-	SGTWGGVCGN	NNACDM-CIR	LEK-ARHG	C-NYVFP-AHK	C-CFFFC	+5,6	+34,78
		M R	RG R	M	R R	W		R IR
								RGFMA R Q
VuDef ₁ A332-42-44Y32-44VuDef (DD)	---KTCENL-	ADTYRGGFCFT	TGSCDDHCKN	KEHLI-SGRC	R-----DDVA	-QWCTRNC	+2	+55,40
PVD ₁	---KTCENL-	ADTYRGGFCFT	TGSCDDHCKN	KEHLIS-GR	R-----DDFR	-AWATR	+2	+21,98 (+20,42)
Y32-44PVD ₁				RS-GR	A-----DFFR	A-ATK	+3,0 (+2,8)	+24,78 (+23,22)
Y31-44PVD ₁ **				RS-GR	A-----DFFR	A-ATK	+7,0 (+2,8)	+21,12 (+23,22)
Y33-44PVD ₁				GR	A-----DFFR	A	+1,0 (+0,9)	+21,05 (+20,01)
Y32-44PVD ₁ **				GR	A-----DFFR	A	+5,0 (+0,9)	+17,39 (+21,05)
VuDef ₁ A332-42-44Y32-44VuDef (DD)	---KTCENL-	ADTYRGGFCFT	TGSCDDHCKN	KEHLI-SGRC	R-----DDVA	-QWCTRNC	+2	+2
MsDef ₁	---KTCENL-	ADKYRGGFCFS	-G-COTFCFT	KENAV-SGR	R-----DDH	C-CTKRC	+2,6	+51,68
NtDef ₁	---KTCENL-	PKKFFGGFCAS	DHCAS-CQT	-ERFS-GGR	R--G--FRFR	C-CTKRC	+5,8	+49,16
MsDef1-R14Q	---KTCENL-	ADKYRGGFCFS	-G-COTFCFT	KENAV-SGR	R-----DDH	C-CTKRC	+1,6	+50,64
MsDef1-V4	---KTCENL-	ADKYRGGFCFS	-G-COTFCFT	KENAV-SGR	R--G--FRFR	C-CTKRC	+6,6	+49,17
GMA ₁				GR	R-----DDFR	C	+0,9 (+0,9)	+20,01 (+20,01)
GMA ₁ -L				GR	R--G--FRFR	C	+4,9 (+4,9)	+17,50 (+17,01)
GMA ₁ -L				R--G--FRFR	R--G--FRFR	C	0 (0)	+17,09 (+17,09)
GMA ₁ -L1				R--G--FRFR	R--G--FRFR	C	+4,0 (+4,0)	+14,58 (+14,58)
GMA ₁ -L2				R--G--FRFR	R--G--FRFR	C	+4,0 (+4,0)	+16,79 (+14,58)
GMA ₁ -C				GR	R-----DDFR	C-CTKRC	+3,0 (+4,0)	+13,27 (+14,58)
GMA ₁ -C				GR	R--G--FRFR	C-CTKRC	+2,7 (+2,7)	+22,74 (+22,74)
				GR	R--G--FRFR	C-CTKRC	+4,8 (+4,8)	+19,73 (+19,73)
VuDef ₁ A332-42-44Y32-44VuDef (DD)	---KTCENL-	ADTYRGGFCFT	TGSCDDHCKN	KEHLI-SGRC	R-----DDVA	-QWCTRNC	+2	+2
SPE10	---KTCENL-	ADTYRGGFCFT	DGSCDDHCKN	KEHLI-RGR	R-----DDVA	-AWATR	+0,7	+59,01
	---KTCENL-	ADTYRGGFCFT	DGSCDDHCKN	KEHLI-RGR	R-----DDVA	-QWCTRNC	+1,7	+56,22
	---KTCENL-	ADTYRGGFCFT	DGSCDDHCKN	KEHLI-RGR	R-----DDVA	-QWCTRNC	+0,7	+61,57

Figura 9: Comparação das estruturas primárias de Vu-Def₁ e DD com algumas das defensinas que relataram a correlação entre a estrutura primária e a atividade biológica. Os quadrados azuis indicam alguns aminoácidos que foram importantes para as atividades biológicas das defensinas e que foram selecionados para alterações direcionadas em DD (Adaptado de Toledo et al., 2021).

Com base nessa análise, foram projetados três novos peptídeos, com modificações direcionadas para otimizar a carga, aumentar a hidrofobicidade e ajustar a quiralidade, visando maximizar sua eficácia antifúngica (Figura 10) (Toledo et al., 2021).

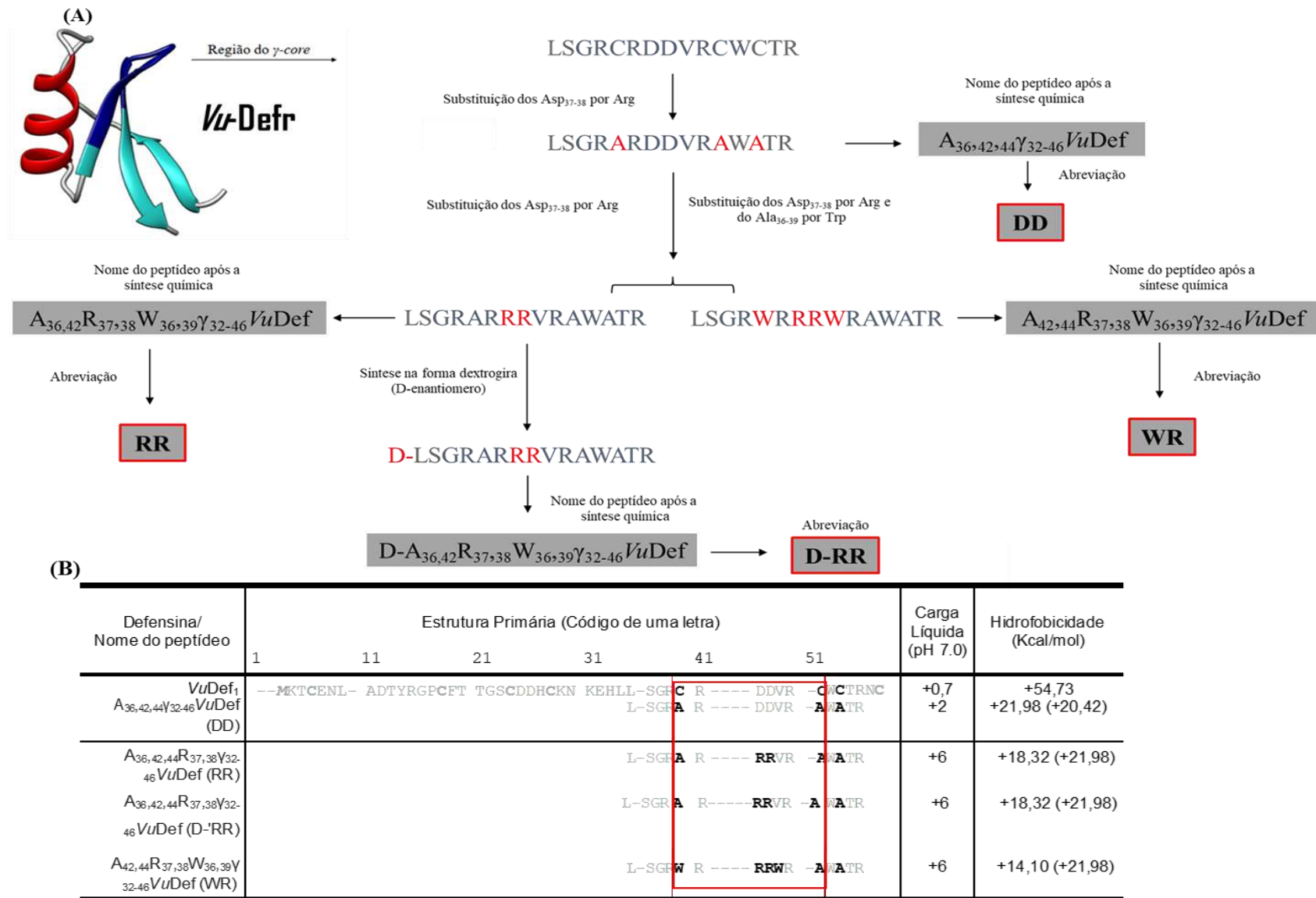


Figura 10: (A) Estrutura primária e modificações de *VuDef*₁ para a bioinspiração dos peptídeos DD, RR e WR. (B) Tabela demonstrativa das estruturas primárias e propriedades físico-químicas em cinza escuro está indicada a metionina inicial, cinza claro os demais resíduos de aminoácidos, preto os resíduos de interesse, a caixa vermelha indica a posição do γ -core (Adaptado de Toledo et al., 2021).

O peptídeo denominado como $A_{36,42,44}R_{37,38}\gamma_{32-46}Vu$ -Def abreviado como RR, teve como mudança troca de dois aminoácidos carregados negativamente, ácido aspártico (Asp), nas posições 37 e 38 por duas argininas (Arg). Esta troca o que fez com que a carga líquida de RR aumentasse de +2 para +6, e sua hidrofobicidade aumentasse de +21.98 para +18.32 kcal/mol (hidrofobicidade calculada de acordo com a escala de *Wimley-White* que quanto maior o valor positivo, mais hidrofílico é o peptídeo, e inversamente, maior valor negativo, mais hidrofóbico é o peptídeo). O peptídeo $D-A_{36,42,44}R_{37,38}\gamma_{32-46}Vu$ -Def (com o prefixo D- indicando a mudança na quiralidade), abreviado como D-RR, diferencia-se do RR pela utilização de aminoácidos em sua forma dextrogira (D-enantiômeros). Essa modificação foi realizada com base em estudos que apontam que aminoácidos na configuração D podem conferir maior resistência a ações enzimáticas, preservando a atividade antimicrobiana do peptídeo. Além disso, peptídeos contendo D-enantiômeros geralmente apresentam menor toxicidade para células de mamíferos, tornando-os alternativas promissoras para aplicações terapêuticas (Zhu et al., 2007; Matsuzaki, 2009; Toledo et al., 2021). O peptídeo $A_{36,42,44}R_{37,38}W_{36,40}\gamma_{32-46}Vu$ Def, apelidado de WR, foi projetado com o objetivo de aumentar sua hidrofobicidade em comparação ao peptídeo RR. Para isso, as substituições dos resíduos alanina na posição 36 (A36) e valina na posição 40 (V40) por triptofano (W), um aminoácido aromático, foram realizadas. Essas alterações, resultaram em um aumento significativo na hidrofobicidade do peptídeo WR, que apresentou um valor de +14,10 kcal/mol, em comparação a RR (+18,32 kcal/mol) e DD (+21,98 kcal/mol). A maior hidrofobicidade pode estar associada a uma interação mais eficiente com membranas biológicas, contribuindo para a atividade antimicrobiana do peptídeo (Toledo et al., 2021).

Os resultados obtidos nos ensaios antimicrobianos demonstraram que as modificações direcionadas nos resíduos de aminoácidos foram eficazes em melhorar a atividade antifúngica dos peptídeos RR, D-RR e WR, em comparação ao peptídeo DD (Figura 11). As alterações estratégicas na carga, hidrofobicidade e quiralidade foram fundamentais para potencializar a interação dos peptídeos com as células fúngicas, refletindo em um desempenho superior nos testes realizados (Toledo et al., 2021).

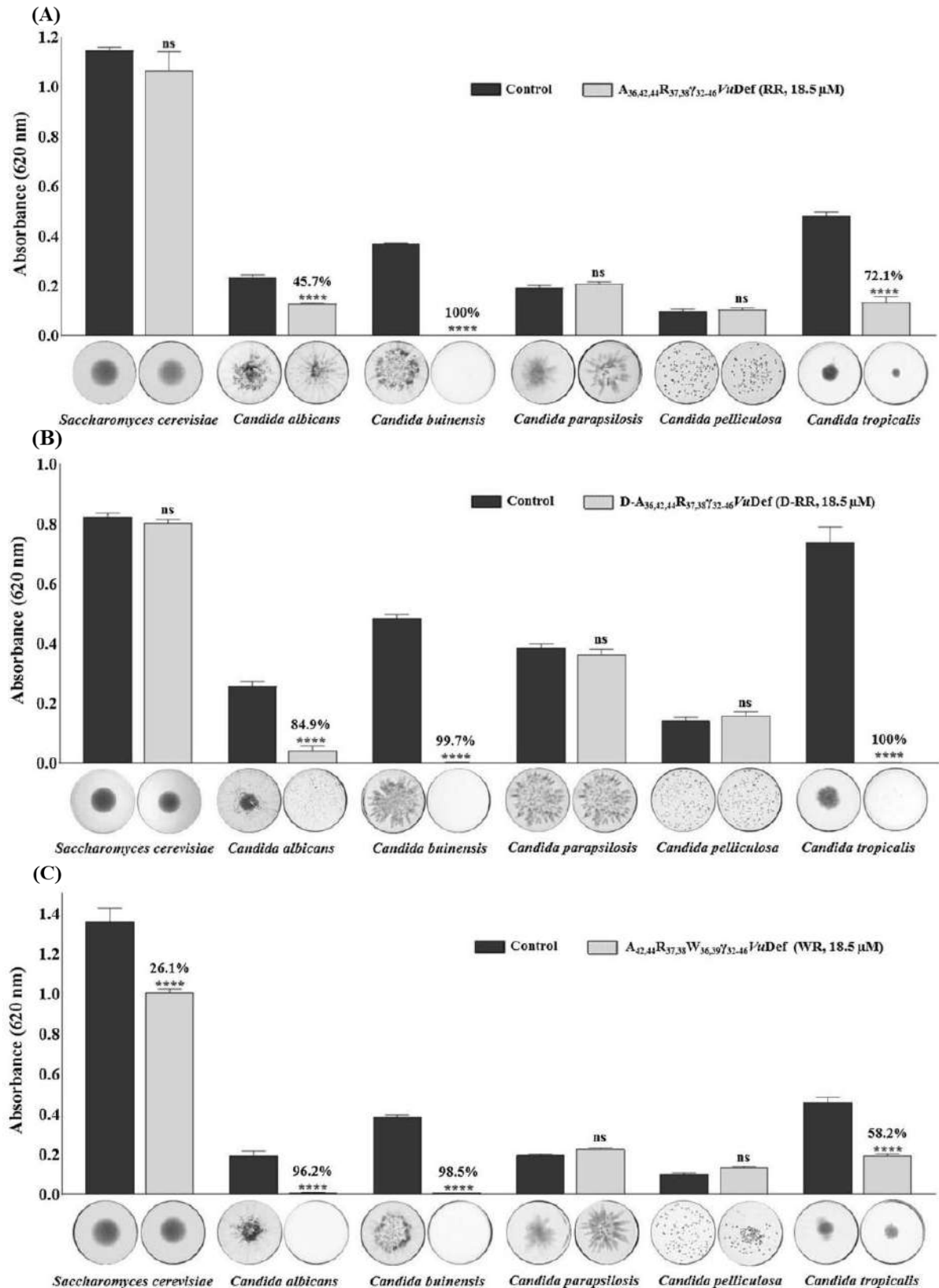


Figura 11: Crescimento das leveduras na ausência (controle) e na presença dos peptídeos sintéticos RR (A), D-RR (B) e WR (C) na concentração de 18,5 μ M por 24 h. As imagens dos fundos dos poços com o padrão de crescimento de cada espécie de levedura são mostradas abaixo das barras. A imagem é representativa de um ensaio em triplicata. ns = não significativo em relação ao controle (Adaptado de Toledo et al., 2021).

1.3 Relevância do Estudo para *Candida* spp. como Alvo Terapêutico

Os resultados obtidos com os peptídeos bioinspirados RR, D-RR e WR evidenciam seu potencial como agentes antifúngicos eficazes, especialmente contra *Candida tropicalis* e *Candida albicans* (Figura 11), espécies amplamente reconhecidas por seu papel como patógenos oportunistas. Infecções fúngicas causadas por *Candida* spp. representam um desafio significativo para a saúde pública, devido à sua elevada morbimortalidade, principalmente em pacientes imunocomprometidos, e à crescente resistência aos antifúngicos convencionais (Stewart & Paterson, 2021; WHO, 2022; Denning, 2024; Thambugala et al., 2024)

Entre as espécies do gênero *Candida*, *C. albicans* é a mais prevalente em infecções sistêmicas e mucocutâneas, enquanto a *C. tropicalis* se destaca como uma das principais causas de candidemia, especialmente em ambientes hospitalares. Reconhecendo a gravidade dessas infecções e a crescente resistência antifúngica, a Organização Mundial da Saúde (OMS) incluiu *C. albicans* e *C. tropicalis* em sua lista de patógenos fúngicos prioritários. *C. albicans* foi classificada no grupo de prioridade crítica, enquanto *C. tropicalis* foi incluída no grupo de alta prioridade. Além disso, ambas apresentam mecanismos adaptativos, como a formação de biofilmes, mecanismos de efluxo, alterações na parede celular, alterações na síntese de ergosterol e modificações na via da calcineurina e também na integridade da parede celular, que dificultam o tratamento e aumentam a resistência aos medicamentos. Evidenciando a urgência em desenvolver novas abordagens terapêuticas para o controle dessas espécies (Fernández de Ullivarri et al., 2020; WHO, 2022; Gow et al., 2022; Lockhart et al., 2023; Thambugala et al., 2024).

Nesse contexto, a busca por novas terapias que combinem eficácia, especificidade e segurança é fundamental para superar essas limitações e ampliar as opções terapêuticas. A relevância do estudo de *Candida* spp. como alvo terapêutico está diretamente ligada à necessidade de compreender os mecanismos de ação dos novos peptídeos bioinspirados e avaliar sua eficácia no combate a essas espécies. Assim, a caracterização detalhada da atividade dos peptídeos RR, D-RR e WR contra *C. albicans* e *C. tropicalis* não apenas fortalece seu potencial como alternativas terapêuticas promissoras, mas também contribui para a ampliação do conhecimento sobre as interações entre os AMPs e os fungos-alvo. Essa investigação é crucial para o desenvolvimento de abordagens mais eficazes e direcionadas no tratamento de infecções fúngicas.

1.4 Modo de Ação de Peptídeos Antifúngicos

No campo da biotecnologia e medicina, compreender os mecanismos pelos quais moléculas bioativas exercem seus efeitos é fundamental para o desenvolvimento de terapias inovadoras, mais eficazes e seguras. Os peptídeos bioinspirados têm se destacado como agentes antimicrobianos promissores, com diversas estratégias de ação descritas, incluindo a desestabilização de membranas celulares, a geração de ROS e a indução de processos intracelulares que levam à inibição do crescimento ou morte das células microbianas (Souza et al., 2019; Parisi et al., 2019).

Esforços significativos têm sido direcionados à identificação, em nível molecular, dos processos e vias de sinalização ativadas por esses peptídeos. Além de ampliar o entendimento de seus modos de ação, essas investigações têm permitido o desenvolvimento de novas moléculas bioativas com maior especificidade e menor toxicidade. Esse conhecimento é crucial para explorar o potencial dos peptídeos como terapias antifúngicas eficazes, especialmente diante da necessidade de mais estudos sobre a relação entre estrutura e mecanismos de ação (Koehbach & Craik, 2019; Toledo et al., 2021).

Nesse contexto, os peptídeos antifúngicos apresentam uma diversidade de modos de ação, desde interações diretas com a membrana celular até processos intracelulares complexos. Por exemplo, o peptídeo LfcinB15 (derivado da lactoferrina bovina) apresenta um modo de ação multifacetado contra *C. albicans*. Inicialmente, liga-se à membrana celular, promovendo sua perturbação, seguido de internalização. Uma vez dentro da célula, pode ser encontrado nos vacúolos e induz a geração de ROS, causando disfunção mitocondrial, perda do potencial de membrana mitocondrial e bloqueio da respiração celular. No entanto, o mecanismo exato de entrada do peptídeo ainda não foi elucidado (Chang et al., 2021).

De forma semelhante, o peptídeo sintético PuroA (baseado no domínio rico em triptofano da puroindolina A do trigo) também atua contra *C. albicans*. Após ligação em um ponto específico da membrana, transloca-se para o citoplasma, onde atinge alvos intracelulares, como o DNA. Esse processo é seguido por ruptura da membrana plasmática entre 25 e 45 min de incubação (Shagaghi et al., 2017).

Já o peptídeo Histatina-5 (um AMP presente na saliva humana) apresenta um modo dependente da concentração. Em baixas concentrações, é internalizado por endocitose e direcionado aos vacúolos, enquanto sua ação letal ocorre apenas após translocação direta para o citoplasma, mediada possivelmente por transportadores. Esse processo causa desbalanço iônico devido ao efluxo de íons, levando à morte celular (Mochon & Liu, 2008; Jang et al., 2010; Kumar et al., 2011).

As defensinas vegetais também têm sido amplamente investigadas. A NaD1 (defensina da planta *Nicotiana glauca*) é internalizada por um processo dependente de energia, sugerido como endocitose, e sua internalização está associada à geração de ROS, permeabilização de membrana e morte celular (Hayes et al., 2018). Modos semelhantes foram descritos para outras defensinas, como a MtDef4 (*Medicago truncatula*) em *Neurospora crassa* (El-Mounadi et al., 2016) e da proteína antifúngica PAF (*Penicillium chrysogenum*) em *Aspergillus nidulans* (Oberparleiter et al., 2003).

Compreender os modos de ação dos AMPs bioinspirados é essencial por várias razões: (1) facilita seu uso como agentes antimicrobianos; (2) identifica possíveis alvos terapêuticos para infecções fúngicas; (3) permite modificações racionais que aumentem sua estabilidade e reduzam a toxicidade em células não-alvo; e (4) aprimora a escolha de estratégias para direcionar os peptídeos ao local de ação (Soares et al., 2017). A relevância médica desses peptídeos impulsiona investigações contínuas sobre seus mecanismos, já que muitos aspectos de sua atuação sobre células-alvo ainda permanecem pouco esclarecidos.

Este documento de tese está estruturado em três capítulos que se referem a três manuscritos científicos elaborados durante o período de doutoramento. Cada capítulo corresponde a um manuscrito completo. No término da tese, são expostas as principais conclusões do estudo.

O Capítulo 1 aborda os diferentes mecanismos de morte celular induzidos pelos peptídeos bioinspirados em leveduras oportunistas. Os dados sobre a cinética de morte, análise morfológica e avaliação da produção de espécies reativas de oxigênio (ROS) foram obtidos durante o meu mestrado. Os experimentos relacionados ao peptídeo WR foram conduzidos durante o doutorado do Dr. Filipe Zaniratti Damica, enquanto os dados referentes aos peptídeos RR e D-RR foram obtidos por mim.

O Capítulo 2 explora o papel do K^+ intracelular na proteção de fungos dimórficos patogênicos contra a morte celular induzida por peptídeos antimicrobianos bioinspirados. Parte dos dados sobre o peptídeo WR foi gerada no doutorado do Dr. Filipe Zaniratti Damica. Já os experimentos com os peptídeos RR e D-RR foram inteiramente conduzidos por mim, assim como as análises de zimografia e microscopia eletrônica de transmissão (MET) para WR.

O Capítulo 3 investiga o mecanismo de internalização dependente de energia, a localização citoplasmática e o impacto dos peptídeos na ultraestrutura fúngica. Parte dos resultados relacionados ao peptídeo WR foi obtida durante o doutorado do Dr. Filipe Zaniratti Damica. Os dados sobre os peptídeos RR e D-RR foram integralmente obtidos por mim, incluindo as análises de microscopia confocal, MET, microscopia eletrônica de varredura e

DNA shift para WR.

2. REFERÊNCIAS

- Bin Hafeez, A., Jiang, X., Bergen, P. J., & Zhu, Y. (2021). Antimicrobial peptides: An update on classifications and databases. *International Journal of Molecular Sciences*, 22(21), 11691. <https://doi.org/10.3390/ijms222111691>
- Brogden, N. K., & Brogden, K. A. (2011). Will new generations of modified antimicrobial peptides improve their potential as pharmaceuticals? *International Journal of Antimicrobial Agents*. <https://doi.org/10.1016/j.ijantimicag.2011.05.004>
- Brunet, K., Verdon, J., Ladram, A., Arnault, S., Rodier, M.-H., & Cateau, E. (2022). Antifungal activity of [K³]temporin-SHa against medically relevant yeasts and moulds. *Canadian Journal of Microbiology*, 68(6), 427–434. <https://doi.org/10.1139/cjm-2021-0250>
- Campoy, S., & Adrio, J. L. (2017). Antifungals. *Biochemical Pharmacology*, 133, 86–96. <https://doi.org/10.1016/j.bcp.2016.11.019>
- Carvalho, A. de O., & Gomes, V. M. (2009). Plant defensins—Prospects for the biological functions and biotechnological properties. *Peptides*, 30(5), 1007–1020. <https://doi.org/10.1016/j.peptides.2009.01.018>
- Carvalho, A. O., Machado, O. L. T., Da Cunha, M., Santos, I. S., & Gomes, V. M. (2001). Antimicrobial peptides and immunolocalization of a LTPin *Vigna unguiculata* seeds. *Plant Physiology and Biochemistry*, 39(2), 137–146. [https://doi.org/10.1016/s0981-9428\(00\)01230-4](https://doi.org/10.1016/s0981-9428(00)01230-4)
- Carvalho, A., S. Filho, G., Ferreira, B., Branco, A., Okorokova-Facanha, A., & Gomes, V. (2006). Cloning and characterization of a cDNA encoding a Cowpea seed defensin and analysis of its expression. *Protein and Peptide Letters*, 13(10), 1029–1036. <https://doi.org/10.2174/092986606778777515>
- Cary, J. W., Rajasekaran, K., Jaynes, J. M., & Cleveland, T. E. (2000). Transgenic expression of a gene encoding a synthetic antimicrobial peptide results in inhibition of fungal growth in vitro and in planta. *Plant Science: An International Journal of Experimental Plant Biology*, 154(2), 171–181. [https://doi.org/10.1016/s0168-9452\(00\)00189-8](https://doi.org/10.1016/s0168-9452(00)00189-8)
- Casadevall, A., Kontoyiannis, D. P., & Robert, V. (2021). Environmental *Candida auris* and the global warming emergence hypothesis. *mBio*, 12(2). <https://doi.org/10.1128/mbio.00360-21>

- Chang, C.-K., Kao, M.-C., & Lan, C.-Y. (2021). Antimicrobial Activity of the Peptide LfcinB15 against *Candida albicans*. *Journal of Fungi (Basel, Switzerland)*, 7(7), 519. <https://doi.org/10.3390/jof7070519>
- de Crecy, E., Jaronski, S., Lyons, B., Lyons, T. J., & Keyhani, N. O. (2009). Directed evolution of a filamentous fungus for thermotolerance. *BMC Biotechnology*, 9(1). <https://doi.org/10.1186/1472-6750-9-74>
- de Oliveira Carvalho, A., & Moreira Gomes, V. (2011). Plant defensins and defensin-like peptides - biological activities and biotechnological applications. *Current Pharmaceutical Design*, 17(38), 4270–4293. <https://doi.org/10.2174/138161211798999447>
- Denning, D. W. (2024). Global incidence and mortality of severe fungal disease. *The Lancet Infectious Diseases*, 24(7), e428–e438. [https://doi.org/10.1016/s1473-3099\(23\)00692-8](https://doi.org/10.1016/s1473-3099(23)00692-8)
- El-Mounadi, K., Islam, K. T., Hernández-Ortiz, P., Read, N. D., & Shah, D. M. (2016). Antifungal mechanisms of a plant defensin MtDef4 are not conserved between the ascomycete fungi *Neurospora crassa* and *Fusarium graminearum*. *Molecular Microbiology*, 100(3), 542–559. <https://doi.org/10.1111/mmi.13333>
- Fernández de Ullivarri, M., Arbulu, S., Garcia-Gutierrez, E., & Cotter, P. D. (2020). Antifungal Peptides as Therapeutic Agents. *Frontiers in cellular and infection microbiology*, 10. <https://doi.org/10.3389/fcimb.2020.00105>
- Fisher, M. C., Alastruey-Izquierdo, A., Berman, J., Bicanic, T., Bignell, E. M., Bowyer, P., Bromley, M., Brüggemann, R., Garber, G., Cornely, O. A., Gurr, S. J., Harrison, T. S., Kuijper, E., Rhodes, J., Sheppard, D. C., Warris, A., White, P. L., Xu, J., Zwaan, B., & Verweij, P. E. (2022). Tackling the emerging threat of antifungal resistance to human health. *Nature Reviews. Microbiology*, 20(9), 557–571. <https://doi.org/10.1038/s41579-022-00720-1>
- Gentilucci, L., Tosi, P., Bauer, A., & De Marco, R. (2016). Modern tools for the chemical ligation and synthesis of modified peptides and proteins. *Future Medicinal Chemistry*, 8(18), 2287–2304. <https://doi.org/10.4155/fmc-2016-0175>
- Gow, N. A. R., Johnson, C., Berman, J., Coste, A. T., Cuomo, C. A., Perlin, D. S., Bicanic, T., Harrison, T. S., Wiederhold, N., Bromley, M., Chiller, T., & Edgar, K. (2022). The importance of antimicrobial resistance in medical mycology. *Nature Communications*, 13(1), 1–12. <https://doi.org/10.1038/s41467-022-32249-5>
- Guinea, J., Sánchez-Somolinos, M., Cuevas, O., Peláez, T., & Bouza, E. (2006). Fluconazole resistance mechanisms in *Candida krusei*: The contribution of efflux-pumps. *Medical*

- Mycology: Official Publication of the International Society for Human and Animal Mycology*, 44(6), 575–578. <https://doi.org/10.1080/13693780600561544>
- Hayes, B., Bleackley, M., Anderson, M., & Van der Weerden, N. (2018). The plant defensin NaD1 enters the cytoplasm of candida albicans via endocytosis. *Journal of Fungi (Basel, Switzerland)*, 4(1), 20. <https://doi.org/10.3390/jof4010020>
- Huan, Y., Kong, Q., Mou, H., & Yi, H. (2020). Antimicrobial peptides: Classification, design, application and research progress in multiple fields. *Frontiers in microbiology*, 11. <https://doi.org/10.3389/fmicb.2020.582779>
- Jang, W. S., Bajwa, J. S., Sun, J. N., & Edgerton, M. (2010). Salivary histatin 5 internalization by translocation, but not endocytosis, is required for fungicidal activity in *Candida albicans*. *Molecular Microbiology*, 77(2), 354–370. <https://doi.org/10.1111/j.1365-2958.2010.07210.x>
- Koehbach, J., & Craik, D. J. (2019). The vast structural diversity of antimicrobial peptides. *Trends in Pharmacological Sciences*, 40(7), 517–528. <https://doi.org/10.1016/j.tips.2019.04.012>
- Kumar, R., Chadha, S., Saraswat, D., Bajwa, J. S., Li, R. A., Conti, H. R., & Edgerton, M. (2011). Histatin 5 uptake by candida albicans utilizes polyamine transporters Dur3 and Dur31 proteins. *The Journal of Biological Chemistry*, 286(51), 43748–43758. <https://doi.org/10.1074/jbc.m111.311175>
- Lockhart, S. R., Chowdhary, A., & Gold, J. A. W. (2023). The rapid emergence of antifungal-resistant human-pathogenic fungi. *Nature Reviews. Microbiology*, 21(12), 818–832. <https://doi.org/10.1038/s41579-023-00960-9>
- Luong, H. X., Thanh, T. T., & Tran, T. H. (2020). Antimicrobial peptides – Advances in development of therapeutic applications. *Life Sciences*, 260(118407), 118407. <https://doi.org/10.1016/j.lfs.2020.118407>
- Matsuzaki, K. (2009). Control of cell selectivity of antimicrobial peptides. *Biochimica et Biophysica Acta. Biomembranes*, 1788(8), 1687–1692. <https://doi.org/10.1016/j.bbamem.2008.09.013>
- Mochon, A. B., & Liu, H. (2008). The antimicrobial peptide histatin-5 causes a spatially restricted disruption on the candida albicans surface, allowing rapid entry of the peptide into the cytoplasm. *PLoS Pathogens*, 4(10), e1000190. <https://doi.org/10.1371/journal.ppat.1000190>
- Nnadi, N. E., & Carter, D. A. (2021). Climate change and the emergence of fungal pathogens. *PLoS Pathogens*, 17(4), e1009503. <https://doi.org/10.1371/journal.ppat.1009503>

- Oberparleiter, C., Kaiserer, L., Haas, H., Ladurner, P., Andratsch, M., & Marx, F. (2003). Active internalization of the *Penicillium chrysogenum* antifungal protein PAF in sensitive aspergilli. *Antimicrobial Agents and Chemotherapy*, 47(11), 3598–3601. <https://doi.org/10.1128/aac.47.11.3598-3601.2003>
- Parisi, K., Shafee, T. M. A., Quimbar, P., van der Weerden, N. L., Bleackley, M. R., & Anderson, M. A. (2019). The evolution, function and mechanisms of action for plant defensins. *Seminars in Cell & Developmental Biology*, 88, 107–118. <https://doi.org/10.1016/j.semcd.2018.02.004>
- Răileanu, M., Borlan, R., Campu, A., Janosi, L., Turcu, I., Focsan, M., & Bacalum, M. (2023). No country for old antibiotics! Antimicrobial peptides (AMPs) as next-generation treatment for skin and soft tissue infection. *International Journal of Pharmaceutics*, 642(123169), 123169. <https://doi.org/10.1016/j.ijpharm.2023.123169>
- Rajasekaran, K., Cary, J. W., Chlan, C. A., Jaynes, J. M., & Bhatnagar, D. (2012). Strategies for controlling plant diseases and mycotoxin contamination using antimicrobial synthetic peptides. In *ACS Symposium Series* (p. 295–315). American Chemical Society.
- Rajasekaran, Kanniah, Sayler, R. J., Sickler, C. M., Majumdar, R., Jaynes, J. M., & Cary, J. W. (2018). Control of *Aspergillus flavus* growth and aflatoxin production in transgenic maize kernels expressing a tachyplesin-derived synthetic peptide, AGM182. *Plant Science: An International Journal of Experimental Plant Biology*, 270, 150–156. <https://doi.org/10.1016/j.plantsci.2018.02.006>
- Shagaghi, N., Bhave, M., Palombo, E. A., & Clayton, A. H. A. (2017). Revealing the sequence of interactions of PuroA peptide with *Candida albicans* cells by live-cell imaging. *Scientific Reports*, 7(1). <https://doi.org/10.1038/srep43542>
- Soares, J. R., José Tenório de Melo, E., da Cunha, M., Fernandes, K. V. S., Taveira, G. B., da Silva Pereira, L., Pimenta, S., Trindade, F. G., Regente, M., Pinedo, M., de la Canal, L., Gomes, V. M., & de Oliveira Carvalho, A. (2017). Interaction between the plant ApDef1 defensin and *Saccharomyces cerevisiae* results in yeast death through a cell cycle- and caspase-dependent process occurring via uncontrolled oxidative stress. *Biochimica et Biophysica Acta. General Subjects*, 1861(1), 3429–3443. <https://doi.org/10.1016/j.bbagen.2016.09.005>
- Souza, G. S., de Carvalho, L. P., de Melo, E. J. T., da Silva, F. C. V., Machado, O. L. T., Gomes, V. M., & de Oliveira Carvalho, A. (2019). A synthetic peptide derived of the β 2– β 3 loop of the plant defensin from *Vigna unguiculata* seeds induces *Leishmania amazonensis*

- apoptosis-like cell death. *Amino Acids*, 51(10–12), 1633–1648. <https://doi.org/10.1007/s00726-019-02800-8>
- Souza, G. S., do Nascimento, V. V., de Carvalho, L. P., de Melo, E. J. T., Fernandes, K. V., Machado, O. L. T., Retamal, C. A., Gomes, V. M., & Carvalho, A. de O. (2013). Activity of recombinant and natural defensins from *Vigna unguiculata* seeds against *Leishmania amazonensis*. *Experimental Parasitology*, 135(1), 116–125. <https://doi.org/10.1016/j.exppara.2013.06.005>
- Stewart, A. G., & Paterson, D. L. (2021). How urgent is the need for new antifungals? *Expert Opinion on Pharmacotherapy*, 22(14), 1857–1870. <https://doi.org/10.1080/14656566.2021.1935868>
- Strickland, A. B., & Shi, M. (2021). Mechanisms of fungal dissemination. *Cellular and Molecular Life Sciences: CMLS*, 78(7), 3219–3238. <https://doi.org/10.1007/s00018-020-03736-z>
- Thambugala, K. M., Daranagama, D. A., Tennakoon, D. S., Jayatunga, D. P. W., Hongsanan, S., & Xie, N. (2024). Humans vs. Fungi: An overview of fungal pathogens against humans. *Pathogens*, 13(5), 426. <https://doi.org/10.3390/pathogens13050426>
- Toledo, E. B., Lucas, D. R., Simão, T. L. B. V., Calixto, S. D., Lassounskaia, E., Muzitano, M. F., Damica, F. Z., Gomes, V. M., & de Oliveira Carvalho, A. (2021). Design of improved synthetic antifungal peptides with targeted variations in charge, hydrophobicity and chirality based on a correlation study between biological activity and primary structure of plant defensin γ -cores. *Amino Acids*, 53(2), 219–237. <https://doi.org/10.1007/s00726-020-02929-x>
- Torres, M. D. T., Sothiselvam, S., Lu, T. K., & de la Fuente-Nunez, C. (2019). Peptide design principles for antimicrobial applications. *Journal of Molecular Biology*, 431(18), 3547–3567. <https://doi.org/10.1016/j.jmb.2018.12.015>
- WHO fungal priority pathogens list to guide research, development and public health action.* (2022, outubro 25). Who.int; World Health Organization. <https://www.who.int/publications/i/item/9789240060241>
- Yount, N. Y., & Yeaman, M. R. (2004). Multidimensional signatures in antimicrobial peptides. *Proceedings of the National Academy of Sciences of the United States of America*, 101(19), 7363–7368. <https://doi.org/10.1073/pnas.0401567101>
- Zhong, C., Zhu, N., Zhu, Y., Liu, T., Gou, S., Xie, J., Yao, J., & Ni, J. (2020). Antimicrobial peptides conjugated with fatty acids on the side chain of D-amino acid promises antimicrobial potency against multidrug-resistant bacteria. *European Journal of*

Pharmaceutical Sciences: Official Journal of the European Federation for Pharmaceutical Sciences, 141(105123), 105123.

<https://doi.org/10.1016/j.ejps.2019.105123>

Zhu, W. L., Nan, Y. H., Hahm, K.-S., & Shin, S.-Y. (2007). Cell selectivity of an antimicrobial peptide melittin diastereomer with D-amino acid in the leucine zipper sequence. *BMB Reports*, 40(6), 1090–1094. <https://doi.org/10.5483/bmbrep.2007.40.6.1090>

([S.d.]). Gaffi.org. Recuperado 26 de janeiro de 2025, de <https://www.gaffi.org/why/fungal-disease-frequency/>.

3-OBJETIVOS

3- OBJETIVOS

3.1 Objetivo Geral

Estudar a interação e o modo de ação dos peptídeos sintéticos $A_{36,42,44}R_{37,38}\gamma_{32-46}Vu$ -Def (RR) e $D-A_{36,42,44}R_{37,38}\gamma_{32-46}Vu$ -Def (D-RR) sobre células de *Candida tropicalis*, e $A_{36,42,44}R_{37,38}W_{36,40}\gamma_{32-46}Vu$ Def (WR) sobre células de *Candida albicans*.

3.2 Objetivos Específicos

- Avaliar as alterações morfológicas e a ultra estruturais induzidas pelos peptídeos em leveduras, incluindo redução no tamanho celular, condensação de cromatina e danos observados por microscopia eletrônica de transmissão e varredura.
- Analisar a funcionalidade mitocondrial em leveduras expostas aos peptídeos, com ênfase na hiperpolarização mitocondrial e na produção de espécies reativas de oxigênio (ROS);
- Identificar os processos de morte celular desencadeados pelos peptídeos, incluindo a ativação de metacaspases, a cinética de morte celular e a caracterização do tipo de morte (programada ou acidental) para cada levedura e peptídeo;
- Verificar o papel de ROS na toxicidade dos peptídeos utilizando antioxidantes;
- Investigar o papel do efluxo de K^+ no encolhimento celular e sua contribuição para a morte fúngica induzida pelos peptídeos;
- Avaliar os efeitos dos peptídeos em processos celulares como estresse oxidativo, hiperpolarização mitocondrial, permeabilização de membrana, acidificação do meio e degradação celular;
- Estudar a interação dos peptídeos, com a membrana celular das leveduras por meio do potencial de membrana, baixa temperatura, inibidor de endocitose e transportadores de poliamina;
- Estimar seletividade dos peptídeos frente às células de mamíferos da linhagem LLC-MK2.

4- CAPÍTULO 1

Bioinspired peptides induce different cell death mechanisms against opportunistic yeasts

4. CHAPTER 1: MANUSCRIPT PUBLISHED

Bioinspired peptides induce different cell death mechanisms against opportunistic yeasts

Douglas Ribeiro Lucas^{a,1}, Filipe Zaniratti Damica^{a,1}, Estefany Braz Toledo^{a,1}, Antônio Jesus Dorighetto Cogo^a, Anna Lvovna Okorokova-Façanha^a, Valdirene Moreira Gomes^a, André de Oliveira Carvalho^{a,*}

^aLaboratório de Fisiologia e Bioquímica de Microrganismos, Centro de Biociências e Biotecnologia, Universidade Estadual do Norte Fluminense Darcy Ribeiro, Campos dos Goytacazes-RJ, 28013-602, Brazil.

¹The authors contributed equally to this manuscript.

Type of article: Research article

Situation: Published

Journal: Probiotics and Antimicrobial Proteins

Impact factor: 4.4 (2023)

RESUMO

O manejo de doenças fúngicas impõe uma necessidade urgente de desenvolvimento de medicamentos antifúngicos eficazes. Entre os novos candidatos a medicamentos estão os peptídeos antimicrobianos, especialmente seus derivados. Neste estudo, investigamos o mecanismo molecular de ação de três peptídeos bioinspirados contra as leveduras oportunistas *Candida tropicalis* e *Candida albicans*. Avaliamos alterações morfológicas, funcionalidade mitocondrial, condensação de cromatina, produção de espécies reativas de oxigênio (ROS), ativação de metacaspases e ocorrência de morte celular. Nossos resultados indicaram que os peptídeos induziram cinéticas de morte celular marcadamente contrastantes: 6 horas para RR e

3 horas para D-RR em *C. tropicalis* e 1 hora para WR em *C. albicans*. As leveduras tratadas com os peptídeos apresentaram aumento nos níveis de ROS, hiperpolarização mitocondrial, redução no tamanho celular e condensação de cromatina. RR e WR induziram necrose em *C. tropicalis* e *C. albicans*, mas D-RR não induziu necrose em *C. tropicalis*. O antioxidante ácido ascórbico reverteu o efeito tóxico de RR e D-RR, mas não de WR, sugerindo que, além de ROS, existe um segundo sinal desencadeado que leva à morte das leveduras. Nossos dados sugerem que RR induziu uma morte celular acidental regulada em *C. tropicalis*, D-RR induziu uma morte celular programada independente de metacaspases em *C. tropicalis*, enquanto WR induziu uma morte celular acidental em *C. albicans*. Os resultados foram obtidos com a LD₁₀₀ e dentro do período em que os peptídeos induzem a morte das leveduras. Nesse intervalo temporal, nossos resultados permitem elucidar os eventos desencadeados pela interação dos peptídeos com as células e sua ordem temporal, proporcionando um melhor entendimento do processo de morte induzido por eles.

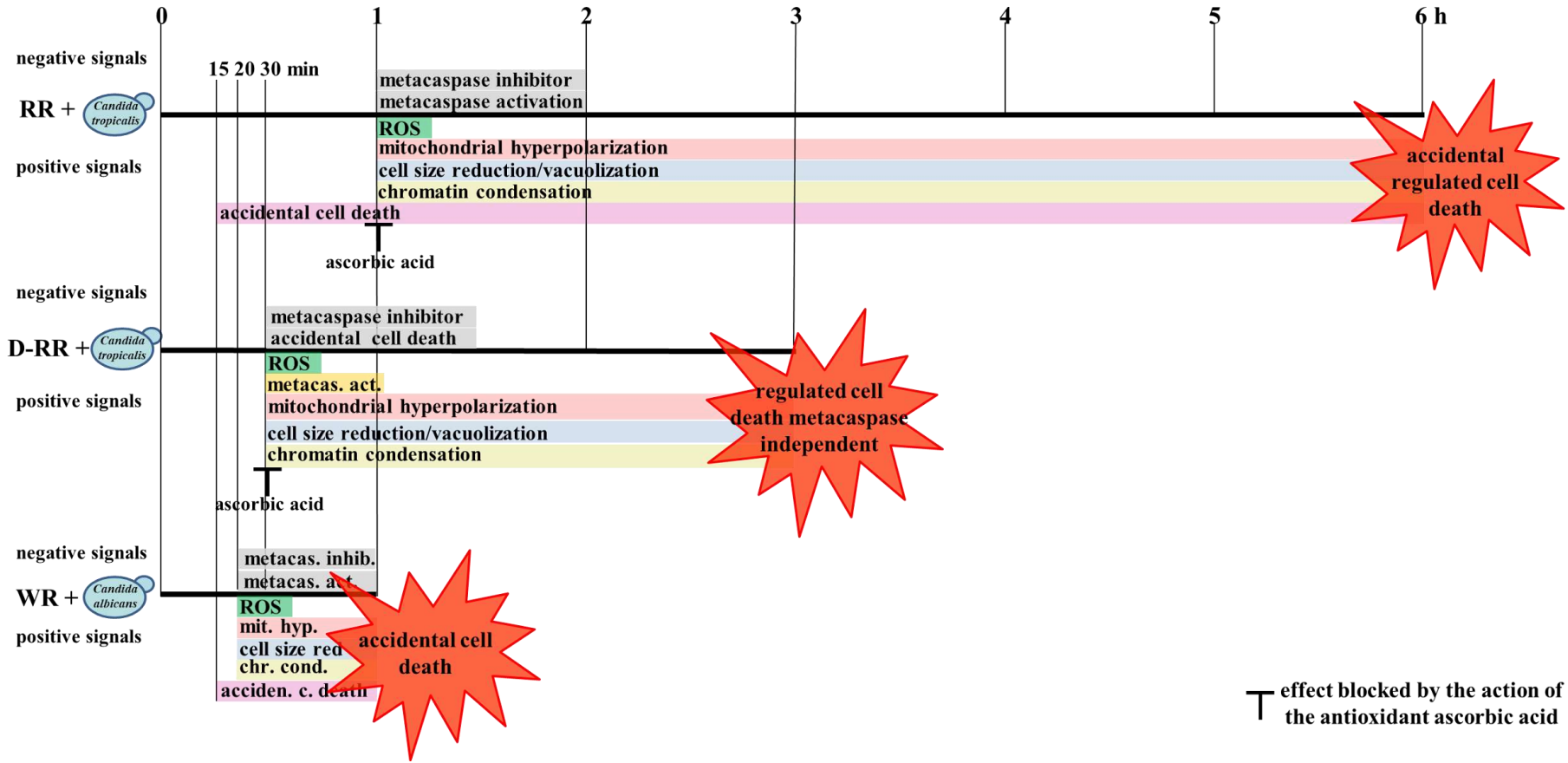
Palavras-chave

peptídeos antimicrobianos; morte celular acidental; morte celular regulada; tempo de morte; hiperpolarização mitocondrial

Destaques

- Há uma necessidade de desenvolver terapias eficazes para o tratamento de doenças fúngicas.
- A indução de ROS por peptídeos bioinspirados está associada à hiperpolarização mitocondrial.
- As ROS não são o executor final da morte das leveduras, sugerindo a atuação de um segundo sinal.
- O destino celular das leveduras é determinado após 15 minutos de interação com os peptídeos.
- Diferentes mecanismos de morte são induzidos por três peptídeos bioinspirados contra leveduras

4.1 Grafical abstract (Resumo gráfico)





Bioinspired peptides induce different cell death mechanisms against opportunistic yeasts

Douglas Ribeiro Lucas¹ · Filipe Zaniratti Damica¹ · Estefany Braz Toledo¹ · Antônio Jesus Dorighetto Cogo¹ · Anna Lvovna Okorokova-Façanha¹ · Valdirene Moreira Gomes¹ · André de Oliveira Carvalho¹

Accepted: 10 March 2023 / Published online: 20 April 2023
 © The Author(s), under exclusive licence to Springer Science+Business Media, LLC, part of Springer Nature 2023

Abstract

The management of fungal diseases imposes an urgent need for the development of effective antifungal drugs. Among new drug candidates are the antimicrobial peptides, and especially their derivatives. Here, we investigated the molecular mechanism of action of three bioinspired peptides against the opportunistic yeasts *Candida tropicalis* and *Candida albicans*. We assessed morphological changes, mitochondrial functionality, chromatin condensation, ROS production, activation of metacaspases, and the occurrence of cell death. Our results indicated that the peptides induced sharply contrasting death kinetics, of 6 h for RR and 3 h for D-RR to *C. tropicalis* and 1 h for WR to *C. albicans*. Both peptide-treated yeasts exhibited increased ROS levels, mitochondrial hyperpolarization, cell size reduction, and chromatin condensation. RR and WR induced necrosis in *C. tropicalis* and *C. albicans*, but not D-RR in *C. tropicalis*. The antioxidant ascorbic acid reverted the toxic effect of RR and D-RR, but not WR, suggesting that instead of ROS there is a second signal triggered that leads to yeast death. Our data suggest that RR induced a regulated accidental cell death in *C. tropicalis*, D-RR induced a programmed cell death metacaspase-independent in *C. tropicalis*, while WR induced an accidental cell death in *C. albicans*. Our results were obtained with the LD₁₀₀ and within the time that the peptides induce the yeast death. Within this temporal frame, our results allow us to gain clarity on the events triggered by the peptide-cell interaction and their temporal order, providing a better understanding of the death process induced by them.

Keywords Antimicrobial peptides · Accidental cell death · Regulated cell death · Time of death · Mitochondrial hyperpolarization

Douglas Ribeiro Lucas, Filipe Zaniratti Damica, and Estefany Braz Toledo contributed equally to this manuscript.

Highlights

- There is a need to develop efficacious therapeutics for the treatment of fungal diseases.
- ROS induction by bioinspired peptides was linked to mitochondria hyperpolarization.
- ROS are not the final yeast death executor and a second signal seems to be operating.
- Cell fate of yeasts is determined after 15 min of interaction with the peptides.
- Different death mechanisms are induced by three bioinspired peptides against yeasts.

✉ André de Oliveira Carvalho
 andre@uenf.br

¹ Laboratório de Fisiologia e Bioquímica de Microrganismos, Centro de Biociências e Biotecnologia, Universidade Estadual do Norte Fluminense Darcy Ribeiro, Av. Alberto Lamego, nº 2000, Campos dos Goytacazes-RJ 28013-602, Brazil

Abbreviations

AA	L-ascorbic acid
AcA	Acetic acid
ACD	Accidental cell death
AMP	Antimicrobial peptides
CoQ	Coenzyme Q
CFU	Colony forming units
DAPI	4',6-Diamidino-2-phenylindole
DIC	Differential interference contrast
DMSO	Dimethyl sulfoxide
D-RR	D-A _{36,42,44} R _{37,38} Y _{32,46} ViDef
ETC	Electron transport chain
GSH	γ-L-glutamyl-L-cysteinyl-glycine
OH [*]	Hydroxyl anion
H ₂ DCFDA	2',7'-Dichlorodihydrofluorescein diacetate
Δψ _m	Mitochondrial membrane potential
O ₂	Molecular oxygen
NAC	N-acetyl-L-cysteine

nd	Not determined
PI	Propidium iodide
RET	Reverse electron transport
ROS	Reactive oxygen species
RR	A _{36,42-44} R ₃₇₋₃₈ Y ₃₂₋₄₆ ViDef
WR	A _{42,44} R ₃₇₋₃₈ W ₃₆₋₃₉ Y ₃₂₋₄₆ ViDef
SD	Standard deviation

Introduction

Our global and industrialized world is facing disheartening problems in the area of human, animal, and plant health. In the medical area, diseases caused by the burgeoning antibiotic-resistant microorganisms menace us to return to the pre-antibiotic era, for example, thwarting medical advances in cancer and transplant treatments [1, 2]. This problem is aggravated by insufficient research and development of new antibiotics by big pharmaceutical companies as a result of the intrinsic process of producing and marketing a new antimicrobial such as research high costs, long development time, and low financial return due to sporadic use compared to chronic or diseases which require drugs of continuous use [3]. Another handicap for pharmaceutical companies is that the development of bacterial resistance can make a newly launched antibiotic obsolete in a short time, undermining the financial return of the pharmaceutical industry that developed it [1, 3]. This fact is clearly demonstrated by the dwindling approval of new antibiotics for clinical use by regulatory agencies in the last two decades, which contrasts strikingly with the increasing rate of resistant bacteria [4, 5].

Besides bacteria, fungi are also of growing concern to medical and environmental areas. In this last one, they have been reported as the cause of drastic fall in wild bat [6] and amphibian [7] populations with serious ecological consequences [8, 9]. In agriculture, the problem caused by fungi is also serious and can put food security at risk [10]. This scenario is very worrying because estimates for the next 20 to 30 years are of a significant increase in the world population, which should reach approximately 9.8 billion humans in 2050 [11]. This population will put more pressure on world food production, and if there is a failure in the production process there would be serious consequences for human health, food security and the economy of some countries whose gross domestic product is heavily based on agribusiness [11]. In the medical area, recent data estimate that fungal infections ranging in severity from superficial to often fatal systemic invasive infections, in addition to being neglected, have increased worldwide, and among them are fungal keratitis, cutaneous mycoses, and airway diseases caused by fungal spores [10, 12, 13]. Those studies estimate that a total of 300 million people suffer from a severe fungal infection each year and about 1.5 million die as a result of these infections worldwide [12, 13]. This scenario has

another complicating factor, the number of elderly patients or patients undergoing medical interventions or living with HIV and *Mycobacterium tuberculosis* infections, as well as the number of immunocompromised patients due to cancer treatment or transplant recipients has been increasing rapidly and all these patients, because of their medical conditions, are more susceptible to fungal infections [12, 13]. Additionally, besides the increase in the number of cases of fungal infections, there is also the report of *Candida* [14, 15] and *Aspergillus* [15] species resistant to clinical antifungals, aggravating the scenario. Moreover, new species *Candida auris* multiresistant to clinical antifungals was reported in 2009 [16]. In a study with four countries, Pakistan, India, South Africa, and Venezuela, and in a total of 54 patients infected with *C. auris*, 93% of the 54 isolates were reported to be resistant to fluconazole, 35% to amphotericin B and 7% the echinocandins. Most worryingly, out of the 54 isolates, 41% were resistant to two classes of antifungals, and 4% were resistant to three classes [17]. This study also shows that *C. auris* is already spread across three continents. In addition to multiple resistance, this emerging species is persistent in the hospital environment as it resists disinfection protocols and is easily propagated among patients, making it a serious threat to human health [16].

Another great concern of the scientific community is the world's post-COVID-19 pandemic future. SARS-COV2 coinfection with other pathogens, including fungi, has been reported to increase the difficulty of diagnosis, treatment, and prognosis of COVID-19, but also exacerbate disease symptoms and mortality [18–20]. Antibiotics overuse to treat COVID-19 patients contributed to the increase in antibiotic-resistant microorganisms [21–24].

The aforementioned data underline the urgent need to develop efficacious therapeutics and rational strategies for both the prevention and treatment of fungal diseases, especially opportunistic ones caused by the yeast of *Candida* genus. Amongst the given alternatives, antimicrobial peptides (AMPs) have been forecasted as possible new therapeutic substances [25, 26]. AMPs are short polymers of up to 100 L-amino acid residues, synthesized by ribosomes, arranged in a linear or cyclic configuration with vast variation in sequence, length, and structure, with a net positive charge at physiological pH, and amphipathic character. The antimicrobial epithet derives from their broad inhibitory activities on various microorganisms, including multi-drug resistant ones. They are constitutively produced or induced in response to the perception of a pathogen attack in complex organisms, where they are part of the innate immune response, and in microorganisms, they are produced to avoid or eliminate competitors [25]. We have used an AMP-based bioinspired peptide design strategy for therapeutic use [27–29]. In our previous study, we gleaned from correlation studies between the primary structure and biological

activities of plant AMPs, namely defensins, the position, and the amino acids required for the biological activity of plant defensins and their derived peptides. Based on this molecular identification, we designed three peptides and tested their antimicrobial activity against opportunistic yeasts of the *Candida* genus, *Saccharomyces cerevisiae*, and tested their toxicity against murine macrophages and human monocytes [29]. We showed that the antifungal activity of three bioinspired peptides was improved by target alterations to increase both charge and hydrophobicity and, in general, exerted low toxicity on the tested mammalian cells [29]. We also started testing strategies to stabilize the bioinspired peptides and introduced D-enantiomer substitutions, which in comparison with the L counterpart, proved to be more potent, likely due to the greater resistance to protease degradation [29]. Our preliminary data also established relevant criteria for the clinical use of bioinspired peptides, such as the small size of biologically active peptides that minimizes the production costs and diminishes the risk of inappropriate host interactions, and increases stability in vivo applications. In the present work, we further investigated the mechanism of action of three bioinspired peptides against opportunistic yeasts to provide an understanding of the intracellular changes triggered by the peptides as a prerequisite to pave the way for clinical trials [30].

Material and methods

All reagents were acquired from Merck unless otherwise stated.

Peptides

The bioinspired peptides $A_{36,42,44}R_{37,38}Y_{32-46}VuDef$ (dubbed RR), $D-A_{36,42,44}R_{37,38}Y_{32-46}VuDef$ (dubbed D-RR), and $A_{32,44}R_{37,38}W_{36,39}Y_{32-46}VuDef$ (dubbed WR) were designed and prepared as described in Toledo et al. [29]. The purity of the peptides was confirmed as $\geq 95\%$ [29].

Yeast strains and antimicrobial assay

The cultivation of the yeasts *Candida tropicalis* (CE017) and *Candida albicans* (CE022), and the antimicrobial assay were done as described in Toledo et al. [29]. In brief, fresh yeast cultures were grown at 30 °C for 24 h and were used to obtain a colony that was resuspended in Sabouraud broth (5 g/L peptone from meat, 5 g/L peptone from casein, and 20 g/L D(+) glucose). The cell number of this stock cell suspension was determined by direct cell counting in a Neubauer chamber (Labor Optik) under an optical microscope (Axio Imager.A2, Zeiss). The antimicrobial assay was performed on a sterile 96-well microplate (polystyrene, U-shaped bottom, Nunc, Thermo Scientific) and consisted of 2,000 cells/mL of each

yeast, the lethal dose of each peptide (27.5 μM RR and 23 μM D-RR for *C. tropicalis*, and 27.5 μM WR for *C. albicans*) filter-sterilized (0.22 μm , Millex-GV, Millipore), and 100 μL (final volume) of Sabouraud broth. Lethal dose or LD_{100} was defined as the lowest peptide concentration that caused 100% cell death of the assay cell population compared to control in the absence of peptide by colony forming units (CFU). Controls were done in the absence of peptides. Blanks were done with culture medium only.

Kinetic analysis of yeasts' cell death induced by the designed peptides

To determine the kinetics of the yeast cell death an assay was carried out to determine the minimum period necessary for the designed peptides, at their LD_{100} , to cause the loss of cell viability. This assay was done as described in Toledo et al. [29] or briefly in the subsection "Yeast strains and antimicrobial assay," with the difference that the entire content of the wells was washed in Sabouraud broth and plated at every 3 h, from 0 to 21 h on plates containing Sabouraud agar (5 g/L peptone from meat, 5 g/L peptone from casein, 20 g/L D(+)glucose, and 17 g/L agar), according to Soares et al. [31]. By 0 h we mean the time needed to set up the experiment, wash the cells and plate them, which takes approximately 5 min. The peptides D-RR and WR were also tested at 1 and 2 h. After plating, CFU were determined at 24 h of incubation at 30 °C h for *C. tropicalis* and *C. albicans*. Cell death was defined as loss of cell division ability and loss of clonogenic capacity in culture medium in the absence of the stressor for 24 h of incubation [32]. The percentage of cell viability loss was calculated according to $\{[(\text{CFU of test samples} \times 100)/\text{CFU of control}] - 100\}$.

Standardization of the number of cells for optical microscopy assays

To validate the antimicrobial activity of the designed peptides, we determined their effect on larger cell density at the LD_{100} and the time of death of each peptide. Cell viability assay was performed with the parameters determined in subsections "Yeast strains and antimicrobial assay" and "Kinetic analysis of yeasts' cell death induced by the designed peptides," with 40,000 cells/mL, as described in Soares et al. [31].

Analysis of endogenous reactive oxygen species production

The detection of reactive oxygen species (ROS) by yeasts after treatment with the bioinspired peptides was performed in antimicrobial assays in the presence of the antioxidant agents L-ascorbic acid (AA), N-acetyl-L-cysteine (NAC), or γ -L-glutamyl-L-cysteinyl-glycine (GSH). The antimicrobial

assay was carried out as described in the subsection “Kinetic analysis of yeasts’ cell death induced by the designed peptides,” with the following modifications: the LD₁₀₀ of the peptides, 70 mM of the antioxidant agent AA (1 M stock solution) added jointly with the peptides, 5 mM NAC (0.6 M stock solution) or 3 mM GSH (0.5 M) both added 30 min prior to addition of the peptides, all dissolved in ultrapure water, filter sterilized (Millex-GV 0.22 µm, Merck Millipore), and incubated at the previously determined time of death of each peptide. Controls also were made with the addition of the antioxidant agents and a positive control (control⁺) constituted of yeast cells incubated with 333 mM of acetic acid (AcA) for 1 h at 30 °C. AcA was used as a control⁺ in this study because it is a well-known inducer of regulated cell death in fungi with apoptosis-like features, and therefore a parameter for comparing the effect of the designed peptides. After this period, the cell viability assay was performed as described in the subsection “Kinetic analysis of yeasts’ cell death induced by the designed peptides.” For RR, samples were diluted fifty times (50x) before plating. Different concentrations of the three antioxidants were previously tested to determine the highest concentration that does not hinder growth without being toxic to the yeasts according to subsections “Yeast strains and antimicrobial assay and Kinetic analysis of yeasts’ cell death induced by the designed peptides.” The antioxidant AA was also incubated in different time intervals in relation to the addition of the peptides, pre- or post-incubated for RR and D-RR, and pre-incubated for WR, within the conditions aforementioned.

The production of ROS was also evaluated by indirect fluorescence microscopy, using 2',7'-Dichlorodihydrofluorescein diacetate (H₂DCFDA, Calbiochem, EMD) according to Mello et al. [27]. Yeast cultures (40,000 cells/mL) were incubated with the designed peptides at their LD₁₀₀ and at the beginning of the time of death, 1 h for RR and *C. tropicalis*, 30 min for D-RR and *C. tropicalis*, and 20 min for WR and *C. albicans*. Controls were done without the addition of the bioinspired peptides. A positive control (control⁺) constituted of yeast cells incubated with 333 mM of acetic acid (AcA) for 1 h at 30 °C was also performed to adjust the parameters of excitation intensity and exposure time for the acquisition of fluorescent images, and these parameters were used for all other treatments. For *C. tropicalis* a control was also done in the presence of 70 mM AA. After peptide treatment, control, and treated cells were incubated with H₂DCFDA (20 µM) for 15 min at 30 °C, transferred to slides, and covered with coverslips. Visualization was performed by differential interference contrast (DIC) (Axio Imager.A2, Zeiss) equipped with fluorescence filters (450 – 490 nm for excitation and 500 nm for emission) and cell images were acquired using an AxioCam MR5 camera (Zeiss) and AxionVision LE software (version 4.8.2,

Zeiss). The results were expressed as percentage of fluorescent cells calculated by cell counting, using the following criteria: 1st—counting of approximately 200 cells in random DIC and fluorescent fields that varied according to the incubation times of the assays; 2nd—if the number of cells was too low (a consequence of the treatment with the bioinspired peptides or with the positive control that causes the death of the yeast cells), 10 random fields for each treatment were counted. The percentage of fluorescent cells, an indication of oxidative stress, was calculated to ([average number of fluorescent cells × 100] / average number of cells observed in DIC) for each sample.

Morphological analysis of yeast cells

Cell morphology was visualized by optical microscopy, as described in the subsection “Standardization of the number of cells for optical microscopy assays” with some modifications. The incubation time for antimicrobial assay for *C. tropicalis* cells with the designed peptides at the LD₁₀₀ was 1 and 6 h with RR, and 30 min and 3 h with D-RR, whereas *C. albicans* cells were incubated for 20 min and 1 h with WR. Yeast cells cultured in the medium without the addition of the peptides were considered controls. Furthermore, three positive controls were included: yeasts heated at 100 °C for 1 min; yeasts incubated with Triton X-100 (2%, V/V) for 15 min; yeasts incubated with 333 mM AcA for 1 h. An assay with 70 mM of the antioxidant agent AA was used (see subsection “Analysis of endogenous reactive oxygen species production” for the description of the antioxidant). After the incubation period of each treatment, the cells were transferred to slides and, after 5 min, covered with coverslips and analyzed under an optical microscope.

Cell size measurements were performed by evaluating the length of the transversal and longitudinal axis of cells after the treatment described above using AxionVision LE software (tool Measure, Length). Fifty randomly selected cells for each treatment were used in different observation fields. To provide uniform measurements, the cells were selected in the same focal plane, and pseudohyphae, non-intact cells, and early budding cells were not considered.

Mitochondrial function assays

Mitochondrial functionality was evaluated by optical fluorescence microscopy using fluorescent probes MitoTracker Red FM (Thermo Fisher) and Rhodamine 123 (Sigma-Aldrich). The assay was carried out as described in the subsection “Analysis of endogenous reactive oxygen species production,” with modifications. Yeast cells were incubated with the designed peptides at the beginning and end of the time of death, 1 and 6 h for RR and *C. tropicalis*, 30 min

and 3 h for D-RR and *C. tropicalis*, and 20 min and 1 h for WR and *C. albicans*. Positive control cells were incubated with 2% Triton X-100 for 15 min. For *C. tropicalis*, a control was also done in the presence of 70 mM AA. Control and peptide-treated cells were incubated with 0.1 µg/mL of the fluorescent probes Mitotracker Red FM or Rhodamine 123 for 15 min at 30 °C and observed under an optical microscope (subsection “Analysis of endogenous reactive oxygen species production”) equipped with a 581 nm for excitation filter and a 644 nm emission filter for Mitotracker Red FM and 506 nm excitation filter and a 530 nm emission filter for Rhodamine 123.

Cell proliferation reagent WST-1 (Roche) was used to access the mitochondrial activity of the yeast cells treated with the designed peptides [33]. The assay for each peptide was prepared according to subsection “Yeast strains and antimicrobial assay” with 80,000 cells/mL. Then, 10 µL of WST-1 reagent and 2 µL of 2,3,5,6-tetramethyl-1,4-benzoquinone (duroquinone) (final concentration 0.24 mM of a stock of 12.24 mM in dimethyl sulfoxide (DMSO)) as an electron couple reagent [34], were added to each sample. A blank was prepared with Sabouraud broth, WST-1, and duroquinone. The optical density was monitored at 450 nm for 20 min and 1 h for WR, 30 min, 2 h, and 3 h for D-RR, and 1, 3, and 6 h for RR in an ELISA microplate reader (Epoch, Biotek) running Gen5 software. The percentage of mitochondrial activity was calculated according to $[(\text{ABS}_{450\text{nm}} \text{ of test samples} \times 100) / \text{ABS}_{450\text{nm}} \text{ of control}]$. Standardization of the minimum number of cells in the assay required for the detection of WST-1 salt conversion by spectrophotometer was previously made. To validate the antimicrobial activity of the designed peptides, we tested their toxic effect on larger cell density at the LD₁₀₀ and time of death of each peptide as described in the subsection “Standardization of the number of cells for optical microscopy assays.”

Regulated cell death analysis

Metacaspase activity was analyzed by optical fluorescence microscopy using fluorescent probe FITC-VAD-FMK (CaspACE, FITC-VAD-FMK In Situ Marker, Promega). The assay was carried out as described in the subsection “Analysis of endogenous reactive oxygen species production,” with modifications. Yeasts were incubated with the designed peptides for 20 min, 1 and 6 h (depending on the yeast and peptide tested), and in the positive control, the cells were incubated with 333 mM AcA for 1 h. For *C. tropicalis*, a control was also done in the presence of 70 mM AA. Control and peptide-treated cells were incubated with 50 µM FITC-VAD-FMK for 15 min 30 °C, washed once in PBS, and observed under a fluorescence microscope (subsection “Analysis of endogenous reactive oxygen species production”) with a 490 nm for excitation filter and a 525 nm emission filter.

To identify whether the death pathway activated by the designed peptides in yeasts is a type of regulated cell death with apoptosis-like features, an antimicrobial assay was performed in the presence of the pan-caspase inhibitor Z-VAD-FMK (Promega). The antimicrobial assay was carried out as described in subsection “Yeasts and antimicrobial assay,” with the following modifications: the LD₁₀₀ of the peptides, 50 µM Z-VAD-FMK (2 mM stock solution in DMSO) were used and incubated at the previously determined death times. Controls were also made with the addition of 50 µM Z-VAD-FMK. Cell viability assay was performed as described in subsection “Kinetic analysis of yeasts’ cell death induced by the designed peptides,” with the following modifications: cells were plated at the time of death for each peptide.

Chromatin condensation was examined by 1 µM DAPI staining (1 mg/mL stock solution in ultrapure water) in cells treated as described in the subsection “Analysis of endogenous reactive oxygen species production” with the following modifications: after the incubation times, the control cells, only cells and medium, and the peptide treated cells were previously permeabilized with 2% Triton X-100 for 2 min prior to DAPI staining for 15 min in the dark at 30 °C and observed under a fluorescence microscope.

Accidental cell death analysis

Accidental cell death (terminology proposed by Carmona-Gutierrez et al. [67] instead of necrosis) was analyzed by fluorescence microscopy using propidium iodide (PI) fluorescent dye. The assay and analysis of the results were carried out as described in subsection “Analysis of endogenous reactive oxygen species production,” with the following modifications: the yeasts were incubated with the peptides at their LD₁₀₀ for 1 and 6 h for RR, 30 min and 3 h for D-RR, and 20 min and 1 h for WR. For positive control, cells were heated for 1 min at 100 °C. Controls and treated cells were incubated with 0.25 µg/mL PI for 15 min in the dark and observed under a fluorescence microscope with a 506 nm excitation filter and a 530 nm emission filter. This analysis was also done with time intervals of 10 and 15 min.

Statistical analysis

All experiments were carried out three times in triplicate, with the exception of optical microscopy assays, carried out in singlicate. A one-way ANOVA test was performed using GraphPad Prism version 8.0.2 for Windows. $P < 0.05$ is considered statistically significant. GraphPad Prism version 8.0.2 and PowerPoint (Microsoft Office 365) were used to illustrate the data.

Results

We first determined the time required for the bioinspired peptides to induce the death of the entire yeast cell population in the antimicrobial assay, *i.e.* 2,000 cells/mL at their respective LD₁₀₀. *C. tropicalis* incubated with 27.5 μM RR caused a 99% decrease in colony forming units (CFU) within 3 h, and induced the death of the entire yeast cell population from 6 h onward, accordingly cell death time of RR was 6 h (Table 1). However, 23 μM D-RR induced the death of *C. tropicalis* cell population already from 3 h onward. This shorter time of death prompted us to verify D-RR antifungal activity at the time intervals of 1 and 2 h, revealing a 98% decrease in CFU at 1 h and a 99% reduction at 2 h; since shorter treatment times were not effective in killing all cell population, D-RR induced time of death was estimated as 3 h (Table 1). Surprisingly, 27.5 μM WR caused 97% decrease in CFU at 0 h, and the death of 100% of *C. albicans* cell population after 3 h (Table 1). We also tested the antifungal activity of WR at 1 and 2 h and found that WR caused 100% death of *C. albicans* cell population after 1 h thus establishing WR time of death of 1 h. By 0 h we mean the time needed to set up the experiment, wash the cells and plate them, which takes approximately 5 min. Based on these experiments we choose the time points that represent the beginning and the end of the time of death interval required for each peptide to induce the death of the assay cell population (based on Table 1) at their respective LD₁₀₀. Therefore, the following assays were done with the LD₁₀₀ and time of death parameters as follows: 27.5 μM RR/1 and 6 h for *C. tropicalis*, 23 μM D-RR/30 min and 3 h for *C. tropicalis*, and 27.5 μM WR/20 min and 1 h for *C. albicans*.

Before we started our study to unravel the mechanism of action of the bioinspired peptides on yeasts, we standardized the number of cells to validate our forthcoming fluorescence microscopy assays. Thus, an antimicrobial assay using 40,000 cells/mL, instead of 2000 cells/mL of the previous assays, was done to determine the toxicity of the bioinspired peptides at higher cell density. It is noteworthy that RR, D-RR, and WR at their same LD₁₀₀ and time of death determined for the assay with 2000 cells/mL retained their toxicity to twenty times more cells than the original antimicrobial assay, causing cell viability loss in almost all cell population (Fig. S1). The CFU were not determined in control samples because of the excessive number of colonies formed, thus the cell death percentage was not calculated. With these results, we ensured that the signals observed at the microscopic analysis are signals that were triggered by the designed peptides that lead to yeast cell death.

Then, we proceeded to test the concentration of the antioxidants AA, NAC, or GSH to select the highest concentration that showed the lowest toxicity (inhibition of CFU in regard to the control) in a viability assay. We chose 70 mM of AA which for *C. tropicalis* incubated at the time of death of RR and D-RR had toxicity of 63% and 45.4% (Table 2), respectively, and the same concentration for *C. albicans* incubated during the time of death of WR did not present toxicity (Table 2). For NAC, we chose 5 mM which for *C. tropicalis* incubated with the time of death of RR and D-RR had a toxicity of 65.6% and 19.2% (Table 2), respectively, and the same concentration for *C. albicans* incubated at the time of death of WR had a toxicity of 3.6% (Table 2). For GSH, we chose 3 mM which for *C. tropicalis* incubated at the time of death of RR and D-RR had a toxicity of 33.3 and

Table 1 Kinetics of cell death induced by 27.5 μM RR, 23 μM D-RR in *Candida tropicalis* and by 27.5 μM WR in *Candida albicans*. Note for each yeast-peptide combination a significant decrease in colony forming units (CFU) in the test samples until complete cell viability loss at 6 h for RR, 3 h for D-RR, and 1 h for WR, which time corresponding to the death time for each peptide

Yeast	Samples	0	1	2	3	6	Time (h)
<i>Candida tropicalis</i>	Control	227 ± 7 ^a	nd	nd	544 ± 46 ^a	overgrowth	CFU
	RR (27.5 μM)	121 ± 24 ^b	nd	nd	1.3 ± 1.5 ^b	0	
	Loss of viability	46	nd	nd	99	100	%
	Control	190 ± 4 ^a	266 ± 3 ^a	401 ± 67 ^a	642 ± 64 ^a	overgrowth	CFU
	D-RR (23 μM)	40 ± 17 ^b	3 ± 1 ^b	2 ± 2 ^b	0 ^b	0	
	Loss of viability	79	98	99	100	100	%
<i>Candida albicans</i>	Control	231 ± 9 ^a	233 ± 22 ^a	287 ± 29 ^a	617 ± 36 ^a	overgrowth	CFU
	WR (27.5 μM)	7 ± 0.6 ^b	0 ^b	0 ^b	0 ^b	0	
	Loss of viability	97	100	100	100	100	%

The CFU values are the means ± SD. nd, not determined. By 0 h we mean the time needed to set up the experiment, wash the cells and plate them, which takes approximately 5 min. Different letter indicates significant differences and the same letter indicates no difference, $P < 0.05$. Assays shown are representative of an independent assay out of three

Table 2 Correlation between oxidative stress and cell death of opportunistic yeasts induced by bioinspired peptides RR, D-RR, and WR at their lethal dose and induced time of death. Yeasts were incubated with the antioxidants ascorbic acid (AA), N-acetyl-L-cysteine (NAC), and glutathione (GSH). Note that AA treatment protects *Candida tropicalis* cells from RR and D-RR-induced death while NAC and GSH did not protect, and any antioxidant protects *Candida albicans* from WR-induced death

Yeast/time of death	Samples	CFU (50 × for RR only)	% of growth (protection)	% of toxicity (death)
<i>Candida tropicalis</i> /6 h	Control	459 ± 26 ^a	nd	nd
	Control + AA (70 mM)	170 ± 1 ^b	37.0	63.0
	RR (27.5 μM) + AA (70 mM)	106 ± 14 ^c	62.4	37.6
	Control + NAC (5 mM)	158 ± 14 ^b	34.4	65.6
	RR (27.5 μM) + NAC (5 mM)	2 ± 1.5 ^c	1.3	98.7
	Control + GSH (3 mM)	306 ± 38 ^b	66.7	33.3
<i>Candida tropicalis</i> /3 h	Control	656 ± 30 ^a	nd	nd
	Control + AA (70 mM)	358 ± 27 ^b	54.6	45.4
	D-RR (23 μM) + AA (70 mM)	228 ± 36 ^c	63.7	36.3
	Control + NAC (5 mM)	530 ± 69 ^b	80.8	19.2
	D-RR (23 μM) + NAC (5 mM)	32 ± 8 ^c	6.0	94.0
	Control + GSH (3 mM)	428 ± 12 ^b	65.2	34.8
<i>Candida albicans</i> /1 h	Control	221 ± 22 ^a	nd	nd
	Control + AA (70 mM)	231 ± 18 ^a	104.5	0
	WR (27.5 μM) + AA (70 mM)	4 ± 2 ^b	1.7	98.3
	Control + NAC (5 mM)	213 ± 20 ^a	96.4	3.6
	WR (27.5 μM) + NAC (5 mM)	1.3 ± 1.5 ^b	0.6	99.4
	Control + GSH (3 mM)	187 ± 28 ^a	84.6	15.4
	WR (27.5 μM) + GSH (3 mM)	3.6 ± 3.6 ^b	1.9	98.1

The colony forming units (CFU) values are means ± standard deviation (SD). (nd), not determined (excessive number of grown colonies that prevented colony counting). Controls correspond to yeast cells cultivated in medium. Controls treated with antioxidants were compared with the control. The yeasts treated with the peptides and the antioxidants were compared with their respective controls with the antioxidants. Different letter denotes significant differences and the same letter denotes no difference, $P < 0.05$. The assay is representative of an independent assay out of three

34.8% (Table 2), respectively, and the same concentration for *C. albicans* incubated at the time of death of WR had a toxicity of 15.4% (Table 2). The viability assay in the presence of AA and *C. tropicalis* cells concurrently incubated with RR showed 62.4% of protection (Table 2), and concurrently incubated with D-RR the protection was 63.7% (Table 2) compared to the peptides alone (Table 1). For *C. albicans* cells concurrently incubated with AA and WR there was no protection (Tables 1 and 2). Two other antioxidants tested, namely NAC and GSH, were both pre-incubated 30 min before the addition of the bioinspired peptides, and presented a very low degree of protection to *C. tropicalis* from the toxic action of RR and D-RR (Table 2). Neither NAC nor GSH protected *C. albicans* cells from the toxic action of WR as they were not protected by AA (Table 2). The protection conferred by AA suggested that *C. tropicalis* was undergoing oxidative stress after treatment with RR and D-RR. The production of ROS was confirmed by the fluorescent probe H₂DCFDA. *C. tropicalis* cells incubated with RR for 1 h presented 88.2% H₂DCFDA positive cells, indicating that those cells were under oxidative stress induced by RR (Table 3 and Fig. S2a). *C. tropicalis* cells incubated with D-RR for 30 min presented 72.3% H₂DCFDA positive cells, indicating that

C. tropicalis cells were also under oxidative stress induced by D-RR (Table 3 and Fig. S2b). We also observed that H₂DCFDA fluorescence signal in *C. tropicalis* cells treated with RR and D-RR was more intense and with a diffuse distribution pattern within the cell which was different from the AcA (control⁺) (Fig. S2a and 2b). *C. albicans* cells incubated with WR for 20 min presented 94.4% of fluorescent cells, indicating that those cells were also under oxidative stress induced by WR and the intensity of the fluorescence in regard to the AcA (control⁺) was weaker (Table 3 and Fig. S2c). Despite being under oxidative stress, *C. albicans* was not protected by any antioxidant tested. Because AA was the only antioxidant protecting *C. tropicalis* from death, we tested it concurrently incubated with *C. tropicalis* cells and RR in the microscopic analysis. This result showed a decline from 88.2 to 21.7% of cells with H₂DCFDA positive signal, whose value was not different from control, therefore indicating a protection in comparison with cells treated only with RR (Table 3 and Fig. S2a). *C. tropicalis* concurrently incubated with D-RR and AA showed a dramatic drop from 72.3 to 1.1% of the cells under oxidative stress, indicating protection in comparison with cells treated with D-RR alone (Table 3 and Fig. S2b). Because all antioxidants tested did

Table 3 Percentage of *Candida tropicalis* and *Candida albicans* cells undergoing oxidative stress after incubation with the bioinspired peptides RR, D-RR, and WR determined by H₂DCF_{DA} positive cells by fluorescence microscopy

Yeast/incubation time	Samples	Number of cells in DIC	Number of H ₂ DCF _{DA} fluorescent cells	% of cells under oxidative stress
<i>Candida tropicalis</i> / 1 h	Control ⁺	205	205 ^a	100
	AcA (333 mM)			
	Control	233	9 ^b	3.8
	RR (27.5 μM)	213	188 ^b	88.2
	RR (27.5 μM) + AA (70 mM)	207	45 ^b	21.7
<i>Candida tropicalis</i> / 30 min	Control ⁺	241	236 ^a	97.9
	AcA (333 mM)			
	Control	258	17 ^b	6.5
	D-RR (23 μM)	268	194 ^a	72.3
	D-RR (23 μM) + AA (70 mM)	255	3 ^b	1.1
<i>Candida albicans</i> / 20 min	Control ⁺	176	171 ^a	97.1
	AcA (333 mM)			
	Control	207	12 ^b	5.7
	WR (27.5 μM)	178	168 ^a	94.4

Controls correspond to yeast cells cultivated in medium, and control⁺ corresponds to acetic acid treatment (AcA). Different letter indicates significant differences and the same letter indicates no difference, $P < 0.05$. The assay is representative of an independent assay out of three

not protect *C. albicans* from the toxic effect of WR, the analysis of WR in the presence of an antioxidant was not done.

Because the antioxidant AA failed to protect the entire population of *C. tropicalis* cells from the toxicity of RR and D-RR in the viability test, we investigated why a fraction of the population of cells, even in the presence of the antioxidant, continued to die. For that, we tested the addition of AA in relation to the incubation time of the peptides, pre and post, in addition to the condition that had already been made of co-incubation. For WR and *C. albicans*, we only tested the pre-addition condition. AA added 30 min before the addition of RR to *C. tropicalis*, the percentage of cells not protected from death increased from 37.6 to 52.3% (Fig. 1A), to D-RR and *C. tropicalis* the percentage of cells not protected from death decreased from 36.3 to 10.6% (Fig. 1A). AA did not protect *C. albicans* cells from WR-induced death (Fig. 1C). AA added 1 h after the addition of RR and D-RR to *C. tropicalis* increased the percentage of cells not protected from death from 37.6 to 82.2% and from 36.3 to 68.6%, respectively (Fig. 1A and B). The percentage of *C. tropicalis* cells not protected from RR and D-RR death decreased even more 2 h after AA addition, reaching 98.4 and 98.9%, respectively (Fig. 1A and B).

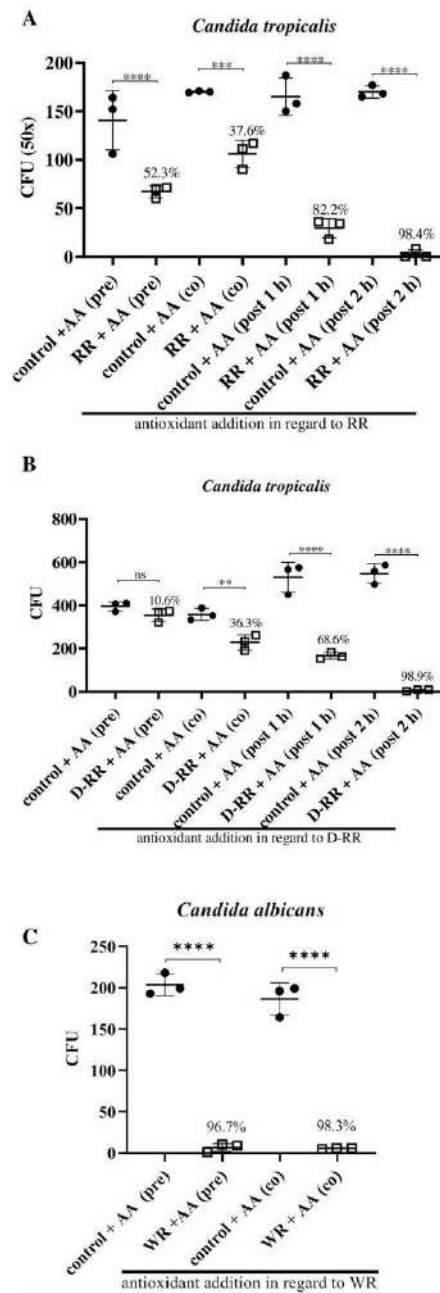
The microscopic observations of cells treated with the designed peptides showed morphological alterations and thus they were further analyzed. We noticed that the cytoplasm of *C. tropicalis*, after 1 and 6 h of incubation with RR (Fig. 2A), and after 30 min and 3 h of incubation with D-RR (Fig. 2A), and *C. albicans* after 20 min and 1 h of incubation with WR (Fig. 2B), all had a granular and/or vacuolated appearance, whereas this morphological alteration was not

detected in the control cells. This granularity of the cytoplasm was also observed in the positive control treatments, mainly those composed of AcA and heat (Fig. 2A and B). Although the antioxidant assays did not show protection for *C. albicans* (Table 2), we used AA as a control for these microscopic analyses. For the first 20 min after incubation, we did not observe changes in cell size, but cytoplasm granularity was attenuated, suggesting that ROS may be involved in the morphological alteration (Fig. 2B). For the time of death, 1 h, cytoplasm granularity, and size reduction were observed (Fig. 2B), which are in accordance with the non-protection of this yeast species by this antioxidant (Table 2). To confirm the overt cell shrinkage (Fig. 2A and B), we measured the longitudinal and transversal axes of the cells at their time of death. *C. tropicalis* cells treated with RR and D-RR presented a reduction of 29.7 and 23.2%, and of 34.9 and 27.4% for the longitudinal and transversal axes, respectively (Fig. 2C). *C. albicans* cells treated with WR presented a reduction of 38.3 and 33.8% for the longitudinal and transversal axes, respectively (Fig. 2D). AA protected *C. tropicalis* from the toxic effect of RR and D-RR (Table 2), and for RR concomitantly incubated with AA, it prevented 13.2% the longitudinal axis reduction, from 29.7 to 16.5%, and 18.9% the transversal axis reduction, from 23.2 to 4.3% (Fig. 2C). For D-RR concomitantly incubated with AA it protected 12.6% the longitudinal axis reduction, from 34.9 to 22.3%, and 23.6% the longitudinal axis reduction, from 27.4 to 3.8% (Fig. 2C). Although AA failed to protect *C. albicans* from death, we used it in this assay, and as observed before, the reduction of cell size was not inhibited and the size of the longitudinal and transversal axes were 38.4 and

Fig. 1 Effect of the antioxidant ascorbic acid (AA) on the antimicrobial activity of the bioinspired peptides. AA was added before (pre), co-incubated (co), and 1 and 2 h after (post) the addition of RR (A) and D-RR (B) to *Candida tropicalis*, and before (pre) and co-incubated (co) the addition of WR (C) to *Candida albicans* cells. The colony forming units (CFU) values are means \pm SD. The data from co-incubation were obtained from Table 1. ** $P < 0.01$; *** $P < 0.001$; **** $P < 0.0001$. (ns) indicates not significantly different. The assay is representative of an independent assay out of three

49.5%, respectively, which were not significantly different from the peptide alone (Fig. 2D). AA protected *C. tropicalis* treated with RR and D-RR against cell shrinkage in comparison with the peptides alone (Fig. 2C). Although this protection in cell shrinkage was statistically different compared to control (cells and medium only) for the longitudinal axis (Fig. 2C) that indicates that the protection was partial. This partial protection was also observed in Table 2. The addition of AcA, an inducer of regulated cell death in fungi with apoptosis-like features, resulted in a reduction in the longitudinal and transversal axes by 19.5 and 9.5% for *C. tropicalis*, and 30.6 and 26% for *C. albicans*, respectively (Fig. 2C and D).

Next, we investigated mitochondrial functionality because ROS stemmed mainly from mitochondrial activity. *C. tropicalis* treated for 1 h with RR in the presence of Mitotracker Red FM showed that the cells had active mitochondrial membrane potential (Fig. 3A). However, a stronger and more diffuse fluorescent labeling of Mitotracker Red FM was observed in the treated cells when compared to the control or those treated with AA (Fig. 3A). The same result was observed for 6 h, *i.e.* the time of death induced by RR. However, the intensity of the fluorescent signal at this latter time was increased even more compared to the initial time point of 1 h (Fig. 3A). *C. tropicalis* treated for 30 min or 3 h with D-RR showed a slightly stronger fluorescent signal in the D-RR treated cells compared to the control (Fig. 3C). *C. albicans* treated for 20 min or 1 h with WR, we observed that likewise *C. tropicalis* treated with RR and D-RR, a slightly stronger fluorescent label of Mitotracker Red FM can be observed in the WR-treated cells compared to the control (Fig. 3E). The positive control with AcA also enhanced mitochondrial activity of both yeasts (Fig. 3B, D, and F), but to a less extent than the bioinspired peptides. To confirm the increase in the membrane potential, we performed WST-1 assay to analyze the mitochondrial metabolic activity. Our results showed that *C. tropicalis* treated with RR and D-RR had an increase of 305.2 and 565.1% in mitochondrial activity within the 1 h and 30 min of incubation, respectively (Fig. 3B and D). This higher activity was kept elevated for 3 and 2 h of incubation, respectively, and was still high at the time of death, 3 and 6 h of incubation, respectively (Fig. 3B



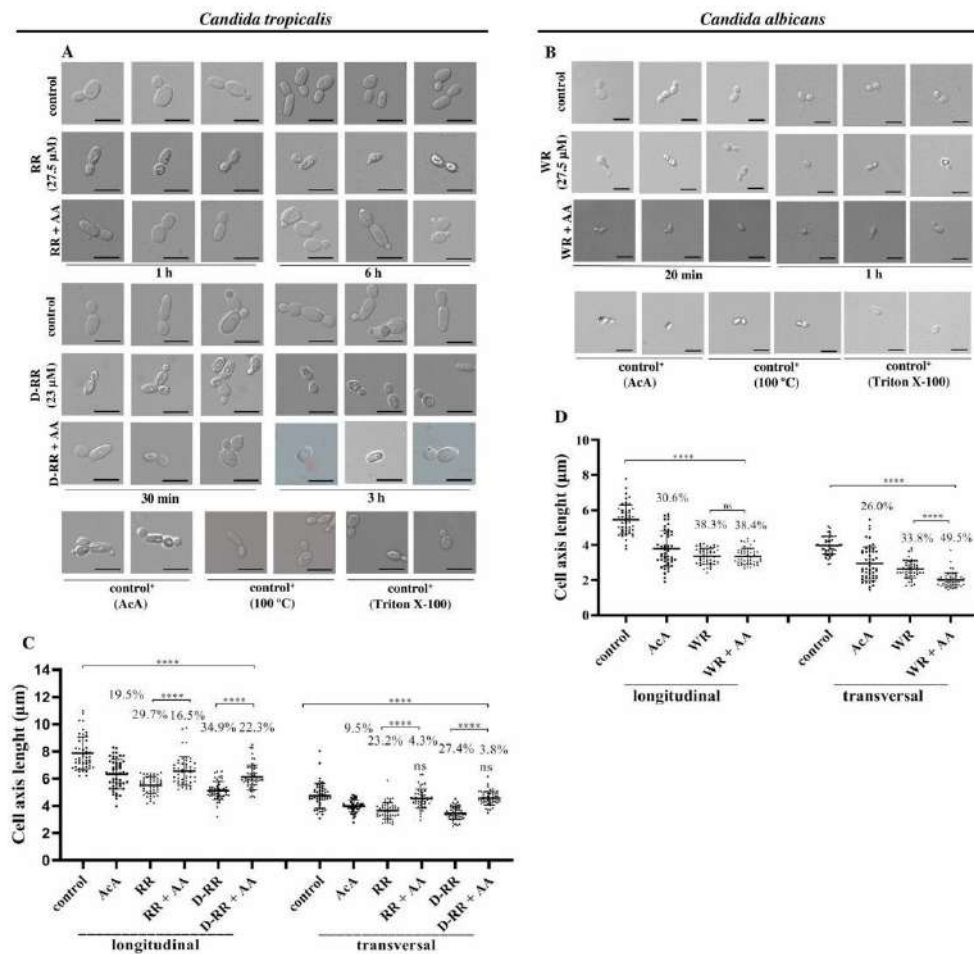


Fig. 2 Morphological changes and size reduction in the yeast cells treated with the bioinspired peptides. **A** Microscopic images of *Candida tropicalis* cells treated with 27.5 μ M RR and 23 μ M D-RR. Scale bar represents 10 μ m. AA, ascorbic acid, AcA, acetic acid. **B** Length of the longitudinal and transverse axes in *C. tropicalis* cells. **C** Microscopic images of *Candida albicans* cells treated with 27.5 μ M WR. **D** Length of the longitudinal and transverse axes of *C. albicans* cells. **A, B** Note the granularity of the cytoplasm and the reduction in cell size. **C, D** The percentage numbers indicate a reduction of the axis in relation to their respective controls. Controls correspond to yeast cells cultivated in medium, control⁺ correspond to AcA or heat or Triton

X-100 treatments. **** $P < 0.0001$. (ns) indicates not significantly different. The average size of each sample for *C. tropicalis* for longitudinal axis is: control 7.8 μ m, AcA 6.3 μ m, RR 5.5 μ m, RR + AA 6.5 μ m, D-RR 5.1 μ m, D-RR + AA 6.1 μ m. The average size of each sample for *C. tropicalis* for transversal axis is: control 4.7 μ m, AcA 4.3 μ m, RR 3.6 μ m, RR + AA 4.5 μ m, D-RR 3.4 μ m, D-RR + AA 4.5 μ m. The average size of each sample for *C. albicans* for longitudinal axis is: control 5.4 μ m, AcA 3.7 μ m, WR 3.3 μ m, WR + AA 3.3 μ m. The average size of each sample for *C. albicans* for the transversal axis is: control 3.9 μ m, AcA 2.9 μ m, WR 2.6 μ m, WR + AA 2.0 μ m. The assay is representative of an independent assay out of three

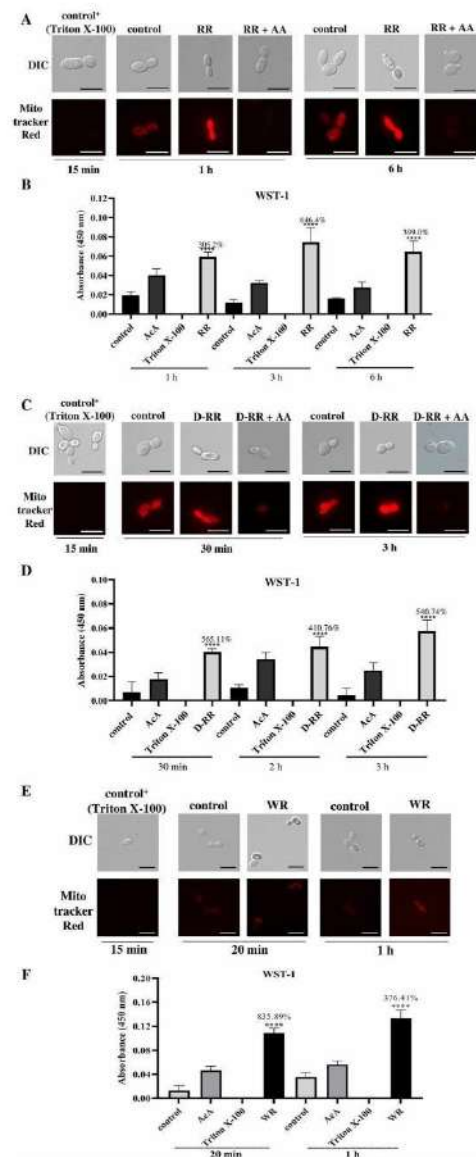
and D). *C. albicans* treated with WR, an increase of 835.9% in mitochondrial activity was also observed within the 20 min of incubation, which was still high, 376.4%, at 1 h,

the time of death (Fig. 3F). Triton X-100, which impaired mitochondrial accumulation of the Mitotracker Red FM probe (Fig. 3A, C, and E), also completely blocked WST-1

Fig. 3 Mitochondrial functionality in opportunistic yeast (**A, B, C, D** *Candida tropicalis*, **E** and **F** *Candida albicans*) cells treated with bioinspired peptides RR, D-RR, and WR lethal dose. **A, C,** and **E** Microscopic images of yeast cells; Mitotracker Red FM fluorescence in the cytoplasm indicates mitochondrial functionality. Scale bar represents 10 μm . Note the hyperpolarization of the mitochondrial membranes of the treated yeast cells. Ascorbic acid (AA) reversed the hyperpolarization. Control⁺ corresponds to Triton X-100 treatment. Controls correspond to yeast cells cultivated in a medium. **B, D,** and **F** Determination of mitochondrial metabolic activity using WST-1. The values above the test bars indicate the mitochondrial activity compared to the control. Controls correspond to yeast cells cultivated in medium, control⁺ correspond to acetic acid (AcA) or Triton X-100 treatments. **** $P < 0.0001$; The assay is representative of an independent assay out of three

reduction in the tested yeasts (Fig. 3B, D, and F); however, the AcA and Triton X-100 treatments were not statistically different from their respective controls.

We also evaluated whether there was activation of metacaspases in the yeasts treated with the peptides with Caspase FITC-VAD-FMK. For *C. tropicalis* treated with RR and for *C. albicans* treated with WR no positive signal was observed at the initial time of induction of death by these peptides (Figs. 4A, B, and 5A, B). *C. tropicalis* cells incubated with D-RR for 30 min presented 94.2% of FITC-VAD-FMK positive cells, indicating that *C. tropicalis* cells had activated metacaspases (Fig. 6A and B). For D-RR and *C. tropicalis*, the induction of metacaspase was inhibited by the coinubation of the cells with AA (Fig. 6A and B). The positive control (AcA) induced metacaspase activation in both yeast species (Figs. 4A, 5A, and 6A). The contribution of metacaspases activation in the death induced by the bioinspired peptides was examined by the pan-caspase inhibitor Z-VAD-FMK in the antifungal assay. It did not protect the tested yeasts from the action of the bioinspired peptides (Figs. 4C, 5C, and 6C). The analysis of chromatin condensation revealed that control cells presented a round shaped nucleus with an even DAPI fluorescent signal, whereas the peptide-treated cells exhibited a stronger and more punctual staining (Figs. 4D, 5D, and 6D). Fluorescent staining was even more conspicuous at the latter incubation times (Figs. 4D, 5D, and 6D). The same fluorescent staining pattern was also observed for AcA, a known inducer of regulated cell death in yeast with apoptosis-like features (Figs. 4D, 5D, and 6D). To better differentiate the type of cell death induced by the bioinspired peptides we investigated whether the death was an accidental cell death (ACD) by propidium iodide (PI) labeling. Our results indicated that *C. tropicalis* treated with RR and *C. albicans* treated with WR both showed positive labeling for PI since the beginning of incubation and also at the ending of the time of death (Table 4, and Fig. S3A and C) reflecting the presence of necrotic cells. Conversely, *C. tropicalis* cells treated with D-RR were PI negative (Table 4 and Fig. S3B). Additionally,



for *C. tropicalis* incubated with RR, the PI positive labeling was reversed by AA co-treatment (Table 4 and Fig. S3A). Noteworthy, the presence of PI positive cells pointed to another result of peptide effect: the plasma membrane permeabilization in *C. tropicalis* treated with RR and in *C. albicans* treated with WR, but not for D-RR-exposed *C.*

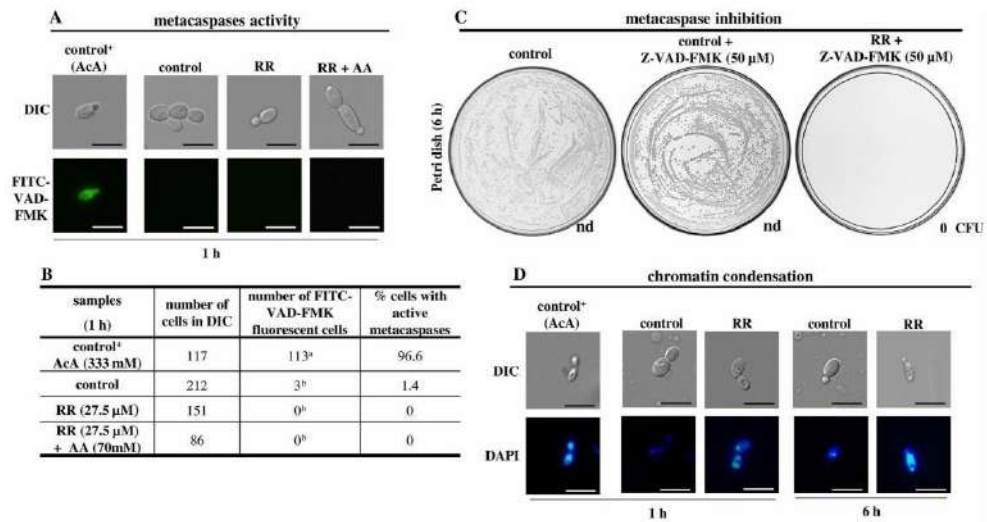


Fig. 4 Cell death analysis in *Candida tropicalis* cells treated with RR lethal dose. **A** Microscopic images of yeast cells; FITC-VAD-FMK green fluorescence in the cytoplasm indicates metacaspase activation. Scale bar represents 10 μm. **B** Number of cells with activated metacaspases, determined after cell count in random DIC and fluorescence fields as observed in **A**. Different letters indicate a statistically significant difference. $P < 0.05$. **C** Viability assay with *C. tropicalis* incubated with RR at its time of death (6 h) and control in the presence of the pan-caspase inhibitor Z-VAD-FMK. Colony forming units

(CFU) values are means \pm SD. (nd), not determined (excessive number of grown colonies that prevented colony counting). **D** Detection of chromatin condensation by DAPI staining. Note that the control cells present a round-shaped nucleus with an even fluorescent signal, whereas the peptide-treated cells present a stronger and more punctual staining indicating chromatin condensation. Scale bar represents 10 μm. **A–D** Controls correspond to yeast cells cultivated in medium. **A, B, D** control⁺ corresponds to acetic acid (AcA) treatment. The assay is representative of an independent assay out of three

tropicalis cells. As the labeling of PI would help us to better differentiate the effect of peptides, we tested early time points for RR and WR and found that PI labeling starts for both peptides and their respective yeasts after 15 min of incubation (Table 5).

Discussion

The broad spectra of microbial inhibitions of AMPs catapulted them to a new pharmaceutical status. Nevertheless, the lack of understanding of their in vivo performance imposes some weaknesses on their pharmaceutical development and stalling their way to the clinic. Such drawbacks are embodied by their toxic action against mammalian cells, which results in a low selective index, poor in vivo pharmacokinetic and pharmacodynamic that render low bioavailability to AMPs, and high production costs, due to their complex structure and length [35]. But embedded in their structures are features that are being explored to circumvent these drawbacks such as wide structural diversity that coupled with correlation studies between activity and

structure are showing both an understanding of positions and nature of amino acids important for activity, as well as, the possibility by chemical synthesis of incorporating unnatural amino acids, improving their stability and activity [36]. These understandings allowed the design of modified AMPs with better therapeutic properties. We used a similar approach correlating the primary structure and biological activities of plant defensins which allowed us to design three new peptides, named RR, D-RR, and WR, with ameliorated antimicrobial activity against opportunistic yeasts and low toxicity toward mammalian cells [29]. Herein, we further characterize these bioinspired peptides and set in motion a series of experiments to unravel the possible mechanism of their action against the opportunistic yeasts in regard to the induced events which led to cell death.

Previously we determined that LD_{100} , which causes 100% of yeast death, was 27.5 μM and 23 μM of RR and D-RR, respectively, for *C. tropicalis*, and 27.5 μM WR for *C. albicans* [29]. Herein we determined the time of death (Table 1) and then chose one time in the beginning and another at the end of the time of death for the next experiments. These parameters are important because they avert

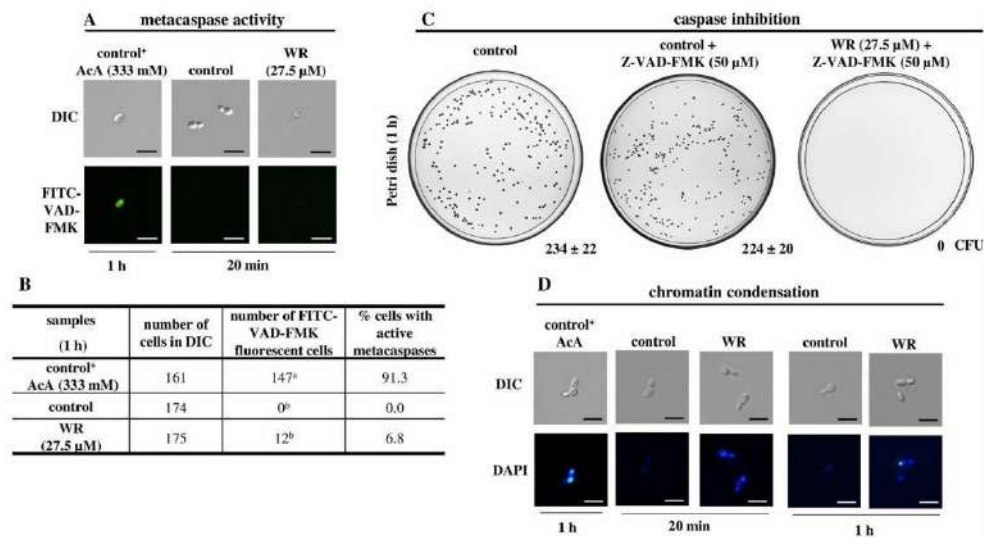


Fig. 5 Cell death analysis in *Candida albicans* cells treated with WR lethal dose. **A** Microscopic images of yeast cells; FITC-VAD-FMK green fluorescence in the cytoplasm indicates metacaspase activation. Scale bar represents 10 μm. **B** Number of cells with activated metacaspases, determined after cell count in random DIC and fluorescence fields as observed in **A**. Different letters indicate a statistically significant difference. $P < 0.05$. **C** Viability assay with *C. albicans* incubated with WR at its time of death (1 h) and control in the presence of the pan caspase inhibitor Z-VAD-FMK. Colony forming units

(CFU) values are means \pm SD. (nd), not determined (excessive number of grown colonies that prevented colony counting). **D** Detection of chromatin condensation by DAPI staining. Note that the control cells present a round shaped nucleus with an even fluorescent signal, whereas the peptide-treated cells present a stronger and more punctual staining indicating chromatin condensation. Scale bar represents 10 μm. **A–D** Controls correspond to yeast cells cultivated in medium. **A, B, D** control⁺ corresponds to acetic acid (AcA) treatment. The assay is representative of an independent assay out of three

misinterpretation of the cell death pathway induced by the bioinspired peptides [31]. Afterwards, we standardized the number of cells for microscopy analysis. The antimicrobial assays carried out so far used a total of 2000 cells/mL; however, this amount of cells is unfeasible for optical microscopy analysis because it is below the detection limit. Therefore, a higher amount of cells was used to allow their visualization under an optical microscope. For that reason, 40,000 cells/mL were used based on Soares et al. [31]. The bioinspired peptides retained their toxicity at higher yeast cell numbers (Fig. S1).

Allegedly, the main mechanism of action involved in microbial growth inhibition or death by AMPs is microbial cell membrane damage. Indeed some AMPs have been reported to interact with microbial membrane components such as phospholipids and sphingolipids [37–39]. Contradictory, some works reported results that do not fully explain that the AMP-membrane interaction is the main event responsible for the microbial growth inhibition or cause of death, and others demonstrated that the membrane damage is a ripple effect, *i.e.* the microbial membrane is a secondary or indirect target of AMPs action with other

primary targets [31, 40–43]. Moreover, other mechanisms of action have been described [44]. However, the interaction of AMPs with microbial membrane components seems to be crucial for growth inhibition and/or death processes. Amongst them are the anchorage points for AMPs at microbial membrane components by opposite charge attraction which allow their accumulation on the membrane surface and their latter entrance into the cell. This view found support in the reports that some known mechanisms of bacterial resistance to AMPs are mediated by camouflaging negative charges of both membrane lipid and cell wall components [45, 46]. One such mechanism of action of several antimicrobial substances, including AMPs, to which the inhibitory activity or the induced death upon microorganisms seems to converge, is the induction of endogenous oxidative stress [47, 48].

Firstly, based on those reports of oxidative stress as the possible primary toxic effect, we analyzed whether bioinspired peptides promoted endogenous oxidative stress in the yeast cells. For that, we analyzed the contribution of oxidative stress to the death induced by the designed peptides by treating the yeasts with the antioxidant agents AA, NAC, or GSH in a viability assay. These substances

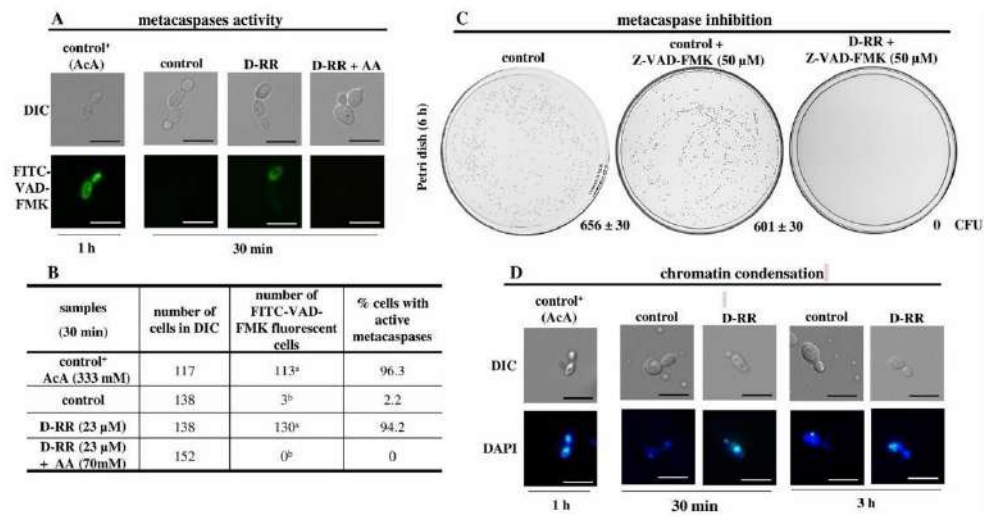


Fig. 6 Cell death analysis in *Candida tropicalis* cells treated with D-RR lethal dose. **A** Microscopic images of yeast cells; FITC-VAD-FMK green fluorescence in the cytoplasm indicates metacaspase activation. Scale bar represents 10 μm. **B** Number of cells with activated metacaspases, determined after cell count in random DIC and fluorescence fields as observed in **A**. Different letters indicate a statistically significant difference. $P < 0.05$. **A, B** Ascorbic acid (AA) reversed the metacaspase activation. **C** Viability assay with *C. tropicalis* incubated with D-RR at its time of death (3 h) and control in the presence of the pan caspase inhibitor Z-VAD-FMK. Colony forming units (CFU)

values are means \pm SD. (nd), not determined (excessive number of grown colonies that prevented colony counting). **D** Detection of chromatin condensation by DAPI staining. Note that the control cells present a round-shaped nucleus with an even fluorescent signal, whereas the peptide-treated cells present a stronger and more punctual staining indicating chromatin condensation. Scale bar represents 10 μm. **A–D** Controls correspond to yeast cells cultivated in medium. **A, B, D** control⁺ corresponds to acetic acid (AcA) treatment. The assay is representative of an independent assay out of three

are non-enzymatic antioxidants capable of protecting cells against the oxidizing action of free radicals [49, 50]. Thus, this analysis makes it possible to infer whether there is ROS generation in yeast cells exposed to the bioinspired peptides and, additionally, to elucidate their mechanistic involvement in yeast death. Our results indicated protection from death to *C. tropicalis* incubated with RR and D-RR, and no protection for *C. albicans* incubated with WR (Table 2). Antioxidant AA were shown to diminish the antifungal activities of NaD₁ (plant defensin from *Nicotiana glauca*) [51], Rs-AFP₂ (plant defensin from *Raphanus sativus*) [41], and ApDef₁ (plant defensin from *Adenantha pavonina*) [31] against *C. albicans* and *S. cerevisiae*. That family of plant AMP is which RR, D-RR, and WR were bioinspired [29], and thus it is expected they share the mechanism of action. Those reports not only are in accordance with our results but also indicate that oxidative stress is involved in the cell death induced by these peptides. Antioxidant NAC is widely used as an ROS scavenger in yeast cells [50, 52, 53] and was shown to protect *C. albicans* from the toxic effect of itraconazole at 5 mM [50], to protect *C. albicans* and *S. cerevisiae* from the toxic effect of KM29 (synthetic AMP derived from *Homo sapiens*

histatin 5) at 10 mM [53], and to protect *C. albicans* from the toxic effect of LfcinB15 (AMP derived from the proteolytic cleavage of lactoferrin) at 60 mM [39]. Nonetheless, it had no effect against the toxic effect of 10 mM farnesol in *S. cerevisiae* [54]. In these three examples, the antioxidant activity was associated with ROS toxicity, to the same extent inferred in our results of co-incubation of RR and D-RR with the antioxidant AA. Having said that, in our test conditions 3 mM NAC was unable to rescue yeast cells from induced death (Table 2). Additionally, in our test conditions, at concentrations higher than 5 mM NAC was toxic for *C. tropicalis* and *C. albicans*, completely abrogating the growth of yeast cells (data not shown). Indeed, Andrés et al. [55] reported the toxic effect of NAC on *C. albicans* at concentrations higher than 15 mM, and AA toxicity for *Candida* was also reported [56]. This toxicity action of the antioxidants on our conditions occurred most likely because the oxidative status of the cells has important signaling roles [57–59] and higher concentrations of exogenous antioxidants might preclude these signaling pathways. One possible explanation for the lower protection of *C. tropicalis* and no protection of *C. albicans* by NAC is that NAC is an optimal scavenger

Table 4 Analysis of accidental cell death (ACD) in *Candida tropicalis* and *Candida albicans* cells treated with the bioinspired peptides RR, D-RR, and WRR lethal dose. Number of cells undergoing necrosis (PI positive cell) was determined after cell counting in random DIC and fluorescence fields after the incubation times indicated. Ascorbic acid (AA) reversed necrosis in *C. tropicalis* incubated with RR

Yeast	Samples	Incubation time	Number of cells in DIC	Number of PI fluorescent cells	% necrotic cells	Incubation time	Number of cells in DIC	Number of PI fluorescent cells	% necrotic cells
<i>Candida tropicalis</i>	Control ⁺ (100 °C)	1 min	207	207 ^a	100	1 min	207	207 ^a	100
	Control	1 h	217	0 ^b	0	6 h	241	5 ^b	2.0
	RR (27.5 μM)		203	108 ^a	53.2		175	71 ^a	40.5
	RR (27.5 μM) + AA (70 mM)		201	4 ^b	1.9		241	6 ^b	2.4
<i>Candida tropicalis</i>	Control ⁺ (100 °C)	1 min	178	175 ^a	98.3	1 min	178	175 ^a	98.3
	Control	1 h	223	0 ^b	0	3 h	214	0 ^b	0
	D-RR (23 μM)								
	D-RR (23 μM) + AA (70 mM)		205	6 ^b	2.9		230	15 ^b	6.5
<i>Candida albicans</i>	Control ⁺ (100 °C)	1 min	191	187 ^a	97.9	1 min	191	187 ^a	97.9
	Control	20 min	228	2 ^b	0.9	1 h	222	14 ^b	6.3
	WR (27.5 μM)		180	175 ^a	97.2		198	198 ^a	100

Control⁺ corresponds to heat (100 °C) treatment. Data from the controls⁺ are the same because the incubation time was 1 min for all of them. Different letter indicates significant differences and the same letter indicates no difference, $P < 0.05$. The assay is representative of an independent assay out of three

for hydroxyl anion (OH[•]) [60]. If it is the case, it points to an irrelevant participation of OH[•] in the peptide-induced death or non-production of it by the yeast species in the conditions studied. Another possibility for the antioxidant activity of NAC is an indirect effect as a precursor used by the cell to synthesize GSH, which ultimately has antioxidant action [61]. At all, GSH synthesis may not have occurred

fast enough to confer antioxidant protection by increasing GSH content since the addition of the peptides, especially WR which toxicity was observed after 0 h of cell contact (Table 1), although GSH failed to rescue the tested yeasts from the toxic action of the bioinspired peptides. GSH by itself is a well-known antioxidant molecule in fungi [62, 63]. Its addition was reported to protect *C. albicans* from death

Table 5 Analysis of accidental cell death (ACD) induced by RR in *Candida tropicalis* and WR in *Candida albicans* at a shorter time

Yeast	Samples	Number of cells in DIC 10 min	Number of PI fluorescent cells	% necrotic cells	Number of cells in DIC 15 min	Number of PI fluorescent cells	% necrotic cells
<i>Candida tropicalis</i>	Control ⁺ (heat 1 min)	157	157 ^a	100	157	157 ^a	100
	Control	150	0 ^b	0	152	0 ^b	0
	RR (27.5 μM)	132	10 ^b	7.6	140	120 ^b	85.7
<i>Candida albicans</i>	Control ⁺ (heat 1 min)	171	167 ^a	97.7	171	167 ^a	97.7
	Control	173	2 ^b	1.1	170	2 ^b	1.2
	WR (27.5 μM)	157	8 ^b	5.1	161	135 ^a	83.8

Different letter indicates significant differences and the same letter indicates no difference, $P < 0.05$. Data from the controls⁺ are the same because the incubation time was 1 min for all of them. The assay is representative of an independent assay out of three

induced by LfcinB15 [40], but in high concentrations, it was toxic to *S. cerevisiae* by extra-mitochondrial Fe–S enzymes maturation [64]. In our test conditions, GSH at 3 mM or higher concentrations negatively impacted *C. tropicalis* growth (33.3% and 34.8% for RR and D-RR, respectively, Table 2) and *C. albicans* (15.4%, Table 2), and therefore, we had chosen in our condition tested the highest GSH concentration that was minimally toxic for the tested yeast cells.

To confirm the endogenous induction of ROS by the yeasts, we used the fluorescent indicator H₂DCFDA. This probe is cell-permeable and once inside the cell it is deacetylated by intracellular esterases and, when oxidized by ROS, generates the fluorescent compound dichlorofluorescein allowing the detection of ROS inside the cell. AcA was used as a positive control in this assay because it is a well-known inducer of regulated cell death in fungi with apoptosis-like features [65, 66]. In the conditions tested, AcA caused 100% of cell death (Table S1), which confirms its cell death induces capability [66]. Additionally, for this fluorescent analysis, cells treated with AcA were used as parameters to adjust the microscope for the control and peptides treatments and all images were captured with the exposure time and excitation intensity adjusted for this positive control (Fig. S2). The time points chosen represented one point at the beginning of the time of death interval required for each peptide to cause the death of the assay cell population (based on Table 1). Our results indicate that RR and D-RR, and WR induced oxidative stress in *C. tropicalis* and *C. albicans*, respectively (Table 3 and Fig. S2), and antioxidants use in the viability assay not only confirm our assumption that *C. tropicalis* cells were undergoing oxidative stress resulting from the action of RR and D-RR, but also that ROS is related to the signal triggered by RR and D-RR that led to cell death, provided that once scavenged by the antioxidant, it rescued *C. tropicalis* cells from death (Table 2). Moreover, *C. tropicalis* death was pharmacologically inhibited, suggesting the occurrence of a regulated cell death (Table 2) [67]. It is of note that the presence of the three different antioxidants did not rescue *C. albicans* from death, even despite cells facing oxidative stress. One explanation might be the rapid rate with which WR induced the death of this yeast species, since immediately after WR addition (0 h time of death), 97% of the cell population was already dead (Table 1). Such rapidity may prevent the antioxidant from having the protective effect even when added before WR (also see discussion of Fig. 1C). Another possibility to explain the absence of antioxidant protection effectiveness is discussed later in this section.

During the analysis of our results of the oxidative stress determination assays, we noted that 37.6 and 36.3% of *C. tropicalis* cells died even in the presence of the AA when incubated with RR and D-RR, respectively (Table 2). These results indicate the antioxidant rescues 62.4 and 63.7% of

C. tropicalis cells from death (Table 2). The death of 37.6 and 36.3% of *C. tropicalis* cells even in the presence of the antioxidant AA (Table 2) raises the question of why the antioxidant did not protect 100% of the assay cell population. The same result was observed in the microscopic assay in which *C. tropicalis* treated with RR and D-RR, simultaneously with AA, did not present a complete reversal of cell size reduction (Fig. 2). Even considering that yeast cells do not have a synchronized division cycle [68], AA should have a higher protection rate if the oxidative stress was the main event leading to peptide-induced yeast death. Based on this incomplete protection, our assumption was that ROS might be an initial stress that once established triggers another cell death executor(s) that lead to the cell death. This assumption explains that even in the presence of the antioxidant, and therefore protected from ROS, yeast cells would still be committed to death. To discriminate this effect, we repeated the antimicrobial and viability assays in the presence of the antioxidant AA, but adding it at different times in relation to the addition of RR and D-RR. AA added 30 min before the addition of RR to *C. tropicalis*, which in theory should provide greater protection against ROS since the cell would be preloaded with the antioxidant and it would promptly eliminate the generated ROS, the percentage of cells not protected from death, unexpectedly, increased from 37.6 to 52.3% (Fig. 1A). We believe that this decrease in protection may be due to the intrinsic toxicity of AA, which in this case lasted a total of 6 h 30 min of incubation with the yeast *C. tropicalis*, 30 min longer than the co-incubation condition and, therefore, ended up being more toxic. In fact, comparing the control co-incubated with AA with the control pre-incubated with the antioxidant we observed a reduction of 17.2% indicating toxicity (Fig. 1A). To D-RR and *C. tropicalis*, as foreseen, the pre-incubation for 30 min with AA, the percentage of cells unprotected from death decreased from 36.3 to 10.6% (Fig. 1B). This higher toxicity observed to RR due to the longer incubation time is also evident when compared with the results of D-RR and the same yeast, in this case, the total incubation time was 3 h and 30 min. AA added 1 h after the addition of RR to *C. tropicalis*, i.e. ROS would have enough time to act on the cell, and the percentage of cells not protected from death, as expected, increased from 37.6 to 82.2% (Fig. 1A). In the case of D-RR, AA was added 1 h after the addition of the peptide and the percentage of cells not protected from death also increased from 36.3 to 68.6% (Fig. 1B), and added 2 h after the addition of the RR and D-RR, the percentage of cells not protected from death dropped even more, reaching 98.4 and 98.9%, respectively (Fig. 1A and B). For WR we adopted a different approach, as this peptide induced the death of *C. albicans* very rapidly (97% of cell death at 0 h of incubation, Table 1), we added AA only 30 min before the addition of the peptide because when AA was added

jointly with WR it did not improve cell death (Table 2), and for this reason, there was no sense to add it later. However, even added 30 min before WR, AA continued to show the same response as when added concomitant to the peptide, no protection (Fig. 1C). *C. albicans* treatment with WR resulted in oxidative stress as confirmed by the fluorescent microscopy analysis (Fig. S2C) and since the peptide induced death of 97% of the cell population of the assay at 0 h (Table 1), we suspect that strong and rapid toxic effect of WR over *C. albicans* may enshroud the protection of the antioxidant even if it added before WR (Fig. 1C). For RR and D-RR, these results, as predicted, showed that ROS is probably not the final executor of *C. tropicalis* death induced by the designed peptides since once it was scavenged by the antioxidant after 1 and 2 h after the addition of the peptides, *C. tropicalis* was still committed to death. This result also raised the question of the nature of another cell death executor triggered instead of ROS or whether there would be a mechanism corresponding to a point-of-no-return during the death process. The point-of-no-return for *C. tropicalis* treated with RR seems to take place before 3 h because at this time 98% of cells were dead, for *C. tropicalis* treated with D-RR this point likely occurred before 1 h because at this time 98% of cells were dead, and for *C. albicans* treated with WR seems to be after 5 min, because at 0 h, our time point correspondent to 5 min, 97% cells were dead (Table 1). Future studies should address the point-of-no-return or the other cell death signal. On the other hand neither the antioxidants used protected *C. albicans* from WR toxic action, suggesting that oxidative stress is not the main mechanism that leads to cell death despite being involved in the process.

Cell morphological analysis indicated that the yeasts treated with the bioinspired peptides exhibited granular cytoplasm and cell shrinkage (Fig. 2). Noteworthy the same phenotypic feature, *i.e.* cytoplasm granularity, was also induced by AcA, well-known inducer of regulated cell death in fungi with apoptosis-like features [66], which, jointly with the results from oxidative stress assays (Table 1), reinforce that regulated cell death may be occurring in the peptide-treated yeasts. Another interesting feature of the treated cells was their shrinkage compared to the control cells (Fig. 2A and B). Both the cytoplasmic alterations and cell shrinkage were observed from the early time until the time of death of the tested yeasts (Fig. 2A and B). Furthermore, it is interesting to note that *C. tropicalis* cells treated with RR and D-RR along with the antioxidant AA did restore both cytoplasmic changes and apparent size reduction (Fig. 2A and B), reinforcing again that these toxic effects of RR and D-RR are mediated by ROS and also pointing out to ROS as the primary stress that leads to both the cytoplasmic changes and cell size reduction. Our measurements confirm the visually observed cell size reduction (Fig. 2C and D). As the same effect, *i.e.* cell shrinkage, was observed for both the

bioinspired peptides and AcA, it is evidencing once again a type of regulated cell death induced by the designed peptides. Cell shrinkage is a well-known hallmark phenotype of several types of regulated cell death in mammalian cells [49]. In fungi, cell shrinkage was characterized during death induced in *C. albicans* by exogenous molecules like chlorogenic acid [69], and histatin 5 (AMP from *Homo sapiens* saliva) [70]. In both examples, the efflux of ions, especially K^+ , was pointed out as the cause of cell shrinkage. If this is the case, it raises two possibilities; first, K^+ efflux is the cause of cell shrinkage, and second, it may be the other signal that is independent of the antioxidant action triggered by the bioinspired peptides, and both possibilities should be investigated in the future studies. Taken together, the death induction by the bioinspired peptides (Table 1), the induction of ROS (Table 2), and cell size reduction (Fig. 2) strongly suggest that designed peptides induced a type of regulated cell death with apoptosis-like features in the tested *Candida* yeasts.

The production of ROS identified in yeasts after treatment with the designed peptides led us to analyze their mitochondrial functionality because mitochondria are the main source of intracellular ROS as a byproduct of cellular respiration due to a leakage of electrons from the determined flow order on the electron transport chain (ETC) directly to molecular oxygen (O_2) [71, 72]. Therefore, we used the membrane potential-dependent probes Mitotracker Red FM and Rhodamine 123 to assess mitochondrial functionality. All three peptides induced mitochondrial dysfunction in the *Candida* yeasts (Fig. 3). These results also indicate by the higher intense fluorescent signal that the alteration induced by the peptides already took place at the beginning of the induced cell death process, *i.e.* 1 h for RR, 30 min for D-RR and 20 min for WR (Fig. 3). It must be emphasized that the comparison of control and peptide-treated samples within the same time point can be interpreted relative to one another because the images were acquired with the same fluorescent intensity and exposure time settings, adjusted to their respective controls (cells and medium). The same results, *i.e.* the increase in the fluorescent intensity signal, were obtained for Rhodamine 123 for all peptides and treated yeasts (data not shown). These results point out that the mitochondria of the peptide-treated yeasts underwent dysfunctional stress and for *C. tropicalis* the anomalous strong signal of the probes, *i.e.* Mitotracker Red FM or Rhodamine 123, was directly linked to the ROS production since co-incubation of AA with RR or D-RR in *C. tropicalis* restored the intensity of the fluorescent signal equal to the control cells for both probes (Fig. 3 and Fig. S2). Additionally, AA also reduced the intensity of the fluorescent signal of ROS probe, that is, the antioxidant relieved the oxidative stress on the mitochondria (Fig. S2). The increased uptake of the mitochondrial probes observed for the peptide-treated yeasts in this work

may indicate a hyperpolarization of the mitochondrial membrane potential. It is also in accordance with the intensified ROS probe signal which also showed an increase in fluorescence intensity as a result of intense ROS production (Fig. S2A and B). These results seem to be related because ROS production depends on a flow of electrons in the mitochondria ETC [73–75]. For a description of mitochondrial ETC please refer to Vendetti et al. [73], Mailloux [74], and Napolitano et al. [75]. One known condition that leads to ROS production in complex I is by reverse electron transport (RET). In RET the mitochondrial membrane must have a high pool of reduced coenzyme Q (CoQ) and a high mitochondrial membrane potential $\Delta\psi_m$ which act together to reverse the flow of electrons back to complex I where at the flavin mononucleotide site, electrons are passed to O_2 generating superoxide anion [76]. *C. albicans* and *C. parapsilosis* are known to possess all five mitochondrial complexes which are denominated classical respiratory pathways, and in addition, two other known pathways were described in these yeasts species denominated as alternative and parallel oxidases [77]. Those last two are considered compensatory pathways when the classical pathway is somehow blocked [78]. The alternative and parallel pathways branch off from the classical pathway at the site of CoQ, therefore they can deoxidize CoQ, thus blocking one of the RET requirements from happening in these yeasts [76, 78]. Some works have demonstrated that the main site of ROS generation in fungi is the mitochondrial complex I [78–80]. Some reports have positively correlate high $\Delta\psi_m$ and low ATP concentration with an increase in endogenous ROS production to the toxic effect of antifungal substances in *Candida* species, for example, in a *C. albicans* fluconazole-resistant strain treated with a combination of fluconazole and berberine [76, 81], and *C. albicans* treated with plagiocin E [82]. The high $\Delta\psi_m$ has also been associated with ROS production in hyperpolarized mitochondria of *S. cerevisiae* treated with the isoprenoid farnesol [54]. Also, protamine sulfate, a drug used in cardiovascular surgery causes a reduction in cardiac oxygen consumption. Its mechanism of action is related to the inhibition of cytochrome c oxidase activity causing respiration inhibition, hyperpolarization of mitochondrial membrane potential, and ROS production [83]. The increase in mitochondrial membrane potential for ROS generation is corroborated by Skulachev [84] who highlighted that for ROS production in both complex I and complex III, an increase in mitochondrial membrane potential is required. Accordingly, our results also correlate with the increase in mitochondrial potential and increased ROS production (Figs. 3 and S2). But what increases the mitochondrial potential in the first place? A possible explanation was given by Pozniakovsky et al. [85], who correlated the increase in mitochondrial potential with the transient rise in intracellular Ca^{2+} in *S. cerevisiae* treated with the antiarrhythmic agent amiodarone,

which in turn increased the activity of mitochondrial NADH dehydrogenases, which ultimately supply electrons to the ETC chain and consequently to ROS production. This explains both the increase in mitochondrial membrane potential and the increase in ROS production by the increase in the flow of electrons. The increased expression of isocitrate dehydrogenase, an enzyme of the Krebs cycle, in *C. albicans* treated with fluconazole and berberine corroborates with the observation of Pozniakovsky et al. [85, 80]. Another possibility for the hyperpolarization of mitochondrial membrane potential was given by Machida and Tanaka [54] who indicated that farnesol precludes cellular signaling which results in the spurring F_1 -ATPase while reversing its activity from ATP synthesis to ATP hydrolysis in *S. cerevisiae*, resulting in proton ions transport back into the intermembrane space, hyperpolarization of the mitochondrial membrane potential and ROS production. It is remarkable that this mitochondrial stress scenario with membrane hyperpolarization nor only tentatively explains the toxic effect of the designed peptides towards *C. albicans* and *C. tropicalis*, but also explains why *S. cerevisiae* that lacks the complex I of the classical respiratory pathway, together with alternative and parallel pathways [86] is resistant to the designed peptides [29], provided that complex I is the site of ROS generation. To confirm the high mitochondrial activity, already observed with the Mitotracker Red FM (Fig. 3A, C, and D) and Rhodamine 123 probes (data not shown), we used WST-1 assay to assess mitochondrial activity on the peptide-treated yeasts based on studies showing that the NADH formed by the mitochondrial Krebs cycle is the leading reductant for WST-1 reduction to water-soluble formazan outside cells in the presence of an intermediate electron acceptor, allowing the quantification of mitochondrial metabolic activity by colorimetric assay [33]. The high activity observed in the reduction of WST-1 at the yeasts' time of death may represent a residual activity of the enzymes involved in the process [66]. Therefore, the results of the WST-1 assay support the results of the stronger staining of the membrane potential-dependent fluorescent probes and confirm that the mitochondria of treated yeasts were hyperpolarized. For the WST-1 assay, we had to standardize the minimum number of cells to give a positive signal in the assay. Initially, we used the 40,000 cells/mL that was already normalized for the microscopy assays (Fig. S1) validating that the peptides had activity at higher cell concentration, but we obtained no positive results within the death incubation time of the peptides, likely because of the low cell density required for this assay (data not shown). Therefore, the cell number of this assay was doubled to 80,000 cells/mL which gave a positive signal (Fig. 3B, D, and F). To validate that the peptides were still active at this 40-fold higher cell concentration than the initial assay (Table 1), we performed a viability assay. It is noteworthy that RR, D-RR, and WR

at the same LD₁₀₀ and time of death determined for the assay with 2,000 cells/mL retained their toxicity to forty times more cells than the original antimicrobial assay, causing cell viability loss of almost all cell population (Fig. S4). Our data clearly indicate that the bioinspired peptides induced hyperpolarization of their mitochondrial membrane potential leading to mitochondrial dysfunction in the tested yeasts. These results may exclude death as an apoptotic-like process because the loss of mitochondrial membrane potential is a hallmark of apoptosis [87]. Future studies should investigate the site of ROS production in the yeast mitochondria to gain a better understanding of how the stress triggered by the bioinspired peptides propagates within yeast cells, reaching and interfering with mitochondria.

Because ROS appear to be essential executors in regulated cell death with apoptotic-like phenotype in yeasts [64, 88] and our results pointed out ROS is linked to this process, we explored some regulated cell death phenotypes in yeasts. Indeed, apoptosis in fungi has been questioned recently [89]. However, it is undeniable that under certain conditions fungal cells die, and whose death exhibits phenotypic characteristics of intrinsic apoptosis in mammalian cells [65]. For this reason, we investigated some known markers of mammalian cell apoptosis to reinforce our results which indicate that a type of regulated cell death with phenotypic characteristics of mammalian cell apoptosis is being induced in *C. tropicalis* and *C. albicans* treated with the designed peptides, as suggested by Carmona-Gutierrez et al. [67]. We initially showed that the treated yeasts are under oxidative stress (Tables 2 and 3, Fig. S2), and exhibited a significant reduction in the cell size when treated with the designed peptides (Fig. 2). Both features are hallmarks of apoptosis in mammalian and yeast cells [48, 66]. We further evaluated whether the yeast metacaspases were activated upon peptides treatment using CaspACE FITC-VAD-FMK, a derivative of the pan-caspase inhibitor carbobenzoxyvalyl-alanyl-aspartyl-[O-methyl]-fluoromethylketone (Z-VAD-FMK), where the N-terminal blocking group was replaced by the fluorescein isothiocyanate (FITC) group. This replacement endowed the pan-caspase inhibitor with fluorescence and the ability to enter cells and bind activated caspases. Only *C. tropicalis* cells incubated with D-RR presented FITC-VAD-FMK positive cells as well as the positive control (AcA) (Figs. 4A, 5A, 6A) which was used to adjust such parameters as exposure time and excitation intensity. The activation of metacaspases in *Candida* by AcA, as well as other AMPs, is in accordance with other works [27, 90, 91] and also with the description of *CaMAC1* gene which encodes a metacaspase in *C. albicans* [92], and therefore, support our results. The inhibition of metacaspase activation by AA in *C. tropicalis* incubated with D-RR (Fig. 6) provided a causal link between the protection of *C. tropicalis* cells from ROS production by this antioxidant (Table 2 and Fig. 2B). To gain a better

comprehension of the role that metacaspase activation plays in the death induced by the bioinspired peptides, we treated yeast cells with the pan-caspase inhibitor Z-VAD-FMK. This inhibitor enters the cell and irreversibly binds to the catalytic site of active caspases, inhibiting their activity. Therefore, if this is the route of death, treatment with Z-VAD-FMK should protect the yeasts from the action of the peptides. We found the addition of 50 μM of the pan-caspase inhibitor in the antifungal assay did not protect *Candida* cells from the action of the bioinspired peptides (Figs. 4C, 5C, 6C). These results point out that the death induced by the designed peptides in *C. tropicalis* and *C. albicans* is metacaspase independent. Guaragnela et al. [93] studied *S. cerevisiae* death by AcA treatment and showed the activation of metacaspases by FITC-VAD-FMK and a non-protection from death by the pan-caspase inhibitor Z-VAD-FMK. Their results indicated that the death induced by AcA in the budding yeast was metacaspase independent. Later studies demonstrated that many factors can induce *S. cerevisiae* death independent of metacaspase activity [94]. The activation of metacaspases was demonstrated by FITC-VAD-FM for *C. albicans* treated with *Rs*-AFP₂, and coinubation with Z-VAD-FMK halted *Rs*-AFP₂-induced yeast death. However, the deletion of the *CaMCA1* did not interfere with the peptide-induced death, indicating that other caspase-like proteases may be involved [90]. Therefore, our results may indicate that the death pathways activated by the designed peptides in yeast are metacaspase independent or there is another signal that once triggered commits cells to death as discussed above. Another regulated death with apoptosis-like features in mammalian cells analyzed in the present study was the detection of chromatin condensation by a fluorescent probe DAPI, which binds to the adenine and thymine-rich sequences of minor grooves of the DNA. Our results showed that the bioinspired peptides induce an alteration in the DAPI staining pattern (Figs. 4D, 5D, 6D). AMPs lead to both caspase-dependent [50] and independent [95] cell death with chromatin condensation. Due to the rapidity with which WR-induced death in *C. albicans* (Table 1), and RR-induced a metacaspase-independent cell death in *C. tropicalis* (Fig. 4A and C), we investigated whether the cell death was an accidental cell death (ACD) type caused by the bioinspired peptides by staining yeast cells with propidium iodide (PI). PI is a fluorescent probe that intercalates DNA and only enters cells with a ruptured cell membrane, being not permeable to the entire plasma membrane, and is excluded from live cells or cells undergoing early apoptosis, but binds to the nucleic acid of cells undergoing ACD and late apoptosis. RR and WR treatment resulted in positive PI labeling in *C. tropicalis* and *C. albicans*, respectively (Table 4), and negative labeling using D-RR and *C. tropicalis* (Table 4). AA had a protective effect on PI labeling in *C. tropicalis* incubated with RR; this result is in accordance with the treatment of *C.*

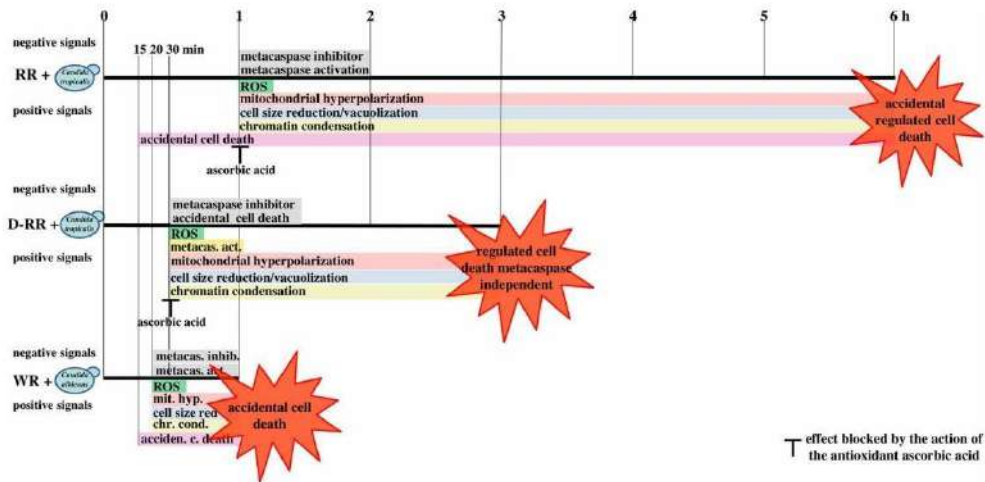


Fig. 7 Schematic depiction of the proposed model describing the mechanism of action of RR and D-RR on *Candida tropicalis*, and WR on *Candida albicans*. Based on the results present study using probes to cellular process (ROS, mitochondrial hyperpolarization, cell size reduction/vacu-

olization, chromatin condensation, accidental cell death, metacaspase activation) and inhibitors (ascorbic acid, metacaspase inhibitor) allowed to differentiate the type of cell death promoted by each peptide

tropicalis concomitantly with RR and AA in which *C. tropicalis* death was prevented (Table 2), and once again linked the toxic effect of RR on *C. tropicalis* to an uncontrolled ROS production. Additionally, the time of 15 min (Table 5) being the earliest that the PI labeling took place ruled out the possibility of death being late apoptosis. The same PI labeling time for *C. tropicalis* and *C. albicans* (Table 5) does not seem to be a mere coincidence and suggests the activation of a conserved mechanism by the peptides. Additionally, this result indicated that the fate of the yeasts after incubation with the peptides is being determined by the cells within this time interval of 15 min, and this finding will be further investigated in the future. In summary, for both RR and D-RR peptides, the induction of death in *C. tropicalis* was reversed by AA (Table 2), therefore suggesting that the death process is a regulated one. For RR and WR our results suggest an ACD once the cells treated with these peptides showed PI-positive labeling (Table 4). Although ACD is characterized by a well-defined feature, the augment in cell volume, in both mammalian and yeast cells [48, 66], our results indicated that *Candida* cells treated with RR and WR were PI positive and were undergoing cell shrinkage (Fig. 2). The permeabilization of the yeast membranes allowed the efflux of ions, including K^+ , and if K^+ leakage was the case, it might explain the shrinkage and not cell volume expansion of the treated yeasts [96, 97].

Conclusions

In this study, we have gleaned information from our previous work on the amino acid residues in the γ -core region of plant defensins important for their biological activity [29]. Next, we designed the RR, D-RR, and WR peptides which exhibited improved antimicrobial activity against opportunistic yeasts and low toxicity to mouse macrophages and human monocytes compared to the original peptide [29]. Herein, we report the effects of these bioinspired peptides on *Candida* yeasts and propose a mechanism of action in regard to distinct types of induced cell death (Fig. 7). We showed that exposure of *C. tropicalis* to RR and D-RR promoted a regulated accidental death (Fig. 7) and metacaspase-independent regulated cell death, respectively (Fig. 7), while WR promoted ACD in *C. albicans* (Fig. 7). Our results were obtained with the LD_{100} and within the time that the peptides induce the yeast death. Within this temporal frame, our results allow us to gain clarity on the events triggered by the peptide-cell interaction and their temporal order, providing a better understanding of the death process induced by these peptides. Future studies should provide further details of the action time course. The understanding of the process of fungal cell death triggered by AMP interaction is important to support the clinical use of antifungal molecules, since the lack of understanding of the mechanism of action leads

to failure in more advanced clinical trials. Our results can be mirrored by other AMPs and derived peptides helping to pave the way for the clinical use of these molecules. Moreover, the understanding of the mode of action of bioinspired peptides is important in light of the fact that regulated cell death pathways are also involved in *Candida* virulence [98] raising the possibility to manipulate these pathways for antifungal therapy purposes.

Supplementary Information The online version contains supplementary material available at <https://doi.org/10.1007/s12602-023-10064-8>.

Acknowledgements The work was supported by the Brazilian agencies *Conselho Nacional de Desenvolvimento Científico e Tecnológico* (CNPq), *Fundação de Amparo à Pesquisa do Estado do Rio de Janeiro* (FAPERJ, process n°. E-26/202.760/2018-Bolsa), and *Coordenação de Aperfeiçoamento de Pessoal de Nível Superior* (Finance Code 001) as well as the *Universidade Estadual do Norte Fluminense Darcy Ribeiro*. We acknowledge Luiz Carlos Dutra de Souza and Valeria Miguelote Kokis for their technical support.

Author contribution D.R.L., F.Z.D., and E.B.T.: investigation, methodology, validation, writing—review and editing. A.J.D.C. and A.L.O.F.: investigation, writing—review and editing. V.M.G. investigation, A.O.C.: conceptualization, methodology, supervision, project administration, funding acquisition, writing—original draft.

Data availability All relevant data are within the manuscript and supplementary information files. Data will be shared upon request with the corresponding author.

Declarations

Competing interests The authors declare no competing interests.

References

- Medina E, Pieper DH (2016) Tackling threats and future problems of multidrug-resistant bacteria. *Curr Top Microbiol Immunol* 398:3–33. https://doi.org/10.1007/82_2016_492/COVER
- Bartoletti M, Giannella M, Tedeschi SE, Viale P (2018) Multi-drug-resistant bacterial infections in solid organ transplant candidates and recipients. *Infect Dis Clin North Am* 32:551–580. <https://doi.org/10.1016/j.idc.2018.04.004>
- Browne K, Chakraborty S, Chen R, Wilcox MD, Black DS, Walsh WR, Kumar N (2020) A new era of antibiotics: the clinical potential of antimicrobial peptides. *Int J Mol Sci* 21:1–23. <https://doi.org/10.3390/ijms21197047>
- Ferri M, Ranucci E, Romagnoli PE, Giaccone V (2017) Antimicrobial resistance: a global emerging threat to public health systems. *Crit Rev Food Sci Nutr* 57:2857–2876. <https://doi.org/10.1080/10408398.2015.1077192>
- Pham TN, Loupias P, Dassonville-Klimpt A, Sonnet P (2019) Drug delivery systems designed to overcome antimicrobial resistance. *Med Res Rev* 39:2343–2396. <https://doi.org/10.1002/MED.21588>
- Lorch JM, Meteyer CU, Behr MJ, Boyles JG, Cryan PM, Hicks AC, Ballmann AE, Coleman JTH et al (2011) Experimental infection of bats with *Geomyces destructans* causes white-nose syndrome. *Nature* 480:376–378. <https://doi.org/10.1038/nature10590>
- Fisher MC, Garner TWJ (2020) Chytrid fungi and global amphibian declines. *Nat Rev Microbiol* 18:332–343. <https://doi.org/10.1038/s41579-020-0335-x>
- Boyles JG, Cryan PM, McCracken GF, Kunz TH (2011) Conservation: economic importance of bats in agriculture. *Science* 332:41–42. <https://doi.org/10.1126/SCIENCE.1201366>
- Colón-Gaud C, Whiles MR, Kilham SS, Lips KR, Pringle CM, Connelly S, Peterson SD (2009) Assessing ecological responses to catastrophic amphibian declines: patterns of macroinvertebrate production and food web structure in upland Panamanian streams. *Limnol Oceanogr* 54:331–343. <https://doi.org/10.4319/LO.2009.54.1.0331>
- Fisher MC, Hawkins NJ, Sanglard D, Gurr SJ (2018) Worldwide emergence of resistance to antifungal drugs challenges human health and food security. *Science* 360:739–742. <https://doi.org/10.1126/SCIENCE.AAP7999>
- Food and Agriculture Organization of the United Nations (2017) Strategic work of FAO for sustainable food and agriculture. 6488EN/1/01.17
- Ashraf N, Kubat RC, Poplin V, Adenis AA, Denning DW, Wright L, McCotter O, Schwartz IS, Jackson BR, Chiller T, Bahr NC (2020) Re-drawing the maps for endemic mycoses. *Mycopathologia* 185:843–865. <https://doi.org/10.1007/s11046-020-00431-2>
- Rodrigues ML, Nosanchuk JD (2020) Fungal diseases as neglected pathogens: a wake-up call to public health officials. *PLoS Negl Trop Dis* 14:e0007964. <https://doi.org/10.1371/JOURNAL.PNTD.0007964>
- Pristov KE, Ghannoum MA (2019) Resistance of *Candida* to azoles and echinocandins worldwide. *Clin Microbiol Infect* 25:792–798. <https://doi.org/10.1016/j.cmi.2019.03.028>
- García-Rubio R, Mellado C-E, E. (2017) Triazole resistance in *Aspergillus* species: an emerging problem. *Drugs* 77:599–613. <https://doi.org/10.1007/s40265-017-0714-4>
- Forsberg K, Woodworth K, Walters M, Berkow EL, Jackson B, Chiller T, Vallabhaneni S (2019) *Candida auris*: the recent emergence of a multidrug-resistant fungal pathogen. *Med Mycol* 57:1–12. <https://doi.org/10.1093/MMY/MYY054>
- Lockhart SR, Etienne KA, Vallabhaneni S, Farooqi J, Chowdhary A, Govender NP et al (2017). Simultaneous emergence of multidrug-resistant *Candida auris* on 3 continents confirmed by whole-genome sequencing and epidemiological analyses. *Clin Infect Dis* 64:134–140. <https://doi.org/10.1093/CID/CJW691>
- Goel RR, Apostolidis SA, Painter MM, Mathew D, Pattekar A, Kuthuru O, Gouma S, Hicks P et al (2021) Distinct antibody and memory B cell responses in SARS-CoV-2 naïve and recovered individuals following mRNA vaccination. *Sci Immunol* 6:1–19. <https://doi.org/10.1126/sciimmunol.abi6950>
- Hoque MN, Akter S, Mishu ID, Islam MR, Rahman MS, Akhter M, Islam I, Hasan MM et al (2021) Microbial co-infections in COVID-19: associated microbiota and underlying mechanisms of pathogenesis. *Microb Pathog* 156:104941. <https://doi.org/10.1016/j.micpath.2021.104941>
- Martins AC, Psaltikidis EM, Lima TC, Fagnani R, Schreiber AZ, Conterno LO, Kamei K et al (2021) COVID-19 and invasive fungal coinfections: a case series at a Brazilian referral hospital. *J Mycol Med* 31:101175. <https://doi.org/10.1016/j.mycmed.2021.101175>
- Rezasoftani S, Yadegar A, Hatami B, Aghdaei HA, Zali MR (2020) Antimicrobial resistance as a hidden menace lurking behind the COVID-19 outbreak: the global impacts of too much hygiene on AMR. *Front Microbiol* 11:3097. <https://doi.org/10.3389/fmicb.2020.590683>
- Ansari S, Hays JP, Kemp A, Okechukwu R, Murugaiyan J, Ekwanzala MD, Alvarez MJR, Paul-Satyaseela M et al (2021) The potential impact of the COVID-19 pandemic on global antimicrobial and biocide resistance: an AMR Insights global perspective. *JAC Antimicrob Resist* 3:dbl038. <https://doi.org/10.1093/JACAMR/DLAB038>
- Knight GM, Glover RE, McQuaid CF, Olanu ID, Gallandat K, Leclerc QJ, Fuller NM et al (2021) Antimicrobial resistance and

- COVID-19: Intersections and implications. *Elife* 10:1–27. <https://doi.org/10.7554/ELIFE.64139>
24. Rusic D, Vilovic M, Bukic J, Leskur D, Perisin AS, Kumric M, Martinovic D, Petric A, Modun D, Bozic J (2021) Implications of COVID-19 pandemic on the emergence of antimicrobial resistance: adjusting the response to future outbreaks. *Elife* 11:220. <https://doi.org/10.3390/LIFE11030220>
 25. Moretta A, Scieuzo C, Petrone AM, Salvia R, Manniello MD, Franco A, Lucchetti D, Vassallo A, Vogel H, Sgambato A, Falabella P (2021) Antimicrobial peptides: a new hope in biomedical and pharmaceutical fields. *Front Cell Infect Microbiol* 11:668632. <https://doi.org/10.3389/FCIMB.2021.668632>
 26. Li X, Zuo S, Wang B, Zhang K, Wang Y (2022) Antimicrobial mechanisms and clinical application prospects of antimicrobial peptides. *Molecules* 27:2675. <https://doi.org/10.3390/MOLECULES27092675>
 27. Mello EO, Taveira GB, Carvalho AO, Gomes VM (2019) Improved smallest peptides based on positive charge increase of the γ -core motif from *PvD₁* and their mechanism of action against *Candida* species. *Int J Nanomedicine* 14:407–420. <https://doi.org/10.2147/IJN.S187957>
 28. Souza GS, Carvalho LP, Melo EJT, Silva FCV, Machado OLT, Gomes VM, Carvalho AO (2019) A synthetic peptide derived of the β 2– β 3 loop of the plant defensin from *Vigna unguiculata* seeds induces *Leishmania amazonensis* apoptosis-like cell death. *Amino Acids* 51:1633–1648. <https://doi.org/10.1007/S00726-019-02800-8>
 29. Toledo EB, Lucas DR, Simão TLBV, Calixto SD, Lassouskaia E, Muzitano MF, Damica FZ, Gomes VM, Carvalho AO (2021) Design of improved synthetic antifungal peptides with targeted variations in charge, hydrophobicity and chirality based on a correlation study between biological activity and primary structure of plant defensin γ -cores. *Amino Acids* 53:219–237. <https://doi.org/10.1007/S00726-020-02929-X>
 30. Schäfer AB, Wenzel M (2020) A how-to guide for mode of action analysis of antimicrobial peptides. *Front Cell Infect Microbiol* 10:540898. <https://doi.org/10.3389/FCIMB.2020.540898>
 31. Soares JR, Melo JTM, da Cunha M, Fernandes KVS, Taveira GB, Silva Pereira L et al (2017) Interaction between the plant *ApDef* defensin and *Saccharomyces cerevisiae* results in yeast death through a cell cycle- and caspase-dependent process occurring via uncontrolled oxidative stress. *Biochim Biophys Acta Gen Subj* 1861:3429–3443. <https://doi.org/10.1016/J.BBAGEN.2016.09.005>
 32. Grosfeld EV, Bidiuk VA, Mitkevich OV, Ghazy ESMO, Kushnirov VV, Alexandrov AI (2021) A systematic survey of characteristic features of yeast cell death triggered by external factors. *J Fungi* 7:886. <https://doi.org/10.3390/JOF7110886>
 33. Berridge MV, Tan HPM, AS. (2005) Tetrazolium dyes as tools in cell biology: new insights into their cellular reduction. *Biotechnol Annu Rev* 11:127–152. [https://doi.org/10.1016/S1387-2656\(05\)11004-7](https://doi.org/10.1016/S1387-2656(05)11004-7)
 34. Tsukatani T, Oba T, Ukeda H, Matsumoto K (2003) Spectrophotometric assay of yeast vitality using 2,3,5,6-tetramethyl-1,4-benzoquinone and tetrazolium salts. *Anal Sci* 19:659–664. <https://doi.org/10.2116/ANALSCI.19.659>
 35. Barreto-Santamaria A, Patarroyo ME, Curtidor H (2019) Designing and optimizing new antimicrobial peptides: all targets are not the same. *Crit Rev Clin Lab Sci* 56:351–373. <https://doi.org/10.1080/10408363.2019.1631249>
 36. Torres MDT, Sothiselvan S, Lu TK, de la Fuente-Nunez C (2019) Peptide design principles for antimicrobial applications. *J Mol Biol* 431:3547–3567. <https://doi.org/10.1016/j.jmb.2018.12.015>
 37. Thevissen K, Terras FRG, Broekaert WF (1999) Permeabilization of fungal membranes by plant defensins inhibits fungal growth. *Appl Environ Microbiol* 65:5451–5458. <https://doi.org/10.1128/AEM.65.12.5451-5458.1999>
 38. Schmitt P, Rosa RD, Destoumieux-Garçon D (2016) An intimate link between antimicrobial peptide sequence diversity and binding to essential components of bacterial membranes. *Biochim Biophys Acta (BBA) - Biomembr* 1858:958–970. <https://doi.org/10.1016/J.BBAMEM.2015.10.011>
 39. Chang CK, Lan KMC, CY. (2021) Antimicrobial activity of the peptide LfcinB15 against *Candida albicans*. *J fungi* 7:519. <https://doi.org/10.3390/JOF7070519>
 40. Park CB, Kim HS, Kim SC (1998) Mechanism of action of the antimicrobial peptide buforin II: buforin II kills microorganisms by penetrating the cell membrane and inhibiting cellular functions. *Biochem Biophys Res Commun* 244:253–257. <https://doi.org/10.1006/BBRC.1998.8159>
 41. Aerts AM, François IEJA, Meert EMK, Li QT, Cammue BPA, Thevissen K (2007) The antifungal activity of *RsaAPP₂*, a plant defensin from *Raphanus sativus*, involves the induction of reactive oxygen species in *Candida albicans*. *Microb Physiol* 13:243–247. <https://doi.org/10.1159/000104753>
 42. Mello EO, Ribeiro SFF, Carvalho AO, Santos JS, da Cunha M, Santa-Catarina C, Gomes VM (2011) Antifungal activity of *PvD₁* defensin involves plasma membrane permeabilization, inhibition of medium acidification, and induction of ROS in fungi cells. *Curr Microbiol* 62:1209–1217. <https://doi.org/10.1007/S00284-010-9847-3>
 43. He J, Krauson AJ, Wimley WC (2014) Toward the de novo design of antimicrobial peptides: lack of correlation between peptide permeabilization of lipid vesicles and antimicrobial, cytolytic, or cytotoxic activity in living cells. *Peptide Sci* 102:1–6. <https://doi.org/10.1002/BIP.22281>
 44. Muñoz A, Gandía M, Harries E, Carmona L, Read ND, Marcos JF (2013) Understanding the mechanism of action of cell-penetrating antifungal peptides using the rationally designed hexapeptide PAF26 as a model. *Fungal Biol Rev* 26:146–155. <https://doi.org/10.1016/J.FBR.2012.10.003>
 45. Peschel A, Jack RW, Otto M, Collins LV, Staubitz P, Nicholson G, Kalbacher H, Nieuwenhuizen WF, Jung G et al (2001) *Staphylococcus aureus* resistance to human defensins and evasion of neutrophil killing via the novel virulence factor MprF is based on modification of membrane lipids with L-lysine. *Exp Med* 193:1067–1076. <https://doi.org/10.1084/JEM.193.9.1067>
 46. Abdi M, Mirkalantari S, Amirzofafari N (2019) Bacterial resistance to antimicrobial peptides. *J Pept Sci* 25e3210. <https://doi.org/10.1002/PSC.3210>
 47. Kusch H, Engelmann S, Albrecht D, Morschhäuser J, Hecker M (2007) Proteomic analysis of the oxidative stress response in *Candida albicans*. *Proteomics* 7:686–697. <https://doi.org/10.1002/PMIC.200600575>
 48. Bortner CD, Cidlowski JA (2020) Ions, the movement of water and the apoptotic volume decrease. *Front Cell Dev Biol* 8:611211. <https://doi.org/10.3389/FCCELL.2020.611211>
 49. Arrigoni O, de Tullio MC (2002) Ascorbic acid: much more than just an antioxidant. *Biochim Biophys Acta Gen Subj* 1569:1–9. [https://doi.org/10.1016/S0304-4165\(01\)00235-5](https://doi.org/10.1016/S0304-4165(01)00235-5)
 50. Lee W, Lee DG (2017) Reactive oxygen species modulate itraconazole-induced apoptosis via mitochondrial disruption in *Candida albicans*. *Free Radic Res* 52:39–50. <https://doi.org/10.1080/10715762.2017.1407412>
 51. Hayes BME, Bleackley MR, Wiltshire JL, Anderson MA, Traven A, van der Weerden NL (2013) Identification and mechanism of action of the plant defensin *NaD₁* as a new member of the antifungal drug arsenal against *Candida albicans*. *Antimicrob Agents Chemother* 57:3667–3675. <https://doi.org/10.1128/AAC.00365-13>
 52. Guaragnella N, Passarella S, Marra E, Giannattasio S (2010) Knock-out of metacaspase and/or cytochrome c results in the activation of a ROS-independent acetic acid-induced programmed cell death pathway in yeast. *FEBS Lett* 584:3655–3660. <https://doi.org/10.1016/J.FEBSLET.2010.07.044>

53. Bullock CB, McNabb DS, Pinto I (2020) Whole-genome approach to understanding the mechanism of action of a histatin 5-derived peptide. *Antimicrob Agents Chemother* 64:e01698–e1719. <https://doi.org/10.1128/AAC.01698-19>
54. Machida K, Tanaka T (1999) Farnesol-induced generation of reactive oxygen species dependent on mitochondrial transmembrane potential hyperpolarization mediated by F_1F_0 -ATPase in yeast. *FEBS Lett* 462:108–112. [https://doi.org/10.1016/S0014-5793\(99\)01506-9](https://doi.org/10.1016/S0014-5793(99)01506-9)
55. Andrés MT, Viejo-Díaz M, Fierro JF (2008) Human lactoferrin induces apoptosis-like cell death in *Candida albicans*: critical role of K^+ -channel-mediated K^+ efflux. *Antimicrob Agents Chemother* 52:4081–4088. <https://doi.org/10.1128/AAC.01597-07>
56. Ojha R, Khan L, Manzoor N (2009) Ascorbic acid modulates pathogenicity markers of *Candida albicans*. *Int J Microbiol Res* 1:19–24. <https://doi.org/10.9735/0975-5276.1.1.19-24>
57. Costa V, Moradas-Ferreira P (2001) Oxidative stress and signal transduction in *Saccharomyces cerevisiae*: insights into ageing, apoptosis and diseases. *Mol Aspects Med* 22:217–246. [https://doi.org/10.1016/S0098-2997\(01\)00012-7](https://doi.org/10.1016/S0098-2997(01)00012-7)
58. Rinnerthaler M, Büttner S, Laun P, Heeren G, Felder TK, Klingler H, Weinberger M et al (2012) Yno1p/Aim14p, a NADPH-oxidase ortholog, controls extramitochondrial reactive oxygen species generation, apoptosis, and actin cable formation in yeast. *Proc Natl Acad Sci USA* 109:8658–8663. <https://doi.org/10.1073/pnas.1201629109>
59. Schippers JHM, Nguyen HM, Lu D, Schmidt R, Mueller-Roeber B (2012) ROS homeostasis during development: an evolutionary conserved strategy. *Cell Mol Life Sci* 69:3245–3257. <https://doi.org/10.1007/S00018-012-1092-4>
60. Arooma OI, Halliwell B, Hoey BM, Butler J (1989) The antioxidant action of N-acetylcysteine: its reaction with hydrogen peroxide, hydroxyl radical, superoxide, and hypochlorous acid. *Free Radic Biol Med* 6:593–597. [https://doi.org/10.1016/0891-5849\(89\)90066-X](https://doi.org/10.1016/0891-5849(89)90066-X)
61. Aldini G, Altomare A, Baron G, Vistoli G, Carini M, Borsani L, Sergio F (2018) N-Acetylcysteine as an antioxidant and disulphide breaking agent: the reasons why. *Free Radic Res* 52:751–762. <https://doi.org/10.1080/10715762.2018.1468564>
62. Pécsi I, Prade RA, Penninckx MJ (2004) Glutathione, altruistic metabolite in fungi. *Adv Microb Physiol* 49:1–76. [https://doi.org/10.1016/S0065-2911\(04\)9001-8](https://doi.org/10.1016/S0065-2911(04)9001-8)
63. Toledano MB, Delaunay-Moisan A, Outten CE, Igbaria A (2013) Functions and cellular compartmentation of the thioredoxin and glutathione pathways in yeast. *Antioxid Redox Signal* 18:699–1711. <https://doi.org/10.1089/ARS.2012.5033>
64. Kumar C, Igbaria A, D'Autreaux B, Planson AG, Junot C, Godat E, Bachhawat AK, Delaunay-Moisan A, Toledano MB (2011) Glutathione revisited: a vital function in iron metabolism and ancillary role in thiol-redox control. *EMBO J* 30:2044–2056. <https://doi.org/10.1038/EMBOJ.2011.105>
65. Madoe F, Fröhlich E, Ligr M, Grey M, Sigris SJ, Wolf DH, Fröhlich KU (1999) Oxygen stress: a regulator of apoptosis in yeast. *J Cell Biol* 145:757–767. <https://doi.org/10.1083/JCB.145.4.757>
66. Chaves SR, Rego A, Martins VM, Santos-Pereira C, Sousa MJ, Côrte-Real M (2021) Regulation of cell death induced by acetic acid in yeasts. *Front Cell Dev Biol* 9:642375. <https://doi.org/10.3389/fcell.2021.642375>
67. Carmona-Gutierrez D, Bauer MA, Zimmermann A, Aguilera A, Austriaco N, Ayseough K, Balzan R, Bar-Nun S, Barrientos A et al (2018) Guidelines and recommendations on yeast cell death nomenclature. *Microbial Cell* 5:4–31. <https://doi.org/10.15698/MIC2018.01.607>
68. Walker GM (1999) Synchronization of yeast cell populations. *Methods Cell Sci* 21:87–93. <https://doi.org/10.1023/A:1009824520278>
69. Yun JE, Lee DG (2017) Role of potassium channels in chlorogenic acid-induced apoptotic volume decrease and cell cycle arrest in *Candida albicans*. *Biochim Biophys Acta Gen Subj* 1861:585–592. <https://doi.org/10.1016/J.BBAGEN.2016.12.026>
70. Baev D, Li XS, Dong J, Keng P, Edgerton M (2002) Human salivary histatin 5 causes disordered volume regulation and cell cycle arrest in *Candida albicans*. *Infect Immun* 70:4777–4784. <https://doi.org/10.1128/IAI.70.9.4777-4784.2002>
71. Kwon YY, Choi KM, Cho CY, Lee CK (2015) Mitochondrial efficiency-dependent viability of *Saccharomyces cerevisiae* mutants carrying individual electron transport chain component deletions. *Mol Cells* 38:1054–1063. <https://doi.org/10.14348/MOLCELLS.2015.0153>
72. Zhao RZ, Jiang S, Zhang L, Yu Z (2019) Mitochondrial electron transport chain, ROS generation and uncoupling. *Int J Mol Med* 44(3–15):72. <https://doi.org/10.3892/IJMM.2019.4188/HTML>
73. Venditti P, di Stefano L, di Meo S (2013) Mitochondrial metabolism of reactive oxygen species. *Int J Mol Med Adv Sci* 13:71–82. <https://doi.org/10.1016/J.MITO.2013.01.008>
74. Mailloux RJ (2015) Teaching the fundamentals of electron transfer reactions in mitochondria and the production and detection of reactive oxygen species. *Redox Biol* 4:381–398. <https://doi.org/10.1016/J.REDOX.2015.02.001>
75. Napolitano G, Fasciolo G, Venditti P (2021) Mitochondrial management of reactive oxygen species. *antioxidants* 10:1824. <https://doi.org/10.3390/ANTIOX10111824>
76. Robb EL, Hall AR, Prime TA, Eaton S, Szibor M, Viscomi C, James AM, Murphy MP (2018) Control of mitochondrial superoxide production by reverse electron transport at complex I. *J Biol Chem* 293:9869–9879. <https://doi.org/10.1074/JBC.RA118.003647>
77. Milani G, Jarmuszkiewicz W, Sluse-Goffart CM, Schreiber AZ, Vercesi AE, Sluse FE (2001) Respiratory chain network in mitochondria of *Candida parapsilosis*: ADP/O appraisal of the multiple electron pathways. *FEBS Lett* 508:231–235. [https://doi.org/10.1016/S0014-5793\(01\)03060-5](https://doi.org/10.1016/S0014-5793(01)03060-5)
78. Ruy F, Vercesi AE, Kowaltowski AJ, Ruy F, Vercesi AE, Kowaltowski AJ (2006) Inhibition of specific electron transport pathways leads to oxidative stress and decreased *Candida albicans* proliferation. *J Bioenerg Biomem* 38(29–135):78. <https://doi.org/10.1007/S10863-006-9012-7>
79. Castro A, Lemos C, Falcão A, Glass NL, Videira A (2008) Increased resistance of complex I mutants to phytohemagglutinin-induced programmed cell death. *J Biol Chem* 283:19314–19321. <https://doi.org/10.1074/JBC.M802112200>
80. Li D, Chen H, Florentino A, Alex D, Sikorski P, Fonzi WA, Calderone R (2011) Enzymatic dysfunction of mitochondrial complex I of the *Candida albicans* goal1 mutant is associated with increased reactive oxidants and cell death. *Eukaryot Cell* 10:672–68280. <https://doi.org/10.1128/EC.00303-10>
81. Xu Y, Wang Y, Yam L, Liang RM, di Dai B, Tang RJ, Gao PH, Jiang YY (2009) Proteomic analysis reveals a synergistic mechanism of fluconazole and berberine against fluconazole-resistant *Candida albicans*: endogenous ROS augmentation. *J Proteome Res* 8:5296–5304. <https://doi.org/10.1021/PR9005074>
82. Wu XZ, Cheng AX, Sun LM, Sun SJ, Lou HX (2009) Plagiochin E, an antifungal bis(benzyl), exerts its antifungal activity through mitochondrial dysfunction-induced reactive oxygen species accumulation in *Candida albicans*. *Biochim Biophys Acta (BBA) - Gen Subj* 1790:770–777. <https://doi.org/10.1016/J.BBAGEN.2009.05.002>
83. Ramzan R, Michels S, Weber P, Rhiel A, Iqbal M, Rastan AJ, Culmsee C, Vogt S (2019) Protamine sulfate induces mitochondrial hyperpolarization and a subsequent increase in reactive oxygen species production. *J Pharmacol Exp Ther* 370:308–317. <https://doi.org/10.1124/JPET.119.257725>
84. Skulachev VP (2006) Bioenergetic aspects of apoptosis, necrosis and mitoptosis. *Apoptosis* 11:473–485. <https://doi.org/10.1007/S10495-006-5881-9>
85. Pozniakovskiy AI, Knorre DA, Ov M, Hyman AA, Skulachev VP, Severin FF (2005) Role of mitochondria in the pheromone- and

- amiodarone-induced programmed death of yeast. *J Cell Biol* 168:257–269. <https://doi.org/10.1083/JCB.200408145>
86. Gabaldón T, Rainey D, Huynen MA (2005) Tracing the evolution of a large protein complex in the eukaryotes. NADH:ubiquinone oxidoreductase (Complex I). *J Mol Biol* 348:857–870. <https://doi.org/10.1016/J.JMB.2005.02.067>
 87. Guaragnella N, Ždravlević M, Antonacci L, Passarella S, Marra E, Giannattasio S (2012) The role of mitochondria in yeast programmed cell death. *Front Oncol* 2:70. <https://doi.org/10.3389/FONC.2012.00070>
 88. Madeo F, Herker E, Maldener C, Wissing S, Lächelt S, Herlan M, Fehr M, Lauber K, Sigris SJ, Wesselborg S, Fröhlich KU (2002) A caspase-related protease regulates apoptosis in yeast. *Mol Cell* 9:911–917. [https://doi.org/10.1016/S1097-2765\(02\)00501-4](https://doi.org/10.1016/S1097-2765(02)00501-4)
 89. Hardwick JM (2018) Do fungi undergo apoptosis-like programmed cell death? *mBio* 9:e00948–18. <https://doi.org/10.1128/MBIO.00948-18>
 90. Acerts AM, Carmona-Gutierrez D, Lefevre S, Govaert G, François IEJA, Madeo F, Santos R, Cammue BPA, Thevissen K (2009) The antifungal plant defensin RsAFP₂ from radish induces apoptosis in a metacaspase independent way in *Candida albicans*. *FEBS Lett* 583:2513–2516. <https://doi.org/10.1016/J.FEBSLET.2009.07.004>
 91. Taveira GB, Mello EO, Souza SB, Monteiro RM, Ramos AC, Carvalho AO, Rodrigues R, Okorokov LA, Gomes VM (2018) Programmed cell death in yeast by thionin-like peptide from *Capsicum annuum* fruits involving activation of caspases and extracellular H⁺ flux. *Biosci Rep* 38:BSR20180119. <https://doi.org/10.1042/BSR20180119/57557>
 92. Cao YY, Huang S, di Dai B, Zhu ZY, Lu H, Dong LL, Cao YB, Wang Y, Gao PH, Chai YF, Jiang YY (2009) *Candida albicans* cells lacking CaMCA1-encoded metacaspase show resistance to oxidative stress-induced death and change in energy metabolism. *Fungal Genet Biol* 46:183–189. <https://doi.org/10.1016/J.FGB.2008.11.001>
 93. Guaragnella N, Pereira C, Sousa MJ, Antonacci L, Passarella S, Corte-Real M, Marra E, Giannattasio S (2006) YCA1 participates in the acetic acid induced yeast programmed cell death also in a manner unrelated to its caspase-like activity. *FEBS Lett* 580:6880–6884. <https://doi.org/10.1016/J.FEBSLET.2006.11.050>
 94. Liang Q, Li W, Zhou B (2008) Caspase-independent apoptosis in yeast. *Biochim Biophys Acta* 1783:1311–1319. <https://doi.org/10.1016/J.BBAMCR.2008.02.018>
 95. Morton CO, dos Santos SC, Coote P (2007) An amphibian-derived, cationic, α -helical antimicrobial peptide kills yeast by caspase-independent but AIF-dependent programmed cell death. *Mol Microbiol* 65:494–507. <https://doi.org/10.1111/J.1365-2958.2007.05801.X>
 96. Xu Y, Ambudkar I, Yamagishi H, Swaim W, Walsh TJ, O'Connell BC (1999) Histatin 3-mediated killing of *Candida albicans*: effect of extracellular salt concentration on binding and internalization. *Antimicrob Agents Chemother* 43:2256–2262. <https://doi.org/10.1128/AAC.43.9.2256>
 97. Lee H, Woo ER, Lee DG (2018) Apigenin induces cell shrinkage in *Candida albicans* by membrane perturbation. *FEMS Yeast Res* 18:foy003. <https://doi.org/10.1093/FEMSYR/FOY003>
 98. Nam M, Kim SH, Jeong JH, Kim S, Kim J (2022) Roles of the pro-apoptotic factors CaNma111 and CaYbh3 in apoptosis and virulence of *Candida albicans*. *Sci Rep* 12:1–9. <https://doi.org/10.1038/s41598-022-11682-y>

Publisher's Note Springer Nature remains neutral with regard to jurisdictional claims in published maps and institutional affiliations.

Springer Nature or its licensor (e.g. a society or other partner) holds exclusive rights to this article under a publishing agreement with the author(s) or other rightsholder(s); author self-archiving of the accepted manuscript version of this article is solely governed by the terms of such publishing agreement and applicable law.

4.2 Figura Suplementar

Probiotics and Antimicrobial Proteins

Supplementary data

Bioinspired peptides induce different cell death mechanisms against opportunistic yeasts

Douglas Ribeiro Lucas¹, Filipe Zaniratti Damica¹, Estefany Braz Toledo¹, Antônio Jesus Dorighetto Cogo¹, Anna Lvovna Okorokova-Façanha¹, Valdirene Moreira Gomes¹, André de Oliveira Carvalho^{1*}

¹Laboratório de Fisiologia e Bioquímica de Microrganismos, Centro de Biociências e Biotecnologia, Universidade Estadual do Norte Fluminense Darcy Ribeiro, Campos dos Goytacazes-RJ, 28013-602, Brazil.

Douglas Ribeiro Lucas, Filipe Zaniratti Damica and Estefany Braz Toledo contributed equally to this work.

*Corresponding author: André de Oliveira Carvalho, Av. Alberto Lamago, nº 2000, Laboratório de Fisiologia e Bioquímica de Microrganismos, Centro de Biociências e Biotecnologia, Universidade Estadual do Norte Fluminense Darcy Ribeiro, Parque Califórnia, Campos dos Goytacazes, RJ, Brazil, CEP 28013-602; Tel (+55) 22 2739-7217; E-mail address: andre@uenf.br

Abbreviations

AA, L-ascorbic acid; AcA, acetic acid; ACD, accidental cell death; AMP, antimicrobial peptides; CoQ, coenzyme Q; CFU, Colony forming units; DAPI, 4',6-diamidino-2-phenylindole; DIC, differential interference contrast; DMSO, dimethyl sulfoxide; D-RR, D-A₃₆₊₄₂₊₄₄R₃₇₊₃₈Y₃₂₋₄₆VuDef; ETC, electron transport chain; GSH, γ -L-glutamyl-L-cysteinyl-glycine; OH⁻, hydroxyl anion; H₂DCFDA, 2',7'-Dichlorodihydrofluorescein diacetate; $\Delta\psi_m$, mitochondrial membrane potential; O₂, molecular oxygen; NAC, N-acetyl-L-cysteine; nd, not determined; PI, propidium iodide; RET, reverse electron transport; ROS, reactive oxygen species; RR, A₃₆₊₄₂₊₄₄R₃₇₊₃₈Y₃₂₋₄₆VuDef; WR, A₄₂₊₄₄R₃₇₊₃₈W₃₆₊₃₉Y₃₂₋₄₆VuDef; SD, standard deviation.

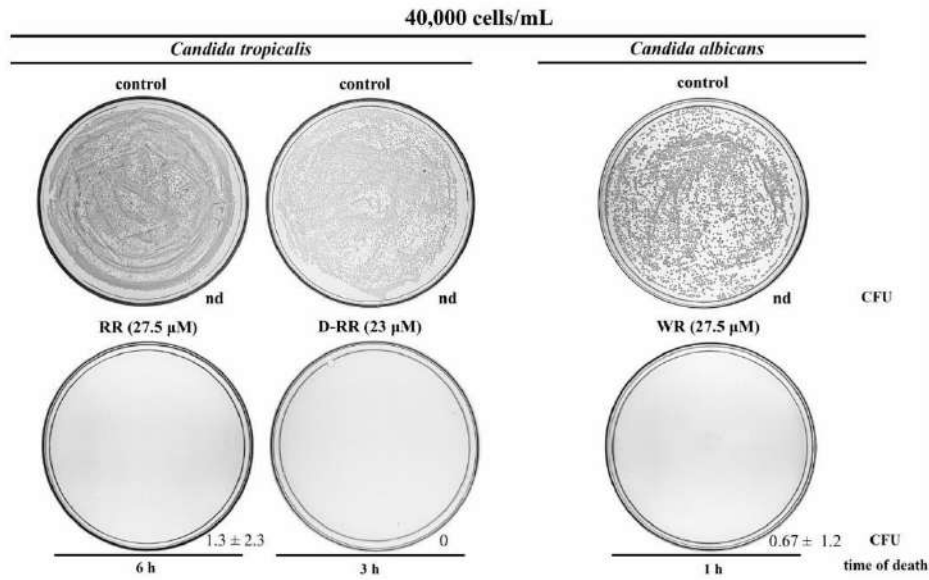


Fig. S1. Determination of cell viability of *Candida tropicalis* incubated with RR at 27.5 μ M for 6 h and D-RR at 23 μ M for 3 h, and *Candida albicans* incubated with WR at 27.5 μ M for 1 h at a cell density of 40,000 cells/mL. The specified times correspond to the time of death of each peptide for each yeast and the concentrations the LD₁₀₀ of each peptide. Note that even with the larger number of cells the bioinspired peptides maintained their toxicities on yeasts. Colony forming units (CFU) are different in controls because the incubation times are different according to the time of death of each peptide. CFU as means with standard deviation. (nd), excessive number of grown colonies that prevented colony counting. The assay is representative of an independent assay out of three.

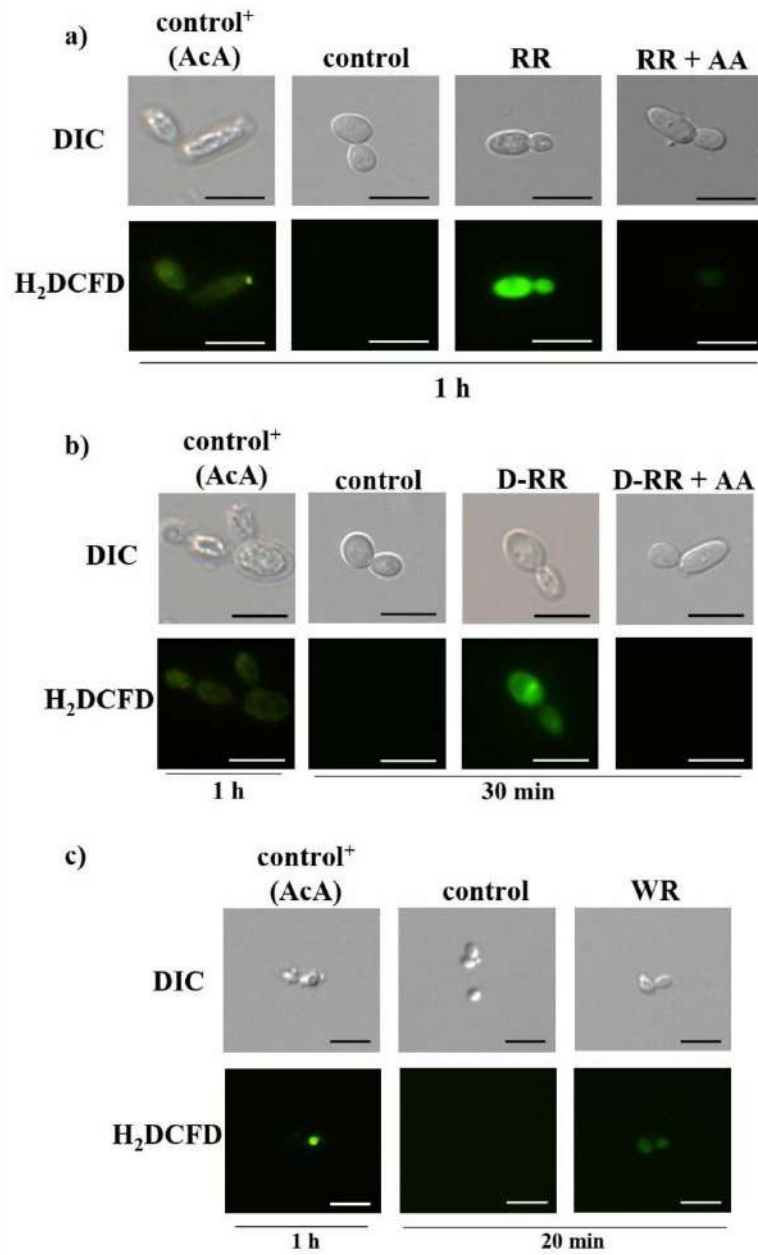


Fig. S2. Reactive oxygen species (ROS) detection in (a) *Candida tropicalis* cells incubated with 27.5 μM RR for 1 h, (b) *C. tropicalis* cells incubated with 23 μM D-RR for 30 min, and (c) *Candida albicans* cells incubated with 27.5 μM WR for 20 min. Acetic acid was used as positive control (control⁺). The H₂DCFDA green fluorescence in the cytoplasm indicates endogenous ROS production. The scale bar represents 10 μm. The assay is representative of an independent assay out of three.

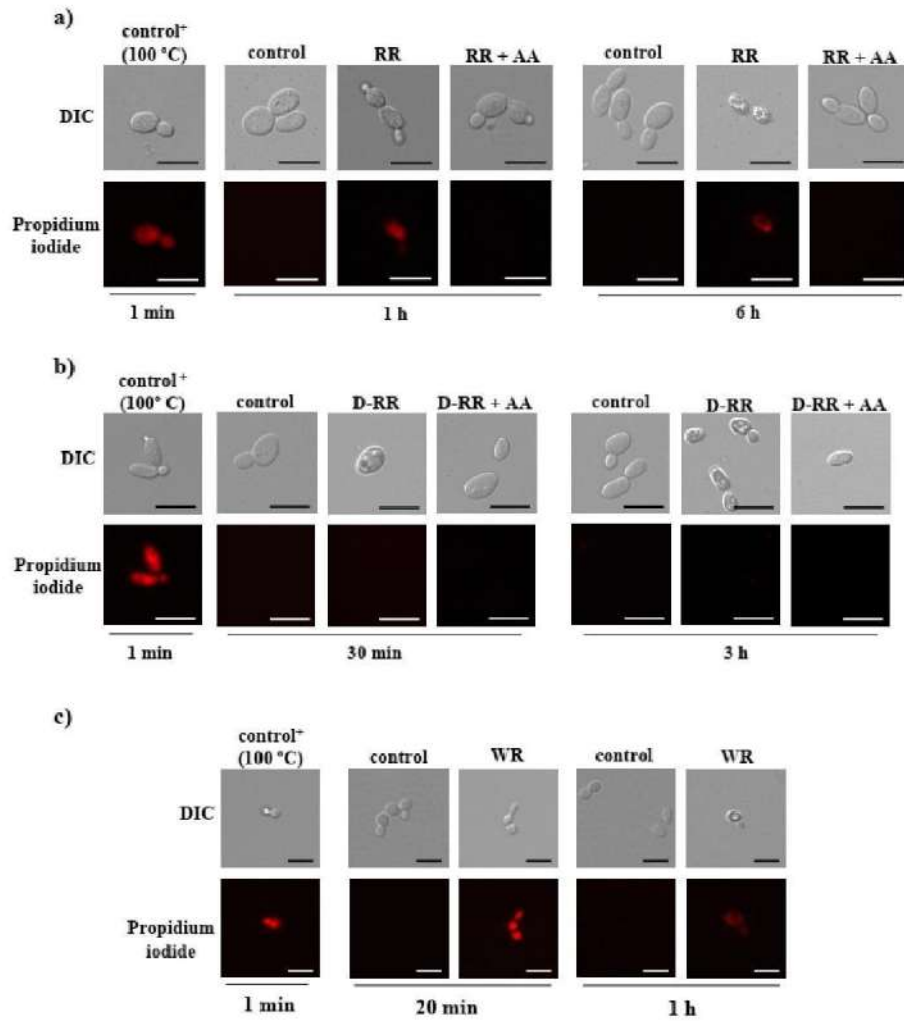


Fig. S3. Microscopic images of yeast cells incubated with propidium iodide (PI). PI red fluorescence in the cytoplasm indicates accidental cell death (necrosis). Ascorbic acid (AA) reversed necrosis. Scale bar represents 10 μ m.

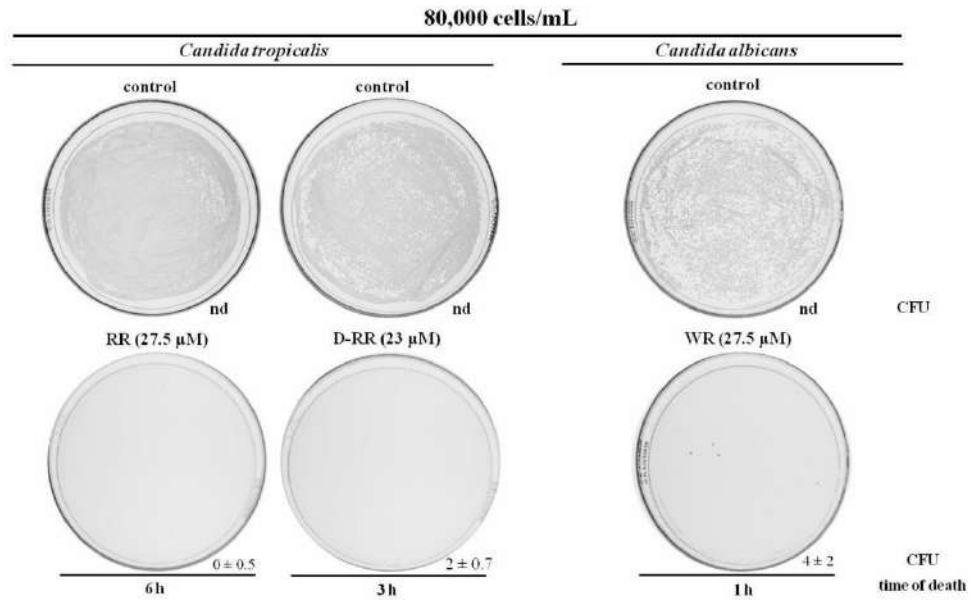


Fig. S4 Determination of cell viability of *Candida tropicalis* incubated with RR at 27.5 μ M for 6 h and D-RR at 23 μ M for 3 h, and *Candida albicans* incubated with WR at 27.5 μ M for 1 h at a cell density of 80,000 cells/mL. The specified times correspond to the time of death of each peptide for each yeast. Note that even with the larger number of cells the bioinspired peptides maintained their toxicities on yeasts. Colony forming units (CFU) are different in controls because the incubation times are different according to the time of death of each peptide. CFU as means with standard deviation. (nd), excessive number of grown colonies that prevented colony counting. The assay is representative of an independent assay out of three.

Table S1. Yeasts were incubated with the acetic acid (AcA, control⁺) for 1 h, washed and spread in Petri dish containing Sabouraud agar and incubated for 24 h. For control sample, please refer to Table 2.

samples	yeast	time (h)	CFU
control ⁺ AcA (333 mM)	<i>Candida tropicalis</i>	1	0
control ⁺ AcA (333 mM)	<i>Candida albicans</i>	1	0

CFU = colony forming units.

5- CAPÍTULO 2

A role in intracellular K^+ in protecting pathogenic dimorphic fungi against induced cell death by bioinspired antimicrobial peptides

5. CHAPTER 2: MANUSCRIPT SUBMITTED

A role in intracellular K⁺ in protecting pathogenic dimorphic fungi against induced cell death by bioinspired antimicrobial peptides

Filipe Zaniratti Damica^{a,1}, Douglas Ribeiro Lucas^{a,1}, Estefany Bras Toledo^a, Marilúcia de Carvalho Ribeiro^a, Anna Lvovna Okorokova Façanha^a, Ana Eliza Zeraik^b, Sérgio Henrique Seabra^c, Juliana Azevedo da Silva^d, Valdirene Moreira Gomes^a, André de Oliveira Carvalho^{a,*}

^aLaboratório de Fisiologia e Bioquímica de Microrganismos, Centro de Biociências e Biotecnologia, Universidade Estadual do Norte Fluminense Darcy Ribeiro, Campos dos Goytacazes-RJ, 28013-602, Brasil.

^bLaboratório de Química e Função de Proteínas e Peptídeos, Centro de Biociências e Biotecnologia, Universidade Estadual do Norte Fluminense Darcy Ribeiro, Campos dos Goytacazes-RJ, 28013-602, Brazil.

^cLaboratório de Biologia Celular e Tecidual, Centro de Biociências e Biotecnologia, Universidade Estadual do Norte Fluminense Darcy Ribeiro, Campos dos Goytacazes-RJ, 28013-602, Brazil.

^dLaboratório de Biologia do Reconhecer, Centro de Biociências e Biotecnologia, Universidade Estadual do Norte Fluminense Darcy Ribeiro, Campos dos Goytacazes-RJ, 28013-602, Brazil.

¹**These authors contributed equally to this work.**

Type of article: Research article

Situation: Submitted

Journal: BBA General Subjects

Impact factor: 2.8

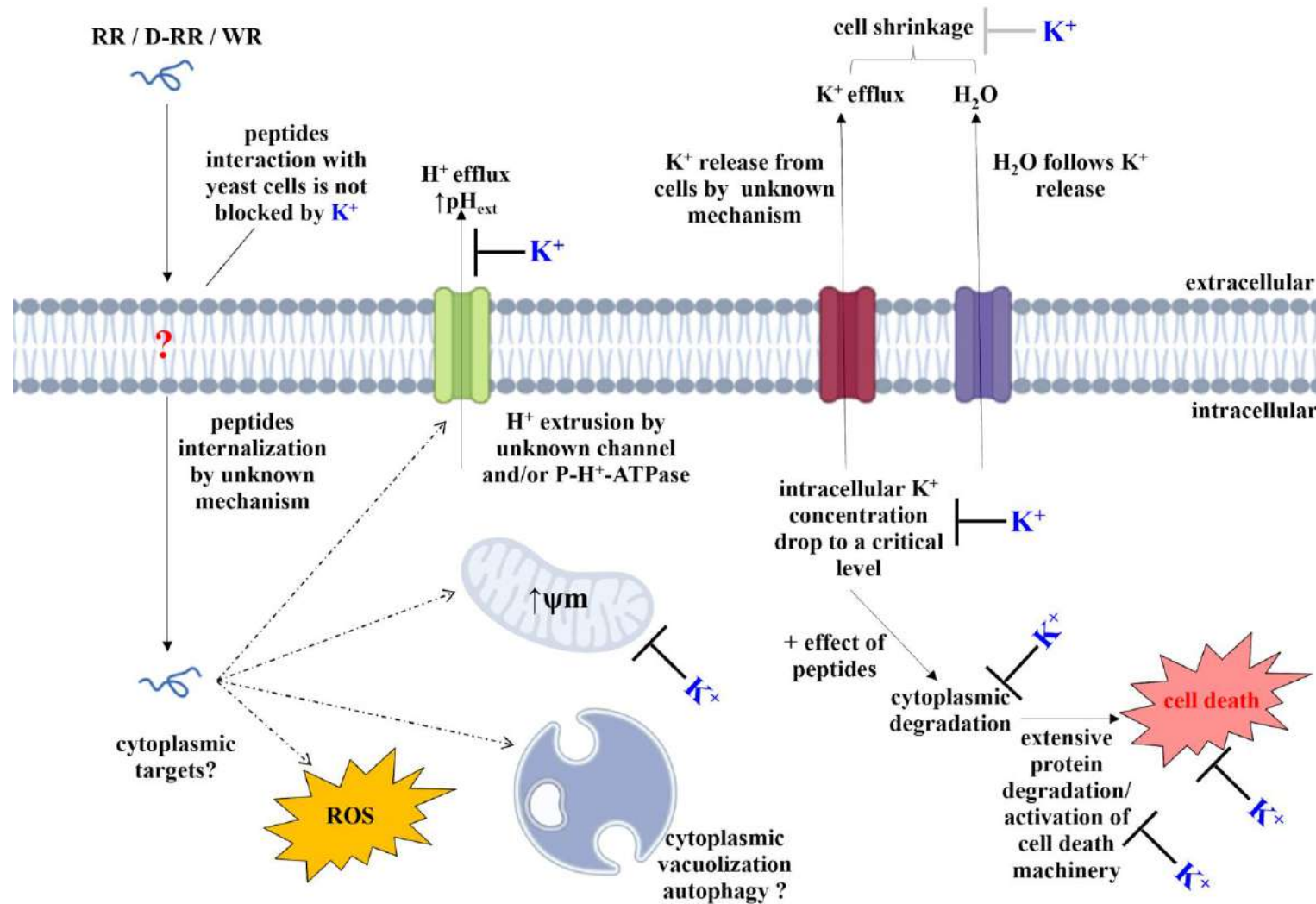
RESUMO

Peptídeos antimicrobianos (AMPs) são medicamentos promissores, embora seus mecanismos de combate a fungos permaneçam parcialmente desconhecidos. Nós projetamos três AMPs (dAMPs) denominados RR, D-RR e WR, e avaliamos suas ações sobre *Candida tropicalis* e *Candida albicans*. Entre suas ações está a redução do volume celular causada pelo efluxo de K^+ das células fúngicas. Investigamos o envolvimento de K^+ na morte fúngica induzida por esses peptídeos. Avaliamos a redução do volume celular, estresse oxidativo, hiperpolarização mitocondrial, permeabilização de membrana, acidificação do meio, atividade antimicrobiana em condições hipo-osmóticas e degradação celular. Ensaio de viabilidade foram realizados com bloqueadores de canais e adição de K^+ em diferentes momentos. As interações dos dAMPs com sais e células fúngicas foram analisadas por difração circular e microscopia. Os canais de K^+ e Cl^- não estiveram diretamente envolvidos na morte induzida pelos dAMPs. A suplementação com K^+ protegeu as células fúngicas da morte. Nos testes, os cátions frequentemente desativaram os peptídeos por neutralização de cargas. Os peptídeos mantiveram sua conformação na presença de K^+ e foram encontrados no citoplasma celular, indicando que K^+ não neutralizou suas cargas. K^+ não preveniu o estresse oxidativo, mas protegeu contra a redução do volume celular e a hiperpolarização mitocondrial. Os dAMPs estimularam rapidamente a acidificação do meio, seguida de inibição após 1 minuto, e K^+ preveniu essa acidificação. A permeabilização da membrana ocorreu após 20 minutos, sendo mais rápida com o peptídeo WR, explicando a ausência de proteção pelos bloqueadores. A morte fúngica foi acelerada em condições hipo-osmóticas. A eletroforese revelou degradação de proteínas, enquanto a análise ultraestrutural das células mostrou vacuolização, indicativa de degradação citoplasmática. Assim, K^+ preveniu a morte celular ao manter seus níveis internos, evitando a ativação do processo de degradação celular.

Palavras-chave

acidificação extracelular; internalização de peptídeos; fluxo iônico; ultraestrutura

5.1 Grafical abstract (Resumo gráfico)



A role in intracellular K^+ in protecting pathogenic dimorphic fungi against induced cell death by bioinspired antimicrobial peptides

Filipe Zaniratti Damica^{a,1}, Douglas Ribeiro Lucas^{a,1}, Estefany Bras Toledo^a, Marilúcia de Carvalho Ribeiro^a, Anna Lvovna Okorokova Façanha^a, Ana Eliza Zeraik^b, Sérgio Henrique Seabra^c, Juliana Azevedo da Silva^d, Valdirene Moreira Gomes^a, André de Oliveira Carvalho^{a,*}

^aLaboratório de Fisiologia e Bioquímica de Microrganismos, Centro de Biociências e Biotecnologia, Universidade Estadual do Norte Fluminense Darcy Ribeiro, Campos dos Goytacazes-RJ, 28013-602, Brasil.

^bLaboratório de Química e Função de Proteínas e Peptídeos, Centro de Biociências e Biotecnologia, Universidade Estadual do Norte Fluminense Darcy Ribeiro, Campos dos Goytacazes-RJ, 28013-602, Brazil.

^cLaboratório de Biologia Celular e Tecidual, Centro de Biociências e Biotecnologia, Universidade Estadual do Norte Fluminense Darcy Ribeiro, Campos dos Goytacazes-RJ, 28013-602, Brazil.

^dLaboratório de Biologia do Reconhecer, Centro de Biociências e Biotecnologia, Universidade Estadual do Norte Fluminense Darcy Ribeiro, Campos dos Goytacazes-RJ, 28013-602, Brazil.

¹These authors contributed equally to this work.

*corresponding author: André de Oliveira Carvalho, Av. Alberto Lamago, nº 2000, Laboratório de Fisiologia e Bioquímica de Microrganismos, Centro de Biociências e Biotecnologia, Universidade Estadual do Norte Fluminense Darcy Ribeiro, Parque Califórnia, Campos dos Goytacazes, RJ, Brazil, CEP 28013-602; Tel (+55) 22 2739-7217; E-mail address: andre@uenf.br

Abbreviations:

AcA, acetic acid; AA, ascorbic acid; 4-AP, 4-aminopyridine; AMP, antimicrobial peptide; dAMP, designed antimicrobial peptide; CFU, colony forming units; DIC, differential interferential contrast; D-RR, D-A_{36,42,44}R_{37,38}γ₃₂₋₄₆VuDef; ΔpH, chemical potential; Δψ, transmembrane potential; 5-FAM, 5-carboxyfluorescein; H₂DCFDA, 2',7'-

dichlorodihydrofluorescein diacetate; FSC, forward light scattering; NPPB, 5-nitro-2-(3-phenylpropylamino) benzoic acid; PI, propidium iodide; ROS, reactive oxygen species; RR, A_{36,42,44}R_{37,38}γ₃₂₋₄₆VuDef; SSC, side light scattering; TEA, tetraethylammonium; WR, A_{42,44}R_{37,38}W_{36,39}γ₃₂₋₄₆VuDef.

Abstract

Antimicrobial peptides (AMPs) are promising drugs, though their fungal combat mechanisms remain partly unclear. We designed three AMPs (dAMPs) named RR, D-RR, WR and assessed their actions on *Candida tropicalis* and *Candida albicans*. Amidst their actions are cell shrinkage caused by K⁺ efflux from fungal cells. K⁺ involvement in fungal death by these peptides was explored. We assessed cell shrinkage, oxidative stress, mitochondria hyperpolarization, membrane permeabilization, medium acidification, antimicrobial activity under hypoosmotic conditions, and cellular degradation. Viability assays were performed with channel blockers and K⁺ addition at various times. The interactions of dAMPs with salts and fungal cells were analyzed using circular dichroism and microscopy. K⁺ and Cl⁻ channels were not directly involved in dAMPs-induced death. Supplementation with K⁺ protected fungal cells from death. In tests, cations often deactivated them through charge neutralization. Peptides maintained their conformation with K⁺ and were found in cell cytoplasm indicating K⁺ did not neutralize charges. K⁺ did not prevent oxidative stress, but protected from cell shrinkage and mitochondria hyperpolarization. dAMPs rapidly stimulated medium acidification, followed by inhibition after 1 min, and K⁺ prevented acidification. Membrane permeabilization occurred after 20 min, faster with WR, explaining lack of protection from blockers. Fungal death was accelerated under hypoosmotic conditions. Electrophoresis revealed protein degradation, while ultrastructural analysis of the cells showed vacuolization, indicative of cytoplasmic degradation. Thus, K⁺ prevented cell death by maintaining internal levels, averting activation of cell degradation process.

Key words

extracellular acidification; internalization of peptides; ion flux, ultrastructure.

1. Introduction

The global incidence of fungal diseases has increased in recent decades, triggered and exacerbated by the growth of the susceptible population, particularly older and

immunocompromised individuals, and is considered a major public health problem [1–4]. Skin mycoses affect more than 1 billion people annually, making cutaneous mycoses one of the world’s most common diseases, and systemic mycoses affect 6.5 million people and cause the death of approximately 3.8 million people per year, ahead of tuberculosis and malaria [1,4–6]. There are also reports of antifungal-resistant fungi, which limits treatment options, and the emergence of new fungal pathogens, such as *Candida auris*, which is intrinsically resistant to available antifungals, further exacerbating the problem of fungal diseases [3,7–9]. In light of this scenario, there is a need to develop new antifungals capable of inhibiting the growth of these microorganisms. Antimicrobial peptides (AMPs) are one such alternative and have attracted considerable interest [10]. As new therapeutic substances, plant defensins are a particularly promising class of AMP that exhibit antifungal activity via different mechanisms, such as interacting with specific lipids, triggering the production of reactive oxygen species (ROS) and inducing cell wall stress [11], with low host toxicity [12,13].

In a previous study, we designed three antimicrobial peptides (dAMPs) based on the γ -core of the *Vu*-Def₁ seed defensin from *Vigna unguiculata* L. Walp. (cowpea). We introduced targeted modifications to their primary structure, altering both amino acid positions and types to increase their net positive charge and hydrophobicity, aiming to enhance their antimicrobial efficacy [14]. These peptides were named A_{36,42,44}R_{37,38}γ₃₂₋₄₆*Vu*Def (abbreviated RR), D-A_{36,42,44}R_{37,38}γ₃₂₋₄₆*Vu*Def (abbreviated D-RR), and A_{42,44}R_{37,38}W_{36,39}γ₃₂₋₄₆*Vu*Def (abbreviated WR). These peptides hold promising clinical relevance due to their potent antifungal activity, combined with their lack of toxicity to mammalian cells, as demonstrated in studies with human monocytes and murine fibroblasts [14]. Understanding the mechanism of action of AMPs on target microorganisms is crucial for their clinical application, thus we set out to investigate the mechanism of action of these three peptides against pathogenic fungi. In a previous study, we established key parameters that will be utilized in this research. *Candida tropicalis* was chosen to study the mechanism of action of RR and D-RR, while *Candida albicans* was selected for WR. We also determined the lethal dose (LD₁₀₀) for each peptide: 27.5 μM for RR and 23 μM for D-RR against *C. tropicalis*, and 27.5 μM for WR against *C. albicans* [14], and we measured the time required for the fungi to die following initial peptide interaction. For *C. tropicalis*, it was 6 h with RR and 3 h with D-RR, while for *C. albicans*, it was 1 h with WR [15]. With these parameters established, we proceeded to investigate the mechanism of action of these peptides against the opportunistic fungi.

We investigated a defined temporal window, starting from the interaction of peptides with fungal cells and continuing through to fungal death. It is important to note that death is a

gradual process initiated by peptide-cell interactions, leading to a series of events that ultimately result in cell death. We systematically organized these events in a temporal sequence to elucidate the initial effects, their interrelationships, and how they culminate in fungal cell death. All three peptides triggered common effects in both *Candida* species studied, including oxidative stress, mitochondrial hyperpolarization, cell shrinkage, cytoplasmic vacuolation, and chromatin condensation [15]. Based on these observations, we reviewed our previous results and proposed that RR induces regulated cell death in *C. tropicalis*, D-RR induced metacaspase-independent regulated cell death in *C. tropicalis*, and WR caused regulated cell death in *C. albicans*, following the nomenclature criteria and death markers suggested by Carmona-Gutiérrez et al. [16]. In earlier work, we showed that when the antioxidant ascorbic acid is co-incubated with the peptides, it protected the fungi from death. However, this protection was lost when the antioxidant was added after peptide exposure, as the death process continued even after the elimination of ROS. For this reason, we suggested that oxidative stress is probably not the primary factor driving fungal cell death. Instead, another event was triggered besides oxidative stress, which continued to occur even in the absence of ROS [15]. Therefore, in this study, we investigated another common effect induced by the three peptides in treated fungi: cell shrinkage. We hypothesized that ion imbalance, particularly K^+ , the primary regulator of cell volume [17-19], might be involved in peptide-induced cell death in both *C. tropicalis* and *C. albicans* [15]. Our findings demonstrate that the addition of exogenous K^+ reverses cell shrinkage, does not prevent ROS production, and blocks mitochondrial hyperpolarization. However, K^+ supplementation does protect fungi from peptide-induced death. This protective effect disappears if K^+ is added after peptide exposure, suggesting that once the peptides initiate their effect, a process is triggered in the fungi that proceed independently of ROS and ion rebalance. We also observed the activation cellular degradation under low cytoplasmic K^+ conditions, which is prevented by K^+ supplementation in the culture medium. This explains why fungal death continued even after K^+ replacement and ROS elimination. Our findings suggest that the dAMPs induced the activation of a cell death machinery which possibly be autophagy.

2. Experimental procedures

All reagents were purchased from Merck-Millipore unless otherwise specified.

2.1. Peptides

The design, preparation, and purity of the three bioinspired peptides $A_{36,42,44}R_{37,38}\gamma_{32-46}VuDef$ (abbreviated RR), $D-A_{36,42,44}R_{37,38}\gamma_{32-46}VuDef$ (abbreviated D-RR) and $A_{42,44}R_{37,38}W_{36,39}\gamma_{32-46}VuDef$ (abbreviated WR) were in accordance with Toledo et al. [14]. Additionally, all three peptides were synthesized conjugated to 5-carboxyfluorescein (5-FAM) fluorophore in their N-terminal portion, with the resulting conjugates denominated 5-FAM_RR, 5-FAM_D-RR and 5-FAM_WR prepared as before but protected from light. The peptides were commercially purchased from Aminotech (São Paulo, Brazil).

2.2. Fungal culture and antimicrobial assay

The dimorphic fungal *Candida tropicalis* (CE017) and *Candida albicans* (CE022) were grown in culture, and antimicrobial tests were carried out following the method described by Toledo et al. [14]. In summary, fresh yeast cultured at 30 °C for 24 h was used to isolate a colony, which was then suspended in Sabouraud broth (containing 5 g/L of meat peptone, 5 g/L of casein peptone, 20 g/L of D(+) glucose, pH 5.6). The yeast cell number in this suspension was determined by direct counting using a Neubauer chamber under an optical microscope (Axio Imager.A2, Zeiss). The antimicrobial assay was conducted in a sterile 96-well microplate (polystyrene, U-bottom, Nunc, Thermo Scientific) with a concentration of 2,000 cells/mL for each yeast strain, along with the lethal dose (LD_{100}) of each peptide (27.5 μ M RR and 23 μ M D-RR for *C. tropicalis*, and 27.5 μ M WR for *C. albicans*), sterilized by filtration (0.22 μ m, Millex-GV, Millipore), and 100 μ L of Sabouraud broth (final volume). The assay was then incubated at 30 °C for the duration required for each peptide to induce cell death: 6 and 3 h for RR and D-RR with *C. tropicalis*, respectively, and 1 h for WR with *C. albicans* [15].

For the viability assay, after the antimicrobial assay, the yeast cells were washed once in Sabouraud broth, plated on Sabouraud agar (5 g/L meat peptone, 5 g/L casein peptone, 20 g/L D (+) glucose, 17 g/L agar, pH 5.6) and then incubated at 30 °C for 24 h. After this period, the number of colony forming units (CFU) was determined. For RR treated cells the samples were diluted fifty folds (x50) before plating. The LD_{100} referred to the peptide concentration (μ M) inducing complete loss of viability in the tested cell population relative to the control lacking the peptide. Loss of viability was characterized by the incapacity of cells to undergo division and growth under optimal medium and temperature conditions following a 24 h incubation period without the peptides. Control samples were prepared without peptides. Biological agent *C. tropicalis* and *C. albicans* was handled following BSL 2 protocols.

2.3. Analysis of K^+ and Cl^- channels in peptide-induced death

The K^+ channel blockers tetraethylammonium (TEA) and 4-aminopyridine (4-AP) and the Cl^- channel blocker 5-nitro-2-(3-phenylpropylamine) benzoic acid (NPPB) were used to analyze the role of ionic flux in cell death caused by the bioinspired peptides. The test was carried out as described in the 2.2. item, with the following modifications: 15 μ M TEA and 3 mM 4-AP were added to the yeast cells 1 h before the addition of the peptides, and 50 μ M NPPB was added 10 min before the addition of the peptides. After the preincubation period, the peptides were added at their LD_{100} and incubated for the cell death time of each peptide, 6, 3, and 1 h for RR, D-RR and WR, respectively.

2.4. Analysis of the role of K^+ in cell death induced by peptides

To assess the role of ions in cell death caused by bioinspired peptides, we repeated the antimicrobial assay described in the 2.2. item, in which *C. tropicalis* and *C. albicans* cells were preincubated for 15 min in the presence of 100 mM potassium chloride or potassium phosphate (both at pH 5.6). For *C. albicans* and WR, salt concentrations of 200 mM were also tested. For potassium phosphate, the same test was repeated at different times; the salt was added at the same time, 10, 20, 30 min and 1 h after incubation with the peptides. Potassium chloride was prepared with ultrapure water, and the pH was adjusted to 5.6 with KOH, which was the same pH as that used for the Sabouraud medium. Potassium phosphate was prepared by mixing K_2HPO_4 and KH_2PO_4 , according to Sambrook and Russel [20] also with pH 5.6.

2.5. Fungal cell shrinkage in the presence of K^+ by flow cytometry

Cell shrinkage was previously observed at the LD_{100} at 6 and 3 h with RR and D-RR, respectively, in *C. tropicalis* cells and at 1 h with WR in *C. albicans* [15]. To determine whether this effect occurs and if it persists in the presence of K^+ , the antimicrobial test was repeated as described in the 2.2. item, with the following differences: the assay was set up with 3,000,000 cells/mL, the incubation times of 1 h for RR and 30 min for D-RR in *C. tropicalis*, and 20 min for WR in *C. albicans*. Yeast cells incubated in media devoid of peptides served as the controls. A positive control was additionally employed with yeast exposed to 333 mM acetic acid (AcA) for 1 h. All treatments were repeated in the presence of 100 and 200 mM potassium chloride previously added to the culture media for *C. tropicalis* and *C. albicans*, respectively. Following the designated treatment duration, cell suspensions were analyzed by flow cytometer FACSibur (BD Biosciences) under argon-ion laser

emitting a 488 nm beam at 15 mW and 20,000 cells per sample were analyzed by the forward (FSC) and side light scattering (SSC). FSC and SSC distribution histograms for cells size and cell granularity were generated on computer from raw data files of flow cytometry (WinMDI versão 2.9), respectively.

2.6. Analysis of endogenous reactive oxygen species (ROS) production in the presence of K^+

ROS production was assessed by fluorescence microscopy in the presence of K^+ using 20 μ M 2',7'-dichlorodihydrofluorescein diacetate (H_2DCFDA , Calbiochem, EMD) in accordance with Lucas et al. [15]. Initially, fungal cultures (40,000 cells/mL) were preincubated with 100 and 200 mM potassium phosphate for *C. tropicalis* and *C. albicans*, respectively, and then incubated with peptides at their LD_{100} and at 1 h and 30 min for *C. tropicalis* with RR and D-RR, respectively, and 20 min for WR and *C. albicans*. The control samples were prepared without the addition of peptides and with 100 and 200 mM potassium phosphate for *C. tropicalis* and *C. albicans*, respectively. The positive control (control⁺) involved fungal cells exposed to 10% ethanol for 10 min at 30 °C. The control⁺ was utilized to calibrate the excitation intensity and exposure duration for fluorescence image capture. These identical parameters were applied for image capture in the other treatments. Following peptide treatment, both control and treated cells underwent incubation with 20 μ M H_2DCFDA for 15 min at 30 °C in the absence of light, then transferred onto slides and covered with coverslips. Visualization was achieved through both differential interference contrast (DIC) microscopy (Axio Imager.A2, Zeiss) and fluorescence filters (excitation at 450 - 490 nm and emission at 515 nm). Cell images were captured using an AxioCam MR5 camera (Zeiss) and AxioVision LE software (version 4.8.2, Zeiss). Results were represented as the percentage of fluorescent cells, determined through cell counting based on predefined criteria. 1 – Around 200 cells were randomly selected from both DIC and fluorescent fields, with variations depending on the preparation and incubation duration of the tests. 2 – If the cell count was notably low (attributed to bioinspired peptide treatment or positive control which cause yeast cell death), cells from ten random fields were enumerated. The percentage of fluorescent cells, serving as an indicator of oxidative stress, was determined using the formula: [average number of fluorescent cells \times 100] divided by the average number of cells observed in DIC for each sample.

2.7. Mitochondria functionality in the presence of K^+

Our previous findings indicated that the mitochondria of fungi treated with the peptides exhibited hyperpolarization [15]. To determine whether this effect occurs in the presence of K^+ and whether it is related to cell death, the assay was repeated as described in the 2.5. item, with the following differences: All treatments were repeated in the presence of 100 and 200 mM potassium chloride previously added to the culture media for *C. tropicalis* and *C. albicans*, respectively, and in the presence of 20 μ M JC-1 (Thermo Fisher), for 20 min. with excitation/emission maxima: 514/529 nm, for the green monomer form, and 585/590 nm for the red J-aggregate form.

2.8. Circular dichroism (CD) spectroscopy

The CD spectra were obtained with a Jasco J-815 CD spectropolarimeter (Jasco Analytical Instruments, Japan) at 25 °C. Each CD spectrum resulted from averaging eight consecutive scans within the wavelength range of 190 to 270 nm, a scan speed of 100 nm/min and a bandwidth of 1 nm. A quartz cuvette with a 0.1 cm path length was used for these measurements. The three peptides were tested separately at a final concentration of 50 μ M in ultra-pure water and in the presence of 100 mM potassium phosphate buffer (pH 5.6) for RR and D-RR and 200 mM potassium phosphate buffer (pH 5.6) for WR. CDtool software was used for spectral analysis [21]. The analysis consisted of subtracting the buffer signal, averaging the data, and then converting the resulting signal to the molar differential extinction coefficient, $\Delta\epsilon$ ($M^{-1} cm^{-1}$).

2.9. Determination of the interaction between 5-FAM-labeled peptides and fungal cells

Peptide interactions were determined by confocal laser scanning microscopy (LSM-710, Zeiss). To that end, we repeated the antimicrobial test described in the 2.2. item, with the following changes: 40,000 cells/mL *C. tropicalis* and *C. albicans* were preincubated for 5 min in the presence of 2% calcofluor white (Sigma–Aldrich). Next, 5-FAM_RR, 5-FAM_D-RR and 5-FAM_WR were added and incubated in the dark for 20 min and then analyzed using a 63x objective lens with Zen Lite Edition 2011 software (Zeiss). Controls were generated in the presence of 2% calcofluor white without the addition of the peptides. 5-FAM was excited at 488 nm and detected at 530 nm, and calcofluor white was excited at 360 nm and detected at 430 nm. This assay was repeated in the presence of 100 mM potassium phosphate (pH 5.6) for *C. tropicalis* cells and 5-FAM_RR and 5-FAM_D-RR and in the presence of 200 mM potassium phosphate (pH 5.6) for *C. albicans* cells and 5-FAM_WR. The molecular weight of 5-FAM was disregarded to prevent interference in peptide molarity calculations.

2.10. Assessment of glucose-induced acidification of the medium

To assess the inhibition of glucose-induced acidification of the medium, *C. tropicalis* and *C. albicans* cells were grown for 24 h at 30 °C, and 20,000,000 cells/mL were then resuspended in 800 µL of 5 mM Tris-HCl (pH 6.0) and kept at a constant temperature of 25 °C under gentle mechanical agitation. The pH was monitored using a benchtop pH meter with a small glass electrode (Q400RS, Quimis). The treatments were carried out by incubating the yeast cells and DL₁₀₀ of the peptides (27.5 µM and 23 µM for RR and D-RR in *C. tropicalis*, respectively, and 27.5 µM for WR in *C. albicans*) at the same time as 200 µL of 0.5 M glucose (final concentration of 0.1 M). The pH was monitored every minute for 30 min. A test was performed under the same conditions, using 0.1 M glucose combined with 100 and 200 mM potassium chloride for *C. tropicalis* and *C. albicans* cells, respectively. The positive control contained no peptides and only 0.1 M glucose, with an additional peptide- and glucose-free control prepared under the same conditions [22,23]. Potassium chloride was prepared with ultrapure water, and the pH was adjusted with KOH to 6.0.

2.11. Analysis of membrane permeabilization

Cell membrane permeabilization was measured via Sytox green uptake, as previously reported by Thevissen et al. [24]. This assay was prepared as described in the 2.2. item (ROS) with some modifications. Yeast cells were treated with the peptides and then incubated with 0.2 µM of Sytox green for 15 min. Additional testing was performed using 100 and 200 mM potassium chloride (pH 5.6) for *C. tropicalis* and *C. albicans*, respectively. A control⁺ containing cells heated at 100 °C for 1 min was included which was also used to calibrate parameters for image capture as described. An untreated control was used to assess basal membrane permeability. The cells were then observed under a DIC microscope (Axio Imager.A2, Zeiss) equipped with a set of fluorescence filters for fluorescein detection (excitation 450–490 nm; emission 515 nm).

2.12. Antimicrobial assay under hypotonic conditions

C. tropicalis and *C. albicans* cells were separately cultivated on Sabouraud agar for 24 h at 30 °C, after which the cells were counted in a Neubauer chamber in Sabouraud broth. An aliquot corresponding to 1,000 cells of each yeast was washed twice in ultrapure water, transferred to ultrapure water and incubated for 5 min before the addition of the peptides at their LD₁₀₀, RR and D-RR for *C. tropicalis*, and WR for *C. albicans*, and incubated for an

additional 1 min at 30 °C. After incubation, the cells were washed in Sabouraud broth and seeded on Sabouraud agar, and the Petri dishes were incubated for 24 h at 30 °C. Controls for each yeast were generated without the addition of the peptides.

2.13. Cellular degradation by electrophoresis

The antimicrobial assay involving *C. tropicalis* and *C. albicans* was established following the protocol outlined in 2.2 item, with the following modifications: 1,000,000 cells/mL were distributed into 10 wells. Treatments were administered for *C. tropicalis* as follows: 80 mM AcA for 1 h, 80 mM AcA plus 50 µM Z-VAD-FMK (Promega) for 1 h, 80 mM AcA plus 100 mM potassium phosphate (pH 5.6) for 1 h, 27.5 µM RR for 20 min, 23 µM D-RR for 20 min, 27.5 µM RR plus 100 mM potassium phosphate (pH 5.6) for 20 min, and 23 µM D-RR plus 100 mM potassium phosphate (pH 5.6) for 20 min. Control groups were treated with medium and 100 mM potassium phosphate (pH 5.6). For *C. albicans* the treatments were: 80 mM AcA for 1 h, 80 mM AcA plus 50 µM Z-VAD-FMK (Promega) for 1 h, 80 mM AcA plus 200 mM potassium phosphate (pH 5.6) for 1 h, 27.5 µM WR for 20 min, 27.5 µM RR plus 200 mM potassium phosphate (pH 5.6) for 20 min. Control groups were treated with medium and 100 mM potassium phosphate (pH 5.6). Upon completion of the incubation period, samples from the wells were combined, subjected to a single wash in phosphate-buffered saline (PBS), pH 7.2, through centrifugation at 7,000xg for 10 min at 4 °C (5414R, Eppendorf). Subsequently, the samples were resuspended in 800 µL of PBS and underwent sonication (Sonifer 150, Branson) with ten pulses of 10 s each in an ice bath, with intervals of 50 s between pulses. Post-sonication, the samples were centrifuged again at 10,000xg for 15 min at 4 °C, and the supernatant was collected and stored at -20 °C.

Gel electrophoresis proceeded on tricine gel according to Schagger and von Jagow [25] with voltage 20 V, and the percentage of acrylamide and bis-acrylamide was 49.5% T and 3% C, respectively.

2.14. Fungal cell ultrastructure

The controls and peptide-treated samples for 10 min were fixed for 16 h in 5% glutaraldehyde. Following fixation, the yeast cells were washed three times with 100 mM sodium cacodylate buffer (pH 7.2) for 10 min each. The samples were then dehydrated over 25 min in a graded ethanol series (30%, 50%, 70%, 90%, and three changes of 100% super dry ethanol) and subsequently infiltrated with LR-White resin (Sigma-Aldrich). The material was left at room temperature for 48 h before being polymerized at 60 °C for 16 h. Ultrathin

sections were prepared using a EM UC7 Ultramicrotome (Leica), stained with uranyl acetate for 5 min and lead citrate for 1 min. Finally, the sections were examined, and images were captured using a JEM 1400 Plus transmission electron microscope (Jeol) operating at an accelerating voltage of 120 kV.

2.15. Statistical analyses

All experiments were performed in triplicate and repeated three times, except for the optical microscopy assays, which were conducted once but repeated thrice. Statistical analysis was carried out using one-way ANOVA in GraphPad Prism software version 8.0.2 for Windows, with significance set at $P < 0.05$. Data visualization was performed using GraphPad Prism version 8.0.2 and PowerPoint (Microsoft Office 365).

3. Results and discussion

3.1. Involvement of K^+ in peptide-induced cell death

Cell shrinkage is a well-known hallmark of apoptosis in eukaryotic cells, including fungi [17-19]. To test our hypothesis linking K^+ efflux to fungal cell death induced by the peptides, we preincubated fungal cells with voltage-dependent K^+ channel blockers TEA and 4-AP for 1 h, and the Cl^- channel blocker NPPB for 10 min. TEA and 4-AP inhibit the Tok1p channel, a voltage-dependent outward rectifier activated by cell membrane depolarization [26,27], while NPPB blocks anion channels, including Cl^- , which plays a role in maintaining the cell's electrically neutral ionic state [28]. Our results showed that none of the channel blockers tested protected *C. tropicalis* from RR- or D-RR-induced death (Fig. 1), nor did they protect *C. albicans* from WR-induced death (Fig. 1). Given that the channel blockers were toxic to control fungal cells, as demonstrated by their reduced viability (Fig. 1), we concluded that the channels were effectively blocked, but blockage had no modulatory effect on peptide-induced cell death. K^+ efflux and the associated cell shrinkage are among the earliest observable events in programmed cell death in metazoans [18,29]. In *C. albicans*, K^+ efflux is a crucial step in initiating the cell death process and is modulated by various substances [30-35]. Inhibiting K^+ channels with chemical agents reduces or abolishes the cytotoxic effects of these molecules, thereby protecting the fungi from cell death. Based on the association between K^+ efflux and cell shrinkage [18,19], our findings suggest that K^+ extrusion, as demonstrated by the reduction in fungal cell size [15], in peptide-induced fungal cell death probably does not occur via ion efflux channels.

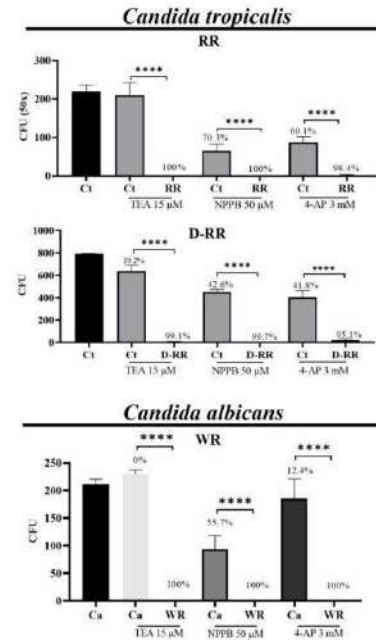


Fig. 1. The viability of fungal cells following incubation with RR, D-RR, and WR at their lethal dose (DL₁₀₀) and induced cell death times in the presence of K⁺ channel blockers TEA and 4-AP, and the Cl⁻ channel blocker NPPB. The percentage of inhibition relative to the control is indicated above the peptide test bars. The percentage of inhibition relative to *C. tropicalis* or *C. albicans* without the blockers is presented above the respective bars. Statistical significance is denoted as ****, $P < 0.05$. The abbreviations used are Ct for *C. tropicalis*, Ca for *C. albicans*, and CFU for colony forming units. The assay is one representative out of three assays.

Thus, we exogenously added K⁺ to the medium to counteract its potential loss from fungal cells, as suggested by cell shrinkage. The chosen salt concentration was based on the cytoplasmic K⁺ concentration in fungi, typically ranging from 200 to 300 mM, including the *Candida* genus [36]. We observed that the salts alone exhibited low toxicity to fungal cells (Table 1). Our results demonstrated that in *C. tropicalis*, preincubation with 100 mM potassium chloride or potassium phosphate 15 min before peptide addition provided protection against RR- and D-RR-induced cell death, respectively (Table 1). For *C. albicans*,

protection was also observed after incubation with WR (Table S1). These results were compared with their respective salt-free controls. Although 100 mM salt concentrations offered minimal protection against WR-induced cell death in *C. albicans*, a slight protective effect was observed in the preincubation test (Table S1), given that WR caused complete cell death under salt-free conditions (Table 1; [15]). To explore whether increasing ion concentration could enhance protection, we repeated the viability test with 200 mM salts. At this concentration, the salts themselves exhibited toxicity (Table 1). Despite this toxicity, preincubation with 200 mM potassium chloride or potassium phosphate 15 min prior to WR addition resulted protection, from death (Table 1). This supports our previous conclusion [15] that WR-induced cell death in *C. albicans* is a regulated process because death is modulated by extracellular K^+ addition [16].

Additionally, a comparison of the salts used, potassium chloride and potassium phosphate and their protective effects against fungal cell death suggested that the phosphate (PO_4^{3-}) and chloride (Cl^-) anions, which are present separately in the two salts, do not appear to prevent peptide-induced death. Therefore, the observed protective effect seems to be attributed to the common ion in both salts, K^+ .

Table 1. Influence of salts on the lethality of RR, D-RR, and WR against opportunistic fungi at their LD₁₀₀ concentrations and corresponding induced death time. Fungi were pre-incubated for 15 min in the presence of KCl or K₂HPO₄ + K₂HPO₄ at specified concentrations. Colony forming unit (CFU, x50 for RR) are presented as the mean ± standard deviation.

fungi	condition/pre-incubation (15 min)	incubation time	samples	CFU	% viability (protection)	% of death (toxicity)
<i>Candida tropicalis</i>	without salt	6 h	control	343 ± 5	100 ^a	0 ^b
			RR (27.5 μM)	0 ± 0	0 ^b	100 ^a
	KCl (100 mM)		control	346 ± 17	100 ^a	0 ^b
			RR (27.5 μM)	327 ± 28	94.2 ^a	5.8 ^b
	KH ₂ PO ₄ + K ₂ HPO ₄ (100 mM)		control	309 ± 17	89.2 ^a	10.8 ^b
			RR (27.5 μM)	291 ± 7	94.6 ^a	5.4 ^b
	without salt	3 h	control	716 ± 15	100 ^a	0 ^b
			D-RR (27.5 μM)	0 ± 0	0 ^b	100 ^a
			control	686 ± 12	95.7 ^a	4.3 ^b
			D-RR (27.5 μM)	706 ± 10	100 ^a	0 ^b
	KCl (100 mM)	control	775 ± 14	92.4 ^a	7.6 ^b	
		D-RR (27.5 μM)	749 ± 9	96.6 ^a	3.4 ^b	
KH ₂ PO ₄ + K ₂ HPO ₄ (100 mM)	3 h	control	716 ± 15	100 ^a	0 ^b	
		D-RR (27.5 μM)	0 ± 0	0 ^b	100 ^a	
		control	686 ± 12	95.7 ^a	4.3 ^b	
		D-RR (27.5 μM)	706 ± 10	100 ^a	0 ^b	
		control	775 ± 14	92.4 ^a	7.6 ^b	
		D-RR (27.5 μM)	749 ± 9	96.6 ^a	3.4 ^b	
<i>Candida albicans</i>	without salt	1 h	control	204 ± 11	100 ^a	0 ^b
			WR (27.5 μM)	0 ± 0	0 ^b	100 ^a
	KCl (200 mM)		control	142 ± 7	69.7 ^c	30.2 ^d
			WR (27.5 μM)	74 ± 7	47.7 ^c	52.2 ^d
	KH ₂ PO ₄ + K ₂ HPO ₄ (200 mM)		control	127 ± 8	62.3 ^c	37.6 ^d
			WR (27.5 μM)	65 ± 2	48.7 ^c	51.3 ^d

Controls consisted of fungal cells without peptide treatment. Comparisons were made between peptide-treated fungi under each salt condition and their respective salt-treated controls. Salt toxicity was evaluated by comparing controls with and without salt addition. Survival percentages were calculated by comparing fungal survival with and without salt treatment. Different letters indicate significant differences ($P < 0.05$), while the same letters indicate no significant difference. The assay is one representative out of three assays.

To determine whether the protective effect of K⁺ diminishes after addition of the peptides, and whether the decrease in cytoplasmic K⁺ concentration may be the secondary event leading to fungal cell death, K⁺ was incorporated into the viability assay both simultaneously and after addition of the peptides. When 100 mM potassium phosphate was added simultaneously with the bioinspired peptides, *C. tropicalis* showed 94.2% and 96.6% protection for RR/6 h and D-RR/3 h, respectively (Fig. 2). However, no protection was observed for WR/1 h in *C. albicans* when incubated simultaneously with 200 mM potassium phosphate (Fig. 2). To explore whether restoring K⁺ cytoplasmic concentration could rescue fungal cells from death, K⁺ was added 10, 20, or 30 min, or 1 h after addition of the peptides. When K⁺ was added 10 min after addition of the peptides, protection decreased to 13.4% and 53.2% for RR and D-RR, respectively (Fig. 2), while *C. albicans* cells showed no protection

when incubated with 200 mM potassium phosphate 10 min after WR addition (Fig. 2). For RR and D-RR, protection further decreased to 14.7% and 28.5%, respectively, when K^+ was added 20 min after addition of the peptides, dropped to 4.3% and 18.2% when added after 30 min (Fig. 2). Adding K^+ 1 h after addition of the peptides provided only 0.7% and 9.5% protection for RR and D-RR, respectively, which was statistically equivalent to the control (Fig. 2). Since K^+ added simultaneously and 10 min after WR no longer provided protection for *C. albicans*, subsequent time points were not considered for testing (Fig. 2).

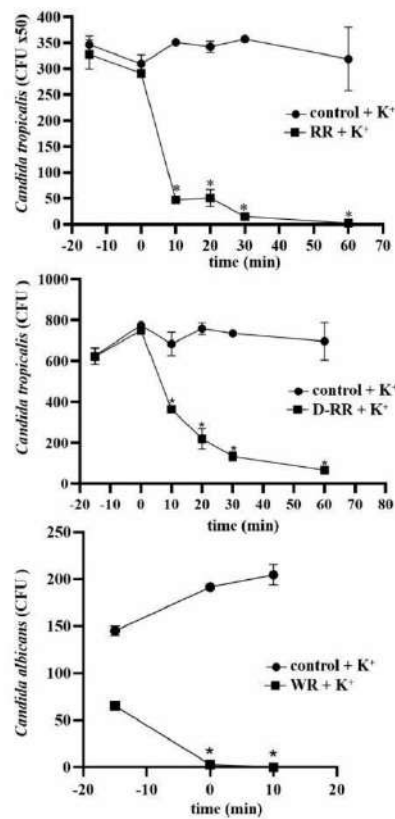


Fig. 2. The viability of fungal cells following incubation with RR, D-RR, and WR at their lethal dose (DL_{100}) and induced cell death to which K^+ was added at various time points, pre- (-15 min), co- (0 min), and post-peptide addition. Pre-incubation data were taken from

Table 1. *, $P < 0.05$. CFU refers to colony-forming units. K^+ refers to the presence of 100 and 200 mM of $K_2HPO_4 + KH_2PO_4$ for *C. tropicalis* and *C. albicans*, respectively. The assay is one representative out of three assays.

These results align with our earlier findings that AA could no longer protect against peptide-induced cell death when added 1 h after addition of the peptides [15]. Taken together, the findings, showing the lack of protection from AA [15] and from K^+ after addition of the peptides, suggest that K^+ -mediated rescue from cell death is also time-sensitive, as the protection provided by AA. This finding suggests that the death process once triggered in the fungi by the dAMPs also proceeds independently of K^+ replacement.

3.3. Analysis of cell shrinkage, ROS induction and mitochondria hyperpolarization in fungal cells treated with peptides and K^+

Cell shrinkage in the presence of K^+ was assessed by measuring forward light scattering (FSC) to estimate overall cell size and side light scattering (SSC) to assess cytoplasmic granularity. The addition of K^+ to the culture media restores cell size (Table 2). As a positive control, we used 333 mM acetic acid (AcA), a known inducer of regulated cell death in fungi, which shares characteristics with apoptosis [37]. Dot plots from this assay are presented in Figures S1 and S2. These results demonstrate that K^+ addition protects fungal cells from shrinkage induced by RR, D-RR, and WR, supporting our hypothesis that the reduction in cytoplasmic K^+ concentration induced by these bioinspired peptides is related to fungal cell shrinkage.

Table 2. Cell size and granularity of *Candida tropicalis* and *Candida albicans* treated with RR, D-RR, and WR in the presence of K⁺. Acetic acid (AcA) was used as control of regulated cell death.

fungi	samples	cell size		cell granularity	
		FSC mean	reduction or increase (%)	SSC mean	reduction or increase (%)
<i>Candida tropicalis</i>	control	419.06	0.00	242.93	0.00
	control + K ⁺	415.54	-0.84	238.20	-1.95
	AcA	316.73	-24.42	292.83	20.54
	AcA + K ⁺	334.79	-20.11	259.42	6.79
	RR	369.06	-11.93	237.46	-2.25
	RR + K ⁺	420.21	0.27	256.26	5.48
	D-RR	343.22	-18.10	238.77	-1.71
	D-RR + K ⁺	434.40	3.66	261.49	7.43
<i>Candida albicans</i>	control	230.10	0.00	118.50	0.00
	control + K ⁺	277.62	20.65	92.37	-22.58
	AcA	217.41	-5.51	225.84	90.58
	AcA + K ⁺	246.50	7.13	119.57	0.90
	WR	179.17	-22.13	176.84	49.23
	WR + K ⁺	228.36	-0.76	240.95	103.33

K⁺ refers to the presence of 100 and 200 mM of K₂HPO₄ + KH₂PO₄ for *C. tropicalis* and *C. albicans*, respectively.

Endogenous ROS production was analyzed in the presence of K⁺. In previous findings, *C. tropicalis* treated with RR and D-RR for 1 h and 30 min showed 88.2% and 72.3% of cells under oxidative stress, respectively. Similarly, *C. albicans* treated with WR for 20 min displayed 94.4% of cells under oxidative stress [15]. In the presence of K⁺, ROS levels in cells treated with the peptides were similar to the previous results from cells without K⁺ treatment (Table 3, Fig. S3). These results indicate that the protection provided by K⁺ does not occur through blocking ROS production, as peptide-treated cells still displayed oxidative stress. This finding reinforces our hypothesis that both ROS production and cell shrinkage are intermediate events in peptide-induced cell death [15].

Table 3. Percentage of fungal cells under oxidative stress after interaction with RR, D-RR, and WR in the presence of K⁺.

fungi	samples	incubation time	number of cells in DIC	number of H ₂ DCFCD fluorescent cells	cells with oxidative stress (%)
<i>Candida tropicalis</i>	control ⁺	10 min	204	190	93.1 ^a
	ethanol + K ⁺	10 min	203	156	76.8 ^a
	control	1 h	200	79	39.5 ^b
	RR (27.5 μM) + K ⁺	1 h	204	159	77.9 ^a
	D-RR (23 μM) + K ⁺	30 min	203	178	87.6 ^a
<i>Candida albicans</i>	control ⁺	10 min	215	202	93.9 ^a
	ethanol + K ⁺	10 min	202	170	84.1 ^a
	control	20 min	198	39	19.7 ^b
	WR (27.5 μM) + K ⁺	20 min	227	221	97.4 ^a

K⁺ refers to the presence of 100 and 200 mM of K₂HPO₄ + KH₂PO₄ for *C. tropicalis* and *C. albicans*, respectively. Different letters denote significant differences and the same letter denotes no difference, P < 0.05. The assay is one representative out of three assays.

We also investigated the mitochondrial hyperpolarization observed in fungi treated with the peptides [15]. *C. tropicalis* treated with RR and D-RR and *C. albicans* treated with WR presented hyperpolarization of the mitochondrial membrane. Treatment with the antioxidant AA prevented mitochondrial hyperpolarization and rescued fungi from peptide-induced death [15]. These results indicated that mitochondria, when not hyperpolarized, protect fungi from death. Since mitochondria are at the intersection of several cell death pathways [38], we used the JC-1 probe to assess mitochondrial functionality at 5 and 10 min after interaction with the peptides and in the presence of K⁺. Our results indicate that all three dAMPs cause mitochondrial hyperpolarization already since 5 min after interaction (Fig. 3). Notably, in the presence of K⁺, no hyperpolarization was observed (Fig. 3). As K⁺ protects against dAMPs-induced cell death (Table 1), these two results suggest that mitochondrial hyperpolarization induced by dAMPs may be related to the fungal cell death process.

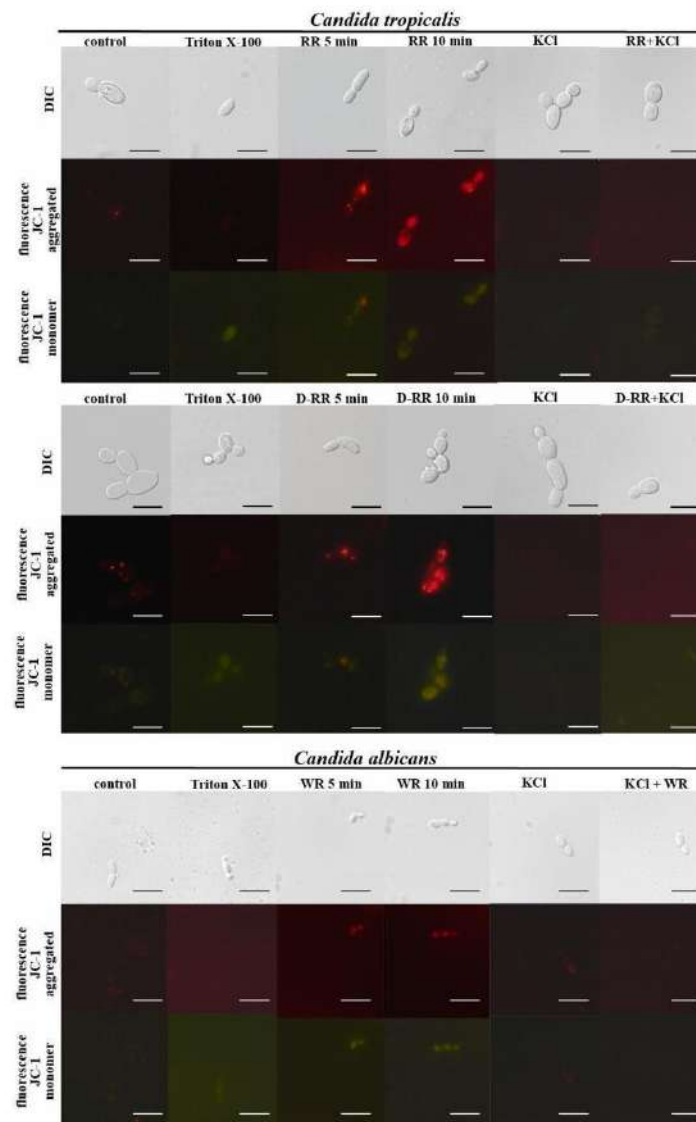


Fig. 3. Mitochondrial functionality in fungal cells treated with RR, D-RR and WR in presence and absence of K^+ at 5 and 10 min of interaction. Green fluorescence indicates JC-1 monomer and red fluorescence indicates JC-1 aggregated. Control images show samples

without peptide treatment. Triton X-100 was used as negative control. K^+ refers to the presence of 100 and 200 mM of $K_2HPO_4 + KH_2PO_4$ for *C. tropicalis* and *C. albicans*, respectively. Scale bars = 10 μm . The assay is one representative out of three assays.

3.4. Analysis of the interaction of peptides with fungal cells in the presence of K^+

A well-established phenomenon in the study of antimicrobial peptides (AMPs) is their inactivation in the presence of ions [39-43], mainly cations, including K^+ [44-45]. Therefore, we investigated whether the death protection in the presence of K^+ is due to the loss of interaction of the three peptides with fungal cells caused by K^+ ions. This lack of interaction is generally attributed to the neutralization of both peptide and cell surface charges by the ions, which may hinder the initial interactions required for the AMPs' toxic effects to occur [41,46].

We first employed circular dichroism (CD) to assess whether the conformation of the RR, D-RR and WR was affected by the presence of K^+ . The CD spectra, characteristic of disordered peptides, remained unchanged in the presence of K^+ , indicating that the ion did not induce any structural changes that would account for inactivation of the peptides (Fig. 4). CD analyses were not performed with KCl due to Cl^- spectral interference, particularly in the far ultraviolet region [47].

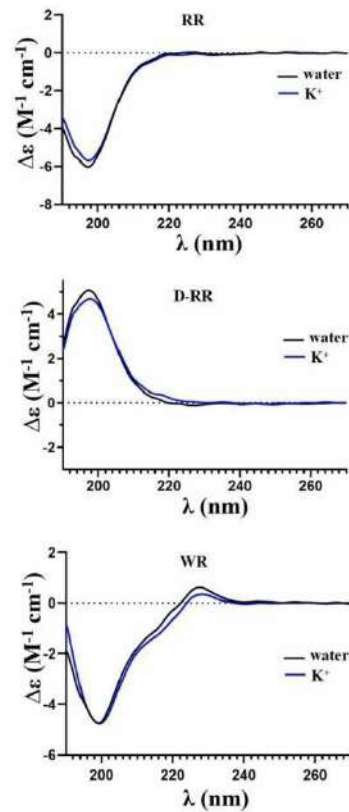


Fig. 4. Far-UV circular dichroism (CD) spectra of the peptides RR, D-RR, and WR were recorded in water (black line) and in the presence of 100 and 200 mM potassium phosphate at pH 5.4 (blue line). K⁺ refers to the presence of 100 and 200 mM of K₂HPO₄ + KH₂PO₄ for *C. tropicalis* and *C. albicans*, respectively.

Next, we used 5-FAM-conjugated peptides to examine their interaction with fungal cells. Conjugation with the 5-FAM molecule did not impair the toxic effect of the peptides (Fig. S4). Consequently, we proceeded with confocal microscopy to analyze the localization of labeled dAMPs. The dAMPs' interaction with fungal cells was studied at the 20 min time point, within the timeframe of cell death induced by the bioinspired peptides. In all treatments, the fluorescence signal of the labeled peptides was observed within the regions defined by cell walls stained with calcofluor white, indicating that the peptides had entered the cytoplasm of the fungal cells (Fig. 5). Additionally, bright green areas near the budding sites suggested localized peptide internalization in these regions (Fig. 5). These findings

indicate that the peptides entered the fungal cells as early as 20 min after incubation. Notably, this suggests that the peptides may target intracellular components.

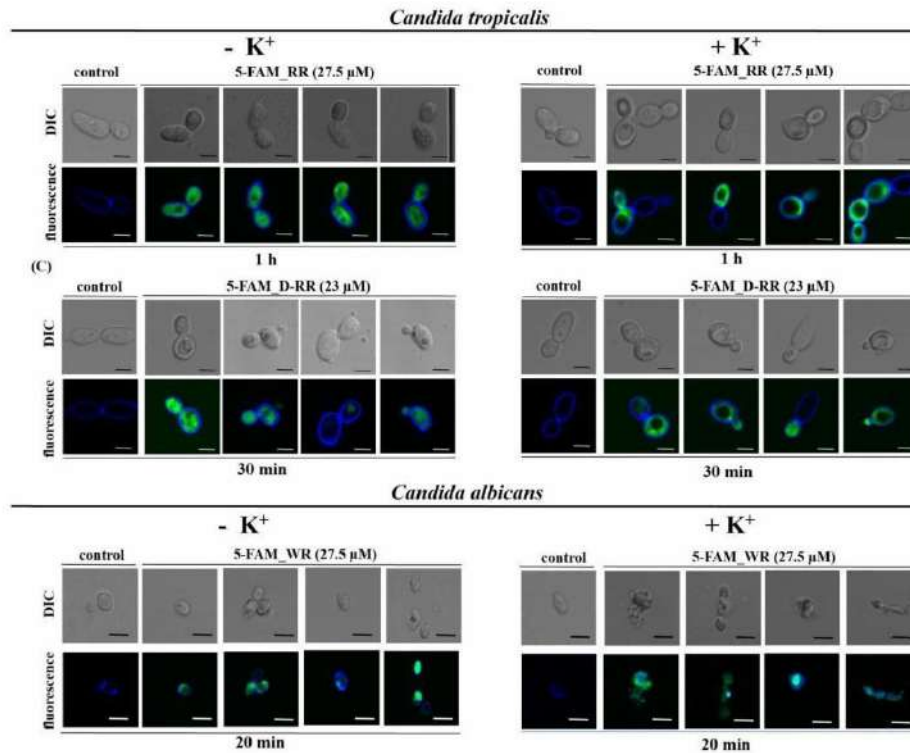


Fig. 5. Interactions of 5-FAM-labeled peptides (5-FAM_RR, 5-FAM_D-RR, and 5-FAM_WR) with *Candida* species in absence and presence of K⁺. Green fluorescence in the cytoplasm indicates the peptide localization, while blue fluorescence marks the yeast cell wall with calcofluor white. Control images show samples without peptide treatment. The images display colocalization observed via confocal microscopy. K⁺ refers to the presence of 100 and 200 mM of K₂HPO₄ + KH₂PO₄ for *C. tropicalis* and *C. albicans*, respectively. Scale bars = 10 μm. The assay is one representative out of three assays.

Several antimicrobial peptides (AMPs) have been shown to enter microbial cells and disrupt cellular functions [48-50]. The role of RR, D-RR, and WR peptides in entering the fungal cytoplasm, as well as their potential cytoplasmic targets, will be explored in future studies. Thus, we repeated the experiment using K^+ . These results demonstrate that the peptides were able to enter fungal cells even in the presence of K^+ , confirming that the observed protection was not due to charge blocking (Fig. 5). The implications of these findings are discussed below.

Our data on peptide interactions with fungal cells, even in the presence of K^+ , contradict previous findings in the literature. Numerous studies have shown that the addition of ions to the culture medium of microorganisms neutralizes the antimicrobial activity of AMPs across various families, involving both monovalent and divalent cations [31,41]. This phenomenon has been observed for several AMPs [25,26,27,40,42,44,45,51-53]. The inhibitory effect of cations is typically attributed to the general characteristics of AMPs, which are cationic at physiological pH [10]. This positive charge is essential for their initial attraction to microbial cells, which possess negatively charged surface components, such as lipopolysaccharides in gram-negative bacteria, teichoic and lipoteichoic acids in gram-positive bacteria [54], mannoproteins in fungi [55], and lipophosphoglycans in trypanosomatids [56]. The importance of charge in AMP antimicrobial activity is supported by several observations. For instance, many AMPs are synthesized as preproteins, with acidic pro-domains that neutralize the AMPs' charge during synthesis or storage. Upon secretion, the cleavage of these pro-domains activates the AMP [57-59]. Additionally, the removal of negatively charged components from microbial membranes or cell walls reduces the effectiveness of AMPs [60]. Various mechanisms of bacterial resistance to AMPs involve the incorporation of positively charged molecules that neutralize the negative charge of membrane or cell wall components, thereby diminishing or blocking the peptide interaction. Examples include the addition of aminoarabinose to lipid A by *Salmonella enterica* serovar Typhimurium [61], the addition of L-lysine to phosphatidylglycerol [62], and the incorporation of D-alanine by *Staphylococcus aureus* [63].

This observation is relevant because it has direct implications for the clinical use of AMPs at host physiological salt concentrations, which is allegedly considered one of the major obstacles to the transfer of AMPs from *in vitro* studies to clinical use. The presence of low K^+ concentrations in host fluids suggests that pathogenic fungi are unlikely to be protected from AMP activity within the host [64]. Indeed, the low K^+ in mammalian fluids may explain the apparent contradiction of AMP efficacy in *in vivo* tests [12], where blockage

of antimicrobial activity by renal clearance and protease degradation plays more preponderant roles than salt inactivation. It is crucial to extend these findings to other AMPs and cell types, as the characteristics shared by many AMPs suggest that these results may be generalizable to other peptides whose antimicrobial activity is impaired by cations. In conclusion, our results indicate that the protective mechanism provided by K^+ is not due to charge neutralization disrupting peptide interactions with fungal cells.

3.5. Analysis of glucose-induced acidification of the extracellular medium in the presence of peptides and K^+

The protection from peptide-induced fungal cell death provided by extracellular K^+ is similar to the protective effect of K^+ observed during glucose-induced cell death in *Saccharomyces cerevisiae* at the stationary phase [23,65]. In this phenomenon, glucose stimulates intracellular acidification, prompting the extrusion of H^+ through the membrane H^+ -ATPase (Pma1). This leads to acidification of the external medium, an increase in transmembrane potential ($\Delta\psi$), a rise in chemical potential (ΔpH), and the induction of ROS. K^+ protects yeast cells from death by dissipating the $\Delta\psi$ and inhibiting ROS production. Moreover, buffering the external medium at pH 7.0 also provides protection by also dissipating ΔpH [23]. Fungal cell death occurs via ATP depletion caused by excessive H^+ pumping into the extracellular environment [23].

All peptides cause a rapid acidification of the external pH within the first two minutes after interaction, followed by an alkalization of the external pH, both in the absence of glucose and in its presence (Fig. 6). In the presence of K^+ added to the medium, the initial acidification is completely abrogated followed by a slow acidification (Fig. 6). In this context, K^+ protection against peptide-induced cell death appears to be due to the inhibition of ΔpH formation, which aligns with the observation that protection is not related to the neutralization of charges on the peptides or the cell surface. The viability and acidification inhibition experiments used glucose concentrations close to each other, Sabouraud medium contained 0.11 M glucose, and the acidification inhibition experiment had 0.1 M, indicating the significance of acidification under both conditions. D-RR exhibits a smaller effect on acidification compared to RR, suggesting a weaker interaction with the target and highlighting the stereodependence of this interaction. These results suggest that H^+ -ATPase may be involved in the process. Future studies will examine the involvement of this pump and whether it is the direct target of the peptides. Acidification analyses were not performed with potassium phosphate due to its buffering capacity. Given the presence of ROS in fungal cells

treated with the peptides and K^+ , we reject the hypothesis that K^+ protection was mediated by $\Delta\psi$ dissipation and ATP depletion, as proposed by Bidiuk et al. [23]. Our data suggest that the rapid acidification within one minute of peptide-fungus interaction might be the trigger for the cell death mechanism. In the presence of peptides and K^+ , cell death is prevented, and the rapid acidification observed in the first minute is completely abrogated. These results indicate that K^+ added to the culture medium impaired the rapid acidification of the medium, thereby preventing ΔpH formation, as demonstrated for mammal cells [66]. Under the condition imposed by the peptides, fungal cells may cause the efflux of K^+ to compensate ΔpH formation, as indicated the importance of K^+ channel Tok1 in transmembrane potential maintenance [67]. Future studies will explore the plasma membrane potential of *Candida* cells and how their energized state is related to peptide-induced fungal death and K^+ efflux.

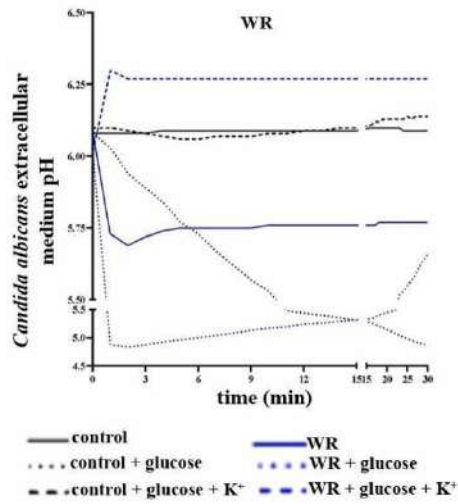
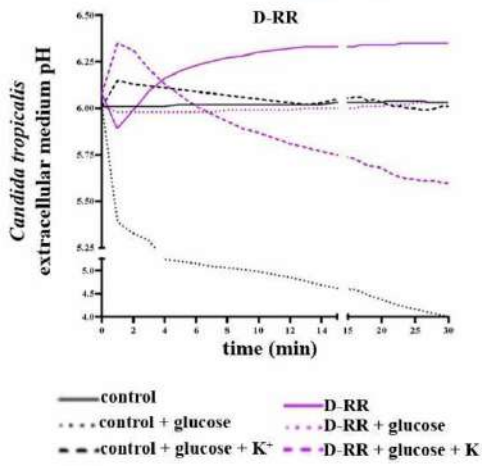
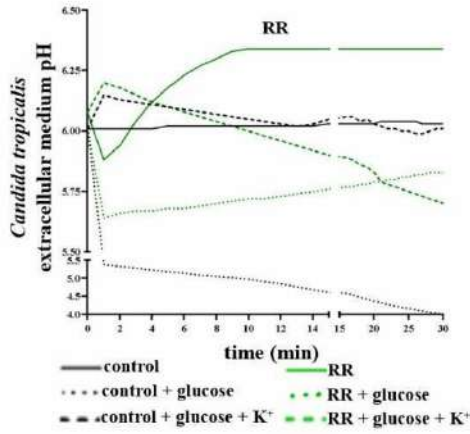


Fig. 6. Acidification of the external media of *Candida tropicalis* and *Candida albicans* cells stimulated with glucose in the presence of RR, D-RR, and WR peptides and K⁺. Glucose stimulation led to acidification, while treatment with the peptides inhibited this effect. Controls for *C. tropicalis* and for both RR and D-RR were the same. K⁺ refers to the presence of 100 and 200 mM of KCl for *C. tropicalis* and *C. albicans*, respectively. The assay is one representative out of three assays.

3.6. Analysis of membrane permeabilization of fungal cells treated with peptides and K⁺

Taken together, our data demonstrate that channel blockers did not protect fungal cells from peptide-induced cell death. Moreover, intracellular effects such as ROS production were not inhibited by K⁺, while cell shrinkage was inhibited in the presence of exogenously added K⁺ to the culture medium. Additionally, the rapid acidification of the medium after glucose addition was inhibited approximately 1 min following the peptide addition. All of these effects could be explained if the fungal cell membranes were permeabilized. The permeabilization of fungal membranes, caused by plant defensins like Rs-AFP2 and Dm-AMP1, could be directly involved in disrupting ion homeostasis, allowing ions to leak back into the cytosol through the compromised plasma membrane [68]. Therefore, it is possible that K⁺, H⁺, and other ions may leak through the structurally compromised cell membrane. Several AMP classes, including plant defensins [24], plant lipid transfer proteins [69], and temporins (AMPs first identified in the skin secretion of *Rana temporaria*) [70], are capable of permeabilizing microbial membranes. For example, the plant defensin NaD1, found in *Nicotiana glauca* flowers, binds to the cell walls of *Fusarium oxysporum* hyphae, causing membrane permeabilization and subsequent extravasation of cytoplasmic content, leading to cell death [71]. Previous we had demonstrated that after 15 min of incubation with the peptides RR and WR, *C. tropicalis* and *C. albicans*, respectively, showed positive propidium iodide (PI) staining, indirectly indicating fungal cell membrane permeabilization. However, this effect was not observed for *C. tropicalis* incubated with D-RR [15]. To further investigate whether the peptides caused fungal membrane permeabilization, we used the Sytox green fluorescent probe. Positive labeling for the probe was observed for all peptides. These results confirm that the yeast membranes were permeabilized, allowing the entry of the Sytox green probe at 1 h for RR, 30 min for D-RR, and 20 min for WR. The addition of K⁺ to the medium did not affect probe labeling in *C. tropicalis* treated with RR or D-RR. However, in *C. albicans* treated with WR, a 41.8% reduction in cells with permeabilized membranes was

observed, though this reduction was not statistically significant (Table 4; Fig. S5). The observed permeability likely explains why channel blockers failed to protect the fungi from cell death, as membrane damage would have allowed K^+ efflux and regulated intracellular effects such as cell shrinkage. Intra- and extracellular ion concentrations may have reached equilibrium due to membrane permeability, partially protecting the fungal cells from shrinkage. The results also explain the inhibition of external medium acidification via dissipation of the H^+ gradient through the permeabilized membrane. This does not exclude the possibility that acidification inhibition is caused by the direct inhibition of H^+ -ATPases.

However, these results do not account for the shift in the slope of acidification observed 1 min after the addition of the peptides. To investigate this, we examined membrane permeabilization within 5 min of dAMPs exposure to determine if permeabilization could explain this shift. In *C. tropicalis* treated with RR and D-RR, no membrane permeabilization was observed (Tables 5 and 6). In *C. albicans* treated with WR, permeabilization was detected at time zero (the time required to set up the assay and perform microscopic observations) (Table 7). These findings suggest that the change in the acidification slope observed in cells treated with the peptides is not associated with membrane permeabilization. The inhibition of acidification, along with the pH variations observed in the peptide treatments both with and without K^+ , likely has a different underlying cause. A plausible mechanism may involve the K^+/H^+ antiporter [72].

Table 4. Plasma membrane permeabilization in fungal cells treated with RR, D-RR, and WR.

fungi	samples	incubation time	number of cells in DIC	number of fluorescent cells	% of permeabilized cells
<i>Candida tropicalis</i>	control [†] (100 °C)	1 min	229	223	97.3 ^a
	control	1 h	213	02	0.9 ^b
	RR (27.5 μM)		211	173	83.0 ^a
	RR (27.5 μM) + K ⁺ (100 mM)		211	165	78.1 ^a
	D-RR (23 μM)	30 min	201	112	55.7 ^a
	D-RR (23 μM) + K ⁺ (100 mM)		209	97	46.4 ^a
<i>Candida albicans</i>	control [†] (100 °C)	1 min	192	183	95.3 ^a
	control	20 min	206	12	5.8 ^b
	WR (27.5 μM)		209	192	92.3 ^a
	WR (27.5 μM) + K ⁺ (200 mM)		204	103	50.5 ^a

K⁺ refers to the presence of 100 and 200 mM of K₂HPO₄ + KH₂PO₄ for *C. tropicalis* and *C. albicans*, respectively. Different letters denote significant differences and the same letter denotes no difference, P < 0.05. The assay is one representative out of three assays.

Table 5. Plasma membrane permeabilization in *Candida tropicalis* cells treated with RR at different times and in the presence of K⁺.

fungus	samples	incubation time	number of cells in DIC	number of fluorescent cells	cells with permeabilized membrane (%)
<i>Candida tropicalis</i>	control	-	168	4	2.3 ^a
	control [†] (heat)	1 min	178	173	97.2 ^b
	K ⁺ (100 mM)	1 h	163	3	1.8 ^a
	RR	0 min	172	13	7.5 ^a
	RR + K ⁺ (100 mM)		179	4	2.2 ^a
	RR	1 min	170	12	7.0 ^a
	RR + K ⁺ (100 mM)		170	7	4.1 ^a
	RR	3 min	189	17	8.9 ^a
	RR + K ⁺ (100 mM)		192	5	2.6 ^a
	RR	5 min	174	25	14.3 ^a
	RR + K ⁺ (100 mM)		191	17	8.9 ^a

Controls correspond to fungal cells without the peptide. Different letters denote significant differences, and the same letter denotes no difference, P < 0.05. K⁺ refers to the presence 100 mM of K₂HPO₄ + KH₂PO₄ incubated with the yeast for 15 min before the addition of RR. The assay is one representative out of three assays.

Table 6. Plasma membrane permeabilization in *Candida tropicalis* cells treated with D-RR at different times and in the presence of K⁺.

fungus	samples	incubation time	number of cells in DIC	number of fluorescent cells	cells with permeabilized membranes (%)
<i>Candida tropicalis</i>	control	-	170	5	2.9 ^a
	control ⁺ (heat)	1 min	178	173	97.2 ^b
	K ⁺ (100 mM)	30 min	163	3	1.8 ^a
	D-RR	0 min	170	10	5.8 ^a
	D-RR + K ⁺ (100 mM)		176	5	2.8 ^a
	D-RR	1 min	170	9	5.2 ^a
	D-RR + K ⁺ (100 mM)		170	5	2.9 ^a
	D-RR	3 min	169	16	9.4 ^a
	D-RR + K ⁺ (100 mM)		185	6	3.2 ^a
	D-RR	5 min	183	19	10.3 ^a
	D-RR + K ⁺ (100 mM)		176	13	7.3 ^a

Controls correspond to fungal cells without the peptide. Different letters denote significant differences, and the same letter denotes no difference, P < 0.05. K⁺ refers to the presence 100 mM K₂HPO₄ + KH₂PO₄ incubated with the yeast for 15 min before the addition of D-RR. The assay is one representative out of three assays.

Table 7. Plasma membrane permeabilization in *Candida albicans* cells treated with WR at different times and in the presence of K⁺.

fungus	samples	incubation time	number of cells in DIC	number of fluorescent cells	cells with permeabilized membranes (%)
<i>Candida albicans</i>	control	-	193	10	5.2 ^a
	control ⁺ (heat)	1 min	189	182	96.3 ^b
	K ⁺ (200 mM)	20 min	182	26	12.6 ^a
	WR	0 min	180	140	77.8 ^b
	WR + K ⁺ (200 mM)		183	22	12.0 ^a
	WR	1 min	178	176	98.9 ^b
	WR + K ⁺ (200 mM)		187	16	8.6 ^a
	WR	3 min	184	184	100 ^b
	WR + K ⁺ (200 mM)		186	26	14 ^a
	WR	5 min	187	186	99.5 ^b
	WR + K ⁺ (200 mM)		189	29	15.3 ^a

Controls correspond to fungal cells without the peptide. Different letters denote significant differences, and the same letter denotes no difference, P < 0.05. K⁺ refers to the presence 200 mM K₂HPO₄ + KH₂PO₄ incubated with the yeast for 15 min before the addition of WR. The assay is one representative out of three assays.

3.7. Fungal cells death under hypoosmotic conditions

Another mechanism involved in the protection provided by K^+ against peptide-induced cell death must be considered. Our results suggest that this protection is linked to maintaining equilibrium between intracellular and extracellular K^+ concentrations, which neutralizes the ion's electrochemical potential. This prevents K^+ from exiting the cell via its electrochemical gradient through channels, transporters [73], or the permeabilized membrane (Tables 5, 6, and 7). This conclusion is primarily supported by the protection from death observed when K^+ was added to the culture medium (Table 1). The external addition of K^+ creates an inversion of the typically low external K^+ concentration to a high concentration, effectively blocking the efflux of K^+ from the cell, which would otherwise follow its electrochemical gradient [73]. K^+ is present in relatively high concentrations in *Candida* species (200-300 mM) and plays crucial roles in cellular functions such as pH regulation, cell volume maintenance, compensation for negative charges, activation of metabolic processes, protein synthesis, and stabilization of membrane potential [36]. Thus, we hypothesize that the protection conferred by exogenously added K^+ is due to the restoration of intracellular K^+ balance, preserving K^+ -dependent cellular processes. This ion may enter the cell through the damaged membrane, restoring internal K^+ levels. If this is true, cells in a hypotonic medium would swell due to water influx, and to regulate volume, the cells would release K^+ , returning cell volume to normal. The K^+ efflux would reduce the intracellular K^+ concentration, rendering cells more susceptible to the action of the peptides, especially if the peptides also promote K^+ efflux, quickly reducing the internal K^+ concentration to a critical level. In this scenario, combined with a toxic stimulus, *e.g.* the peptide action, the cell death pathway is activated, and the cells become non-viable [73,74]. Our results showed that all three peptides killed the fungi much faster when the cells were pre-incubated in water as hypothesized (Table 8).

Table 8. Viability of *Candida tropicalis* and *Candida albicans* treated with RR, D-RR, and WR in Sabouraud medium and in water.

fungi	samples	incubation time	condition	number of surviving cells (UFC)	viability (protection) (%)	death (toxicity)(%)	
<i>Candida tropicalis</i>	control	0 min	Sabouraud medium	1035 ± 15	100 ^b	0 ^a	
	RR (27.5 μM)			879 ± 18	84.9 ^b	15.1 ^a	
	control		water	680 ± 27	100 ^b	0 ^a	
	RR (27.5 μM)			1 ± 2	0.1 ^a	99.9 ^b	
	<i>Candida tropicalis</i>	control	0 min	Sabouraud medium	1035 ± 15	100 ^b	0 ^a
		D-RR (23 μM)			875 ± 18	85.5 ^b	14.5 ^a
control		water		680 ± 27	100 ^b	0 ^a	
D-RR (23 μM)				0 ± 0	0 ^a	100 ^b	
<i>Candida albicans</i>	control	0 min	Sabouraud medium	902 ± 21	100 ^b	0 ^a	
	WR (27.5 μM)			46 ± 5	5.1 ^a	94.9 ^b	
	control		water	1025 ± 39	100 ^b	0 ^a	
	WR (27.5 μM)			0 ± 0	0 ^a	100 ^b	

CFU (colony forming units) values are mean ± standard deviation. Controls correspond to fungal cells without the peptides. The percentage of survival was calculated by comparing fungal cells treated in the presence of water with those treated in Sabouraud medium. Different letters denote significant differences and the same letter denotes no difference, $P < 0.05$. The assay is one representative out of three assays.

3.8. Assessment of cytoplasmic degradation

Taken together, the above results indicate that cell death is triggered by low cytoplasmic K^+ levels. Low cytoplasmic K^+ levels have been associated with cell death processes in mammalian cells [18,73] and with the activation of autophagy in *S. cerevisiae* with degradation of cellular constituents [75]. To investigate whether the fungal cells were undergoing cytoplasmic degradation, we assessed protein profile by electrophoresis under conditions of low intracellular K^+ induced as an effect of the bioinspired peptides. To improve visualization of low molecular weight proteins, we used Tricine gels, which clearly showed the disappearance of protein bands in the dAMPs- and AcA-treated samples, with preservation of the bands when K^+ was added (Fig. 7). Overall, the maintenance of protein bands in the presence of K^+ suggests that supplementation of external K^+ replenish intracellular ion concentrations to levels that prevent the activation of a degradative process responsible for cellular degradation and cell collapse.

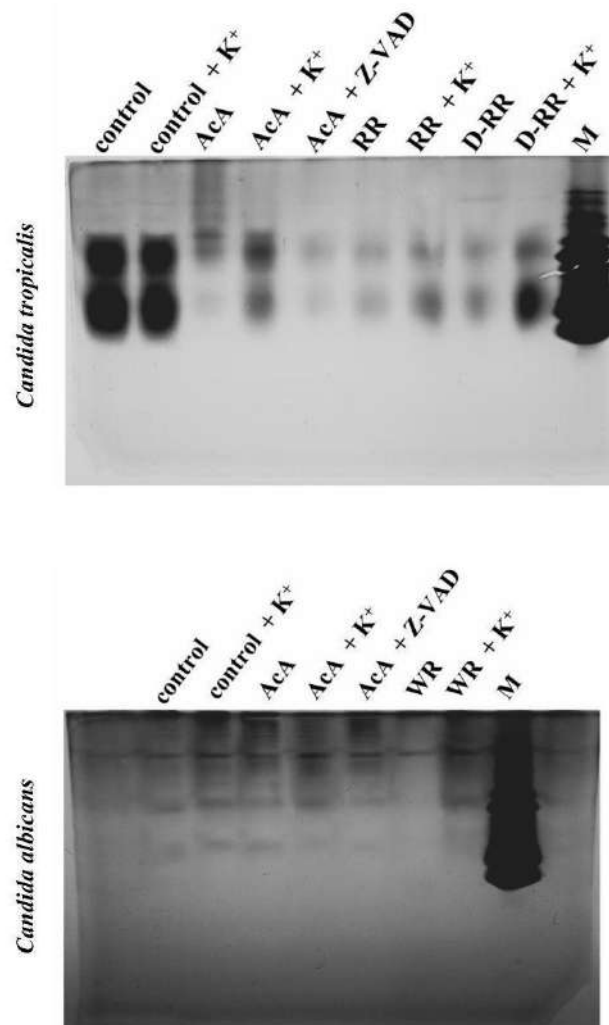


Fig. 7. Cytoplasmic degradation accompanied by electrophoresis in protein extracts from fungal cells treated with RR, D-RR, and WR. The degradation of proteins is indicated by the disappearance of the corresponding band in treated samples. Fungal cells were treated as described. K^+ ions were supplied as 100 mM $K_2HPO_4 + KH_2PO_4$. AcA refers to acetic acid, while Z-VAD represents Z-VAD-FMK, a broad-spectrum caspase inhibitor. M refers to molecular weight marker. RR and D-RR denote the peptides used in the study. The assay is one representative out of three assays.

To further characterize the cellular degradation process, we examined the fungal cell ultrastructure. Our results revealed extensive cytoplasmic disorganization and vacuolization in peptide-treated cells. Notably, these cells displayed membrane-compartment vesicles within the vacuole that suggest peptide-treated fungal cells are undergoing autophagy (Fig. 8). Therefore, the cellular degradation in the peptide-treated fungal may be caused by activation of autophagy triggered by the low intracellular K^+ concentration induced after peptide interaction [75].

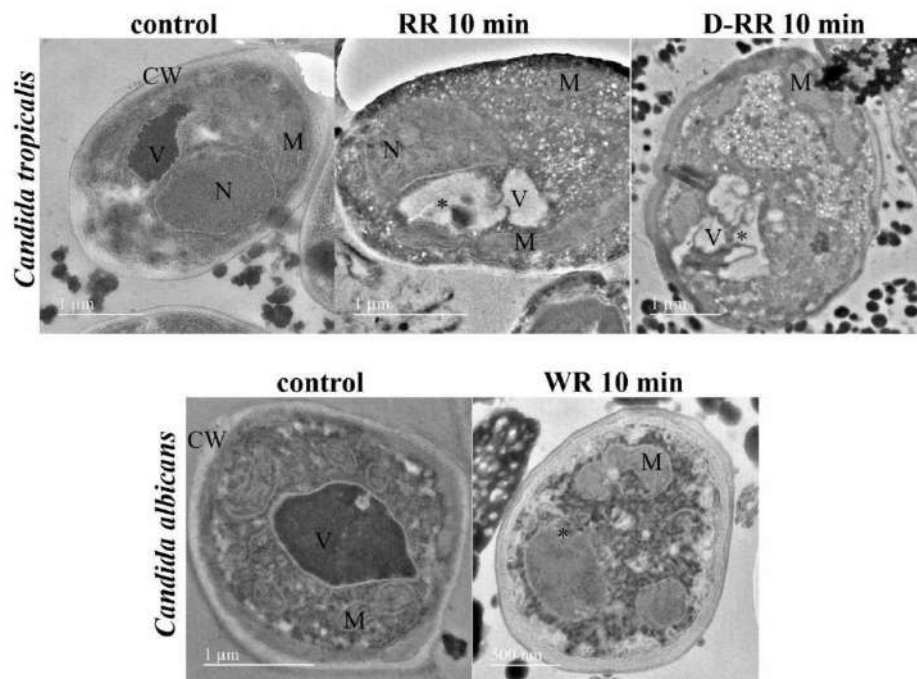


Fig. 8. Ultrastructure of fungal cells treated with RR, D-RR, and WR for 10 min. M refers to nucleus, V to vacuole, M to mitochondrion, and * to the cytoplasm vacuolization. The assay is one representative out of three assays.

4. Conclusion

Our research is focused on the mechanism of action of peptides on fungi, we have demonstrated that these peptides induce fungal cell death, accompanied by cell shrinkage, reactive oxygen species (ROS) production, vacuolization, and mitochondrial hyperpolarization [15]. In our studies, when death modulators such as ascorbic acid were added after peptide treatment, protection from death was no longer observed. Based on this, we postulated that fungal cells reach a stage in the death process where recovery becomes impossible. We termed this the 'point of no return' [15]. Supporting this hypothesis, we observed that within 15 min of incubation with RR and WR, *C. tropicalis* and *C. albicans*, respectively, exhibited positive staining for propidium iodide (PI). This suggests that, at this stage, the cells had already committed to the death pathway, marking a potential point of no return [15]. In fungi, this point was suggested to occur when the cell membrane loses its barrier function, allowing the entry of PI [76]. Notably, PI staining was absent in *C. tropicalis* treated with D-RR, indicating a possible distinct mechanism of action [15].

In this study, we assessed cell shrinkage and K^+ leakage in fungal cells treated with the dAMPs. We found that supplementing the medium with K^+ protected fungal cells from death (Table 1). However, when K^+ was added after dMAPs treatment, this protection was lost (Fig. 2), reinforcing our hypothesis of a 'point of no return' in the cell death process. At this critical juncture, cells appear to lose the ability to reverse the peptide-triggered death process. The ionic environment, particularly K^+ levels, plays a pivotal role in determining this outcome. Beyond this point, the death process is likely irreversibly activated, making both AA (in *C. tropicalis*) [15] and K^+ (in both *C. tropicalis* and *C. albicans*) ineffective in halting or reversing cell death once it has begun.

K^+ supplementation halted three processes induced by the dAMPs: mitochondrial hyperpolarization (Fig. 3), medium acidification (Fig. 6), and cellular degradation (Figs. 7 and 8). Mitochondrial hyperpolarization likely is the critical point in this peptide-mediated cell death process, as exogenous K^+ blocked hyperpolarization (Fig. 3) and cell death (Table 1). The important participation of mitochondria in cell death process is well established [38]. Furthermore, some studies demonstrated its hyperpolarization as a toxic effect on fungi by RsAFP2 and Plagiochin E (a macrocyclic bis(bibenzyl) from liverwort *Marchantia polymorpha* L.) [77,78], and the hyperpolarization within the death process triggered by Ppdef1 (plant defensin from *Picramnia pentandra*) [79] on *S. cerevisiae*. Therefore, the

mitochondrial dysfunction observed in the dMAPs-treated fungal cells may be involved in the cell death.

Our findings suggest that the dAMPs trigger K^+ extrusion (Table 2) through an as-yet-unknown mechanism, possibly as compensation for ΔpH formation via H^+ extrusion (Fig. 6) [67]. K^+ extrusion causes a reduction in its intracellular levels below a critical threshold that activate cell degradation (Fig. 7), as demonstrated in *S. cerevisiae* [75]. Thus, K^+ added to the medium protects fungal cells from death by maintaining intracellular K^+ concentrations above this critical level, preventing the activation of the regulated cell death signaling cascade that leads to cell death (Figs. 7 and 8). This explains the rapid decline in fungal cell viability caused by the dMAPs, a response typically mediated by rapid ion flux at the plasma membrane. Additionally, the lack of protection from ascorbic acid [15] or K^+ (Fig. 2) following dMAPs treatment can be attributed to the activation of cell degradation driving the death pathway, which proceeds independently of ROS scavenging by antioxidants or K^+ replenishment once initiated (Fig. 9).

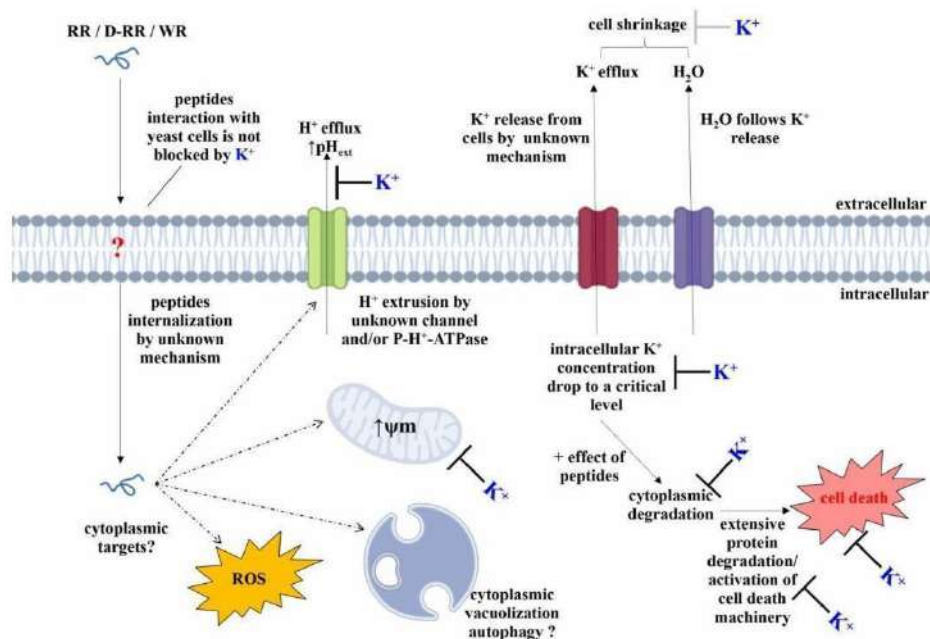


Fig. 9. Proposed mechanism of fungal cell death induced by bioinspired peptides, along with the protective role of K⁺ ions. (K⁺) represents potassium added to the medium. (⊖) indicates complete blockage, while (⊓) indicates partial blockage. (pHex) refers to extracellular pH. (----) represents related mechanisms. (↑) represents increased effect. (ψm) refers to mitochondrial membrane potential.

CRedit authorship contribution statement

Filipe Zaniratti Damica: Writing – original draft, Methodology, Investigation, Formal analysis, Data curation. **Douglas Ribeiro Lucas:** Writing – original draft, Methodology, Investigation, Formal analysis, Data curation. **Estefany Bras Toledo:** Methodology, Investigation. **Marilúcia de Carvalho Ribeiro:** Methodology, Investigation. **Anna Lvovna Okorokova Façanha:** Methodology, Investigation. **Ana Eliza Zeraik:** Methodology, Investigation. **Sérgio Henrique Seabra:** Methodology, Investigation. **Juliana Azevedo da Silva:** Methodology, Investigation. **Valdirene Moreira Gomes:** Methodology, Investigation. **André de Oliveira Carvalho:** Writing – review & editing, Conceptualization, Visualization, Supervision, Resources, Project administration, Methodology, Funding acquisition, Formal analysis.

Declaration of Competing Interest

Data availability

Data will be made available on request.

This article contains supporting information.

Funding

The work was supported by Brazilian agencies *Conselho Nacional de Desenvolvimento Científico e Tecnológico* (CNPq) (number 306429/2023-3), *Fundação Carlos Chagas Filho de Amparo à Pesquisa do Estado do Rio de Janeiro* (FAPERJ) (number E-26/210.484/2024, APQ1), and *Coordenação de Aperfeiçoamento de Pessoal de Nível Superior* (CAPES) (Financial Code 001), as well as by the University State of Norte Fluminense Darcy Ribeiro.

Notes

The authors declare no competing financial interest.

ACKNOWLEDGMENTS

We thank Luis Carlos Souza, Valéria Miguelote Kocks, and Zila Macedo for their technical assistance.

References

- [1] S. Banerjee, D. Denning, A. Chakrabarti, One health aspects and priority roadmap for fungal diseases: a mini-review. *Indian J. Med. Res.* 153 (2021) 311. https://doi.org/10.4103/ijmr.IJMR_768_21.
- [2] A. Spallone, I.S. Schwartz, Emerging fungal infections. *Infect Dis. Clin. North Am.* 35 (2021) 261–277. <https://doi.org/10.1016/j.idc.2021.03.014>.
- [3] World Health Organization. WHO fungal priority pathogens list to guide research, development and public health action. 2022 1–15.
- [4] D.W. Denning, Global incidence and mortality of severe fungal disease. *Lancet Infect. Dis.* (2024) S1473-3099(23)00692-8. [https://doi.org/10.1016/S1473-3099\(23\)00692-8](https://doi.org/10.1016/S1473-3099(23)00692-8).
- [5] N. Ashraf, R.C. Kubat, V. Poplin, A.A. Adenis, D.W. Denning, L. Wright, O. McCotter, I.S. Schwartz, B.R. Jackson, T. Chiller, N.C. Bahr, Re-drawing the maps for endemic mycoses. *Mycopathologia* 185 (2020) 843–65. <https://doi.org/10.1007/S11046-020-00431-2>.
- [6] M.L. Rodrigues, L.J.D. Nosanchuk, Fungal diseases as neglected pathogens: a wake-up call to public health officials. *PLoS Negl. Trop. Dis.* 14 (2020) e0007964. <https://doi.org/10.1371/JOURNAL.PNTD.0007964>.
- [7] D. Sanglard, Emerging threats in antifungal-resistant fungal pathogens. *Front. Med.* 3 (2016) 11. <https://doi.org/10.3389/fmed.2016.00011>.
- [8] K. Forsberg, K. Woodworth, M. Walters, E.L. Berkow, B. Jackson, T. Chiller, S. Vallabhaneni, *Candida auris*: the recent emergence of a multidrug-resistant fungal pathogen. *Med. Mycol.* 57 (2019) 1–12. <https://doi.org/10.1093/MMY/MYY054>.

- [9] S. Costa-de-Oliveira, A.G. Rodrigues, *Candida albicans* antifungal resistance and tolerance in bloodstream infections: the triad yeast-host-antifungal. *Microorganisms* 8(2) (2020) 154. <https://doi.org/10.3390/microorganisms8020154>.
- [10] P. Ioannou, S. Baliou, D.P. Kofteridis, Antimicrobial peptides in infectious diseases and beyond—a narrative review. *Life* 13 (2023) 1651. <https://doi.org/10.3390/life13081651>.
- [11] K. Parisi, T.M.A. Shafee, P. Quimbar, N.L. van der Weerden, M.R. Bleackley, M.A. Anderson, The evolution, function and mechanisms of action for plant defensins. *Semin. Cell Dev. Biol.* 88 (2019) 107–118. <https://doi.org/10.1016/j.semcdb.2018.02.004>.
- [12] P.M. Tavares, K. Thevissen, B.P.A. Cammue, I.E.J.A. François, E. Barreto-Bergter, C.P. Taborda, A.F. Marques, M.L. Rodrigues, L. Nimrichter, *In vitro* activity of the antifungal plant defensin *RsAFP₂* against *Candida* isolates and its *in vivo* efficacy in prophylactic murine models of candidiasis. *Antimicrob. Agents Chemother.* 52 (2008) 4522–4525. <https://doi.org/10.1128/AAC.00448-08>.
- [13] N. Ishaq, M. Bilal, H. Iqbal, Medicinal potentialities of plant defensins: a review with applied perspectives. *Medicines* 6 (2019) 29. <https://doi.org/10.3390/medicines6010029>.
- [14] E.B. Toledo, D.R. Lucas, T.L.B.V. Simão, S.D. Calixto, E. Lassounskaia, M.F. Muzitano, F.Z. Damica, V.M. Gomes, A.O. Carvalho, Design of improved synthetic antifungal peptides with targeted variations in charge, hydrophobicity and chirality based on a correlation study between biological activity and primary structure of plant defensin γ -cores. *Amino Acids* 53 (2021) 219–237. <https://doi.org/10.1007/s00726-020-02929-x>.
- [15] D.R. Lucas, F.Z. Damica, E.B. Toledo, A.J.D. Cogo, A.L. Okorokova-Façanha, V.M. Gomes, A.O. Carvalho, Bioinspired peptides induce different cell death mechanisms against opportunistic yeasts. *Probiotics Antimicrob Proteins* 16 (2024) 649–672. <https://doi.org/10.1007/s12602-023-10064-8>.
- [16] D. Carmona-Gutierrez, M.A. Bauer, A. Zimmermann, A. Aguilera, N. Austriaco, K. Ayscough, R. Balzan, S. Bar-Nun, A. Barrientos, P. Belenky, M. Blondel, R.J. Braun, M. Breitenbach, W.C. Burhans, S. Büttner, D. Cavalieri, M. Chang, K.F. Cooper, M. Côte-Real, V. Costa, C. Cullin, I. Dawes, J. Dengjel, M.B. Dickman, T. Eisenberg, B. Fahrenkrog, N. Fasel, K.-U. Fröhlich, A. Gargouri, S. Giannatasio, P. Goffrini, C.W. Goutlay, C.M. Grant, M.T. Greenwood, N. Guaragnella, T. Heger, J. Heinisch, E.

- Herker, J.M. Herrmann, S, Hofer, A. Jiménez-Ruiz, H. Jungwrith, K. Kainz, D.P. Kontoyiannis, P. Ludovico, S. Manon, E. Martegani, C. Mazzoni, L.A. Megeney, C. Meisinger, J. Nielsen, T. Nyström, H.D. Osiewacz, T.F. Outeiro, H.-O. Park, T. Pendl, D. Petranovic, S. Picot, P. Pločič, T. Powers, M. Ramsdale, M. Rinnerthaler, P. Rockenfeller, C. Ruckenstuhl, R. Schaffrath, M. Segovia, F.F. Severin, A. Sharon, S.J. Sigrist, C. Sommer-Ruck, M.J. Souza, J.M. Thevelein, K. Thevissen, V. Tintorenko, M.B. Toledano, M. Yuite, F.-N. Vögtle, B. Westermann, J. Winderickx, S. Wissing, S. Wölfi, Z.J. Zhang, R.Y. Zhao, B. Zhou, L. Galluzzi, G. Kroemer, F. Madeo, Guidelines and recommendations on yeast cell death nomenclature. *Microb. Cell* 1,5(1) (2018) 4–31. <https://doi.org/10.15698/MIC2018.01.607>.
- [17] O. Arrigoni, M.C.D. Tullio, Ascorbic acid: much more than just an antioxidant. *Biochim. Biophys. Acta (BBA) - General Subjects* 1569 (2002) 1–9. [https://doi.org/10.1016/S0304-4165\(01\)00235-5](https://doi.org/10.1016/S0304-4165(01)00235-5).
- [18] C.D. Bortner, J.A. Cidlowski. Ions, the movement of water and the apoptotic volume decrease. *Front. Cell. Dev. Biol.* 8 (2020) 1415. <https://doi.org/10.3389/FCELL.2020.611211>.
- [19] J. Yun, D.G. Lee, Role of potassium channels in chlorogenic acid-induced apoptotic volume decrease and cell cycle arrest in *Candida albicans*. *Biochim. Biophys. Acta (BBA) - General Subjects* 1861 (2017) 585–92. <https://doi.org/10.1016/j.bbagen.2016.12.026>.
- [20] J.F. Sambrook, D.W. Russell. *Molecular cloning: a laboratory manual*. Third ed. Cold Spring Harbor Laboratory Press, 2001.
- [21] J.G. Lees, B.R. Smith, F. Wien, A.J. Miles, B.A. Wallace, CDtool—an integrated software package for circular dichroism spectroscopic data processing, analysis, and archiving. *Anal. Biochem.* 332 (2004) 285–289. <https://doi.org/10.1016/j.ab.2004.06.002>.
- [22] M.S.S. Diz, A.O. Carvalho, R. Rodrigues, A.G.C. Neves-Ferreira, M. Da Cunha, E.W. Alves, A.L. Okorokova-Façanha, M.A. Oliveira, J. Perales, O.L.T. Machado, V.M. Gomes, Antimicrobial peptides from chilli pepper seeds causes yeast plasma membrane permeabilization and inhibits the acidification of the medium by yeast cells. *Biochim Biophys Acta (BBA) - General Subjects* 1760 (2006) 1323–1332. <https://doi.org/10.1016/j.bbagen.2006.04.010>.
- [23] V.A. Bidiuk, A.I. Alexandrov, A.Y. Valiakhmetov, Extracellular pH and high concentration of potassium regulate the primary necrosis in the yeast *Saccharomyces*

- cerevisiae*. Arch Microbiol 204 (2022) 35. <https://doi.org/10.1007/s00203-021-02708-6>.
- [24] K. Thevissen, F.R.G. Terras, W.F. Broekaert, Permeabilization of fungal membranes by plant defensins inhibits fungal growth. Appl. Environ. Microbiol. 65 (1999) 5451–5458. <https://doi.org/10.1128/AEM.65.12.5451-5458.1999.x>
- [25] H. Schägger, G. von Jagow, Tricine-sodium dodecyl sulfate-polyacrylamide gel electrophoresis for the separation of proteins in the range from 1 to 100 kDa. Anal. Biochem. 166 (1987) 368–379. [https://doi.org/10.1016/0003-2697\(87\)90587-2](https://doi.org/10.1016/0003-2697(87)90587-2).
- [26] Y. Li, L. Sun, C. Lu, Y. Gong, M. Li, S. Sun, Promising antifungal targets against *Candida albicans* based on ion homeostasis. Front. Cell Infect. Microbiol. 8 (2018) 286. <https://doi.org/10.3389/fcimb.2018.00286>.
- [27] M.T. Andrés, M. Acosta-Zaldívar, J. González-Seisdedos, J.F. Fierro, Cytosolic acidification is the first transduction signal of lactoferrin-induced regulated cell death pathway. Int. J. Mol. Sci. 20(23) (2019) 5838. <https://doi.org/10.3390/ijms20235838>.
- [28] T. Tanida, T. Okamoto, E. Ueta, T. Yamamoto, T. Osaki, Antimicrobial peptides enhance the candidacidal activity of antifungal drugs by promoting the efflux of ATP from *Candida* cells. J. Antimicrob. Chemother. 57 (2006) 94–103. <https://doi.org/10.1093/jac/dki402>.
- [29] C.V. Remillard, J.X.-J. Yuan, Activation of K⁺ channels: an essential pathway in programmed cell death. Am. J. Physiol. Lung. Cell. Mol. Physiol. 286 (2004) L49–67. <https://doi.org/10.1152/ajplung.00041.2003>.
- [30] W. Lee, D.G. Lee, Potential role of potassium and chloride channels in regulation of silymarin-induced apoptosis in *Candida albicans*. IUBMB Life. 70(3) (2018) 197–206. doi: 10.1002/iub.1716.
- [31] M.T. Andrés, M. Viejo-Díaz, J.F. Fierro, Human lactoferrin induces apoptosis-like cell death in *Candida albicans*: critical role of K⁺-channel-mediated K⁺ efflux. Antimicrob. Agents Chemother. 52 (2008) 4081–4088. <https://doi.org/10.1128/AAC.01597-07>.
- [32] J.E. Yun, D.G. Lee, Role of potassium channels in chlorogenic acid-induced apoptotic volume decrease and cell cycle arrest in *Candida albicans*. Biochim. Biophys. Acta – Gen. Subj. 1861 (2017) 585–592. <https://doi.org/10.1016/J.BBAGEN.2016.12.026>.
- [33] J. Yun, D.G. Lee, Cecropin A-induced apoptosis is regulated by ion balance and glutathione antioxidant system in *Candida albicans*. IUBMB Life 68 (2016) 652–662. <https://doi.org/10.1002/iub.1527>.

- [34] D. Baev, A. Rivetta, X.S. Li, S. Vylkova, E. Bashi, C.L. Slayman, M. Edgerton, Killing of *Candida albicans* by human salivary histatin 5 is modulated, but not determined, by the potassium channel TOK1. *Infect. Immun.* 71 (2003) 3251–3260. <https://doi.org/10.1128/IAI.71.6.3251-3260.2003>.
- [35] J. Han, M.A. Jyoti, H.–Y. Song, W.S. Jang. Antifungal activity and action mechanism of histatin 5-halocidin hybrid peptides against *Candida* ssp. *PLoS One* 11 (2016) e0150196. <https://doi.org/10.1371/journal.pone.0150196>.
- [36] J. Ariño, J. Ramos, H. Sychrová. Alkali metal cation transport and homeostasis in yeasts. *Microbiol. Mol. Biol. Rev.* 74 (2010) 95–120. <https://doi.org/10.1128/MMBR.00042-09>.
- [37] S.R. Chaves, A. Rego, V.M. Martins, C. Santos-Pereira, M.J. Sousa, M. Côrte-Real, Regulation of cell death induced by acetic acid in yeasts. *Front. Cell Dev. Biol.* 9 (2021) 642375. <https://doi.org/10.3389/FCELL.2021.642375>.
- [38] F.J. Bock, S.W.G. Tait, Mitochondria as multifaceted regulators of cell death. *Nat. Rev. Mol. Cell Biol.* 21 (2020) 85–100. <https://doi.org/10.1038/s41580-019-0173-8>.
- [39] J.J. Smith, S.M. Travis, E.P. Greenberg, M.J. Welsh, Cystic fibrosis airway epithelia fail to kill bacteria because of abnormal airway surface fluid. *Cell* 85 (1996) 229–236. [https://doi.org/10.1016/S0092-8674\(00\)81099-5](https://doi.org/10.1016/S0092-8674(00)81099-5).
- [40] M.J. Goldman, G.M. Anderson, E.D. Stolzenberg, U.P. Kari, M. Zasloff, J.M. Wilson, Human β -defensin-1 is a salt-sensitive antibiotic in lung that is inactivated in cystic fibrosis. *Cell* 88 (1997) 553–560. [https://doi.org/10.1016/S0092-8674\(00\)81895-4](https://doi.org/10.1016/S0092-8674(00)81895-4).
- [41] T. Ganz, R.I. Lehrer, Antibiotic peptides from higher eukaryotes: biology and applications. *Mol Med Today* 5(7) (1999) 292–297. [https://doi.org/10.1016/S1357-4310\(99\)01490-2](https://doi.org/10.1016/S1357-4310(99)01490-2).
- [42] M. Viejo-Díaz, M.T. Andrés, J.F. Fierro, Modulation of *in vitro* fungicidal activity of human lactoferrin against *Candida albicans* by extracellular cation concentration and target cell metabolic activity. *Antimicrob Agents Chemother.* 48(4) (2004) 1242–8. doi: 10.1128/AAC.48.4.1242-1248.2004.
- [43] R.E.W. Hancock, H.–G. Sahl, Antimicrobial and host-defense peptides as new anti-infective therapeutic strategies. *Nat. Biotechnol.* 24 (2006) 1551–1557. <https://doi.org/10.1038/nbt1267>.
- [44] F.R.G. Terras, S. Torrekens, F. Van Leuven, R.W. Osborn, J. Vanderleyden, B.P.A. Cammue, W.F. Broekaert, A new family of basic cysteine-rich plant antifungal

- proteins from Brassicaceae species. *FEBS Lett.* 316(3) (1993) 233–240. [https://doi.org/10.1016/0014-5793\(93\)81299-F](https://doi.org/10.1016/0014-5793(93)81299-F).
- [45] S. Vylkova, N. Nayyar, W. Li, M. Edgerton, Human β -defensins kill *Candida albicans* in an energy-dependent and salt-sensitive manner without causing membrane disruption. *Antimicrob. Agents Chemother.* 51 (2007) 154–161. <https://doi.org/10.1128/AAC.00478-06>.
- [46] R.C. Anderson, P.–L. Yu, Factors affecting the antimicrobial activity of ovine-derived cathelicidins against *E. coli* 0157:H7. *Int. J. Antimicrob. Agents* 25 (2005) 205–210. <https://doi.org/10.1016/j.ijantimicag.2004.10.010>.
- [47] S.M. Kelly, N.C. Price, The use of circular dichroism in the investigation of protein structure and function. *Curr. Protein Pept. Sci.* 1 (2000) 349–384. <https://doi.org/10.2174/1389203003381315>.
- [48] C.B. Park, H.S. Kim, S.C. Kim, Mechanism of action of the antimicrobial peptide buforin II: buforin II kills microorganisms by penetrating the cell membrane and inhibiting cellular functions. *Biochem. Biophys. Res. Commun.* 244 (1998) 253–257. <https://doi.org/10.1006/BBRC.1998.8159>.
- [49] A.B. Mochon, H. Liu, The antimicrobial peptide histatin-5 causes a spatially restricted disruption on the *Candida albicans* surface, allowing rapid entry of the peptide into the cytoplasm. *PLoS Pathog.* 4(10) (2008) e1000190. doi: 10.1371/journal.ppat.1000190.
- [50] B. Hayes, M. Bleackley, M. Anderson, N. Van der Weerden, The plant defensin NaD1 enters the cytoplasm of *Candida albicans* via endocytosis. *J. Fungi* 4 (2018) 20. <https://doi.org/10.3390/jof4010020>.
- [51] T. Saito, S. Kawabata, T. Shigenaga, Y. Takayenoki, J. Cho, H. Nakajima, M. Hirata, S. Iwanaga, A novel big defensin identified in horseshoe crab hemocytes: isolation, amino acid sequence, and antibacterial activity. *J. Biochem.* 117 (1995) 1131–1137. <https://doi.org/10.1093/oxfordjournals.jbchem.a124818>.
- [52] J. Turner, Y. Cho, N.–N. Dinh, A.J. Waring, R.I. Lehrer, Activities of LL-37, a cathelin-associated antimicrobial peptide of human neutrophils. *Antimicrob. Agents Chemother.* 42 (1998) 2206–2214. <https://doi.org/10.1128/AAC.42.9.2206>.
- [53] M. Tetorya, H. Li, A.T. Djami–Tchatchou, G.W. Buchko, K.J. Czymmek, D.M. Shah, Plant defensin *MtDef4*-derived antifungal peptide with multiple modes of action and potential as a bio-inspired fungicide. *Mol. Plant Pathol.* 24 (2023) 896–913. <https://doi.org/10.1111/mpp.13336>.

- [54] B.C. Monk, K. Niimi, S. Lin, A. Knight, T.B. Kardos, R.D. Cannon, R. Parshot, D. Lun, D.R.K. Harding, Surface-active fungicidal D-peptide inhibitors of the plasma membrane proton pump that block azole resistance. *Antimicrob. Agents Chemother.* 49 (2005) 57–70. <https://doi.org/10.1128/AAC.49.1.57-70.2005>.
- [55] P.N. Lipke, R. Ovalle, Cell Wall Architecture in yeast: new structure and new challenges. *J. Bacteriol.* 180 (1998) 3735–3740. <https://doi.org/10.1128/JB.180.15.3735-3740.1998>.
- [56] C.A. Buscaglia, V.A. Campo, A.C.C. Frasci, J.M.D. Noia, *Trypanosoma cruzi* surface mucins: host-dependent coat diversity. *Nat. Rev. Microbiol.* 4 (2006) 229–236. <https://doi.org/10.1038/nrmicro1351>.
- [57] A. Mor, V.H. Nguyen, A. Delfour, D. Migliore-Samour, P. Nicolas, Isolation, amino acid sequence and synthesis of dermaseptin, a novel antimicrobial peptide of amphibian skin. *Biochemistry* 30 (1991) 8824–8830. <https://doi.org/10.1021/bi00100a014>.
- [58] D. Michaelson, J. Rayner, M. Couto, T. Ganz, Cationic defensins arise from charge-neutralized propeptides: a mechanism for avoiding leukocyte autotoxicity?. *J. Leukoc. Biol.* 51 (1992) 634–639. <https://doi.org/10.1002/jlb.51.6.634>.
- [59] C.L. Wilson, A.J. Ouellette, D.P. Satchell, T. Ayabe, Y.S. López-Boado, J.L. Stratman, S.J. Hultegren, L.M. Matrisian, W.C. Parks, Regulation of intestinal α -defensin activation by the metalloproteinase matrilysin in innate host defense. *Science* 286 (1999) 113–117. <https://doi.org/10.1126/science.286.5437.113>.
- [60] A. Bera, S. Singh, R. Nagaraj, T. Vaidya, Induction of autophagic cell death in *Leishmania donovani* by antimicrobial peptides. *Mol. Biochem. Parasitol.* 127 (2003) 23–35. [https://doi.org/10.1016/S0166-6851\(02\)00300-6](https://doi.org/10.1016/S0166-6851(02)00300-6).
- [61] J.S. Gunn, K.B. Lim, J. Krueger, K. Kim, L. Guo, M. Hackett, S.I. Miller, PmrA–PmrB-regulated genes necessary for 4-aminoarabinose lipid A modification and polymyxin resistance. *Mol. Microbiol.* 27 (1998) 1171–1182. <https://doi.org/10.1046/j.1365-2958.1998.00757.x>.
- [62] A. Peschel, R.W. Jack, M. Otto, L.V. Collins, P. Staubitz, G. Nicholson, H. Kalbacher, W.F. Nieuwenhuizen, G. Jung, A. Tarkowski, K.P. van Kessel, J.A. van Trijp, *Staphylococcus aureus* resistance to human defensins and evasion of neutrophil killing via the novel virulence factor mprf is based on modification of membrane lipids with L-lysine. *J. Exp. Medicine* 193 (2001) 1067–1076. <https://doi.org/10.1084/JEM.193.9.1067>.

- [63] A. Peschel, M. Otto, R.W. Jack, H. Kalbacher, G. Jung, F. Götz, Inactivation of the *dlt* operon in *Staphylococcus aureus* confers sensitivity to defensins, protegrins, and other antimicrobial peptides. *J. Biol. Chem.* 274 (1999) 8405–8410. <https://doi.org/10.1074/jbc.274.13.8405>.
- [64] B.-S. Yu, L.-H. Nie, S.-Z. Yao, Ion chromatographic study of sodium, potassium and ammonium in human body fluids with bulk acoustic wave detection. *J. Chromatogr. B Biomed. Sci. Appl.* 693 (1997) 43–49. [https://doi.org/10.1016/S0378-4347\(97\)00019-4](https://doi.org/10.1016/S0378-4347(97)00019-4).
- [65] D. Granot, A. Levine, E. Dorhefetz, Sugar-induced apoptosis in yeast cells. *FEMS Yeast Res.* 4 (2003) 7–13. [https://doi.org/10.1016/S1567-1356\(03\)00154-5](https://doi.org/10.1016/S1567-1356(03)00154-5).
- [66] S. Salvioli, A. Ardizzoni, C. Franceschi, A. Cossarizza, JC-1, but not DiOC6(3) or rhodamine 123, is a reliable fluorescent probe to assess delta psi changes in intact cells: implications for studies on mitochondrial functionality during apoptosis. *FEBS Lett.* 1997 7;411(1):77-82. doi: 10.1016/s0014-5793(97)00669-8. PMID: 9247146.
- [67] L. Maresova, E. Urbankova, D. Gaskova, H. Sychrova, Measurements of plasma membrane potential changes in *Saccharomyces cerevisiae* cells reveal the importance of the Tok1 channel in membrane potential maintenance. *FEMS Yeast Res.* 6 (2006) 1039–1046. <https://doi.org/10.1111/j.1567-1364.2006.00140.x>.
- [68] K. Thevissen, A. Ghazi, G.W. De Samblanx, C. Brownlee, R.W. Osborn, W.F. Broekaert, Fungal membrane responses induced by plant defensins and thionins. *J. Biol. Chem.* 271 (1996) 15018–1525. <https://doi.org/10.1074/jbc.271.25.15018>.
- [69] M.C. Regente, A.M. Giudici, J. Villalain, L.D.L. Canal, The cytotoxic properties of a plant lipid transfer protein involve membrane permeabilization of target cells. *Lett. Appl. Microbiol.* 40 (2005) 183–189. <https://doi.org/10.1111/j.1472-765X.2004.01647.x>.
- [70] M.L. Mangoni, J.M. Saugar, M. Dellisanti, D. Barra, M. Simmaco, L. Rivas, Temporins, small antimicrobial peptides with leishmanicidal activity. *J. Biol. Chem.* 280 (2005) 984–990. <https://doi.org/10.1074/jbc.M410795200>.
- [71] N.L. Van der Weerden, F.T. Lay, M.A. Anderson. The plant defensin, *NaD₁*, enters the cytoplasm of *Fusarium oxysporum* hyphae. *J. Biol. Chem.* 283 (2008) 14445–14452. <https://doi.org/10.1074/jbc.M709867200>.
- [72] F.J. Ruiz-Castilla, F.S. Ruiz Pérez, L. Ramos-Moreno, J. Ramos, *Candida albicans* potassium transporters. *Int. J. Mol. Sci.* 23 (2022) 4884. <https://doi.org/10.3390/ijms23094884>.

- [73] F.M. Hughes Jr., J.A. Cidlowski, Potassium is a critical regulator of apoptotic enzymes *in vitro* and *in vivo*. *Adv. Enzyme Regul.* 39 (1999) 157–171. [https://doi.org/10.1016/S0065-2571\(98\)00010-7](https://doi.org/10.1016/S0065-2571(98)00010-7).
- [74] C.D. Bortner, F.M. Hughes, J.A. Cidlowski, A primary role for K⁺ and Na⁺ efflux in the activation of apoptosis. *J. Biol. Chem.* 272 (1997) 32436–32442. <https://doi.org/10.1074/jbc.272.51.32436>.
- [75] N. Rangarajan, I. Kapoor, S. Li, P. Drossopoulos, K.K. White, V.J. Madden, H.G. Dohlman, Potassium starvation induces autophagy in yeast. *J Biol Chem.* 41 (2020) 14189-14202. doi: 10.1074/jbc.RA120.014687.
- [76] A. Rego, A. Ribeiro, M. Côrte-Real, S.R. Chaves, Monitoring yeast regulated cell death: trespassing the point of no return to loss of plasma membrane integrity. *Apoptosis* 27 (2022) 778–786. <https://doi.org/10.1007/s10495-022-01748-7>.
- [77] A.M. Aerts, I.E. François, E.M. Meert, Q.-T. Li, B.P. Cammue, K. Thevissen, The antifungal activity of RsAFP2, a plant defensin from *Raphanus sativus*, involves the induction of reactive oxygen species in *Candida albicans*. *Microb. Physiol.* 13 (2007) 243–247
- [78] X.-Z. Wu, A.-X. Cheng, L.-M. Sun, S.-J. Sun, H.-X. Lou, Plagiochin E, an antifungal bis (bibenzyl), exerts its antifungal activity through mitochondrial dysfunction-induced reactive oxygen species accumulation in *Candida albicans*. *Biochim. Biophys. Acta Gen. Subj.* 1790 (2009) 770–777.
- [79] K. Parisi, J.A. McKenna, R. Lowe, K.S. Harris, T. Sha3.4ee, R. Guarino, E. Lee, N.L. van der Weerden, M.R. Bleackley, M.A. Anderson, Hyperpolarisation of mitochondrial membranes is a critical component of the antifungal mechanism of the plant defensin, Ppdef1. *J. Fungi (Basel)* 10 (2024) 54. <https://doi.org/10.3390/jof10010054>.

5.2 Figura Suplementar

Supplementary material

A role in intracellular K⁺ in protecting pathogenic dimorphic fungi against induced cell death by bioinspired antimicrobial peptides

Filipe Zaniratti Damica^{a,1}, Douglas Ribeiro Lucas^{a,1}, Estefany Bras Toledo^a, Marilúcia de Carvalho Ribeiro^a, Anna Lvovna Okorokova Façanha^a, Ana Eliza Zeraik^b, Sérgio Henrique Seabra^c, Juliana Azevedo da Silva^d, Valdirene Moreira Gomes^a, André de Oliveira Carvalho^{a,*}

^aLaboratório de Fisiologia e Bioquímica de Microrganismos, Centro de Biociências e Biotecnologia, Universidade Estadual do Norte Fluminense Darcy Ribeiro, Campos dos Goytacazes-RJ, 28013-602, Brasil.

^bLaboratório de Química e Função de Proteínas e Peptídeos, Centro de Biociências e Biotecnologia, Universidade Estadual do Norte Fluminense Darcy Ribeiro, Campos dos Goytacazes-RJ, 28013-602, Brazil.

^cLaboratório de Biologia Celular e Tecidual, Centro de Biociências e Biotecnologia, Universidade Estadual do Norte Fluminense Darcy Ribeiro, Campos dos Goytacazes-RJ, 28013-602, Brazil.

^dLaboratório de Biologia do Reconhecer, Centro de Biociências e Biotecnologia, Universidade Estadual do Norte Fluminense Darcy Ribeiro, Campos dos Goytacazes-RJ, 28013-602, Brazil.

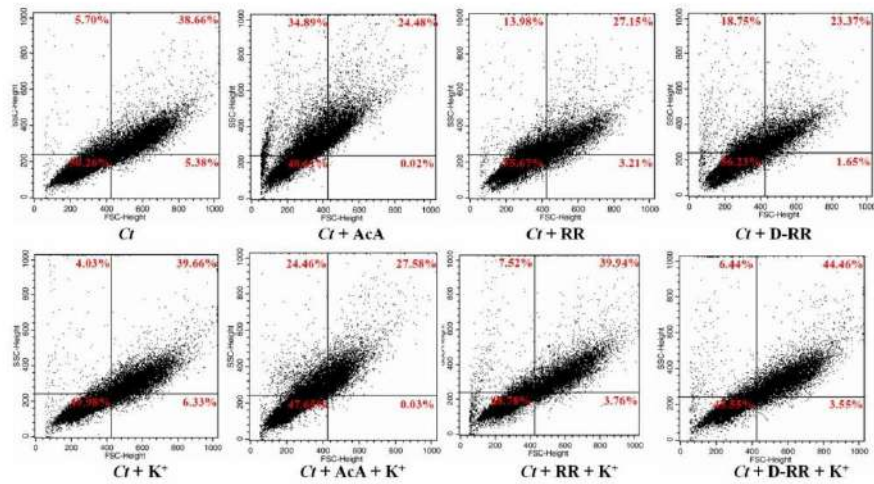
¹These authors contributed equally to this work.

*corresponding author: André de Oliveira Carvalho, Av. Alberto Lamego, nº 2000, Laboratório de Fisiologia e Bioquímica de Microrganismos, Centro de Biociências e Biotecnologia, Universidade Estadual do Norte Fluminense Darcy Ribeiro, Parque Califórnia, Campos dos Goytacazes, RJ, Brazil, CEP 28013-602; Tel (+55) 22 2739-7217; E-mail address: andre@uenf.br

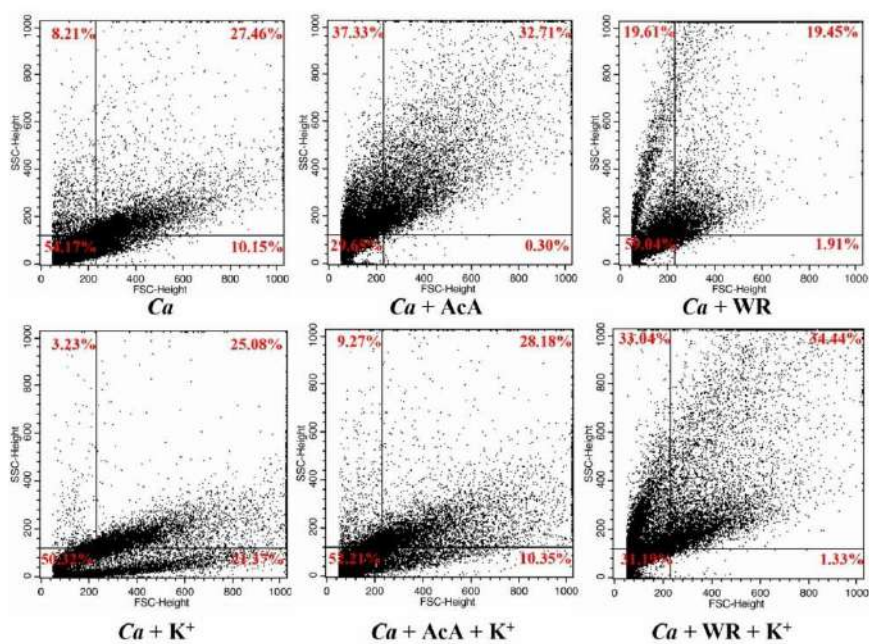
Table S1. Influence of salts on the lethality of opportunistic fungus *Candida albicans* induced by WR at its LD₁₀₀ concentration and induced time of death. The fungus was pre-incubated for 15 min in the presence of KCl or K₂HPO₄ + K₂HPO₄ at specified concentrations. Colony-forming unit (CFU) counts are presented as the mean ± standard deviation.

condition/pre-incubation (15 min)	incubation time	samples	CFU	% viability (protection)	% of death (toxicity)
without salt	20 min	control	212 ± 5	100 ^a	0 ^b
		WR (27.5 µM)	0 ± 0	0 ^b	100 ^a
KCl (100 mM)		control	187 ± 11	88.1 ^a	11.9 ^b
		WR (27.5 µM)	26 ± 14	14.2 ^b	85.8 ^a
KH ₂ PO ₄ + K ₂ HPO ₄ (100 mM)		control	205 ± 12	96.3 ^a	3.7 ^b
		WR (27.5 µM)	27 ± 5	13.3 ^b	86.7 ^a

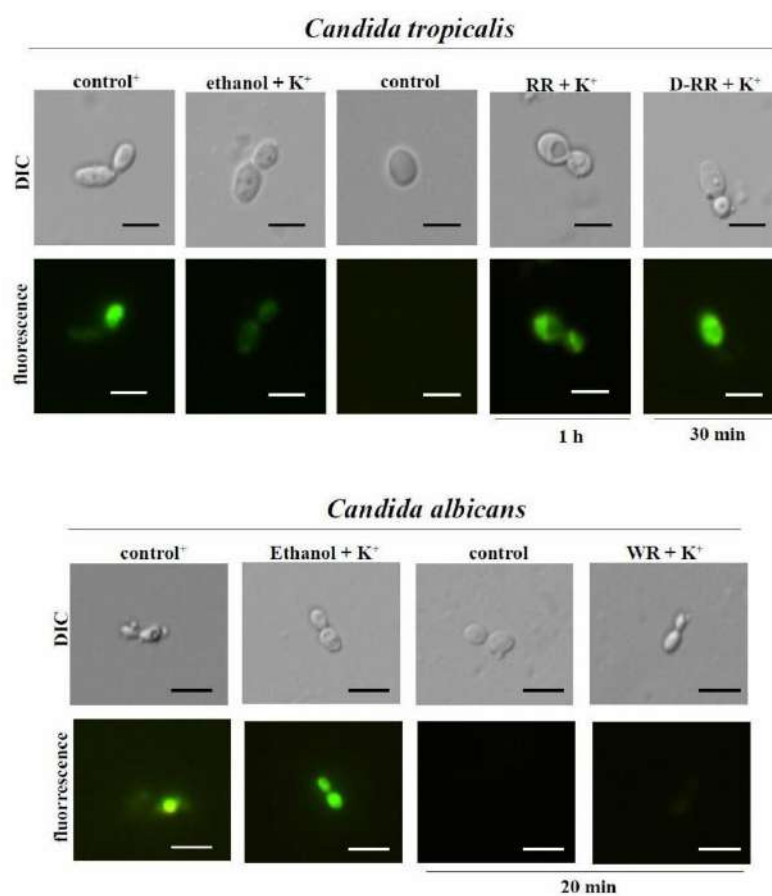
Controls consisted of fungal cells without peptide treatment. Comparisons were made between peptide-treated fungus in each salt condition and their respective salt-treated controls. Salt toxicity was assessed by comparing the controls with and without salt addition. Survival percentages were calculated by comparing fungus survival with salt treatment to those without salt treatment. Different letters indicate significant differences ($P < 0.05$), while the same letters indicate no significant difference. The assay is one representative out of three assays.



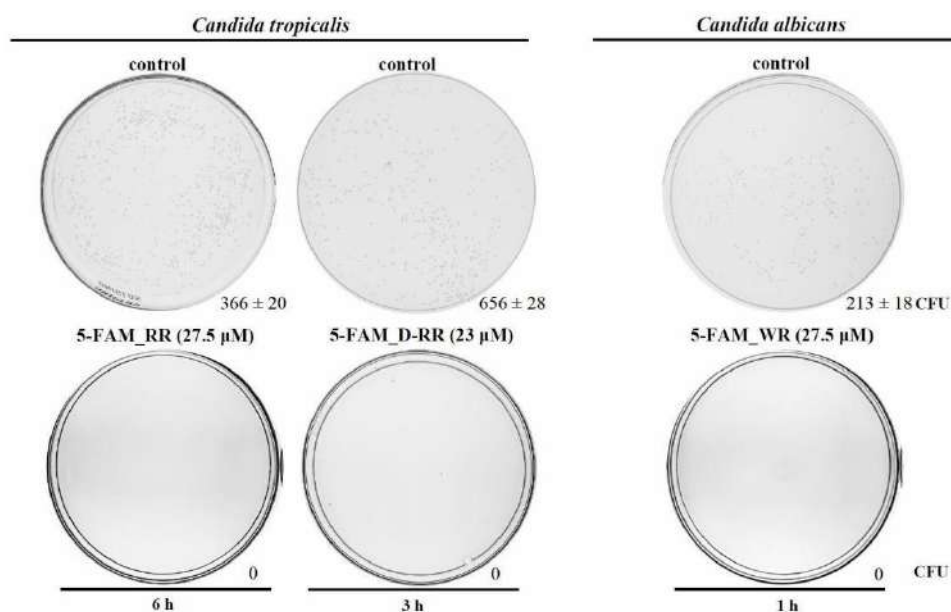
Supplementary figure 1. Density plot quadrants of *Candida tropicalis* in Sabouraud medium, in the presence of acetic acid (AcA), the peptides RR and D-RR, and in the presence of K⁺. Cell subpopulations were analyzed by forward light scattering (FSC) to estimate overall cell size and side light scattering (SSC) to assess cytoplasmic granularity.



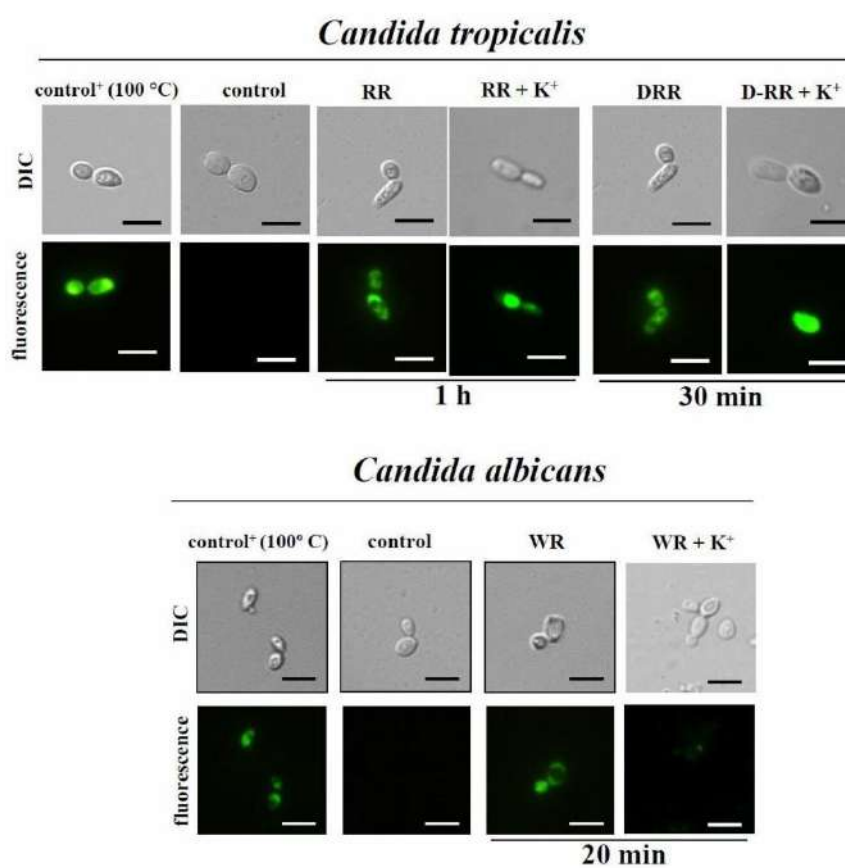
Supplementary figure 2. Density plot quadrants of *Candida albicans* in Sabouraud medium, in the presence of acetic acid (AcA), the peptide WR, and in the presence of K^+ . Cell subpopulations were analyzed by forward light scattering (FSC) to estimate overall cell size and side light scattering (SSC) to assess cytoplasmic granularity.



Supplementary Figure 3. Oxidative stress in *Candida tropicalis* and *Candida albicans* cells treated with bioinspired peptides. Microscope images show cells under various conditions in culture media supplemented with K⁺. Green fluorescence in the cytoplasm indicates the presence of reactive oxygen species. Scale bars = 10 μm. Images are representative of the assay detailed in Table 2.



Supplementary Figure 4. Antimicrobial activity of 5-FAM-labeled peptides RR, D-RR, and WR at their LD₁₀₀ (μM) and cell death induced times (h) against *Candida albicans* and *Candida tropicalis*. The absence of colonies in the treated samples indicates that the 5-FAM-labeled peptides retained their biological activity. Images show the assay Petri dishes. CFU = Colony-forming units, presented as means ± standard deviations. Data represent one of three independent assays. For the control peptide, refer to peptide DD in Fig. 1 of the article E.B. Toledo, D.R. Lucas, T.L.B.V. Simão, S.C. Calixto, E. Lassounskaia, M.F. Muzitano, F.Z. Damica, V.M. Gomes, A.O. Carvalho, Design of improved synthetic antifungal peptides with targeted variations in charge, hydrophobicity and chirality based on a correlation study between biological activity and primary structure of plant defensin γ-cores. *Amino Acids*. 53(2) (2021) 219–237. doi: 10.1007/s00726-020-02929-x.



Supplementary Figure 5. Plasma membrane permeabilization in *Candida tropicalis* and *Candida albicans* cells treated with bioinspired peptides. Microscope images show cells under various conditions in culture media supplemented with K⁺. Green fluorescence in the cytoplasm indicates plasma membrane permeabilization. Scale bars = 10 μm. Images are representative of the assay detailed in Table 5.

6- CAPÍTULO 3

Energy-dependent internalization mechanism, cytoplasmic localization, and impact on the ultrastructure of pathogenic fungi of the genus *Candida* by three bioinspired antimicrobial peptides

6. CHAPTER 3: MANUSCRIPT SUBMITTED

Energy-dependent internalization mechanism, cytoplasmic localization, and impact on the ultrastructure of pathogenic fungi of the genus *Candida* by three bioinspired antimicrobial peptides

Douglas Ribeiro Lucas^{a,1}, Filipe Zaniratti Damica^{a,1}, Felipe Figueirôa Moreira^b, Juliana Azevedo da Silva^c, Felipe Perissé Duarte Lopes^d, Noil Gomes de Freitas^a, Sérgio Henrique Seabra^b, Anna Lvovna Okorokova-Façanha^a, Valdirene Moreira Gomes^a, André de Oliveira Carvalho,*

^aLaboratório de Fisiologia e Bioquímica de Microrganismos, Centro de Biociências e Biotecnologia, Universidade Estadual do Norte Fluminense Darcy Ribeiro, Campos dos Goytacazes-RJ, 28013-602, Brazil.

^bLaboratório de Biologia Celular e Tecidual, Centro de Biociências e Biotecnologia, Universidade Estadual do Norte Fluminense Darcy Ribeiro, Campos dos Goytacazes-RJ, 28013-602, Brazil. ^cLaboratório de Biologia do Reconhecer, Centro de Biociências e Biotecnologia, Universidade Estadual do Norte Fluminense Darcy Ribeiro, Campos dos Goytacazes-RJ, 28013-602, Brazil.

^dLaboratório de Materiais Avançados, Centro de Ciência e Tecnologia, Universidade Estadual do Norte Fluminense Darcy Ribeiro, Campos dos Goytacazes-RJ, 28013-602, Brazil.

¹**These authors contributed equally to this work.**

Type of article: Research article

Situation: submitted

Journal: ACS ômega

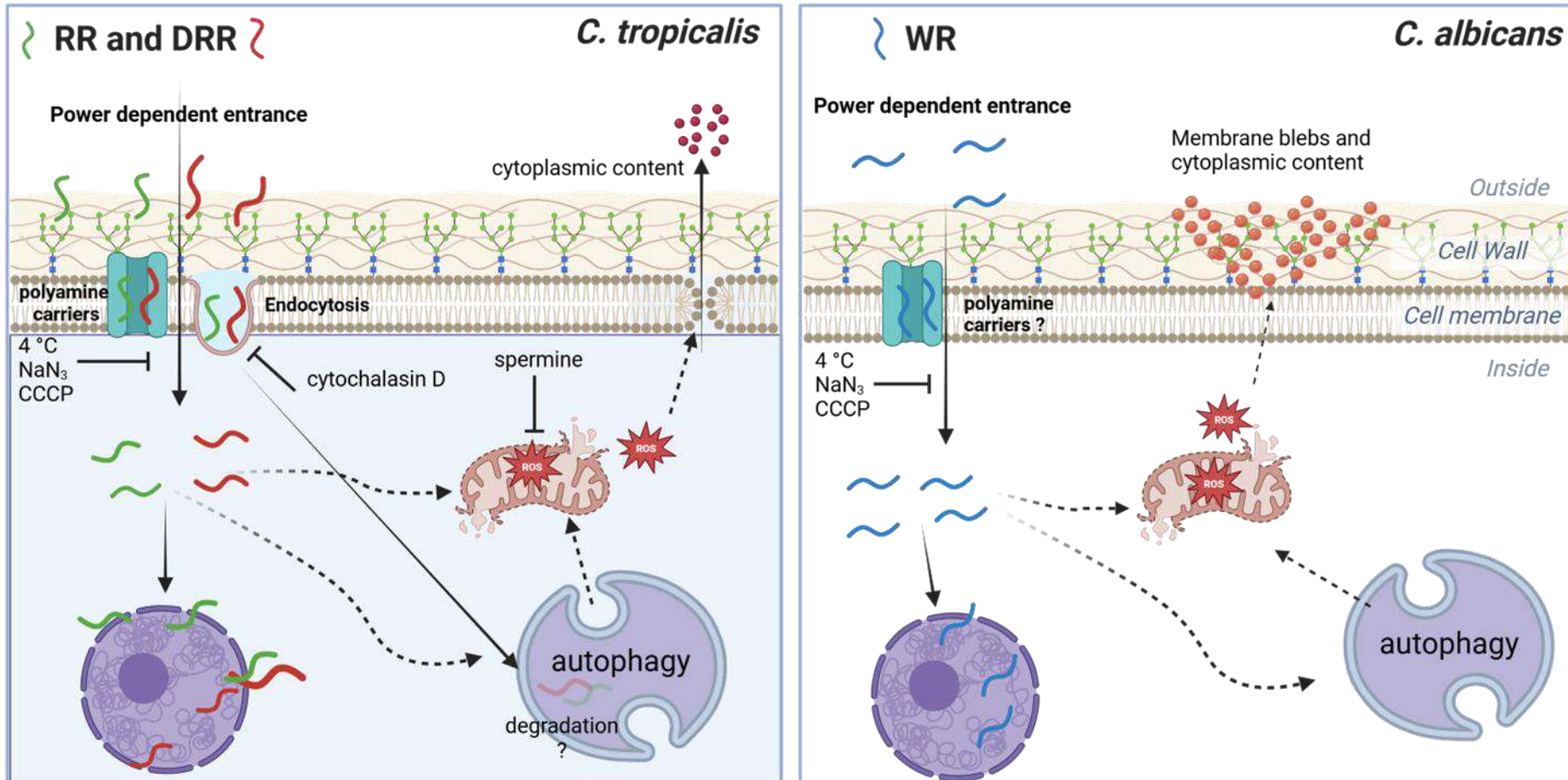
Impact factor: 3.7

RESUMO

As doenças fúngicas e a resistência aos agentes antifúngicos estão aumentando globalmente, destacando a necessidade de terapêuticas inovadoras. Os peptídeos bioinspirados RR, D-RR e WR exibem potente atividade antifúngica. Estudamos o mecanismo de ação desses peptídeos, com foco na internalização celular e nos danos induzidos. RR e D-RR são internalizados em *C. tropicalis* em 1,2 e 1 minuto, respectivamente, enquanto WR é internalizado em *C. albicans* em 20 segundos. CCCP, NaN₃ e temperaturas de 4 °C prejudicaram a internalização e protegeram os fungos contra a morte induzida pelos peptídeos. A espermina reduziu os níveis de espécies reativas de oxigênio, conferindo proteção aos fungos sem bloquear a internalização. Em conjunto, nossos resultados indicam que a entrada ocorre principalmente por transportadores de poliaminas. Os peptídeos causaram extensos danos celulares, afetando vacúolos, mitocôndrias e a parede celular, levando ao vazamento citoplasmático e à formação de poros. WR induziu exclusivamente a formação de blebs em *C. albicans*. Estruturas semelhantes a autofagia foram observadas. Os peptídeos não apresentaram toxicidade detectável em células LLC-MK2 de mamíferos. Esses achados reforçam o potencial dos peptídeos RR, D-RR e WR como candidatos promissores para novas terapêuticas.

Palavras-chave: transportador de poliaminas; autofagia; endocitose

6.1 Grafical abstract (Resumo gráfico)



Energy-dependent internalization mechanism, cytoplasmic localization, and impact on the ultrastructure of pathogenic fungi of the genus *Candida* by three bioinspired antimicrobial peptides

Douglas Ribeiro Lucas¹, Filipe Zaniratti Damica¹, Felipe Figueirôa Moreira, Juliana Azevedo da Silva, Felipe Perissé Duarte Lopes, Noil Gomes de Freitas, Sérgio Henrique Seabra, Anna Lvovna Okorokova-Façanha, Valdirene Moreira Gomes, and André de Oliveira Carvalho*

¹ These authors contributed equally to this manuscript.

Abbreviations:

BSA, bovine serum albumin; CCCP, carbonyl cyanide 3-chlorophenylhydrazone; Cyt D, cytochalasin D; CFW, calcofluor white; DMEM, Dulbecco's Modified Eagle Medium; 5-FAM, 5-carboxyfluorescein; Lat A, latrunculin A; TEM, transmission electron microscope; SEM, scanning electron microscope; MTT, 3-(4,5-dimethylthiazol-2-yl)-2,5-diphenyltetrazolium bromide; Noc, nocodazole; 5-FAM_RR, RR peptide linked to 5-FAM; 5-FAM_D-RR, D-RR peptide linked to 5-FAM; 5-FAM_WR, WR peptide linked to 5-FAM; b_RR, RR peptide linked to biotin; b_D-RR, RR peptide linked to biotin; b_WR, RR peptide linked to biotin; Spm, spermine.

Abstract

Fungal diseases and resistance to antifungal agents are escalating globally, emphasizing the need for novel therapeutics. The bio-inspired peptides RR, D-RR, and WR exhibit potent antifungal activity. We studied the mechanism of action of these peptides, focusing on cellular internalization and induced damage. RR and D-RR are internalized within 1.2 and 1 min in *C. tropicalis*, and within 20 s for WR in *C. albicans*. CCCP, NaN₃ and 4 °C impaired internalization and protect fungi from peptide-induced death. Spermine reduces reactive oxygen species levels, conferring fungal protection without blocking internalization. Taken together our results indicate the entrance via is mainly by polyamine transporters. The peptides caused extensive cellular damage, affecting vacuoles, mitochondria, and cell wall, leading to cytoplasmic leakage and pore formation. WR uniquely induced blebs in *C. albicans*. Autophagic-like structures were observed. The peptides exhibited no detectable toxicity toward mammalian LLC-MK2 cells. These findings reinforce the potential of RR, D-RR, and WR peptides as promising candidates for novel therapeutics.

Keywords: polyamine transporter; autophagy; endocytosis.

Introduction

Fungal infections and associated mortality have been increasing worldwide, raising global concern.¹⁻³ Estimates indicate an annual incidence of 6.5 million invasive fungal infections and 3.8 million deaths, with approximately 2.5 million deaths directly attributable to fungal infections globally.^{4,5} Mycoses rank among the deadliest infectious diseases, exceeding the combined mortality rates of malaria and tuberculosis.⁶

Several factors contribute to this increase. Evidence suggests that rising global temperatures have played a significant role in the appearance of invasive mycoses. Although mammals are endothermic and typically more resistant to fungal infections, this new climatic condition exposes them to higher infection risks whereas fungi are adapting to higher temperatures closer to that of mammalian body.^{7,8} An example is the emergence of *Candida auris*, a yeast adapted to higher temperatures that causes infections in humans.⁸ Additionally, global warming is altering the geographical distribution of fungal pathogens.⁹ For instance, coccidioidomycosis, historically endemic to arid regions of the United States of America, Central, and South America, is expanding northward to Canada and new regions in the Americas, with projections showing a significant increase in cases due to climate change.¹⁰

Another factor contributing to the rise in fungal infections is the expanding population of vulnerable individuals, including the elderly, those immunocompromised by acquired immunodeficiency syndrome, cancer patients, organ transplant recipients on immunosuppressants, and individuals with severe viral infections.¹¹ This scenario is further complicated by the growing resistance of many fungi to paucity of five clinical classes of antifungal drugs. This resistance is driven by widespread use of azole fungicides in agriculture, as seen in *Aspergillus fumigatus*, which complicates the treatment of aspergillosis in humans.^{10,11} Additionally, *C. auris* has emerged as resistant to multiple antifungal classes.¹² Given this alarming reality, the development of new effective antifungal agents to combat emerging infections and reduce associated mortality, particularly among vulnerable populations, has become urgent.^{13,14}

Antimicrobial peptides (AMPs) are natural defense molecules produced by most living organisms, from microorganisms to humans, and are considered potential candidates for the development of new antifungals to address antifungal resistance.¹⁵⁻¹⁷ The mechanism of action of AMPs, which leads to the inhibition or death of target microorganisms, is complex and only partially understood. Fully exploring their therapeutic potential requires a comprehensive understanding of their mechanism of action.¹⁸

In a previous study, we analyzed the primary structure of the γ -core region responsible for the biological activity of various plant defensins. Based on that study, we designed three bioinspired peptides derived from the γ -core of *Vu*-Def₁, a defensin from *Vigna unguiculata* L. Walp. (cowpea) seeds, with specific amino acid modifications to increase net positive charge and hydrophobicity, thereby enhancing biological activity.¹⁹ These peptides were designated as A_{36,42,44}R_{37,38}γ₃₂₋₄₆*Vu*Def (abbreviated RR), D-A_{36,42,44}R_{37,38}γ₃₂₋₄₆*Vu*Def (abbreviated D-RR), and A_{42,44}R_{37,38}W_{36,39}γ₃₂₋₄₆*Vu*Def (abbreviated WR). These three peptides demonstrated inhibitory activity against various fungal species and low toxicity to mammalian cells.¹⁹

Based on these findings, we selected two fungi classified as priority pathogens by WHO¹ to

investigate the mechanism of action of the peptides. Specifically, *Candida tropicalis* was chosen to study the mechanism of action of RR and D-RR, and *Candida albicans* to investigate WR.¹⁹ In preliminary studies, the lethal dose (DL₁₀₀) was determined as 27.5 μ M for RR, 23 μ M for D-RR, and 27.5 μ M for WR, with the times required to induce fungal death being 6 h for RR, 3 min for D-RR, and 1 h for WR.²⁰ Previous research by our group showed that RR induced regulated cell death in *C. tropicalis*, D-RR caused metacaspase-independent regulated cell death in *C. tropicalis*,²⁰ and WR induced regulated cell death in *C. albicans* (personal communications). Furthermore, we demonstrated that all three peptides interact with fungal cells, disrupt ionic balance, especially K⁺ and H⁺, and are internalized into the fungal cytoplasm (personal communications). Notably, the peptides exhibited no toxicity to mammalian cells under the tested conditions, making them promising candidates for drug development.¹⁹

This study examines the process by which peptides enter the fungal cytoplasm and their intracellular effects using an integrated approach that includes real-time confocal fluorescence microscopy, scanning and transmission electron microscopy (SEM and TEM), and viability assays with specific modulators. Our findings reveal an energy-dependent internalization mechanism, primarily mediated by transporters, the intracellular localization of peptides, particularly within the cell nucleus, and extensive damage to the fungal cell ultrastructure. Additionally, we demonstrate the selectivity of these peptides, showing no interaction or toxicity toward mammalian cells.

Results

Dynamics of cytoplasmic entry of 5-FAM-labeled peptides into cells and cell viability

As described previously, the mechanism of action of the peptides has been partially described, and their internalization in the cytoplasm of fungi at 1 h for RR, 30 min for D-RR, and 20 min for WR has already been demonstrated (personal communications). The cytoplasmic entry of the peptides was analyzed during the initial moments by time-lapse confocal microscopy, using peptides labeled with 5-FAM at the N-terminal portion. Images were acquired at 20 s intervals over the first 15 min after interaction. Figure 1A illustrates the dynamics of the 5-FAM_RR peptide in *C. tropicalis*: at 80 s, fluorescence appears in the bud, completing its labeling at 520 s, with the mother cell starting to be labeled at 560 s. A bud organelle, probably the vacuole, is labeled at 620 s. The labeling in the mother cell intensifies at 660 s, followed by the increase of another organelle, suggested to be the vacuole, at 740 s, followed by its labeling at 760 s. After 780 s, no new changes in labeling occur, but the fluorescence increases, indicating accumulation of the peptide within the cell. Flow cytometry confirmed that 97.5% of the cells were labeled by the 5-FAM_RR peptide, considering 20,000 events (Supplementary Figure 2 Ai, Aii). For 5-FAM_D-RR in *C. tropicalis*, fluorescence in the bud starts at 60 s, with the mother cell being labeled at 120 s. At 280 s, the entire cytoplasm of the mother cell is labeled excluding two organelles, and at 300 s two non-fluorescent organelles, possibly vacuoles, appear. The labelling of the smaller vacuole occurs between 700 and 740 s, and the larger one between 840 and 860 s. After 880 s, the fluorescence shows no changes, only increases, indicating accumulation of the peptide in the cell (Figure 1B). Flow cytometry revealed labeling in 97.75% of the cell population (Supplementary Figure 2 Bi, Bii). For 5-FAM_WR in *C. albicans*, fluorescence starts since 0 s, with the cytoplasm starting to be labeled at 20 s.

Between 300 and 380 s, the labeling of an organelle, possible vacuole, occurs, and at 400 s the cell is already completely labeled. From 620 s, the fluorescence increases, suggesting greater internalization of the peptide (Figure 1C). Flow cytometry showed 98.63% of the cells are fluorescent, indicating interaction with WR_5-FAM (Supplementary Figure 2 Ci, Cii). Supplementary Figure 2 A, B and C were combined to create a video that demonstrates the dynamics of interaction of the three peptides (Supplementary Video 1 A, B, C).

To associate the cytoplasmic entry of peptides into cells with toxicity, we monitored fungal cell viability after 20 min of incubation with the peptides. In *C. tropicalis*, treatment with RR and D-RR showed only 1% cells remain viable (Figure 1 B, D), while in *C. albicans* treatment with WR led to no detectable viable cells (Figure 1 F). These findings indicate that initiation and execution of the cell death process occur within 20 min and are temporally coincident with the accumulation of peptides in the cytoplasm of fungal cells.

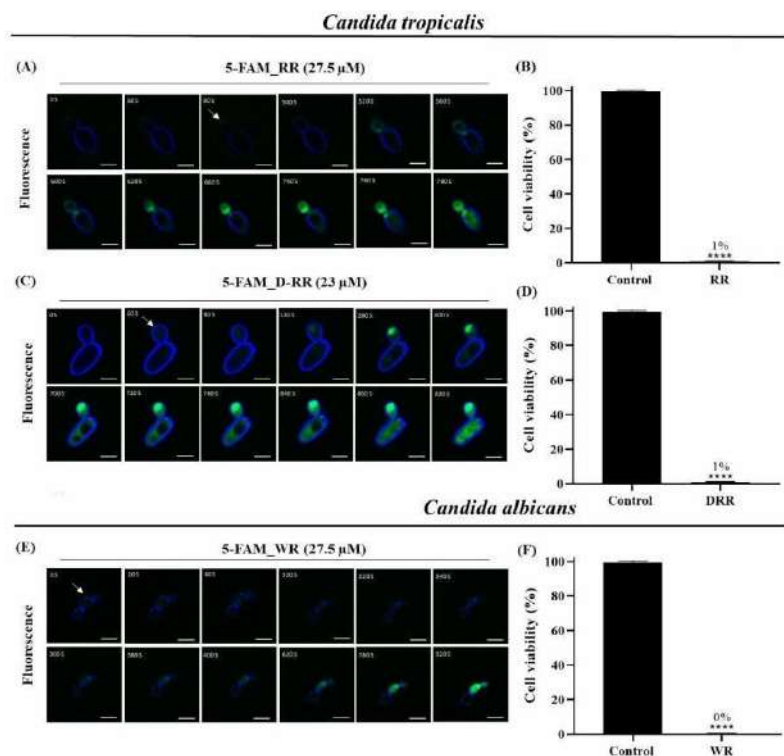


Figure 1. Dynamics of cytoplasmic entry of 5-FAM-labeled peptides into fungal cells and loss of cell viability. Confocal microscopy time lapse within the first 15 min of interaction of the peptides with the fungal cells (A) 5-FAM_RR and (C) 5-FAM_D-RR with *Candida tropicalis*, and (E) 5-FAM_WR with *Candida albicans*. Green fluorescence in the cytoplasm indicates the presence of the peptide, while blue fluorescence marks the fungal cell wall with calcofluor white. Scale bars = 10 μ m. The result is representative of triplicate assays. Cell viability of *C. tropicalis* treated with RR (B) and D-RR (D), and *C. albicans* treated with WR (F), after 20 min of incubation at the LD₅₀ of the peptides. Above the bars of the treatments, the percentage of viability is shown. The data are a representative example of three independent experiments. Statistical significance is indicated as ****, $P < 0.05$.

Effect of cell energy on the internalization and antifungal activities of bioinspired peptides

To investigate whether the entry of peptides depends on cellular processes or the energy state of the cells, we performed experiments blocking cellular processes. At first, we used low temperature. In *C. tropicalis*, the viability of fungi treated with RR and D-RR was 1% at 30 °C, but it increased to 62% and 37%, respectively, at 4 °C (Figures 2 A, E). In *C. albicans*, WR reduced viability to 0% at 30 °C, but reached 41% at 4 °C (Figure 2 I). These results indicate that low temperature protects fungi from peptide-induced death. Flow cytometry showed lower interaction of peptides with cells at 4 °C (Supplementary Figure 3 Ai, Aii, D, Dii, G, Gii), and confocal microscopy confirmed that labeling was restricted to the cell surface, notably in restricted binding sites, indicating blockage of cytoplasmic entry (Figure 2 D, H, L). With this, we conclude that the entry of peptides is dependent on energy or membrane fluidity, and toxicity is seemingly triggered in the cytoplasm, not in the cell surface.

Sodium azide (NaN₃) was used to assess the cytoplasmic entry of peptides and their impact on cell death. *C. tropicalis* cells treated with NaN₃ and RR showed 57% viability, while those treated with RR alone had 1% (Figure 2 B). With D-RR, viability was 48% in the presence of NaN₃ and 1% in its absence (Figure 2 F). For *C. albicans*, viability was 59% in the presence of NaN₃ and 0% without treatment when exposed to the WR peptide (Figure 2 I). Flow cytometry revealed a reduction in the fluorescence intensity of 5-FAM-labeled peptides, especially in *C. albicans*, where 38% of cells showed no fluorescence (Supplementary Figure 3 B, Bi, E, Ei, H, Hi). Confocal microscopy confirmed that the peptides remained on the cell surface, with no entry into the cytoplasm (Figure 2 D, H, L). This result reinforces the low temperature result and again indicates the energy dependence for the entry of peptides into fungal cells and the existence of a cytoplasmic target.

We continued the study of energy dependence using CCCP. *C. tropicalis* cells treated with RR and CCCP showed 42% viability, while those without CCCP had only 1% (Figure 2 C). With D-RR, viability was 28% in the presence of CCCP and 1% in the absence (Figure 2 G). For *C. albicans* and WR, viability was 19% with CCCP and 0% without treatment (Figure 2 K). Flow cytometry revealed an increase in the fluorescence of 5-FAM-labeled peptides in CCCP-treated cells, indicating a change in the interaction pattern (Supplementary Figure 3 C, Ci, F, Fi, I, Ii). Confocal microscopy confirmed higher fluorescence intensity and a change in the localization pattern: the peptides concentrated in organelles and not in the cytoplasm, in addition to being present on the cell surface (Figure 2 D, H, L). These results suggest that CCCP changes the cytoplasmic localization of the peptides, being in this condition the peptides redirected to an organelle. Besides CCCP demonstrating the energy dependence of the entry process, it also demonstrated the peptides need to remain in the cell cytoplasm to exert their toxic effect, which possibly indicates a cytoplasmic target.

Comparison of the three substances used indicates that membrane fluidity, as affected by treatment at 4 °C, does not influence peptide entry. Collectively, the inhibition of both peptide entry and cell death under energy-depleted conditions suggests that peptide entry is energy-dependent and mediated by a cellular mechanism. However, the 4 °C and NaN₃ treatments besides halting peptide entry, it is visible that the peptides accumulate in the cell surface at spatially restricted sites. These sites were not observed with CCCP treatment. Therefore, comparing the effect of the substances used, it seems that the

peptides interact with the cell surface at specific sites before cell entry.

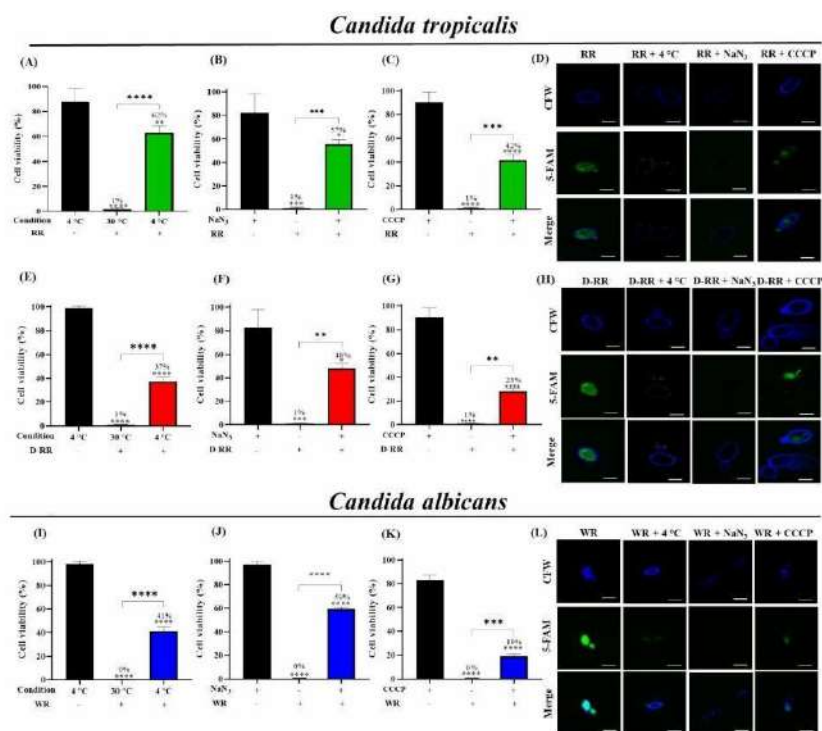


Figure 2. Influence of cell energy on the interaction of bioinspired peptides with fungal cells. Cell viability of *C. tropicalis* treated with RR and D-RR at 4 °C (A and E), with NaNO₃ (B and F), and CCCP (C and G), and of *C. albicans* treated with WR at 4 °C (I), NaNO₃ (J), and CCCP (K). Cells were treated with the peptides at their respective LD₁₀₀ for 20 min and the specified substances. Confocal microscopy of cells treated with RR (D), D-RR (H), and WR (L) showing peptide localization patterns for each treatment condition. Green fluorescence indicates the presence of the peptides, while blue fluorescence marks the cell wall with the dye calcofluor white. The images show different treatment conditions, with overlap of labels (Merge). The data presented represent the mean of three independent experiments. Statistical significance is indicated as **** (P < 0.05). The cells displayed were chosen randomly.

Role of endocytosis in the internalization and antifungal activities of the bioinspired peptides

After confirming that the entry of peptides depends on energy and is mediated by a cellular mechanism, we investigated the role of endocytosis as a possible uptake mechanism. We used endocytosis inhibitors, including nocodazole (Noc), which interferes with microtubule polymerization, latrunculin A (Lat A) and cytochalasin D (Cyt D), which affect actin filaments. The results show that Noc and Lat A did not influence cell viability in *C. tropicalis* treated with RR and D-RR (Supplementary Figure 4 A, B, C, and D), nor in *C. albicans* treated with WR (Supplementary Figure 4 E and F), suggesting that microtubules and the actin cytoskeleton are not essential for the uptake of these peptides.

However, *C. tropicalis* treated with Cyt D showed increased viability from 1% to 21% for RR and 22% for D-RR (Figure 3 A, C), indicating that interference with actin filaments at the periphery of

cells impacts the antifungal activity of these peptides. WR, on the other hand, showed no significant change in viability (Supplementary Figure 4 G). Flow cytometry revealed changes in the 5-FAM labeling profile in Cyt D-treated cells, suggesting lower cytoplasmic entry of RR and D-RR peptides (Supplementary Figure 5 A, Ai, B, Bii). Confocal microscopy confirmed less intense labeling restricted to the inner periphery of the cells (Figure 3 B and D). These results indicate that the entry of RR and D-RR may be partially associated with endocytosis, possibly involving mechanisms dependent on actin filaments responsible for growth at the cell periphery.

Candida tropicalis

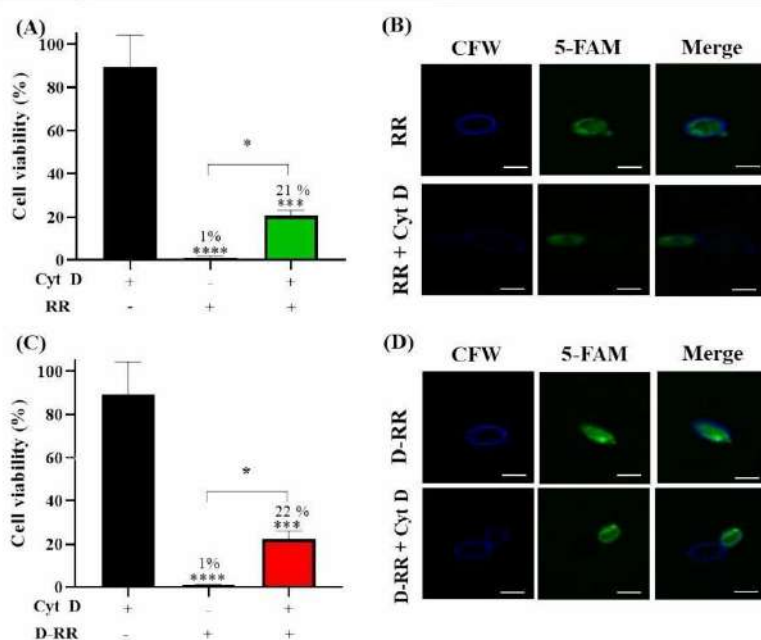


Figure 3. Role of endocytosis in the interaction of bioinspired peptides in *Candida tropicalis*. Cell viability of *C. tropicalis* treated with RR (A) and D-RR (C). Cells were treated with the peptides at their respective LD₁₀₀ for 20 min of incubation at 30 °C with and without the addition of Cytochalasin D (Cyt D). Statistical significance is indicated as ****, P < 0.05. Confocal microscopy of *C. tropicalis* cells treated with RR (B) and D-RR (D). Cells incubated in the presence and absence of Cyt D with the respective LD₁₀₀ of the peptides shown in three conditions, green fluorescence indicates the presence of the peptide, blue fluorescence marks the yeast cell wall with calcofluor white, and Merge indicates the overlap of labels. The data and images are representative of three independent experiments. The cells shown were chosen randomly.

Role of polyamine transporters in the internalization and cytotoxic activities of bioinspired peptides

To evaluate a possible route of entry of peptides via polyamine transporter, *C. tropicalis* and *C. albicans* cells were treated with spermine (Spm) to saturate the transporter. Spm conferred relevant protection to *C. tropicalis* cells: 54% viability for RR and 31% for D-RR (Figure 4 A and D). For *C. albicans* treated with WR, Spm had no protective effect (Supplementary Figure 6 C). Flow cytometry revealed changes in the 5-FAM fluorescence profile for RR and D-RR in the presence of Spm, indicating

an increase in labeling intensity (Supplementary Figure 5 A, Ai, B, Bii). Confocal microscopy confirmed intense intracellular fluorescent labeling, showing that the Spm does not prevent the cytoplasmic entry of peptides (Figure 4 B and E). To investigate the mechanism of Spm protection, endogenous ROS levels were evaluated. Treatment with RR increased ROS levels by 271% compared to the control, whereas a reduction of 62% by Spm coincubation (Figure 4 C). With D-RR, ROS levels increased by 156%, being reduced by 53% with Spm (Figure 4 F). These data suggest that the protection conferred by Spm is related to the mitigation of oxidative stress induced by peptides, and not to the inhibition of their internalization.

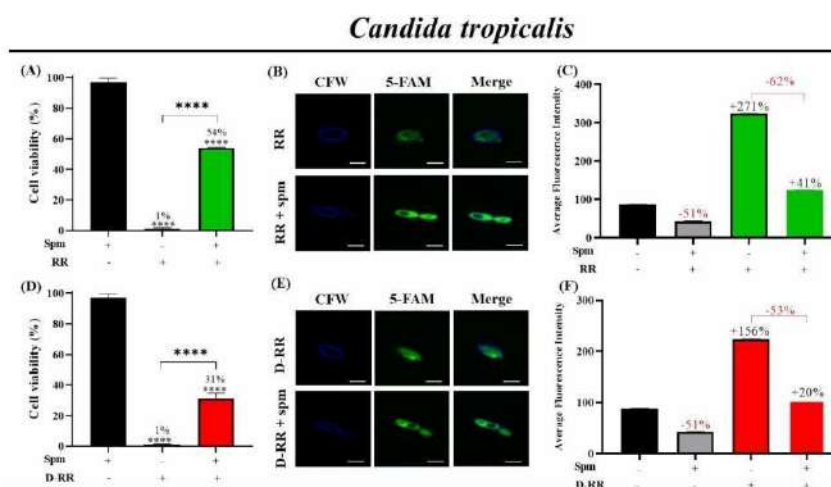


Figure 4. Role of spermine (Spm) in the interaction of bioinspired peptides in *Candida tropicalis*. Cell viability of *C. tropicalis* treated with RR (A) and D-RR (D), at their LD₁₀₀, for 20 min at 30 °C, with and without the addition of Spm. Data represent the mean of three independent experiments, with statistical significance indicated as **** (P < 0.05). Confocal microscopy of cells treated with RR (B) and D-RR (E), showing peptide localization patterns. Green fluorescence indicates the presence of the peptides, while blue fluorescence marks the cell wall with the dye calcofluor white. Images include the overlap of labels (Merge). The cells displayed were chosen randomly. Analysis of reactive oxygen species (ROS) levels by flow cytometry in cells treated with RR (C) and D-RR (F), in the presence and absence of Spm. Cells were incubated with the peptides at their LD₁₀₀ for 20 min at 30 °C. The graph shows the mean fluorescence intensity of the H₂DCFDA probe, an indicator of ROS, with representative data of 10,000 events. The percentages of ROS increase compared to the control are indicated above the bars, and the bracket highlights the reduction of ROS levels in treatments with Spm.

Cytoplasmic entry and localization of peptides by colloidal gold labeling by TEM

To investigate the dynamics and localization of peptides in the cytoplasm, we used peptides labeled with biotin at the N-terminal region, visualized by transmission electron microscopy with streptavidin-gold (40 nm). Within 1 min of interaction, the peptides b_{RR}, b_{D-RR}, and b_{WR} were detected in the cell wall (Figure 5 A, B, D, E, G, and H). In addition, b_{D-RR} and b_{WR} were already present in the cytoplasm (Figure 5 E and H). After 5 min, all peptides were found in the cytoplasm, with b_{RR} interacting with the nuclear membrane (Figure 5 C) and b_{D-RR} and b_{WR} located inside the nucleus (Figure 5 F, I). b_{RR} and b_{D-RR} were also observed associated with the cytoplasmic side of the membrane (Figure 5 C, D).

The interaction of peptides with the nucleus suggests that the nucleus may act as an intracellular target for these bioinspired peptides. Furthermore, the occurrence of the spatially restricted site at the fungal cell surface where the peptides accumulated before entering was evident in the TEM images at one minute after initial interaction (Figure 5).

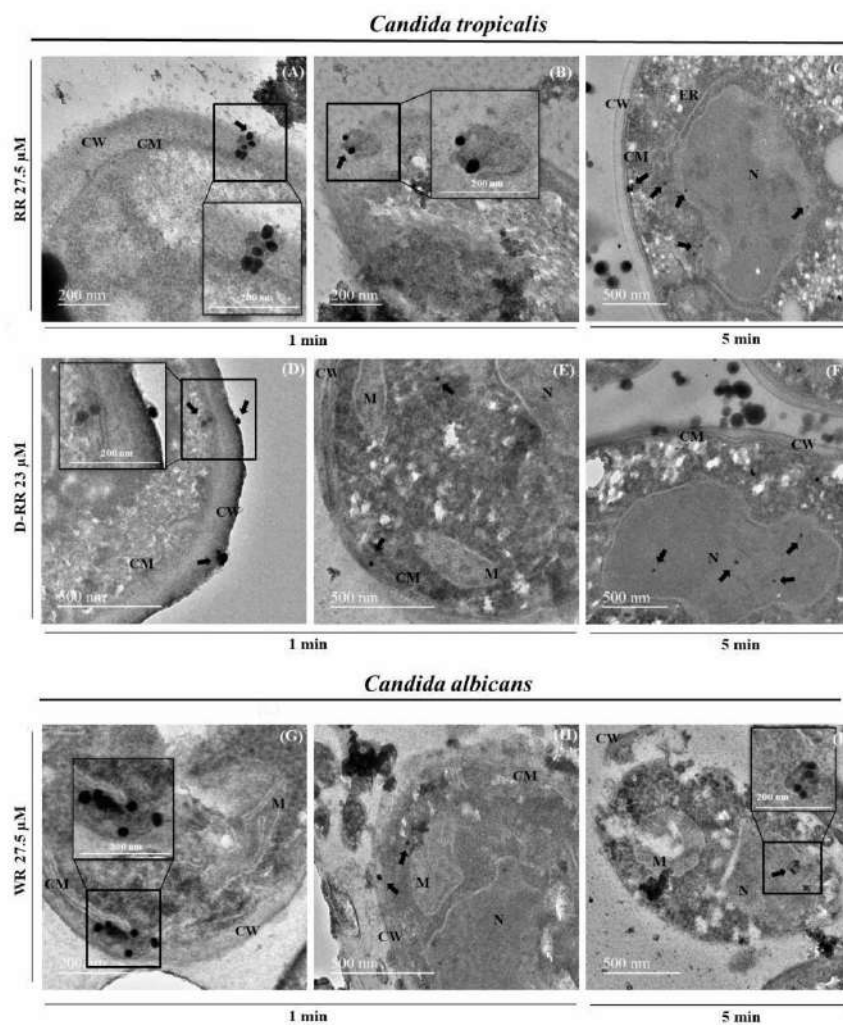


Figure 5. Localization of peptides by colloidal gold labeling in *Candida tropicalis* cells treated with b_{RR} and b_{D-RR}, and *Candida albicans* cells treated with peptide b_{WR} by transmission electron microscopy. Cells were treated with the peptides at their respective LD₅₀ for 1 and 5 min of incubation at 30 °C. Black arrows indicate the location of colloidal gold. Black boxes indicate image magnification. (CW) cell wall, (CM) cell membrane, (M) mitochondria, (N) nucleus. The images are a representative example of three independent experiments. The cells shown were chosen randomly.

Because the three peptides were localized in the nucleus of the fungal cells after 5 min of initial

interaction, we analyzed whether the peptides could interact with DNA. Gel shift assay indicated that the three peptides interact with fungal DNA forming a complex that completely inhibits its electrophoretic migration (Supplementary Figure 7). The DNA extraction was contaminated with RNA, nonetheless this contamination also indicated that the three peptides also interact with RNA *in vitro* also inhibiting its electrophoretic migration (Supplementary Figure 7).

Ultrastructural alterations in fungal cells caused by bioinspired peptides

Transmission electron microscopy revealed significant alterations in the ultrastructure of fungal cells treated with bioinspired peptides. Control cells exhibited a uniform cell wall (CW), intact cell membrane (CM), and well-defined organelles, including the nucleus (N), endoplasmic reticulum (ER), electron-dense vacuoles (V), and mitochondria (M) with transverse or tubular cristae (Figure 6 A, B, C). *C. tropicalis* cells treated with RR at LD₁₀₀ showed, as early as 5 min, larger and less electron-dense vacuoles, in addition to swollen mitochondria with reduced cristae. The cell wall became slightly more electron-dense (Figure 6 D). At 10 min, the damage to the organelles was more pronounced: swollen and disorganized vacuoles, deformed mitochondria, and release of cellular material outside the cell (Figure 6 F). With D-RR, the damage was even faster. At 1 min, less electron-dense vacuoles and membrane-enclosed vesicles were observed, in addition to mitochondria with poorly defined cristae (Figure 6 G). At 5 min, vacuolar swollen and degradation progressed, with increased extracellular electron-dense material and mitochondrial deformation. After 10 min, deformed mitochondria were seemed to be endocytosed by vacuoles, and the formation of structures that resembles autophagosomes (As) and autophagic bodies (Ab) was observed (Figure 6 I). In *C. albicans* cells treated with WR, the structural alterations were immediate and intense. At 1 min, mitochondria exhibited swelling and deformation, accompanied by thinning of the cell wall and vesicle formation (Figure 6 J). At 5 min, mitochondrial damage was more intense, with vesicles near the mitochondria and swelled vacuoles containing internal vesicles. At 10 min, the mitochondria were endocytosed by the vacuoles, indicating mitochondrial and vacuolar degradation (Figure 6 L). These results suggest that bioinspired peptides induce autophagy, culminating in vacuolar degradation.

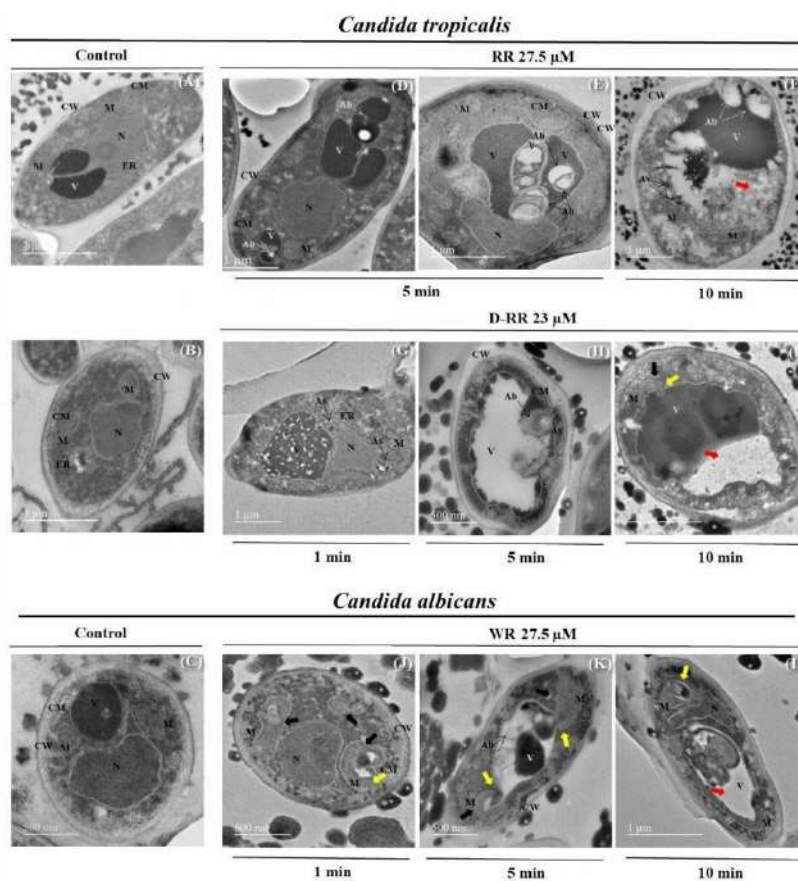


Figure 6. Ultrastructure of *Candida tropicalis* cells treated with RR and D-RR, and *Candida albicans* cells treated with peptide WR by transmission electron microscopy. Cells were treated with the peptides at their respective LD₅₀ for different times of incubation at 30 °C. Black arrows indicate deformed mitochondria. Yellow arrows indicate mitochondria being endocytosed by vacuoles. Red arrows indicate vacuole degradation. (*) indicate leakage of cytoplasmic content. Cell wall (CW), plasma membrane (CM), vacuole (V), nucleus (N), mitochondrion (M), endoplasmic reticulum (ER), autophagosomes (As), autophagic bodies (Ab). The images are a representative example of three independent experiments. The cells shown were chosen randomly.

The effect of bioinspired peptides on the morphology of fungal cells using SEM

Morphological analysis revealed striking alterations in cells treated with bioinspired peptides, compared to controls. The control cells of *C. tropicalis* (Figure 7 A, B) and *C. albicans* (Figure 7 I) showed regular cell shape, with an intact cell wall and no signs of structural damage. In *C. tropicalis* cells

treated with RR and D-RR at LD₁₀₀ (27.5 μ M and 23 μ M, respectively), cytoplasmic material leakage was observed (yellow arrows, Figure 7 C-H). In cells treated with D-RR, pores on the cell wall surface were identified (red arrow, Figure 7 H), in addition to a decrease in cell volume and wrinkling of the cell wall (white arrows, Figure 7 E, G). For *C. albicans* cells treated with WR, the formation of membrane "blebs" was evident (indicated by, Figure 7 J-L), suggesting a response to peptide-induced damage. These results highlight the occurrence of severe structural alterations, including cytoplasmic leakage, pore formation and "blebs", and compromised cell integrity, induced by bioinspired peptides in both fungal species.

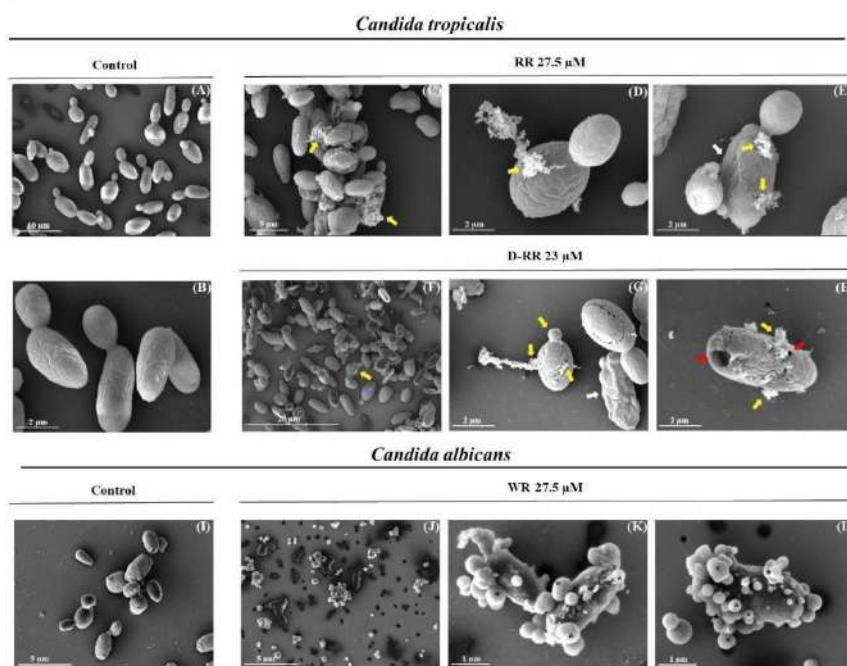


Figure 7. Morphology of *Candida tropicalis* cells treated with RR and D-RR, and *Candida albicans* cells treated with peptide WR by scanning electron microscopy. Cells were treated with the peptides at their respective LD₁₀₀ for 20 min of incubation at 30 °C. Yellow arrows indicate cytoplasmic material leakage, white arrows indicate cell wall wrinkling, red arrows indicate pore formation, asterisks (*) indicate the formation of membrane "blebs". Control cells without peptide treatment. The images are representative of three independent experiments. The cells shown were chosen randomly.

Interaction and cytotoxicity of bioinspired peptides with mammalian cells

The toxicity of the peptides RR, D-RR, and WR was evaluated in LLC-MK2 cells (from *Rhesus* monkey kidney) using the MTT assay. The three peptides showed no toxicity, maintaining 100% cell viability at the concentration corresponding to the LD₁₀₀ for yeasts (RR and WR: 27.5 μ M; D-RR: 23 μ M). Even at five times higher concentrations (RR and WR: 137.5 μ M; D-RR: 113 μ M), cell viability was not affected (Figure 8 A). The interaction of peptides with LLC-MK2 cells was investigated by confocal microscopy with 5-FAM-labeled peptides. After 20 min of incubation, the cells remained intact, and there was no green fluorescence in the cytoplasm, confirming the absence of peptide internalization

(Figure 8 B). Cell surfaces of the LLC-MK2 cells were delimited by labeling them at the same time as the peptides with DBA-Texas Red, which recognizes N-acetylgalactosamine residues on the cell surface. These results demonstrate the selectivity of peptides for fungal cells, reinforcing their safety and potential as antifungal agents.

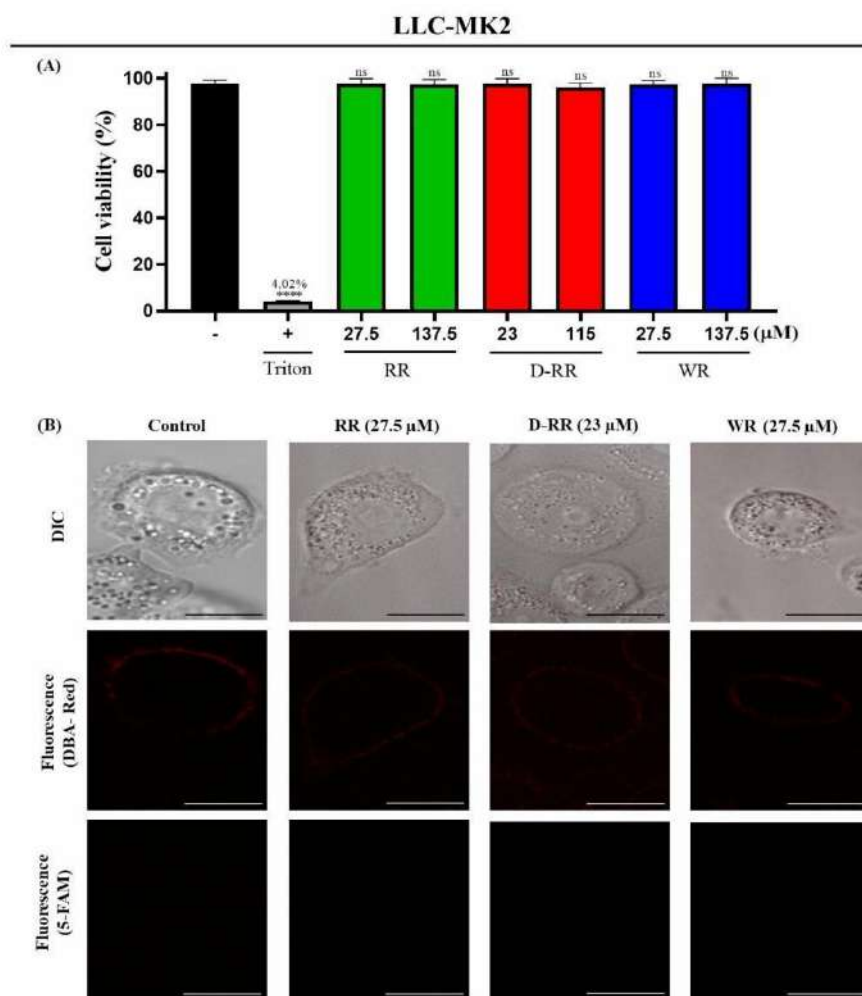


Figure 8. Effect of bioinspired peptides on LLC-MK2 mammalian cells. (A) Viability of LLC-MK2 cells in response to bioinspired peptides after 24 h of treatment at LD₁₀₀ and at a 5x higher concentration for fungi. Cell viability was assessed by the MTT-based colorimetric assay. Statistical significance is indicated as *****, $P < 0.05$. ns, non significant. (B) Confocal microscopy of LLC-MK2 cells treated with bioinspired peptides. Cells seen in differential interference contrast, green fluorescence indicates the presence of the peptide, red fluorescence DBA-Texas Red that specifically binds to certain types of carbohydrates, for the delimitation of the cell surface. The images are representative of three independent experiments. The cells shown were chosen randomly.

Discussion

The capability of AMPs to interact with and penetrate microbial cells has garnered significant interest, as these processes are closely linked to their mechanisms of action.^{18,21-28} Three basic processes had been proposed as the entry mechanism of AMPs into fungal cells. Receptor-mediated endocytosis,^{22,23,26,27,29} polyamine transporters,^{25,30} and direct translocation.^{23,24,26,31} In several of the studies mentioned above, different concentrations were employed to investigate the mechanism of action of AMPs in the same microorganisms. Notably, the mechanism described varies depending on the peptide concentration used. For instance, histatin-5 (AMP from human saliva) at low concentration enters cells and is directed to the vacuole by receptor mediated endocytosis, whereas at higher concentration the peptide directly translocates into the cytoplasm in *C. albicans*.^{23,24} The cytotoxicity of histatin-5 was associated with its cytoplasmic localization rather than its presence in the vacuole.^{23,24} PAF26 (a synthetic hexapeptide identified by a combinatorial screening against the filamentous fungus *Penicillium digitatum*) was also demonstrated that at low 2 to 5 μM concentrations gains access to the cell cytoplasm of *Neurospora crassa* by endocytosis and at higher 20 μM the entry process is energy independent, translocation.³¹ These findings underscore the importance of using concentrations that effectively induce cell death to avoid ambiguous interpretations of the underlying mechanism of action against microorganisms. For this reason, we used the lethal dose (LD_{100}) in our study.

In the present study, we investigated the dynamics of internalization of the bio-inspired peptides RR and D-RR in *C. tropicalis* and WR in *C. albicans* cells. Real-time dynamics of internalization and intracellular localization provided insights into the kinetics of entry and cytoplasmic distribution patterns of the bio-inspired peptides, as shown in Figure 1 and Supplementary Video 1. We observed that peptide internalization into fungal cells occurred rapidly, at 1.2 min for RR, 1 min for D-RR in *C. tropicalis*, and 20 s for WR in *C. albicans*. To confirm that cytoplasmic invasion by the peptides was associated with loss of cell viability, we conducted a viability assay after 20 min of incubation. Our results confirmed that, after 20 min of incubation, 99% of the cells lost viability (Figure 1). This time interval refines the previously studied time²⁰ and indicates that the toxic action of the peptides that leads to the fungal cell death occurs in a narrow time window after initial interaction of only 20 min. Consequently, all subsequent experiments were conducted using this 20-minute interval.

Reconstructing our results from external cell interaction to the cytoplasmic location, the bioinspired peptides initially bind to specific sites on the surface of fungal cells. This restricted binding site was demonstrated when the inhibition of the entry process in fungal cells was blocked by treatment at 4 °C (Figure 2) and in the presence of NaN_3 (Figure 2) freezing the peptides interaction at this restricted site just prior the entrance. Low temperatures (4 °C) influence energy-dependent processes such as endocytosis, viability, oxidative stress responses, and alter the fluidity of the cell membrane, making it more rigid.^{32,33} These changes may affect peptide interactions with the membrane, hindering penetration and activity.³⁴ NaN_3 inhibits cytochrome c oxidase, a key enzyme in the electron transport chain (complex IV). NaN_3 blocks ATP production and catalase activity, critical for ROS detoxification.³⁵ These substances effectively interrupt energy-dependent cellular processes.^{31,36,37} Additionally, transmission electron microscopy (TEM) visualized the localization of biotinylated peptides, confirming their surface interaction at these restricted binding sites within the first minute of interaction (Figure 5). Similar point-

specific binding has been reported for the antimicrobial peptides histatin-5²³ and dermaseptin S3 (AMP derived from the South American arboreal frog *Phyllomedusa sauvagii*).³⁸

The treatment at 4 °C, NaN₃, and CCCP (Figure 2) indicates that the bio-inspired peptides enter fungal cells by both an energy dependent mechanism and a cellular process, such as endocytosis or transporters. To differentiate the energy-dependent cellular mechanisms used by the peptides, inhibitors were used. Inhibitors of the cell cytoskeleton, such as Noc, that disrupts microtubule polymerization, structures essential for various cellular processes, including cell division and intracellular transport.³⁹ However, microtubule depolymerization and endosome transport do not appear to be involved in the cytoplasmic entry of the peptides (Supplementary Figure 4). This finding is consistent with the antifungal activity of NaD1 (a defensin from *Nicotiana glauca*), where Noc did not reduce its toxic activity against *C. albicans*.²⁷ We also tested Lat A, a sponge-derived toxin that forms a complex with actin monomers inhibiting its polymerization, causing complete disruption of the actin cytoskeleton in fungi.⁴⁰ Lat A did not alter the activity of the bio-inspired peptides (Supplementary Figure 4). Cyt D is a cell-permeable fungal toxin that targets the barbed ends of actin filaments, therefore inhibiting actin polymerization, affecting processes such as endocytosis.⁴¹ Cyt D, Noc, and Lat A did not affect WR uptake nor viability in *C. albicans*, but affects loss of viability in *C. tropicalis* treated with RR and D-RR, however it did not affect the entrance of the peptides in the *C. tropicalis* cytoplasm (Figure 3). Although both Lat A and Cyt D inhibit actin polymerization, they operate through distinct mechanisms. Lat A directly targets actin monomers, while Cyt D targets the barbed ends of actin filaments, preventing both the addition and removal of subunits. This results in the disruption of actin filaments and inhibits actin polymerization⁴² and these differences may explain the different results obtained between the two inhibitors. Lat A effectively reduced the uptake of NaD1 in *C. albicans*.²⁷ For MtDef4 defensin, actin polymerization inhibitors Lat A and Cyt D did not affect peptide uptake by *N. crassa* cells. However, its internalization was significantly inhibited by brefeldin A and filipin, which block retrograde transport and lipid raft-mediated endocytosis, respectively. In contrast, none of the endocytosis inhibitors tested blocked MtDef4 internalization in *Fusarium graminearum*.²⁶ TEM images did not show vesicles surrounding the peptides at their entrance in fungal cytoplasm (Figure 5). However, an electron dense cytoplasm is observed around the peptide-labeled gold particles which may indicate that the peptides are in fact surrounded by a membrane. Nonetheless, the membrane may be not preserved by the fixation technique. Additionally, the protection from death provided by Cyt D may be caused by endocytosis inhibition although it is elusive and will require further investigation. Taken together, these results highlight that the entry mechanism of the bio-inspired peptide in *Candida*, is energy dependent, mainly performed by polyamine transporters, see below, and secondary by endocytosis.

To confirm that cytoplasmic entry of the peptides is energy-dependent, we employed CCCP, a protonophore that disrupts ATP production by dissipating the proton gradient essential for oxidative phosphorylation in mitochondria and the transmembrane electrical potential at plasma membrane.^{43,44,45} Cells treated with CCCP were protected from peptide-induced death (Figure 2). Flow cytometry and confocal microscopy demonstrated that the peptides maintained their ability to bind to the cell surface, indicating that this binding is independent of the plasma membrane potential. However, in the presence of CCCP, the intracellular localization of the peptides was altered. Instead of accumulating in the fungal

cytoplasm, the peptides were localized to an internal organelle, likely the vacuole (Figure 2). This observation suggests that the energy dissipation caused by CCCP prevents peptide entry into the cytoplasm, reinforcing the hypothesis that cytoplasmic accumulation is critical for toxicity. A similar phenomenon has been reported for histatin-5, which, at lower concentrations, is directed to the vacuole, thereby reducing its toxicity.²³ The vacuole, a key organelle involved in substance degradation and detoxification, plays critical roles in ionic homeostasis, pH regulation, and cytoplasmic ion balance.⁴⁶ Redirecting peptides to the vacuole may represent a degradation mechanism that protects fungal cells from peptide-induced death (Figures 1 and 2). Our results indicate that the peptides initially bind to restricted sites on the fungal cell surface (Figure 2). These restricted binding sites may correspond to lipid rafts, specialized microdomains within the fungal membrane. The peptides RR, D-RR, and WR were designed based on the γ -core motif of Vu-Def1.¹⁹ This γ -core motif is essential for the biological activity of AMPs that contain it.^{47,48} The interaction of plant defensins with lipids and ceramides in fungal membranes, mediated by the γ -core motif, has been well-documented.⁴⁹⁻⁵² Lipid rafts, enriched with ceramides and ergosterol, have also been identified in fungal membranes.⁵³ Thus, the observed restricted binding sites suggest that the peptides interact with lipid rafts in the fungal membrane (Figure 2). One pathway of endocytosis is mediated by lipid raft-mediated⁵⁴ and may explain the internalization of the peptides into an organelle after CCCP treatment. Under the experimental conditions, CCCP likely disrupted the transmembrane potential without fully impairing ATP production, allowing lipid raft-mediated endocytosis to remain functional. This mechanism could direct the peptides from the cell surface to the vacuole for degradation. A similar process has been described for edelfosine in *S. cerevisiae*⁵⁵ and proposed as a potential entry mechanism for NaD1 in *C. albicans*.²⁷

Because the possibility that endocytosis is not the main entry mechanism of the bio-inspired peptides, we tested another entry energy dependence via the polyamine transporters. Polyamine transporter dependency has been observed for the cytosolic internalization of histatin-5 in *C. albicans*.²⁵ Also the peptides CP29 (an insect cecropin-bee melittin hybrid), BMAP28 (a bovine cathelicidin variant), Bac2a (a bovine batenecin variant), HBD2 (a human β -defensin), and NaD1 are all dependent of the polyamine transporter to exert their toxic effect in fungi.³⁰ The high amine content of our peptides suggested potential uptake via these transporters. We used Spm, a low molecular weight aliphatic cation critical for cell survival, as a competitive inhibitor of polyamine transporters.⁵⁶ Spm might also modulate membrane fluidity and permeability by interacting with acidic phospholipids, reducing membrane surface charge density precluding initial peptide interaction by opposite charge at cell surface.⁵⁷ However, using fluorescence and transmission microscopy, we observed that the bio-inspired peptides did not extensively bind to the fungal cell surface, except at specific sites (Figure 2). This finding rules out the possibility that the peptides bind broadly to negatively charged surface components whose charges could be blocked by the action of Spm and therefore, decreasing or blocking the toxicity of the peptides as proposed by Bleackley.³⁰ Spm did not affect WR peptide toxic activity in *C. albicans* cells (Supplementary Figure 6), but protects *C. tropicalis* from RR- and D-RR-induced death (Figure 4). Flow cytometry and confocal microscopy revealed increased RR and D-RR internalization in the presence of Spm (Figure 4). This result contrasts with findings from experiments with 4 °C, NaN₃, and CCCP (Figure 2), which indicated that peptide internalization is required for cytotoxicity. Also the energy depletion caused by 4 °C, NaN₃,

and CCCP may explain the inhibition from death induced by the peptide since these substance affects negatively the function of the polyamine transporters as demonstrated by their inhibition with NaN_3 .⁵⁸ Spm likely participates in cellular defense mechanisms against oxidative damage by scavenging free radicals, directly neutralizing ROS, and regulating ion transport.^{57,59,60} This antioxidative role could explain the observed protection, given that ROS generation and ion efflux are key mechanisms in RR- and D-RR-induced cell death²⁰ (personal communications). Confirming this hypothesis, Spm addition reduced ROS generation in peptide-treated cells (Figure 4), highlighting its antioxidative role. These results confirm that Spm-mediated protection is due to its antioxidative properties rather than blocking peptide entry.

Transmission electron microscopy (TEM) with streptavidin-gold labeled peptides corroborates the cytoplasmic entry and intracellular localization of the peptides. Images revealed gold particles associated with the cell wall and plasma membrane (Figures 5 D, E, G, and H) and peptides localized inside the cells (Figures 5C, F, and I), including their association with nuclei (Figures 5 C, F, and I). These results also indicated the restricted binding of the peptides at specific points in the cell surface within the first minute after initial interaction (Figure 1). Recent studies suggest that AMP interactions with nuclear structures may relate to their mechanism of action, either by disrupting critical intracellular processes or inducing cell death pathways.^{18,61,62} For example, Psd1 (a defensin from *Pisum sativum*) interacts directly with cyclin F in *Neurospora crassa*, a protein involved in cell cycle control.⁶³ Our results indicated the localization of the bio-inspired peptides at the nucleus of the treated fungus. Additionally, gel shift assay indicates the interaction of the peptides with DNA and RNA (Supplementary Figure 7). Thus, the location of the peptides in the cell nucleus as well as their ability to bind DNA may indicate a relevant effect for the inhibition of fungi. These results may indicate that the peptides may interfere with macromolecular synthesis,⁶⁴ which will be investigated in the future.

Membranous structures observed inside the vacuole suggest the formation of autophagic bodies indicating that engulfed material is released into the vacuole lumen for degradation, representing an intermediate stage of autophagy.^{65,66} This phenomenon may reflect an attempt by the cell to counteract the lethal effects of the peptides, as previously observed in other contexts. For example, autophagy has been implicated in oxidative stress responses in various fungal species.⁶⁷ Struyfs⁶⁸ demonstrated that HsAFP1 (a defensin from *Heuchera sanguinea*) increases intracellular ROS and induces autophagy in *C. albicans*, potentially as a tolerance mechanism to the peptide. The three peptides induce efflux of K^+ from fungal cells and extensive cellular degradation²⁰ (personal communications). The addition of 100 and 200 mM of potassium chloride or potassium phosphate to *C. tropicalis* and *C. albicans*, respectively, rescue cells from peptide induced death and halt cellular degradation indicated by the preservation of proteins (personal communications). The salt addition did not halt interaction as observed that the salt-treated cell continues to internalize the peptides, indicating that the protection from death is caused by K^+ replenishment (personal communications). The efflux of K^+ from fungal cells causes autophagy.⁶⁹ Therefore, the presence of autophagosomes aligns with the hypothesis that autophagy is activated as a cellular stress response, potentially aiming to isolate or degrade cytotoxic peptides or damaged organelles caused by peptide action^{70,71} or to replenish the K^+ loss caused by peptide treatment.⁶⁹

SEM analysis further supports and expands on TEM observations, highlighting the

morphological impacts of peptides on treated cells (Figure 7). After 20 min of incubation, RR and D-RR peptides caused severe cell wall damage in *C. tropicalis*, including cytoplasmic content leakage, cell wall wrinkling, and pore formation (Figure 7). These events suggest that after peptide internalization and subsequent impacts on intracellular processes, pore formation emerges as a secondary mechanism amplifying cellular damage. Supporting this idea, previous studies demonstrated that peptide-induced ROS generation damages the plasma membrane, reversible with antioxidant treatment (personal communications). Similar findings have been reported for peptides like HsAFP1 and PuroA, where ROS increase and intracellular target impacts precede plasma membrane pore formation.^{16,68} Pore formation by peptides leads to cytoplasmic content and ion loss, explaining cell size reduction (personal communications). This phenomenon may be linked to excessive autophagic degradation, compromising cell integrity. In *C. albicans* cells treated with WR, membrane blebbing was observed, differing from the effects of RR and D-RR. These surface alterations likely result from changes in cell permeability, indicating that WR exhibits higher permeabilization levels in *C. albicans*. Such cell wall and membrane disturbances resemble the effects of miconazole in *C. albicans*, where necrosis progresses more slowly and involves progressive cell wall degradation.⁷² Similarly, SEM studies of plantaricin E, F, and J fungicidal activity revealed extracellular vesicles (blebs), convolutions, and cell wall disturbances initiating apoptosis and progressing to necrosis due to toxicity.⁷³ P113Du and P113Tri (a duplicate and triplicate 12-mer amino acid fragment of Hst5, respectively) induce blebbing *C. albicans* cells in biofilm. The induction of blebbing was correlated with ROS induction in the treated fungus provided that co-treatment with ascorbic acid, a ROS scavenger, suppressed blebbing formation.⁷⁴ ROS is induced in *C. albicans* treated with WR,²⁰ therefore, might be related to ROS production and will be addressed in the future.

Thus, SEM morphological analyses reinforce TEM findings, showing that internal damage, such as mitochondrial and vacuolar dysfunction, has evident external manifestations. These observations provide insights into the lethal mechanisms of peptide action, suggesting that initial intracellular effects promote a progressive structural collapse, intensified especially in WR activity, leading to cell death.

The ability of peptides to internalize into cells and destabilize microbial membranes is a critical mechanism underlying antimicrobial action.⁷⁵⁻⁷⁷ However, this membrane interaction can also occur in mammalian cells,⁷⁸ potentially resulting in cytotoxicity, as observed with peptide-lipid antibiotics like iturin A (a cyclic lipopeptide from *Bacillus subtilis*) and bacillomycin L (a iturinic lipopeptide from *Bacillus amyloliquefaciens*), which cause erythrocyte lysis.⁷⁹ Cytotoxicity is also noted in cathelicidin peptides, where the cytotoxic concentration varies depending on the cell type and assay used.⁸⁰ Consequently, when developing new antimicrobial therapies, assessing cytotoxicity is a crucial factor.⁷⁸ In this study, we evaluated the cytotoxicity and internalization capability of our peptides in mammalian LLC-MK2 cells, a well-established cell line for virological studies and vaccine development due to its stability and susceptibility to various viruses.⁸¹ Our results were promising: none of the bio-inspired peptides demonstrated toxicity toward LLC-MK2 cells (Figure 8). Even at concentrations five times higher, the peptides did not interact with or internalize into these mammalian cells, demonstrating their selectivity for fungal cells. This specificity positions them as strong candidates for therapeutic applications.^{16,82}

Our findings advance the understanding of these peptides' mechanisms of action. Deciphering drug mechanisms at the molecular level is pivotal for predicting their efficacy against specific targets, representing a critical step in the clinical development of new therapeutics.^{11,76,78}

CONCLUSION

This study elucidated the initial aspects of the mechanism of action of the bioinspired peptides RR, D-RR, and WR, designed based on the γ -core of the defensin Vu-Def1. These peptides demonstrated high antifungal efficacy against *C. tropicalis* and *C. albicans*, acting selectively and with low toxicity to mammalian cells. Rapid, energy-dependent cytoplasmic internalization was identified as a critical step for antifungal activity. The peptides likely utilized polyamine transport as a main entry route.

Spm exhibited an antioxidant role, reducing the ROS levels generated by RR and D-RR, providing partial protection to fungal cells without blocking internalization. However, Spm did not affect the cell death induced by WR, indicating that ROS scavenge by polyamine did not protect *C. albicans* from the toxic effect of WR as previously demonstrated for ascorbic acid.²⁰ Moreover, intracellular damage included vacuolar disorganization, mitochondrial alterations, and cell wall lesions, which likely contributed to cell death. Autophagy activation was also observed, suggesting a cellular stress response induced by the peptides.

The absence of toxicity to mammalian cells and the selectivity for fungal cells highlight the potential of these peptides as promising candidates for the development of novel antifungal therapies, particularly in a context of increasing resistance to conventional treatments. These findings strengthen the relevance of bio-inspired peptides in the search for innovative and effective therapeutic alternatives. Parallel to these results we had tested the three bio-inspired peptides in a *in vivo* fungal infection model in the larva of *Galleria mellonella* which indicated lack of toxicity to the insect and the effectiveness in control the infection with clinical strains of *C. tropicalis* and *C. albicans*.

Materials and Methods

Cells

Yeasts *Candida tropicalis* (CE017) and *Candida albicans* (CE022) were grown on Sabouraud agar (10 g/L peptone, 20 g/L D(+)glucose, 17 g/L agar, Merck) at 30 °C for 24 h. Stocks of each yeast were then maintained at 4 °C and transferred to fresh medium every 3 months.

LLC-MK2 cells (from *Rhesus* monkey kidney) (ATCC CCL-7.1) were grown in Dulbecco's Modified Eagle Medium (DMEM) supplemented with 5% bovine serum albumin (BSA) in 5% CO₂ at 37 °C in the Laboratório de Biologia Celular e Tecidual, from CBB, UENF, Campos dos Goytacazes, Rio de Janeiro, Brazil.

Peptides

The design and preparation of the three bioinspired peptides A_{36,42,44}R_{37,38}Y₃₂₋₄₆VuDef (abbreviated RR), D-A_{36,42,44}R_{37,38}Y₃₂₋₄₆VuDef (abbreviated D-RR), and A_{42,44}R_{37,38}W_{36,39}Y₃₂₋₄₆VuDef (abbreviated WR) were performed according to Toledo¹⁹. The peptides were also synthesized conjugated

with the fluorescent molecule 5-carboxyfluorescein (5-FAM) at the N-terminal portion and were named 5-FAM_{RR}, 5-FAM_{D-RR}, and 5-FAM_{WR}. The peptides were also synthesized conjugated with biotin at the N-terminal portion and were named b_{RR}, b_{D-RR}, and b_{WR}. Peptides were acquired commercially by Aminotech Brazil. All synthetic peptides were >95% pure by high performance liquid chromatography analysis performed by the manufacturer (Supplementary figure 1).

Antimicrobial and viability assays

Briefly, fresh cultures of the fungi were grown at 30 °C for 24 h and used to obtain a colony that was resuspended in Sabouraud broth (5 g/L meat peptone, 5 g/L casein peptone, 20 g/L D(+)glucose, 17 g/L agar, pH 5.7). The number of cells in this stock cell suspension was determined by direct counting in a Neubauer chamber (LaborOptik) under a light microscope (Axio Imager.A2, Zeiss). The antimicrobial assay was performed in a sterile 96-well microplate (polystyrene, U-bottom, Nunc, Thermo Scientific) and consisted separately of 2,000 cells/mL of each fungus, the lethal dose (LD₁₀₀) of each peptide determined by Lucas²⁰ sterilized by filtration (0.22 µm, Millex-GV, Millipore), and 100 µL (final volume) of Sabouraud broth. Different incubations times were used according to the experiment. For the viability assay, after the incubation time, the fungal cells were washed once in Sabouraud broth and plated in Sabouraud medium. After incubation at 30 °C for 24 h, the colonies were counted to determine the colony-forming units (CFU). The LD₁₀₀ was defined as the lowest peptide concentration that caused 100% cell death in the assay cell population compared to the control in the absence of peptide, by CFU counting. Controls were performed in the absence of peptides and were considered 100% viable. Blank samples were made with culture medium only.

Determination of cytoplasmic entry by confocal microscopy

To determine the cytoplasmic entry of the peptides into the fungal cells, we used the 5-FAM_{RR}, 5-FAM_{D-RR}, and 5-FAM_{WR}. Fungal cultures (40,000 cells/mL) were incubated with calcofluor white (CFW) (Sigma-Aldrich) for chitin staining at 30 °C for 5 min, then the 5-FAM-labeled peptides at their LD₁₀₀ were added and incubated for 20 min at 30 °C. Controls were performed without the addition of the bioinspired peptides. For time-lapse analysis, 100 µL aliquots (in 1.5 mL microcentrifuge tubes) were pretreated with 2% CFW for 5 min before the addition of the 5-FAM-labeled peptides. For the time-lapse assay, images were captured every 20 s for a 15 min interval. The cells were monitored using a Zeiss LSM-710/ConfoCor confocal microscope, the 5-FAM-labeled peptides were excited at 488 nm and the emission was detected in the 530 nm range. The CFW was excited at 380 nm, and the fluorescence was monitored in the 475 nm range. Images were captured using Zen2011 software.

Flow cytometry

C. tropicalis and *C. albicans* cells were obtained as described in the **Antimicrobial and viability assays** item, with modifications. The assays were performed with 10⁶ cells/mL in 300 µL (value referring to 3 wells of the antifungal assay) with the respective LD₁₀₀ for 20 min of 5-FAM_{RR}, 5-FAM_{D-RR}, and 5-FAM_{WR}. Analyses were performed using the FACS Calibur™ flow cytometer (BD

Sciences). For the 5-FAM-labeled peptides, samples were excited at 488 nm and emission was detected using a 505 to 530 nm filter. Data were analyzed with WinMDI software version 2.9.

Analysis of the influence of low temperature (4 °C) on peptide activity

Cells for this assay were obtained as described in the **Antimicrobial and viability assays** item, but the peptides were incubated with the cells for 20 min at their LD₁₀₀ at 4 °C. The controls were performed in the absence of the peptides and with peptides incubated at 30 °C. After this period, the cells were treated as described in the **Antimicrobial and viability assays** item. For the analysis of cytoplasmic entry, the cells were treated as described in the **Flow cytometry** item, at a temperature of 4 °C for 20 min with the 5-FAM-labeled peptides. Immediately afterward, they were treated as described in the **Determination of cytoplasmic entry by confocal microscopy** item.

Analysis of the interference in the membrane potential and energy metabolism of fungi from the interaction of peptides

This experiment was performed as described in the **Antimicrobial and viability assays** item, up to the quantification of cells, with the following differences: the cells were pre-incubated with 10 µM of carbonyl cyanide 3-chlorophenylhydrazone (CCCP) (Sigma-Aldrich) and 5 mM of sodium azide (NaN₃) (Sigma-Aldrich) for 15 min at 30 °C. After this period, the peptides were added and incubated for 20 min. Untreated cells, cells treated only with the peptides, and cells treated only with CCCP or NaN₃ were used as controls. At the end of the assay, the treated cells were plated as described in the **Antimicrobial and viability assays** item. This experiment was repeated three times. For the analysis of cytoplasmic entry, the cells were treated as described in the **Flow cytometry** item, with the same parameters, but with the 5-FAM-labeled peptides. Soon after they were treated as described in the **Determination of cytoplasmic entry by confocal microscopy** item.

Study of endocytosis inhibitors in the interaction of the peptide with the cell

This experiment followed the protocol detailed in the **Antimicrobial and viability assays** item, with the exception of some specific steps. The cells were initially exposed to 20 µM of Latrunculin A (Lat A) (Sigma-Aldrich) for a period of 15 min at 30 °C. Subsequently, the peptides were added and incubated for another 20 min. The control groups consisted of untreated cells and cells submitted only to Lat A exposure. The same procedure was applied using Nocodazole (Noc) (Sigma-Aldrich) at a concentration of 20 µM, maintaining the experimental parameters. The endocytosis inhibitor Cytochalasin D (Cyt D) (Sigma-Aldrich) was also tested at a concentration of 100 µg/mL pre-incubated for 30 min, the peptides were added and incubated for another 20 min maintaining the experimental parameters. At the end of the assays, the treated cells were submitted to the plating process as described in the **Antimicrobial and viability assays** item. For the analysis of cytoplasmic entry, the cells were treated as described in the **Flow cytometry** item and in the **Determination of cytoplasmic entry by confocal microscopy** item.

Study of polyamine transporters in peptide internalization

This experiment was performed as described in the **Antimicrobial and viability assays** item, up

to the quantification of cells, with the following differences: Cells were initially exposed to 100 μM of the polyamine spermine (Spm) (Sigma-Aldrich) for a period of 15 min at 30 °C. Subsequently, the peptides were added and incubated for another 20 min. The control groups consisted of untreated cells and cells submitted only to Spm exposure. At the end of the assays, the treated cells were submitted to the plating process as described in the **Antimicrobial and viability assays** item. For the analysis of cytoplasmic entry, the cells were treated as described in the **Flow cytometry** item, with the same parameters, but with the 5-FAM-labeled peptides, soon after they were treated as described in the **Determination of cytoplasmic entry by confocal microscopy** item. To evaluate the intracellular ROS levels of *C. tropicalis* cells treated with Spm, the assay was performed as described in the **Flow cytometry** item, with the same parameters, but with RR and D-RR, and in the presence of 20 μM of the probe 2',7'-dichlorodihydrofluorescein diacetate (H₂DCFDA, Calbiochem, EMD) and Spm.

Ultrastructural analysis by transmission electron microscopy

This experiment was performed as described in the **Antimicrobial and viability assays** item with the following differences: for this assay was used 10⁶ cells/mL. The controls and the samples treated with the peptides for 1, 5, and 10 min were fixed with 5% glutaraldehyde overnight. After fixation, the yeasts were washed three times with 100 mM sodium cacodylate buffer, pH 7.2 for 10 min. The samples were dehydrated for 25 min in different concentrations of ethanol (30%, 50%, 70%, 90%, and 100% super dry 3 times), followed by infiltration in hydrophilic resin (LR-White). After this process, the material was left at room temperature for 48 h, and after this time taken to an oven at 60 °C, for 16 h for polymerization. Ultrathin sections of the samples were obtained, using an Ultramicrotome Leica EM UC7, which were stained with uranyl acetate for 5 min and lead citrate for 1 min. Then, the samples were observed, and images were obtained using a Jeol JEM 1400 Plus transmission electron microscope with an acceleration voltage of 120 kV.

Localization of peptides by transmission electron microscopy

This experiment was performed as described in the **Antimicrobial and viability assays** item with the following differences: for this assay was used 10⁶ cells/mL and fungal cells were treated with b_RR, b_D-RR, and b_WR for 1, 5, and 10 min. After the incubation the samples were treated as described in **Ultrastructural analysis by transmission electron microscopy** item with the following differences: and the streptavidin-gold conjugate (40 nm) was used for visualization. After the ultrathin sections were made. The sections were incubated in a closed humid chamber at 4 °C overnight at a 1:50 ratio of streptavidin-gold conjugate (from *Streptomyces avidinii* with 40 nm gold particle size, Sigma-Aldrich) in PBS and 1% BSA. They were washed four times in PBS and 1% BSA, four times in PBS, three times in distilled water and contrasted with uranyl acetate for 5 min and lead citrate for 1 min, then examined in a Jeol JEM 1400 Plus transmission electron microscope with an acceleration voltage of 120 kV.

DNA gel shift assay

The DNA of *C. tropicalis* and *C. albicans* fresh cultures were extracted according to the DNeasy plant mini kit (Qiagen), after the extraction, DNA was quantified by NanoDrop 2000 (Thermo Scientific).

Gel shift assay was performed as Soares²¹ with 1000 ng of the extracted DNA.

Ultrastructural analysis by scanning electron microscopy

Cells for this assay were obtained as described in the **Antimicrobial and viability assays** item with the following differences: Fungal cells at 1×10^6 cells/mL were treated with the bioinspired peptides for 20 min. Control samples were prepared in the absence of the peptides. All samples were subjected to three washes with 100 mM sodium cacodylate, pH 7.2, immediately after they were fixed for 1 h in a Karnovsky solution (2.5% glutaraldehyde, 2.5% formaldehyde in 50 mM sodium cacodylate buffer, pH 7.2). After fixation, the fungi were washed three times with 100 mM sodium cacodylate buffer, pH 7.2 for 10 min. After washing again in the same buffer, the cells were dehydrated in an increasing series of acetone (30%, 50%, 70%, 90%, and 3 times 100% super dry), lasting 20 min at each stage. After dehydration, the cells were subjected to a critical point to replace all acetone with liquid CO₂ under high pressure conditions (Bal-Tec Critical Point Dryer - CPD 030). Images were obtained with a scanning electron microscope (FEG-SEM Mira, Tescan) with an acceleration voltage of 5 - 10 kV.

Study of the interaction of peptides with LLC-MK2 cells

The viability of LLC-MK2 cells after treatment with the peptides was assessed based on the reduction of 3-(4,5-dimethylthiazol-2-yl)-2,5-diphenyltetrazolium bromide (MTT) (Sigma-Aldrich). In 96-well plates, 1×10^4 cells per well were cultured in Dulbecco's Modified Eagle's Medium (DMEM) supplemented with 5% BSA. After 24 h, the cells were washed and treated with the peptides at different concentrations. As a negative control, cells were cultured under the same conditions, without the addition of peptides. As a positive control, cells were treated with 10% Triton X-100. After 24 h of treatment, 15 μ L of MTT solution (5 mg/mL in DMEM) were added to the cells in each well of the plate, incubated for 4 h at 37 °C and 5% CO₂. The formazan crystals formed were solubilized by the addition of 100 μ L of DMSO. A volume of 100 μ L of the supernatant from each well was transferred to a new 96-well plate and read at 570 nm in a VersaMax microplate reader (Molecular Devices) using SoftMax Pro 6.0 software. Data were plotted using GraphPad Prism 5.0 software. For analysis of cytoplasmic entry, the cells after cultivation were treated as described in the **Determination of cytoplasmic entry by confocal microscopy** item, with modifications, using 1 mg/mL of the DBA-Texas Red dye (*Dolichos biflorus* agglutinin, (Sigma-Aldrich) which is a lectin, *i.e.*, a protein that specifically binds to certain types of carbohydrates, for the delimitation of the cell surface.

Statistical analysis

All tests were performed in three replicates, in triplicate, with the exception of the confocal microscopy, TEM and SEM tests, which were performed in one replicate. The data obtained were statistically analyzed using the GraphPad Prism 8 program, using the one-way ANOVA test, considering a P-value < 0.05 as significant.

ASSOCIATED CONTENT

Supporting Information

The Supporting Information is available free of charge at

AUTHOR INFORMATION

Corresponding author

André de Oliveira Carvalho - Laboratory of Physiology and Biochemistry of Microorganisms, Center of Biosciences and Biotechnology, Northern Fluminense State University Darcy Ribeiro, Av. Alberto Lamego, nº 2000, Parque Califórnia, Campos dos Goytacazes, RJ, Brazil, CEP 28013-602; Tel: (+55) 22 2739-7217; E-mail: andre@uenf.br

Authors

Douglas Ribeiro Lucas - *Laboratório de Fisiologia e Bioquímica de Microrganismos, Centro de Biociências e Biotecnologia, Universidade Estadual do Norte Fluminense Darcy Ribeiro, Campos dos Goytacazes-RJ, 28013-602, Brazil*

Filipe Zaniratti Damica - *Laboratório de Fisiologia e Bioquímica de Microrganismos, Centro de Biociências e Biotecnologia, Universidade Estadual do Norte Fluminense Darcy Ribeiro, Campos dos Goytacazes-RJ, 28013-602, Brazil*

Felipe Figueirôa Moreira - *Laboratório de Biologia Celular e Tecidual, Centro de Biociências e Biotecnologia, Universidade Estadual do Norte Fluminense Darcy Ribeiro, Campos dos Goytacazes-RJ, 28013-602, Brazil*

Juliana Azevedo da Silva - *Laboratório de Biologia do Reconhecer, Centro de Biociências e Biotecnologia, Universidade Estadual do Norte Fluminense Darcy Ribeiro, Campos dos Goytacazes-RJ, 28013-602, Brazil*

Felipe Perissé Duarte Lopes - *Laboratório de Materiais Avançados, Centro de Ciência e Tecnologia, Universidade Estadual do Norte Fluminense Darcy Ribeiro, Campos dos Goytacazes-RJ, 28013-602, Brazil*

Noíl Gomes de Freitas - *Laboratório de Fisiologia e Bioquímica de Microrganismos, Centro de Biociências e Biotecnologia, Universidade Estadual do Norte Fluminense Darcy Ribeiro, Campos dos Goytacazes-RJ, 28013-602, Brazil*

Sérgio Henrique Seabra - *Laboratório de Biologia Celular e Tecidual, Centro de Biociências e Biotecnologia, Universidade Estadual do Norte Fluminense Darcy Ribeiro, Campos dos Goytacazes-RJ, 28013-602, Brazil*

Anna Lvovna Okorokova-Façanha - *Laboratório de Fisiologia e Bioquímica de Microrganismos, Centro de Biociências e Biotecnologia, Universidade Estadual do Norte Fluminense Darcy Ribeiro, Campos dos Goytacazes-RJ, 28013-602, Brazil*

Valdirene Moreira Gomes - *Laboratório de Fisiologia e Bioquímica de Microrganismos, Centro de Biociências e Biotecnologia, Universidade Estadual do Norte Fluminense Darcy Ribeiro, Campos dos Goytacazes-RJ, 28013-602, Brazil*

Notes

The authors declare no competing financial interest.

ACKNOWLEDGMENTS

We thank Luis Carlos Souza, Valéria Miguelote Kocks, and Zila Macedo for their technical assistance. The work was supported by Brazilian agencies *Conselho Nacional de Desenvolvimento Científico e Tecnológico* (CNPq) (number 306429/2023-3), *Fundação Carlos Chagas Filho de Amparo à Pesquisa do Estado do Rio de Janeiro* (FAPERJ) (number E-26/210.484/2024, APQ1), and *Coordenação de Aperfeiçoamento de Pessoal de Nível Superior* (CAPES) (Financial Code 001), as well as by the University State of Norte Fluminense Darcy Ribeiro.

REFERENCES

- (1) WHO fungal priority pathogens list to guide research, development and public health action. Geneva: World Health Organization; 2022. Licence: CC BY-NC-SA 3.0 IGO. <https://www.who.int/publications/i/item/9789240060241>
- (2) Garcia-Bustos, V.; Cabañero-Navalon, M. D.; Ruiz-Gaitán, A.; Salavert, M.; Tomo-Mas, M. Á.; Pemán, J. Climate change, animals, and *Candida auris*: insights into the ecological niche of a new species from a One Health approach. *Clin. Microbiol. Infect.* **2023**, *29* (7), 858–862.
- (3) Thambugala, K. M.; Daranagama, D. A.; Tennakoon, D. S.; Jayatunga, D. P. W.; Hongsanan, S.; Xie, N. Humans vs. Fungi: An overview of fungal pathogens against humans. *Pathogens* **2024**, *13* (5), 426
- (4) *GAFFI annual report 2022*. (2023, julho 15). Gaffi. <https://gaffi.org/gaffi-annual-report-2022/>
- (5) Denning, D. W. Global incidence and mortality of severe fungal disease. *Lancet Infect. Dis.* **2024**, *24* (7), e428–e438.
- (6) Banerjee, S.; Denning, D.; Chakrabarti, A. One Health aspects & priority roadmap for fungal diseases: A mini-review. *Indian J. Med. Res.* **2021**, *153* (3), 311.
- (7) de Crecy, E.; Jaronski, S.; Lyons, B.; Lyons, T. J.; Keyhani, N. O. Directed evolution of a filamentous fungus for thermotolerance. *BMC Biotechnol.* **2009**, *9* (1), 74.
- (8) Casadevall, A.; Kontoyiannis, D. P.; Robert, V. Environmental *Candida auris* and the global warming emergence hypothesis. *MBio* **2021**, *12* (2), e00360-21.
- (9) Nnadi, N. E.; Carter, D. A. Climate change and the emergence of fungal pathogens. *PLoS Pathog.* **2021**, *17* (4), e1009503.
- (10) Seidel, D.; Wurster, S.; Jenks, J. D.; Sati, H.; Gangneux, J.-P.; Egger, M.; Alastruey-Izquierdo, A.; Ford, N. P.; Chowdhary, A.; Sprute, R.; Cornely, O.; Thompson, G. R.; Hoenigl, M.; Kontoyiannis, D. . Impact of climate change and natural disasters on fungal infections. *Lancet Microbe* **2024**, *5* (6), e594–e605.
- (11) Fisher, M. C.; Alastruey-Izquierdo, A.; Berman, J.; Bicanic, T.; Bignell, E. M.; Bowyer, P.; Bromley, M.; Brüggemann, R.; Garber, G.; Cornely, O. A.; Gurr, S. J.; Harrison, T. S.; Kuijper, E.; Rhodes, J.; Sheppard, D. C.; Warris, A.; White, P. L.; Xu, J.; Zwaan, B.; Verweij, P. E.

- Tackling the emerging threat of antifungal resistance to human health. *Nat. Rev. Microbiol.* **2022**, *20* (9), 557–571.
- (12) Du, H.; Bing, J.; Hu, T.; Ennis, C. L.; Nobile, C. J.; Huang, G. *Candida auris*: Epidemiology, biology, antifungal resistance, and virulence. *PLoS Pathog.* **2020**, *16* (10), e1008921.
- (13) Campoy, S.; Adrio, J. L. Antifungals. *Biochem. Pharmacol.* **2017**, *133*, 86–96.
- (14) Stewart, A. G.; Paterson, D. L. How urgent is the need for new antifungals? *Expert Opin. Pharmacother.* **2021**, *22* (14), 1857–1870.
- (15) Carvalho, A. de O.; Gomes, V. M. Plant defensins - Prospects for the biological functions and biotechnological properties. *Peptides* **2009**, *30* (5), 1007–1020.
- (16) Carvalho, A. de O.; Gomes, V. M. Plant defensins and defensin-like peptides - biological activities and biotechnological applications. *Curr. Pharm. Des.* **2011**, *17* (38), 4270–4293.
- (17) Răileanu, M.; Borlan, R.; Campu, A.; Janosi, L.; Turcu, I.; Focsan, M.; Bacalum, M. No country for old antibiotics! Antimicrobial peptides (AMPs) as next-generation treatment for skin and soft tissue infection. *Int. J. Pharm.* **2023**, *642*, 123169.
- (18) Shagaghi, N.; Bhawe, M.; Palombo, E. A.; Clayton, A. H. A. Revealing the sequence of interactions of PuroA peptide with *Candida albicans* cells by live-cell imaging. *Sci. Rep.* **2017**, *7* (1), 42542.
- (19) Toledo, E. B.; Lucas, D. R.; Simão, T. L. B. V.; Calixto, S. D.; Lassounskaia, E.; Muzitano, M. F.; Damica, F. Z.; Gomes, V. M.; de Oliveira Carvalho, A. Design of improved synthetic antifungal peptides with targeted variations in charge, hydrophobicity and chirality based on a correlation study between biological activity and primary structure of plant defensin γ -cores. *Amino Acids* **2021**, *53* (2), 219–237.
- (20) Lucas, D. R.; Damica, F. Z.; Toledo, E. B.; Cogo, A. J. D.; Okorokova-Façanha, A. L.; Gomes, V. M.; de Oliveira Carvalho, A. Bioinspired peptides induce different cell death mechanisms against opportunistic yeasts. *Probiotics Antimicrob. Proteins* **2024**, *16* (2), 649–672.
- (21) Soares, J. R.; José Tenório de Melo, E.; da Cunha, M.; Fernandes, K. V. S.; Taveira, G. B.; da Silva Pereira, L.; Pimenta, S.; Trindade, F. G.; Regente, M.; Pinedo, M.; de La Canal, L.; Gomes, V. M.; Carvalho, A. O. Interaction between the plant ApDef1 defensin and *Saccharomyces cerevisiae* results in yeast death through a cell cycle- and caspase-dependent process occurring via uncontrolled oxidative stress. *Biochim. Biophys. Acta Gen. Subj.* **2017**, *1861* (1), 3429–3443.
- (22) Oberparleiter, C.; Kaiserer, L.; Haas, H.; Ladurner, P.; Andratsch, M.; Marx, F. Active internalization of the *Penicillium chrysogenum* antifungal protein PAF in sensitive *aspergilli*. *Antimicrob. Agents Chemother.* **2003**, *47* (11), 3598–3601.
- (23) Mochon, A. B.; Liu, H. The antimicrobial peptide histatin-5 causes a spatially restricted disruption on the *Candida albicans* surface, allowing rapid entry of the peptide into the cytoplasm. *PLoS Pathog.* **2008**, *4* (10), e1000190.
- (24) Jang, W. S.; Bajwa, J. S.; Sun, J. N.; Edgerton, M. Salivary histatin 5 internalization by translocation, but not endocytosis, is required for fungicidal activity in *Candida albicans*. *Mol. Microbiol.* **2010**, *77* (2), 354–370.

- (25) Kumar, R.; Chadha, S.; Saraswat, D.; Bajwa, J. S.; Li, R. A.; Conti, H. R.; Edgerton, M. Histatin 5 uptake by candida albicans utilizes polyamine transporters Dur3 and Dur31 proteins. *J. Biol. Chem.* **2011**, *286* (51), 43748–43758.
- (26) El-Mounadi, K.; Islam, K. T.; Hernández-Ortiz, P.; Read, N. D.; Shah, D. M. Antifungal mechanisms of a plant defensin MtDef4 are not conserved between the ascomycete fungi *Neurospora crassa* and *Fusarium graminearum*. *Mol. Microbiol.* **2016**, *100* (3), 542–559.
- (27) Hayes, B.; Bleackley, M.; Anderson, M.; Van der Weerden, N. The plant defensin NaD1 enters the cytoplasm of candida albicans via endocytosis. *J. Fungi (Basel)* **2018**, *4* (1), 20.
- (28) Chang, C.-K.; Kao, M.-C.; Lan, C.-Y. Antimicrobial Activity of the Peptide LfcinB15 against *Candida albicans*. *J. Fungi (Basel)* **2021**, *7* (7), 519.
- (29) Rossignol, T.; Kelly, B.; Dobson, C.; d'Enfert, C. Endocytosis-mediated vacuolar accumulation of the human ApoE apolipoprotein-derived ApoEdpL-W antimicrobial peptide contributes to its antifungal activity in *Candida albicans*. *Antimicrob. Agents Chemother.* **2011**, *55* (10), 4670–4681.
- (30) Bleackley, M. R.; Wiltshire, J. L.; Perrine-Walker, F.; Vasa, S.; Burns, R. L.; van der Weerden, N. L.; Anderson, M. A. Agp2p, the plasma membrane transregulator of polyamine uptake, regulates the antifungal activities of the plant defensin NaD1 and other cationic peptides. *Antimicrob. Agents Chemother.* **2014**, *58* (5), 2688–2698.
- (31) Muñoz, A.; Gandía, M.; Harries, E.; Carmona, L.; Read, N. D.; Marcos, J. F. Understanding the mechanism of action of cell-penetrating antifungal peptides using the rationally designed hexapeptide PAF26 as a model. *Fungal Biol. Rev.* **2013**, *26* (4), 146–155.
- (32) Iacopetta, B. J.; Morgan, E. H. The kinetics of transferrin endocytosis and iron uptake from transferrin in rabbit reticulocytes. *J. Biol. Chem.* **1983**, *258* (15), 9108–9115.
- (33) Aguilera, J.; Rande-Gil, F.; Prieto, J. A. Cold response in *Saccharomyces cerevisiae*: new functions for old mechanisms. *FEMS Microbiol. Rev.* **2007**, *31* (3), 327–341.
- (34) Omardien, S.; Brul, S.; Zaat, S. A. J. Antimicrobial activity of cationic antimicrobial peptides against gram-positives: Current progress made in understanding the mode of action and the response of bacteria. *Front. Cell Dev. Biol.* **2016**, *4*, 111.
- (35) Tat, J.; Heskett, K.; Satomi, S.; Pilz, R. B.; Golomb, B. A.; Boss, G. R. Sodium azide poisoning: a narrative review. *Clin. Toxicol. (Phila.)* **2021**, *59* (8), 683–697.
- (36) Hoffmann, J.; Mendgen, K. Endocytosis and Membrane Turnover in the Germ Tube of *Uromyces fabae*. *Fungal Genet. Biol.* **1998**, *24* (1–2), 77–85.
- (37) Atkinson, H. A.; Daniels, A.; Read, N. D. Live-cell imaging of endocytosis during conidial germination in the rice blast fungus, *Magnaporthe grisea*. *Fungal Genet. Biol.* **2002**, *37* (3), 233–244.
- (38) Coote, P. J.; Holyoak, C. D.; Bracey, D.; Ferdinando, D. P.; Pearce, J. A. Inhibitory action of a truncated derivative of the amphibian skin peptide dermaseptin s3 on *Saccharomyces cerevisiae*. *Antimicrob. Agents Chemother.* **1998**, *42* (9), 2160–2170.
- (39) Tomasinsig, L.; Skerlavaj, B.; Papo, N.; Giabbai, B.; Shai, Y.; Zanetti, M. Mechanistic and functional studies of the interaction of a proline-rich antimicrobial peptide with mammalian cells. *J. Biol. Chem.* **2006**, *281* (1), 383–391.

- (40) Ayscough, K. R.; Stryker, J.; Pokala, N.; Sanders, M.; Crews, P.; Drubin, D. G. High rates of actin filament turnover in budding yeast and roles for actin in establishment and maintenance of cell polarity revealed using the actin inhibitor latrunculin-A. *J. Cell Biol.* **1997**, *137* (2), 399–416.
- (41) Dutta, D.; Donaldson, J. G. Search for inhibitors of endocytosis: Intended specificity and unintended consequences. *Cell. Logist.* **2012**, *2* (4), 203–208.
- (42) Wakatsuki, T.; Schwab, B.; Thompson, N. C.; Elson, E. L. Effects of cytochalasin D and latrunculin B on mechanical properties of cells. *J. Cell Sci.* **2001**, *114* (5), 1025–1036.
- (43) Veerman, E. C. I.; Valentijn-Benz, M.; Nazmi, K.; Ruissen, A. L. A.; Walgreen-Weterings, E.; van Marle, J.; Doust, A. B.; van't Hof, W.; Bolscher, J. G. M.; Amerongen, A. V. N. Energy depletion protects candida albicans against antimicrobial peptides by rigidifying its cell membrane. *J. Biol. Chem.* **2007**, *282* (26), 18831–18841.
- (44) Podda, E.; Benincasa, M.; Pacor, S.; Micali, F.; Mattiuzzo, M.; Gennaro, R.; Scocchi, M. Dual mode of action of Bac7, a proline-rich antibacterial peptide. *Biochim. Biophys. Acta Gen. Subj.* **2006**, *1760* (11), 1732–1740.
- (45) Greco, I.; Hansen, J. E.; Jana, B.; Molchanova, N.; Oddo, A.; Thulstrup, P. W.; Damborg, P.; Guardabassi, L.; Hansen, P. R. Structure–activity study, characterization, and mechanism of action of an antimicrobial peptoid D2 and its d- and l-peptide analogues. *Molecules* **2019**, *24* (6), 1121.
- (46) Veses, V.; Richards, A.; Gow, N. A. R. Vacuoles and fungal biology. *Curr. Opin. Microbiol.* **2008**, *11* (6), 503–510.
- (47) Utesch, T.; de Miguel Catalina, A.; Schattenberg, C.; Paegle, N.; Schmieder, P.; Krause, E.; Miao, Y.; McCammon, J. A.; Meyer, V.; Jung, S.; Mroginski, M. A. A computational modeling approach predicts interaction of the antifungal protein AFP from *Aspergillus giganteus* with fungal membranes via its γ -core motif. *mSphere* **2018**, *3* (5), e00377-18.
- (48) Slezina, M. P.; Istomina, E. A.; Korostyleva, T. V.; Odintsova, T. I. The γ -core motif peptides of plant AMPs as novel antimicrobials for medicine and agriculture. *Int. J. Mol. Sci.* **2022**, *24* (1), 483.
- (49) Neves de Medeiros, L.; Domitrovic, T.; Cavalcante de Andrade, P.; Faria, J.; Barreto Bergter, E.; Weissmüller, G.; Kurtenbach, E. Psd1 binding affinity toward fungal membrane components as assessed by SPR: The role of glucosylceramide in fungal recognition and entry. *Biopolymers* **2014**, *102* (6), 456–464.
- (50) Fernandes, C. M.; de Castro, P. A.; Singh, A.; Fonseca, F. L.; Pereira, M. D.; Vila, T. V. M.; Atella, G. C.; Rozental, S.; Savoldi, M.; Del Poeta, M.; Goldman, G. H.; Kurtenbach, E. Functional characterization of the *Aspergillus nidulans* glucosylceramide pathway reveals that LCB $\Delta 8$ -desaturation and C9-methylation are relevant to filamentous growth, lipid raft localization and Psd1 defensin activity. *Mol. Microbiol.* **2016**, *102* (3), 488–505.
- (51) Järvä, M.; Lay, F. T.; Hulett, M. D.; Kvangsakul, M. Structure of the defensin Nsd7 in complex with PIP₂ reveals that defensin: lipid oligomer topologies are dependent on lipid type. *FEBS Lett.* **2017**, *591* (16), 2482–2490.
- (52) Amaral, V. S. G.; Fernandes, C. M.; Felício, M. R.; Valle, A. S.; Quintana, P. G.; Almeida, C. C.; Barreto-Bergter, E.; Gonçalves, S.; Santos, N. C.; Kurtenbach, E. Psd2 pea defensin shows a

- preference for mimetic membrane rafts enriched with glucosylceramide and ergosterol. *Biochim. Biophys. Acta Biomembr.* **2019**, *1861* (4), 713–728.
- (53) Martin, S. W.; Konopka, J. B. Lipid raft polarization contributes to hyphal growth in *Candida albicans*. *Eukaryot. Cell* **2004**, *3* (3), 675–684.
- (54) Lajoie, P.; Nabi, I. R. Regulation of raft-dependent endocytosis. *J. Cell. Mol. Med.* **2007**, *11* (4), 644–653.
- (55) Cuesta-Marbán, Á.; Botet, J.; Czyz, O.; Cacharro, L. M.; Gajate, C.; Hornillos, V.; Delgado, J.; Zhang, H.; Amat-Guerri, F.; Acuña, A. U.; McMaster, C. R.; Revuelta, J. L.; Zaremberg, V.; Mollinedo, F. Drug uptake, lipid rafts, and vesicle trafficking modulate resistance to an anticancer lysophosphatidylcholine analogue in yeast. *J. Biol. Chem.* **2013**, *288* (12), 8405–8418.
- (56) Tabor, C. W.; Tabor, H. Polyamines. *Annu. Rev. Biochem.* **1984**, *53* (1), 749–790.
- (57) Schuber, F. Influence of polyamines on membrane functions. *Biochem. J.* **1989**, *260* (1), 1–10.
- (58) Uemura, T.; Kashiwagi, K.; Igarashi, K. Polyamine Uptake by DUR3 and SAM3 in *Saccharomyces cerevisiae*. *J. Biol. Chem.* **2007**, *282* (10), 7733–7741.
- (59) Rider, J. E.; Hacker, A.; Mackintosh, C. A.; Pegg, A. E.; Woster, P. M.; Casero, R. A., Jr. Spermine and spermidine mediate protection against oxidative damage caused by hydrogen peroxide. *Amino Acids* **2007**, *33* (2), 231–240.
- (60) Cavalheiro, M.; Romão, D.; Santos, R.; Mil-Homens, D.; Pais, P.; Costa, C.; Galocha, M.; Pereira, D.; Takahashi-Nakaguchi, A.; Chibana, H.; Fialho, A. M.; Teixeira, M. C. Role of CgTpo4 in polyamine and antimicrobial peptide resistance: Determining virulence in *Candida glabrata*. *Int. J. Mol. Sci.* **2021**, *22* (3), 1376.
- (61) Li, R.-F.; Yan, X.-H.; Lu, Y.-B.; Lu, Y.-L.; Zhang, H.-R.; Chen, S.-H.; Liu, S.; Lu, Z.-F. Anticandidal activity of a novel peptide derived from human chromogranin A and its mechanism of action against *Candida krusei*. *Exp. Ther. Med.* **2015**, *10* (5), 1768–1776.
- (62) Parisi, K.; Shafee, T. M. A.; Quimbar, P.; van der Weerden, N. L.; Bleackley, M. R.; Anderson, M. A. The evolution, function and mechanisms of action for plant defensins. *Semin. Cell Dev. Biol.* **2019**, *88*, 107–118.
- (63) Lobo, D. S.; Pereira, I. B.; Fragel-Madeira, L.; Medeiros, L. N.; Cabral, L. M.; Faria, J.; Bellio, M.; Campos, R. C.; Linden, R.; Kurtenbach, E. Antifungal *Pisum sativum* defensin 1 interacts with *Neurospora crassa* cyclin F related to the cell cycle. *Biochemistry* **2007**, *46* (4), 987–996.
- (64) Park, C. B.; Kim, H. S.; Kim, S. C. Mechanism of action of the antimicrobial peptide buforin II: Buforin II kills microorganisms by penetrating the cell membrane and inhibiting cellular functions. *Biochem. Biophys. Res. Commun.* **1998**, *244* (1), 253–257.
- (65) Ma, T.; Yu, Q.; Ma, C.; Mao, X.; Liu, Y.; Peng, X.; Li, M. Role of the inositol polyphosphate kinase Vip1 in autophagy and pathogenesis in *Candida albicans*. *Future Microbiol.* **2020**, *15* (14), 1363–1377.
- (66) Wójcik-Mieszawska, S.; Lewtak, K.; Skwarek, E.; Dębowski, D.; Gitlin-Domagalska, A.; Nowak, J.; Wydrych, J.; Pawelec, J.; Fiolka, M. J. Autophagy of *Candida albicans* cells after the action of earthworm Venetin-I nanoparticle with protease inhibitor activity. *Sci. Rep.* **2023**, *13* (1), 14228.

- (67) Yun, H. R.; Jo, Y. H.; Kim, J.; Shin, Y.; Kim, S. S.; Choi, T. G. Roles of autophagy in oxidative stress. *Int. J. Mol. Sci.* **2020**, *21* (9), 3289.
- (68) Struyfs, C.; Cools, T. L.; De Cremer, K.; Sampaio-Marques, B.; Ludovico, P.; Wasko, B. M.; Kaerberlein, M.; Cammue, B. P. A.; Thevissen, K. The antifungal plant defensin HsAFP1 induces autophagy, vacuolar dysfunction and cell cycle impairment in yeast. *Biochim. Biophys. Acta Biomembr.* **2020**, *1862* (8), 183255.
- (69) Rangarajan, N.; Kapoor, I.; Li, S.; Drossopoulos, P.; White, K. K.; Madden, V. J.; Dohlman, H. G. Potassium starvation induces autophagy in yeast. *J. Biol. Chem.* **2020**, *295* (41), 14189–14202.
- (70) Klionsky, D. J.; Ohsumi, Y. Vacuolar import of proteins and organelles from the cytoplasm. *Annu. Rev. Cell Dev. Biol.* **1999**, *15* (1), 1–32.
- (71) Mijaljica, D.; Prescott, M.; Klionsky, D. J.; Devenish, R. J. Autophagy and vacuole homeostasis: A case for self-degradation? *Autophagy* **2007**, *3* (5), 417–421.
- (72) De Nollin, S.; Borgers, M. Scanning electron microscopy of *Candida albicans* after in vitro treatment with miconazole. *Antimicrob. Agents Chemother.* **1975**, *7* (5), 704–711.
- (73) Sharma, A.; Srivastava, S. Anti-Candida activity of two-peptide bacteriocins, plantaricins (PIn E/F and J/K) and their mode of action. *Fungal Biol.* **2014**, *118* (2), 264–275.
- (74) Lin, G.-Y.; Chen, H.-F.; Xue, Y.-P.; Yeh, Y.-C.; Chen, C.-L.; Liu, M.-S.; Cheng, W.-C.; Lan, C.-Y. The antimicrobial peptides P-113Du and P-113Tri function against *Candida albicans*. *Antimicrob. Agents Chemother.* **2016**, *60* (10), 6369–6373.
- (75) Patrzykat, A.; Friedrich, C. L.; Zhang, L.; Mendoza, V.; Hancock, R. E. W. Sublethal concentrations of pleurocidin-derived antimicrobial peptides inhibit macromolecular synthesis in *Escherichia coli*. *Antimicrob. Agents Chemother.* **2002**, *46* (3), 605–614.
- (76) Otvos, L., Jr.; Snyder, C.; Condie, B.; Bulet, P.; Wade, J. D. Chimeric antimicrobial peptides exhibit multiple modes of action. *Int. J. Pept. Res. Ther.* **2005**, *11* (1), 29–42.
- (77) Roversi, D.; Luca, V.; Aureli, S.; Park, Y.; Mangoni, M. L.; Stella, L. How many antimicrobial peptide molecules kill a bacterium? The case of PMAP-23. *ACS Chem. Biol.* **2014**, *9* (9), 2003–2007.
- (78) Fernández de Ullivarri, M.; Arbulu, S.; Garcia-Gutierrez, E.; Cotter, P. D. Antifungal peptides as therapeutic agents. *Front. Cell. Infect. Microbiol.* **2020**, *10*, 105.
- (79) Latoud, C.; Peypoux, F.; Michel, G.; Genet, R.; Morgat, J. L. Interactions of antibiotics of the iturin group with human erythrocytes. *Biochim. Biophys. Acta Biomembr.* **1986**, *856* (3), 526–535.
- (80) Benincasa, M.; Scocchi, M.; Pacor, S.; Tossi, A.; Nobili, D.; Basaglia, G.; Busetti, M.; Gennaro, R. Fungicidal activity of five cathelicidin peptides against clinically isolated yeasts. *J. Antimicrob. Chemother.* **2006**, *58* (5), 950–959.
- (81) Xiao, X.; Wang, C.; Chang, D.; Wang, Y.; Dong, X.; Jiao, T.; Zhao, Z.; Ren, L.; Dela Cruz, C. S.; Sharma, L.; Lei, X.; Wang, J. Identification of potent and safe antiviral therapeutic candidates against SARS-CoV-2. *Front. Immunol.* **2020**, *11*, 586572.
- (82) ay, F. T.; Ryan, G. F.; Caria, S.; Phan, T. K.; Veneer, P. K.; White, J. A.; Kvensakul, M.; Hulett, M. D. Structural and functional characterization of the membrane-permeabilizing activity of *Nicotiana occidentalis* defensin NoD173 and protein engineering to enhance oncolysis. *FASEB J.* **2019**, *33* (5), 6470–6482.

6.2 Figura Suplementar

Supplementary figures

Energy-dependent internalization mechanism, cytoplasmic localization, and impact on the ultrastructure of pathogenic fungi of the genus *Candida* by three bioinspired antimicrobial peptides

Douglas Ribeiro Lucas^{a,1}, Filipe Zaniratti Damica^{a,1}, Felipe Figueirôa Moreira^b, Juliana Azevedo da Silva^c, Felipe Perissé Duarte Lopes^d, Noil Gomes de Freitas^a, Sérgio Henrique Seabra^b, Anna Lvovna Okorokova-Façanha^a, Valdirene Moreira Gomes^a, André de Oliveira Carvalho^{a,*}

^aLaboratório de Fisiologia e Bioquímica de Microrganismos, Centro de Biociências e Biotecnologia, Universidade Estadual do Norte Fluminense Darcy Ribeiro, Campos dos Goytacazes-RJ, 28013-602, Brazil.

^bLaboratório de Biologia Celular e Tecidual, Centro de Biociências e Biotecnologia, Universidade Estadual do Norte Fluminense Darcy Ribeiro, Campos dos Goytacazes-RJ, 28013-602, Brazil.

^cLaboratório de Biologia do Reconhecer, Centro de Biociências e Biotecnologia, Universidade Estadual do Norte Fluminense Darcy Ribeiro, Campos dos Goytacazes-RJ, 28013-602, Brazil.

^dLaboratório de Materiais Avançados, Centro de Ciência e Tecnologia, Universidade Estadual do Norte Fluminense Darcy Ribeiro, Campos dos Goytacazes-RJ, 28013-602, Brazil.

¹These authors contributed equally to this work.

*Corresponding author: André de Oliveira Carvalho, Av. Alberto Lamego, nº 2000, Laboratory of Physiology and Biochemistry of Microorganisms, Center of Biosciences and Biotechnology, Universidade Estadual do Norte Fluminense Darcy Ribeiro, Parque Califórnia, Campos dos Goytacazes, RJ, Brazil, CEP 28013-602; Tel: (+55) 22 2739-7217; E-mail: andre@uenf.br

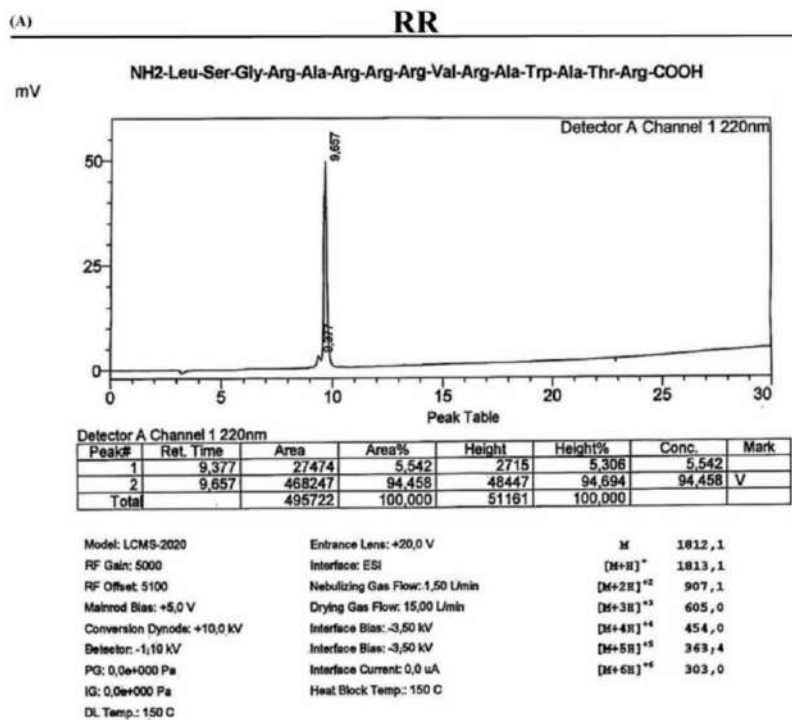
Abbreviations:

BSA, bovine serum albumin; CCCP, carbonyl cyanide 3-chlorophenylhydrazone; Cyt D, cytochalasin D; CFW, calcofluor white; DMEM, Dulbecco's Modified Eagle Medium; 5-FAM, 5-carboxyfluorescein; Lat A, latrunculin A; TEM, transmission electron microscope; SEM, scanning electron microscope; MTT, 3-(4,5-dimethylthiazol-2-yl)-2,5-diphenyltetrazolium bromide; Noc, nocodazole; 5-FAM_RR, RR peptide linked to 5-FAM; 5-FAM_D-RR, D-RR peptide linked to 5-FAM; 5-FAM_WR, WR peptide linked to 5-FAM; b_RR, RR peptide linked to biotin; b_D-RR, RR peptide linked to biotin; b_WR, WR peptide linked to biotin; Spm, spermine.

Content of SI:

1. Liquid Chromatography-Mass Spectrometry Analysis of the synthetic peptides.....	2
2. Dynamics of cytoplasmic entry of 5-FAM-labeled peptides into fungal cells.....	11
3. Influence of cell energy on the interaction of bioinspired peptides with fungal cells.....	13
4. Role of endocytosis in the interaction of bioinspired peptides in fungal cells.....	14

5. Role of endocytosis in the interaction of bioinspired peptides in *Candida tropicalis*.....15
6. Role of spermine (Spm) in the interaction of bioinspired peptides in *Candida tropicalis*.....16
7. Gel shift assay showing the interaction of RR, D-RR, and WR with DNA of fungal cells.....17

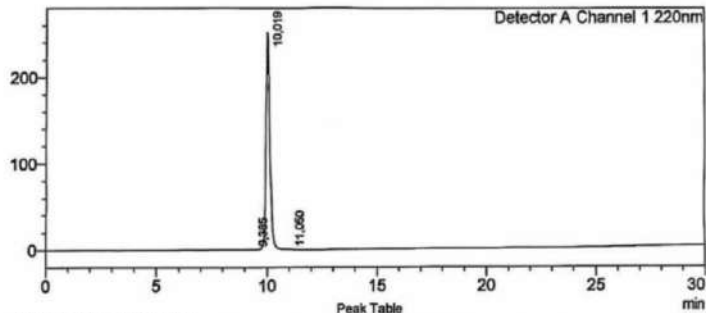


(B)

D-RR

NH₂-(d)Leu-(d)Ser-Gly-(d)Arg-(d)Ala-(d)Arg-(d)Arg-(d)Val-(d)Arg-(d)Ala-(d)Trp-(d)Ala-(d)Thr-(d)Arg-COOH (todos d-aminoacidos)

mV



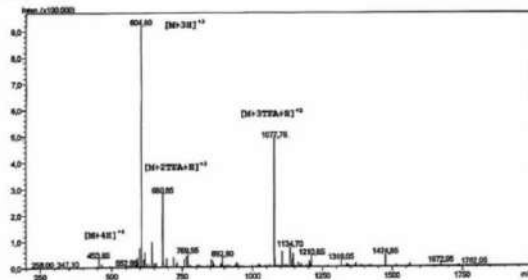
Peak Table

Peak#	Ret. Time	Area	Area%	Height	Height%	Conc.	Mark
1	9.385	316	0.010	43	0.017	0.010	
2	10.019	3088613	99.945	250658	99.910	99.945	S
3	11.050	1375	0.044	183	0.073	0.044	T
Total		3090303	100.000	250884	100.000		

Model: LCMS-2020
 RF Gols: 5000
 RF Offset: 5100
 Mainrod Bias: +5.0 V
 Conversion Dynode: +10.0 kV
 Detector: -1.10 kV
 PG: 0.0e+000 Pa
 IG: 0.0e+000 Pa
 DL Temp.: 150 C

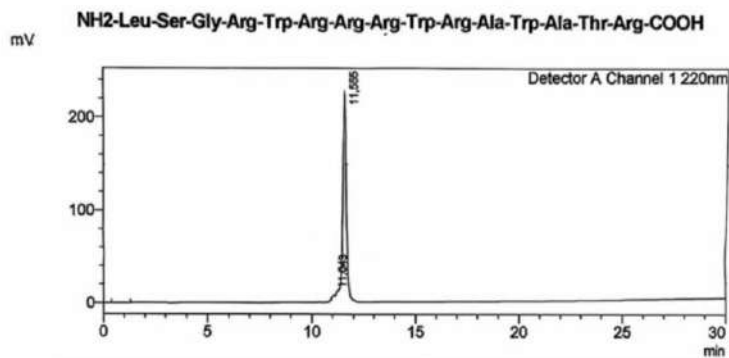
Entrance Lens: +20.0 V
 Interface: ESI
 Nebulizing Gas Flow: 1.50 L/min
 Drying Gas Flow: 15.00 L/min
 Interface Bias: -3.50 kV
 Interface Bias: -3.50 kV
 Interface Current: 0.0 uA
 Heat Block Temp.: 150 C

M 1812, 1
 [M+H]⁺ 1813, 1
 [M+2H]²⁺ 907, 1
 [M+3H]³⁺ 605, 0
 [M+4H]⁴⁺ 454, 0
 [M+5H]⁵⁺ 363, 4
 [M+6H]⁶⁺ 303, 0



(C)

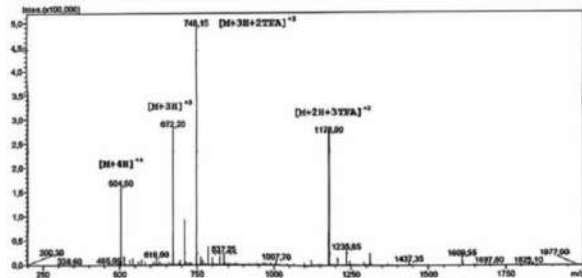
WR



Peak Table

Peak#	Ret. Time	Area	Area%	Height	Height%	Conc.	Mark
1	11.043	68877	2.382	7026	3.016	2.382	
2	11.555	2822380	97.618	226003	96.984	97.618	V
Total		2891257	100.000	233032	100.000		

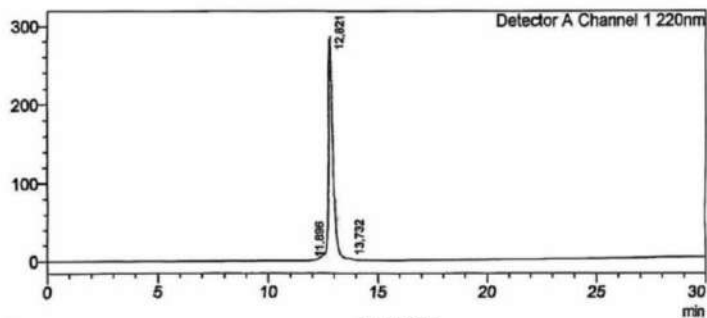
Model: LCMS-2020	Entrance Lens: +20.0 V	M	2014,3
RF Gain: 5000	Interface: ESI	[M+H]⁺	2015,3
RE Offset: 5100	Nebulizing Gas Flow: 1.50 L/min	[M+2H]²⁺	1008,2
Makrod Bias: +5.0 V	Drying Gas Flow: 15.00 L/min	[M+3H]³⁺	672,4
Conversion Dynodo: +10.0 kV	Interface Bias: -3.50 kV	[M+4H]⁴⁺	504,6
Detector: -1,10 kV	Interface Bias: -3.50 kV	[M+5H]⁵⁺	403,9
PG: 0,0e+000 Pa	Interface Current: 0.0 uA	[M+6H]⁶⁺	336,7
IG: 0,0e+000 Pa	Heat Block Temp.: 150 C		
Q1 Temp.: 150 C			



(D)

5-FAM_RR

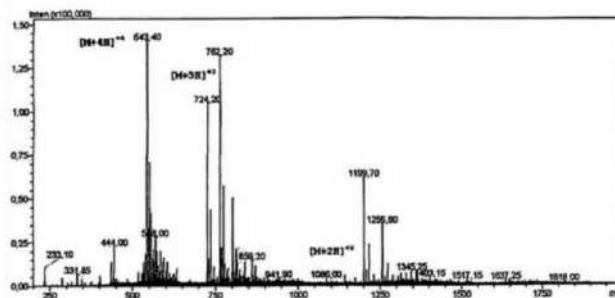
mV 5-FAM-Leu-Ser-Gly-Arg-Ala-Arg-Arg-Arg-Val-Arg-Ala-Trp-Ala-Thr - Arg-COOH

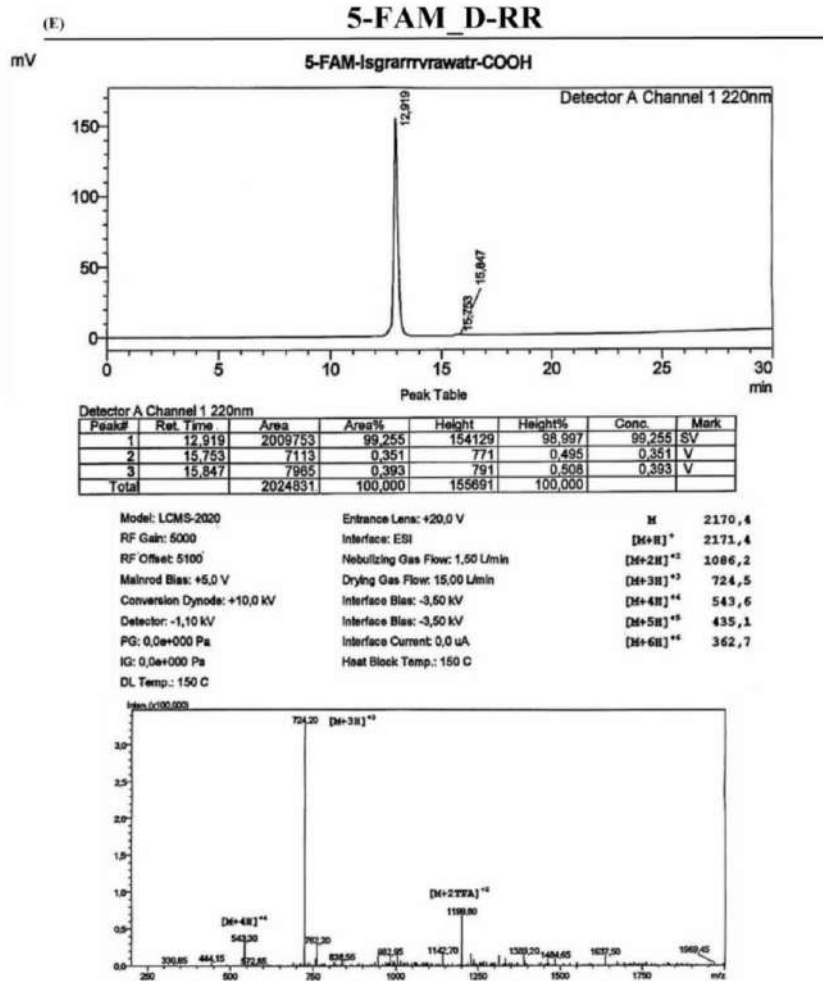


Peak Table

Peak#	Ret. Time	Area	Area%	Height	Height%	Conc.	Mark
1	11,896	1904	0,046	137	0,048	0,046	
2	12,821	4156041	99,781	285963	99,724	99,781	SV
3	13,732	7203	0,173	655	0,228	0,173	T
Total		4165148	100,000	286755	100,000		

Model: LCMS-2020	Entrance Lens: +20,0 V	X	2170,4
RF Gain: 5000	Interface: ESI	[M+R] ⁺	2171,4
RF Offset: 5100	Nebulizing Gas Flow: 1.50 L/min	[M+2R] ⁺⁺	1086,2
Mainrod Bias: +5,0 V	Drying Gas Flow: 15,00 L/min	[M+3R] ⁺⁺⁺	724,5
Conversion Dynode: +10,0 kV	Interface Bias: -3,50 kV	[M+4R] ⁺⁺⁺⁺	543,6
Detector: -1,10 kV	Interface Bias: -3,50 kV	[M+5R] ⁺⁺⁺⁺	435,1
PG: 0,0e+000 Pa	Interface Current: 0,0 uA	[M+6R] ⁺⁺⁺⁺	362,7
IG: 0,0e+000 Pa	Heat Block Temp.: 150 C		
DL Temp.: 150 C			



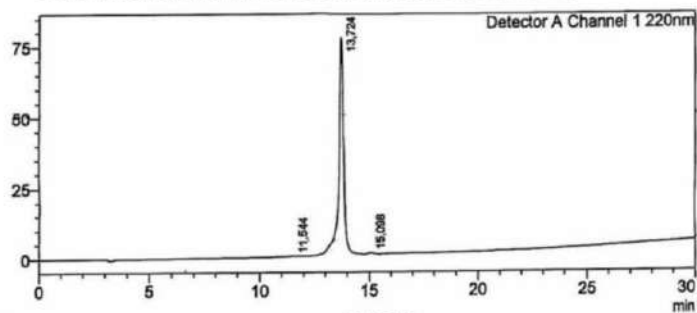


(F)

5-FAM_WR

mV

5-FAM-Leu-Ser-Gly-Arg-Trp-Arg-Arg-Trp-Arg-Ala-Trp-Ala-Thr-Arg-COOH

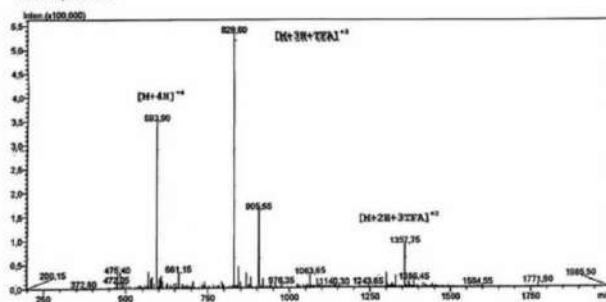


Detector A Channel 1 220nm

Peak Table

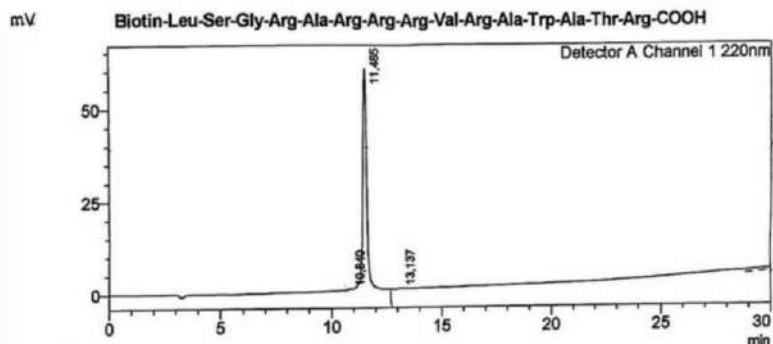
Peak#	Ret. Time	Area	Area%	Height	Height%	Conc.	Mark
1	11.544	3497	0.281	206	0.266	0.281	M
2	13.724	1231836	99.005	76691	98.899	99.005	V
3	15.098	8878	0.714	647	0.835	0.714	
Total		1244210	100.000	77545	100.000		

Model: LCMS-2020	Entrance Lens: +20.0 V	M	2372,6
RE Gas: 5000	Interface: ESI	[M+2] ⁺	2373,6
RF Offset: 5100	Nebulizing Gas Flow: 1.50 L/min	[M+2H] ²⁺	1187,3
Mainrod Bias: +5.0 V	Drying Gas Flow: 15.00 L/min	[M+3H] ³⁺	791,9
Conversion Dynode: +10.0 kV	Interface Bias: -3.50 kV	[M+4H] ⁴⁺	594,2
Detector: -1,10 kV	Interface Bias: -3.50 kV	[M+5H] ⁵⁺	475,5
PG: 0.0e+000 Pa	Interface Current: 0.0 uA	[M+6H] ⁶⁺	396,4
IS: 0.0e+000 Pa	Heat Block Temp.: 150 C		
DL Temp.: 150 C			



(G)

b RR

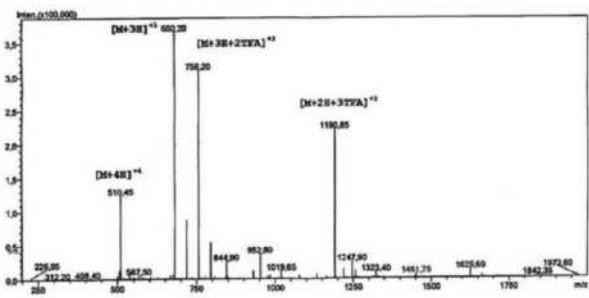


Peak#	Ret. Time	Area	Area%	Height	Height%	Conc	Mark
1	10.840	4523	0.588	359	0.615	0.588	
2	11.485	762708	99.119	59383	99.022	99.119	V
3	13.137	2256	0.293	218	0.363	0.293	
Total		769488	100.000	59970	100.000		

Model: LCMS-2020
 RE Gain: 5000
 RF Offset: 5100
 Mainrod Bias: +5.0 V
 Conversion Dynode: +10.0 kV
 Detector: -1.10 kV
 PG: 0.0e+000 Pa
 IG: 0.0e+000 Pa
 DL Temp.: 150 C

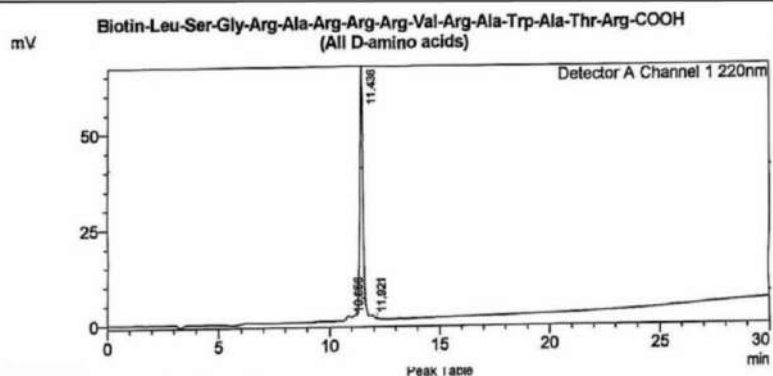
Entrance Lens: +20.0 V
 Interface: ESI
 Nebulizing Gas Flow: 1.50 L/min
 Drying Gas Flow: 15.00 L/min
 Interface Bias: -3.50 kV
 Interface Bias: -3.50 kV
 Interface Current: 0.0 uA
 Heat Block Temp.: 150 C

M 2039,3
 [M+H]⁺ 2039,3
 [M+2H]²⁺ 1020,2
 [M+3H]³⁺ 680,4
 [M+4H]⁴⁺ 510,6
 [M+5H]⁵⁺ 408,7
 [M+6H]⁶⁺ 340,7



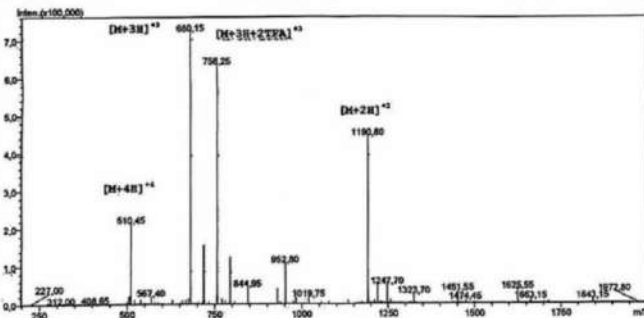
(II)

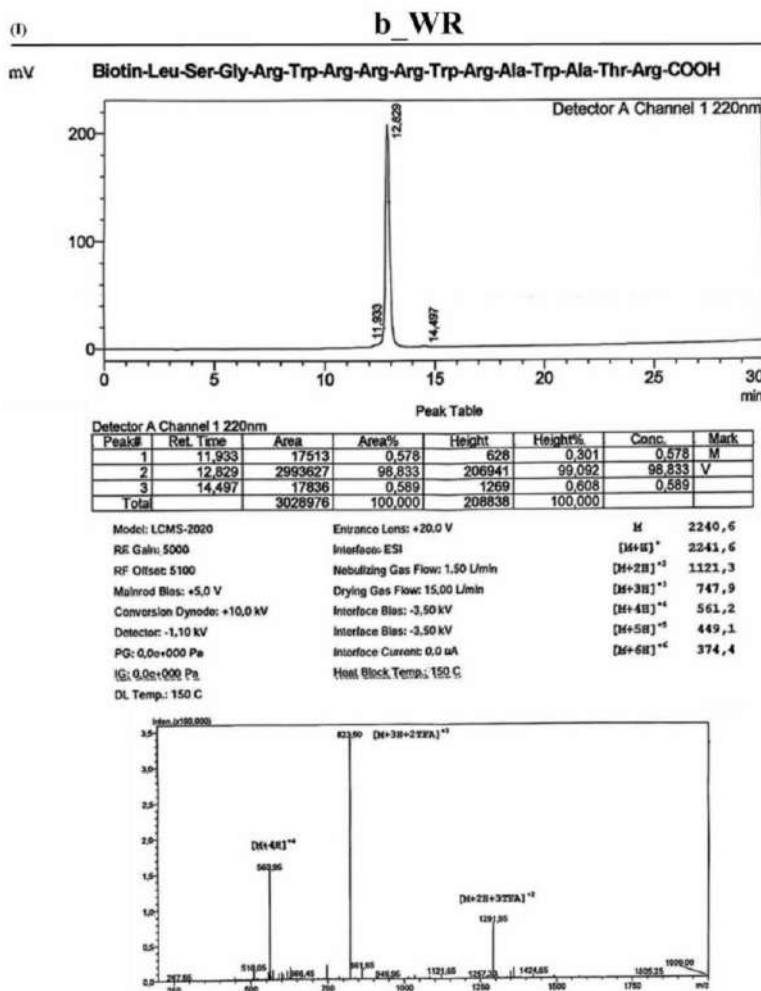
b D-RR



Peak#	Ret. Time	Area	Area%	Height	Height%	Conc.	Mark
1	10.856	16463	2.301	1269	1.843	2.301	
2	11.436	680912	95.158	68441	96.487	95.158	V
3	11.921	18187	2.542	1149	1.669	2.542	V
Total		715562	100.000	68860	100.000		

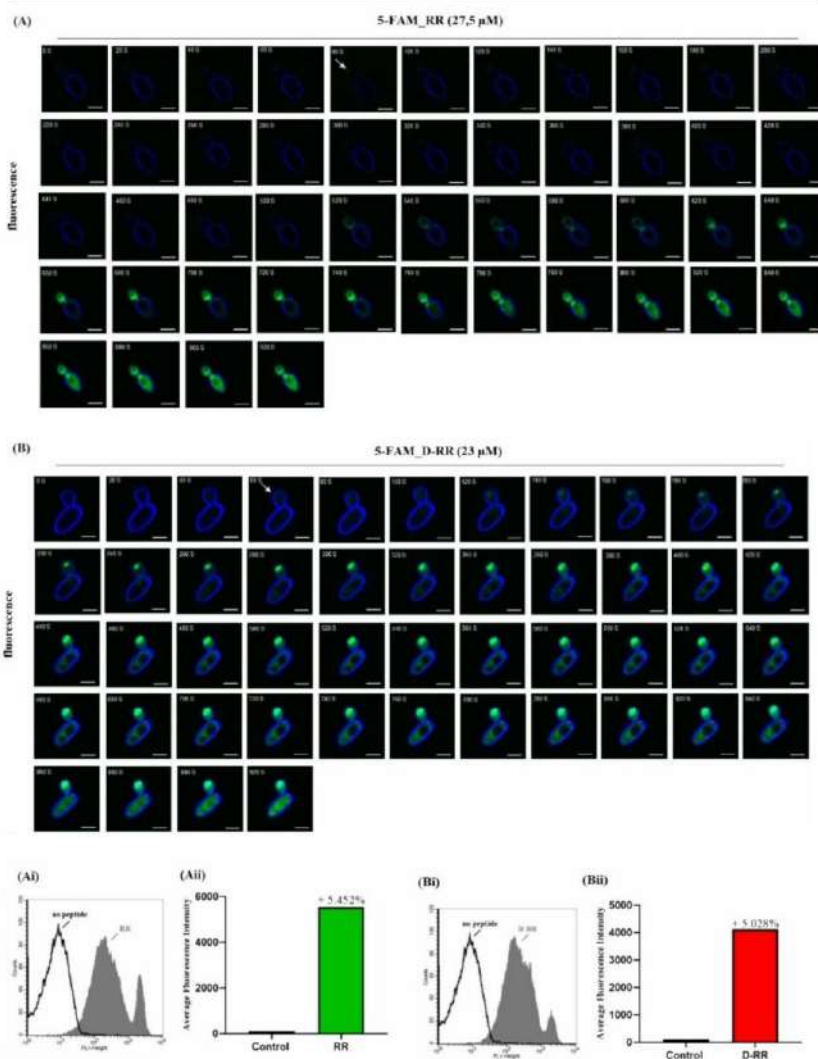
Model: LCMS-2020	Entrance Lens: +20.0 V	X	2038,3
RG Gain: 5000	Interface: ESI	[M+H] ⁺	2039,3
RF Offset: 5100	Nebulizing Gas Flow: 1.50 L/min	[M+2H] ²⁺	1020,2
Mistrod Bias: +5.0 V	Drying Gas Flow: 15.00 L/min	[M+3H] ³⁺	680,4
Conversion Dynode: +10.0 kV	Interface Bias: -3.50 kV	[M+4H] ⁴⁺	510,6
Detector: -1.10 kV	Interface Bias: -3.50 kV	[M+5H] ⁵⁺	408,7
PG: 0.0e+000 Pa	Interface Current: 0.0 uA	[M+6H] ⁶⁺	340,7

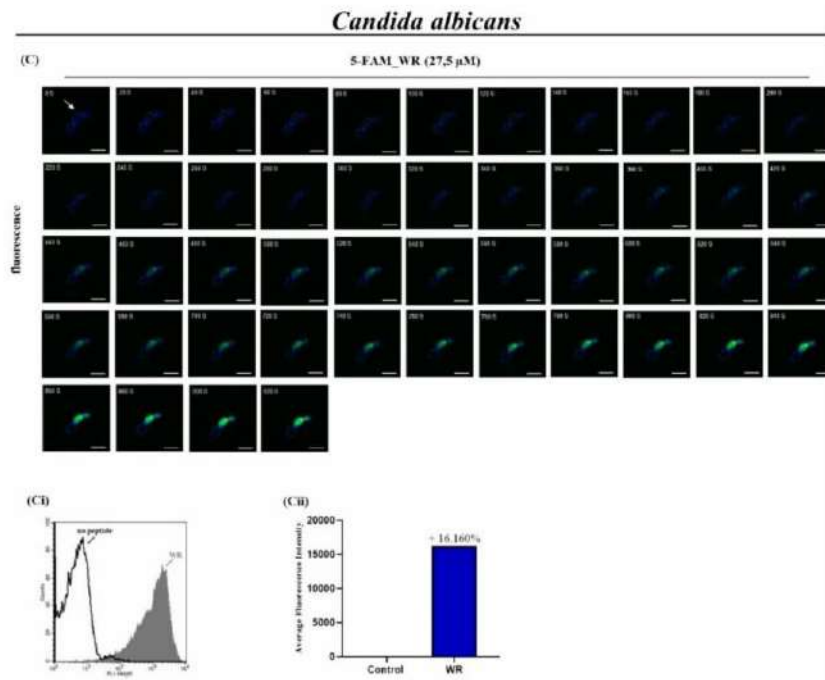




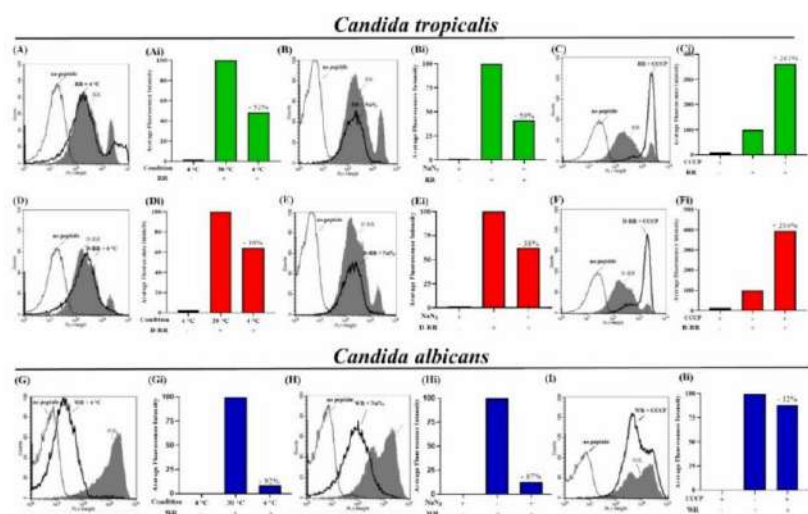
Supplementary Figure 1. Liquid Chromatography-Mass Spectrometry Analysis of the synthetic peptides (A) RR, (B) D-RR, (C) WR, its 5-FAM conjugates (D) 5-FAM_RR, (E) 5-FAM_D-RR, (F) 5-FAM_WR, and its biotin conjugates (G) b_RR, (H) b_D-RR, and (I) b_WR. Analysis conditions: RP-C18 column, 4.6x250 mm - Flow: 1 mL/min Solvents: A=TFA 0.1%/H₂O, B=CH₃CN/H₂O 9:1 with TFA 0.1% Detector: 220 nm - Gradient: 5 to 100% of B in 25 min. Note: due to the cationic character, the presence of signals of ions aggregated with trifluoroacetate is noted as a mere artifact of the analysis.

Candida tropicalis

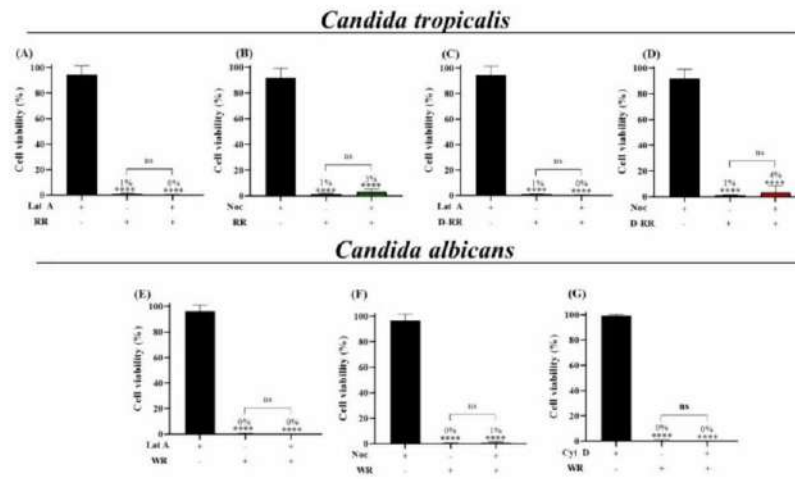




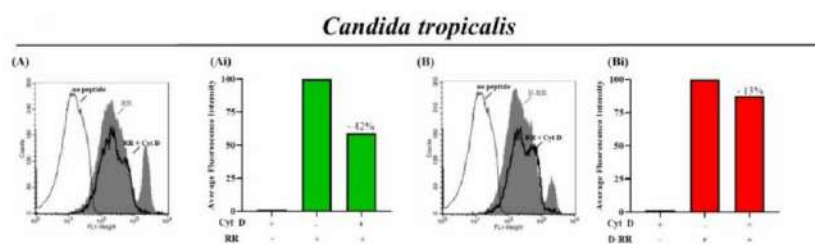
Supplementary Figure 2. Dynamics of cytoplasmic entry of 5-FAM-labeled peptides into fungal cells. Confocal microscopy time lapse within the first 15 min of interaction of the peptides with the fungal cells. (A) 5-FAM_RR and (B) 5-FAM_D-RR with *Candida tropicalis*, and (C) 5-FAM_WR with *Candida albicans*. Green fluorescence in the cytoplasm indicates the presence of the peptide, while blue fluorescence marks the fungal cell wall with calcofluor white. Scale bars = 10 μ m. The result is representative of triplicate assays. Fluorescence patterns and cell count by flow cytometry of *C. tropicalis* cells treated with 5-FAM_RR (Ai) and 5-FAM_D-RR (Bii) and *C. albicans* treated with 5-FAM_WR (Ci) at 30 °C (grey shading) untreated cells (black line). Data representative of 20,000 events. Graphs representing mean fluorescence intensity of *C. tropicalis* cells treated with 5-FAM_RR (Aii) and 5-FAM_D-RR (Bii) and *C. albicans* treated with 5-FAM_WR (Cii) at 30 °C. Data representative of 20,000 events.



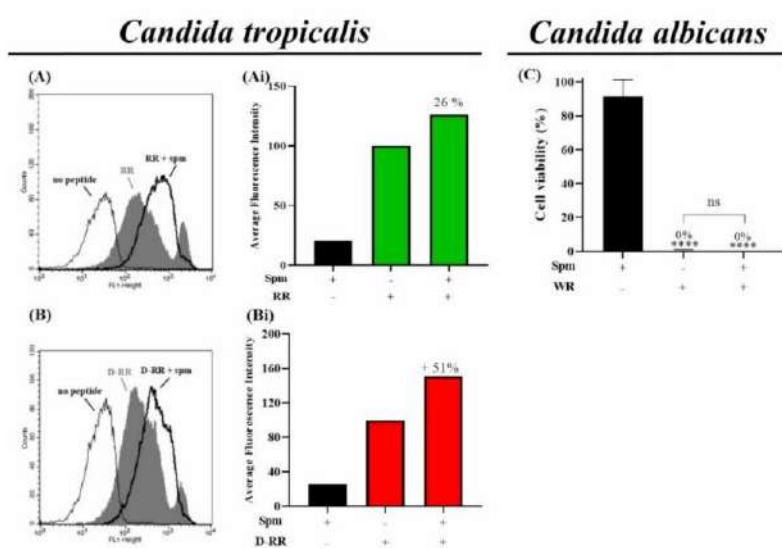
Supplementary Figure 3. Influence of cell energy on the interaction of bioinspired peptides with fungal cells. Cell count and mean fluorescence intensity obtained by flow cytometry for *C. tropicalis* cells treated with 5-FAM-RR (A, Ai) and 5-FAM-D-RR (D, Di), and *Candida albicans* cells treated with 5-FAM-WR (G, Gi). Analyses were performed at 30 °C (gray shading) and 4 °C (thick black line), with untreated cells represented by the thin black line. For experiments in the presence of NaN₃: *C. tropicalis* cells treated with 5-FAM-RR (B, Bi) and 5-FAM-D-RR (E, Ei), and *C. albicans* cells treated with 5-FAM-WR (H, Hi) at 30 °C (gray shading), with untreated cells represented by the thin black line. For experiments in the presence of CCCP: *C. tropicalis* cells treated with 5-FAM-RR (C, Ci) and 5-FAM-D-RR (F, Fi), and *C. albicans* cells treated with 5-FAM-WR (I, Ii) at 30 °C (gray shading), with untreated cells represented by the thin black line. Data are representative of 20,000 events.



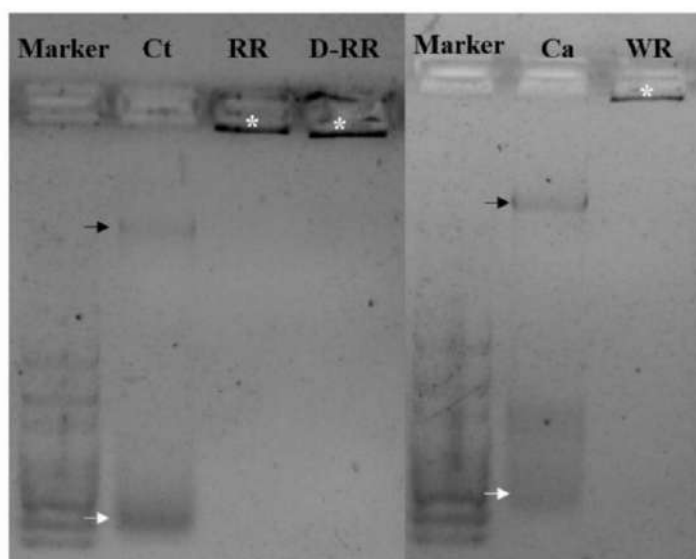
Supplementary Figure 4. Role of endocytosis in the interaction of bioinspired peptides in fungal cells. Cell viability in response to bioinspired peptides. **(A)** *C. tropicalis* cells treated with RR peptide in the presence and absence of latrunculin A (Lat A) and **(B)** in the presence and absence of Nocodazole (Noc). **(C)** *C. tropicalis* cells treated with D-RR peptide in the presence and absence of Lat A and **(D)** in the presence and absence of Noc. **(E)** *C. albicans* cells treated with WR peptide in the presence and absence of Lat A, **(F)** in the presence and absence of Noc, and **(G)** in the presence and absence of Cyt D. Cells were treated with the peptides at their respective LD₁₀₀ for 20 min incubation at 30 °C. Data are a representative example of three independent experiments. Statistical significance with the control is indicated as ****, $P < 0.05$. ns, not significant.



Supplementary Figure 5. Role of endocytosis in the interaction of bioinspired peptides in *Candida tropicalis*. Fluorescence patterns and cell count by flow cytometry of *C. tropicalis* cells treated with 5-FAM_RR (**A**) and 5-FAM_D-RR (**B**) at 30 °C (grey shading), in the presence of Cyt D (thick black line) untreated cells (thin black line). Data representative of 20,000 events. Graphs representing mean fluorescence intensity of *C. tropicalis* cells treated with 5-FAM_RR (**Ai**) and 5-FAM_D-RR (**Bi**) in the presence and absence of Cyt D. Data representative of 20,000 events.



Supplementary Figure 6. Role of spermine (Spm) in the interaction of bioinspired peptides in *Candida tropicalis*. Fluorescence patterns and cell count by flow cytometry of *C. tropicalis* cells treated with 5-FAM_RR (A) and 5-FAM_D-RR (B) at 30 °C (grey shading), in the presence of Spm (thick black line) untreated cells (thin black line). Data representative of 20,000 events. Graphs representing mean fluorescence intensity of *C. tropicalis* cells treated with 5-FAM_RR (Ai) and 5-FAM_D-RR (Bi) in the presence and absence of Spm. Data representative of 20,000 events. Cell viability of *C. albicans* treated with WR (C), at their LD₁₀₀, for 20 min at 30 °C, with and without the addition of Spm. Data represent the mean of three independent experiments, with statistical significance indicated as **** ($P < 0.05$).



Supplementary Figure 7. Gel shift assay showing the interaction of RR, D-RR, and WR with DNA of fungal cells. Note that the peptides impair que migration of DNA which is retained inside the well. Black arrow indicates DNA band, white arrow indicates the RNA bands, (*) indicates the retention of DNA/RNA inside the well.

7. CONCLUSÕES

As doenças fúngicas representam um desafio crescente para a saúde global, especialmente devido ao aumento da resistência aos antifúngicos disponíveis. Nesse contexto, os AMPs surgem como uma promissora alternativa terapêutica. Nesta tese, investigamos os mecanismos de ação dos peptídeos bioinspirados RR, D-RR e WR contra *Candida tropicalis* e *Candida albicans*, destacando sua internalização, indução de danos celulares e papel no desencadeamento da morte fúngica.

Nossos achados demonstraram que esses peptídeos possuem mecanismos de internalização distintos e rápidos, mediados principalmente por transportadores de poliaminas. A inibição desse transporte e a redução da temperatura prejudicaram a entrada dos peptídeos nas células fúngicas, conferindo proteção aos microrganismos. Além disso, identificamos que a espermina, um antioxidante, reduziu os níveis de ROS e protegeu as células fúngicas da toxicidade induzida pelos peptídeos, reforçando a importância do estresse oxidativo no processo de morte celular.

Os danos celulares induzidos pelos peptídeos incluíram encolhimento celular devido ao efluxo de K^+ , hiperpolarização mitocondrial, acidificação do meio, permeabilização da membrana e degradação citoplasmática. Alterações estruturais, como vacuolização, dano à parede celular e formação de poros, foram observadas, evidenciando a extensão da disrupção celular causada por esses peptídeos. WR, em particular, induziu a formação de *blebs* em *C. albicans*, sugerindo um mecanismo de ação diferenciado. Além disso, a observação da ligação dos peptídeos ao núcleo celular indica um possível alvo citoplasmático relevante para sua atividade antifúngica.

Importante ressaltar que os peptídeos estudados não demonstraram toxicidade detectável em células LLC-MK2, reforçando seu potencial como agentes antifúngicos seguros. Os resultados obtidos contribuem significativamente para a compreensão dos mecanismos de ação dos AMPs e abrem novas perspectivas para o desenvolvimento de terapias antifúngicas inovadoras e eficazes.

Dessa forma, esta tese reforça a relevância dos peptídeos bioinspirados como candidatos promissores no combate às infecções fúngicas, fornecendo bases científicas para futuras aplicações terapêuticas e aprimoramento do design de novos antifúngicos.